TECHNISCHE UNIVERSITÄT MÜNCHEN

TUM School of Engineering and Design

Micromechanical Foundations of Mechanobiology in Soft Tissues

Jonas Felix Eichinger

Vollständiger Abdruck der von der TUM School of Engineering and Design der Technischen Universität München zur Erlangung des akademischen Grades eines

Doktors der Ingenieurwissenschaften

genehmigten Dissertation.

Vorsitz:	Priv.-Doz. Dr.-Ing. Christian Krempaszky
Prüfer der Dissertation:	
	1. Prof. Dr.-Ing. Christian J. Cyron
	2. Prof. Jay D. Humphrey, Ph.D.
	3. Prof. Dr.-Ing. Wolfgang A. Wall

Die Dissertation wurde am 17.06.2021 bei der Technischen Universität München eingereicht und durch die Fakultät für Maschinenwesen am 28.09.2021 angenommen.

Danksagung

"Gratia pro rebus merito debetur inemptis." — *Ovid*

Die vorliegende Dissertation entstand in den Jahren 2016 bis 2021 im Rahmen meiner Tätigkeit als wissenschaftlicher Mitarbeiter am Lehrstuhl für Numerische Mechanik der Technischen Universität München. In dieser Zeit hatte ich das Privileg, von großartigen Menschen begleitet und auf vielfältige Weise selbstlos unterstützt zu werden. An dieser Stelle möchte ich den Versuch wagen, mich dafür angemessen zu bedanken.

Allen voran möchte ich meinem Doktorvater Prof. Christian Cyron meinen herzlichen Dank aussprechen. Seine Begeisterung für die Wissenschaft, seine herausragende fachliche Kompetenz sowie sein Ansatz, Probleme stets als Chance wahrzunehmen, haben mich inspiriert und nachhaltig geprägt. Auch die vielen langen Gespräche fernab des Fachlichen (und manchmal Sachlichen) habe ich immer sehr genossen. In ähnlichem Maße möchte ich mich bei meinem zweiten Betreuer Prof. Jay Humphrey bedanken – sowohl für die Möglichkeit, mehrere Monate in seinem Lab an der Yale University verbringen zu dürfen, als auch für das, was ich über das Schreiben wissenschaftlicher Artikel sowie gelebte Integrität in der Wissenschaft lernen durfte. Neben meiner Dankbarkeit gilt ihm als Mensch meine ehrliche Bewunderung. Des Weiteren möchte ich mich bei meinem Mentor Prof. Wolfgang Wall für die vielen vertrauensvollen Gespräche sowie die Übernahme des zweiten Mitberichts bedanken. Das Privileg, Wissenschaft von drei so unterschiedlichen Persönlichkeiten mit jedoch ähnlichen zugrundeliegenden Werten hautnah erleben und erlernen zu dürfen, empfinde ich als unschätzbares Glück. Herrn Priv.-Doz. Christian Krempaszky, den ich bereits zu Studienzeiten sehr zu schätzen lernte, danke ich für die Übernahme des Prüfungsvorsitzes. Frau Renata Nagl danke ich für viele Jahre angenehmer und vertrauensvoller Zusammenarbeit in allen organisatorischen Belangen.

Während meiner Zeit am Lehrstuhl durfte ich mit wunderbaren Kollegen und Kolleginnen zusammenarbeiten, zusammen wachsen und zusammenwachsen – viele sind über die Jahre zu Freunden geworden. Die morgendliche Kaffeerunde, das gemeinsame Mittagessen, Fußballspielen oder Bouldern nach der Arbeit sowie gemeinsame Unternehmungen in der Freizeit prägten für mich die letzten Jahre. Maximilian Grill danke ich für die von gegenseitiger Wertschätzung geprägte enge fachliche Zusammenarbeit über viele Jahre, ohne die der numerische Teil dieser Arbeit in seiner jetzigen Form nicht möglich gewesen wäre. In selbem Maße bedanke ich mich bei Daniel Paukner für seine Beiträge zum experimentellen Teil der Arbeit. Jason Szafron, Ramak Khosravi und Abhay Ramachandra gebührt mein Dank für ihre ausdauernde Geduld, einem Numeriker wie mir das notwendige Handwerk sowie die Freude am experimentellen Arbeiten zu vermitteln. Darüber hinaus danke ich auch allen anderen Kollegen aus Jays Lab für die vielen gemeinsamen sozialen Aktivitäten während meiner beiden Aufenthalte in den USA. Andreas Rauch danke ich für die Betreuung meiner Semester- sowie Masterarbeit am Lehrstuhl. Dem gesamten Adminteam danke ich für die hervorrgende Unterstützung in IT-Belangen. Christoph Schmidt danke ich für seinen altruistischen Einsatz und das stete Bemühen um unsere Cluster. Bei Karl Wichmann, Georg Hammerl und Michael Hiermeier möchte ich mich für wertvollen Input zum Thema Coding bedanken. Meinem ehemaligen Bürokollegen Benjamin Krank bin ich für all seine Hilfe gerade zu Beginn meiner Promotion dankbar. Bei Anna Birzle und Christoph Meier bedanke ich mich für viele unterhaltsame Gespräche während und außerhalb der Arbeits-

zeit sowie für unsere gemeinsame Zeit in den USA. Tiefe Dankbarkeit auf vielen Ebenen gilt Carolin Geitner, Sebastian Brandstäter, Sebastian Fuchs und Johannes Kremheller. Herzlichen Dank für alle Gespräche, allen Zuspruch und die gemeinsamen Erlebnisse in den vergangenen Jahren. Unbedingt möchte ich auch all meinen Studierenden, insbesondere Lydia Ehmer, Lea Häusel und Jonas Koban für ihren Einsatz und ihre Beiträge zu dieser Arbeit in Form von Studienarbeiten oder Hiwi-Tätigkeiten Dank sagen.

Abschließend möchte ich mich herzlich bei meiner Familie und meinen Freunden für die Unterstützung und das mir entgegengebrachte Vertrauen bedanken. Besonderer Dank gilt meiner Schwester Annick für ihren Rückhalt in allen Höhen und Tiefen der Promotion.

München, im Dezember 2021 Jonas F. Eichinger

Abstract

The emerging research field of *mechanobiology*, which focuses on the active interaction between biology and mechanics, has revolutionized our understanding of the origin and progression of various diseases over the past decades. A major milestone in this field was the finding that living soft tissues appear to promote the development and maintenance of a preferred mechanical state within a defined tolerance around a so-called set-point. This phenomenon is often referred to as *mechanical homeostasis*. Homeostasis requires both mechanosensitive and mechanoregulatory processes; failure or malfunction of just one of these complimentary processes is inseparably linked to some of the most predominant causes of death, such as cancer and cardiovascular diseases such as aneurysms or hypertension.

Even though mechanobiology and, in particular, mechanical homeostasis play a central role in various (patho-)physiological processes, its micromechanical and biophysical principles remain elusive. It is not yet known which mechanosensitive and mechanoregulatory processes act collaboratively on the various length scales from molecules to cells to entire tissues and on different time scales from minutes to days to years to promote what is macroscopically called mechanical homeostasis.

Both experiments with tissue equivalents such as cell-seeded collagen gels and mathematical modeling have been proven to be tremendously helpful in understanding soft tissue mechanobiology. Yet, many central questions remain open, because available experimental approaches and current mathematical models suffer from critical shortcomings.

A major drawback of available experimental data is the restriction to uniaxial data, although most tissues are subject to multiaxial loading *in vivo*. To close this gap, the first computer-controlled bioreactor that enables accurate measurements of the evolution of mechanical tension and deformation of tissue equivalents under well-controlled biaxial loads is custom-built and validated in this thesis. Subsequently, diverse studies are performed to examine how cells establish a homeostatic state of biaxial tension, and within which tolerance they maintain this state in response to mechanical perturbations. Moreover, the impact of cell and matrix density, cell type, and different types of uni- and biaxial loading conditions (uniaxial, strip-biaxial, and biaxial) on mechanobiological processes is studied.

Current micromechanical computational models primarily focus on the passive mechanical properties of fiber networks or suffer from an unsatisfactory experimental foundation and rely on heuristic assumptions in many crucial aspects. Therefore, a highly efficient micromechanical finite element model resolving the interaction of individual cells and matrix fibers is introduced in this thesis. In various numerical examples, agreement between results of the novel computational framework, experimental data, and theoretical predictions is shown.

Finally, experimental data and simulation data are combined with theoretical considerations based on a novel mechanical analog model for active soft tissue mechanics to identify a likely candidate for the target quantity of cellular mechanoregulation, at least on short time scales. These considerations are then extended to longer times scales by including mass turnover, i.e., production and degradation of matrix fibers, to propose a set of mechanosensitive mechanisms which potentially control mechanical homeostasis on time scales longer than two days.

The results and conclusions presented in this thesis allow a better bottom-up understanding of mechanobiology and homeostasis in soft tissues.

Zusammenfassung

Das Forschungsgebiet der Mechanobiologie, das sich mit der Interaktion von Biologie und Mechanik beschäftigt, hat über die letzten Jahrzehnte unser Verständnis der Entstehung und des Verlaufs verschiedener Krankheiten revolutioniert. Ein wichtiger Meilenstein dieses Gebiets war die Erkenntnis, dass lebendes Weichgewebe die Entwicklung und Aufrechterhaltung eines bevorzugten mechanischen Zustands innerhalb einer definierten Toleranz um einen Sollwert zu fördern scheint. Dieses Phänomen wird oft als mechanische Homöostase bezeichnet. Diese erfordert sowohl mechanosensitive als auch mechanoregulatorische Prozesse. Das Versagen eines dieser komplementären Prozesse steht in direkter Verbindung zu einigen der häufigsten Todesursachen wie Krebs und Herz-Kreislauf-Erkrankungen.

Im Widerspruch zur zentralen Rolle, die Mechanobiologie in verschiedenen (patho-)physiologischen Prozessen spielt, sind ihre mikromechanischen und biophysikalischen Prinzipien weitgehend unerforscht. Im Besonderen ist noch unbekannt, welche mechanosensitiven und mechanoregulatorischen Prozesse auf verschiedenen Längen- und Zeitskalen zusammenwirken, um auf makroskopischer Ebene mechanische Homöostase zu bewirken.

Sowohl Experimente mit Gewebeäquivalenten als auch mathematische Modelle haben sich als enorm hilfreich erwiesen, um Mechanobiologie in Weichgeweben zu untersuchen. Dennoch bleiben viele zentrale Fragen offen, da sowohl die verfügbaren experimentellen Ansätze als auch die aktuellen mathematischen Modelle einige kritische Defizite aufweisen.

Ein wesentlicher Nachteil der verfügbaren experimentellen Daten ist die Beschränkung auf uniaxiale Daten, obwohl die meisten Gewebe *in vivo* einer multiaxialen Belastung unterliegen. Um diese Lücke zu schließen, wird im Rahmen dieser Arbeit der erste computergesteuerte Bioreaktor entwickelt und validiert, der genaue Messungen der Entwicklung der mechanischen Spannung in Gewebeäquivalenten unter präzise kontrollierbaren biaxialen Belastungen ermöglicht. Anschließend werden verschiedene Studien durchgeführt, unter anderem um zu ermittlen, wie Zellen einen homöostatischen Spannungszustand entwickeln und innerhalb welcher Toleranz sie diesen als Reaktion auf mechanische Störungen wiederherstellen. Darüber hinaus wird der Einfluss der Zell- und Faserdichte, des Zelltyps und verschiedener Arten von biaxialen Belastungsbedingungen auf mechanobiologische Prozesse untersucht.

Mathematische Computermodelle der Weichgewebemikromechanik konzentrieren sich häufig nur auf die passiven mechanischen Eigenschaften oder leiden unter einer unbefriedigenden experimentellen Grundlage und basieren in entscheidenden Aspekten auf heuristischen Annahmen. Daher wird in dieser Arbeit ein hocheffizientes mikromechanisches Finite-Elemente-Modell vorgestellt, das die Interaktion von einzelnen Zellen und Matrixfasern auflöst. In verschiedenen numerischen Beispielen wird eine große Übereinstimmung von Simulationsdaten und experimentellen Ergebnissen sowie theoretischen Vorhersagen gezeigt.

Anschließend werden Experiment- und Simulationsdaten mit theoretischen Überlegungen, die auf einem neuartigen mechanischen Analogmodell für aktive Weichteilmechanik basieren, kombiniert und somit die wahrscheinliche Zielgröße der zellulären Mechanoregulation auf kurzen Zeitskalen identifiziert. Abschließend werden diese Überlegungen auf längere Zeitskalen ausgedehnt, indem auch die Produktion und der Abbau von Matrixfasern berücksichtigt wird, und so ein Satz von mechanosensitiven Mechanismen postuliert, der hinreichend ist, um mechanische Homöostase auf langen Zeitskalen zu steuern.

Contents

Chapter 1

Introduction

1.1 Motivation

Human health is to a large extent controlled by mechanical principles. *Mechanobiology*, as the emerging field of science at the interface of biology, physics, and mechanics, studies how mechanical quantities such as forces influence form and function of tissues on various length and time scales. Achievements in this field have transformed our understanding of various diseases over the past decades. Mechanobiological processes have been shown to be inseparably linked to some of the most predominant causes of death, such as cancer (Weaver et al. 1997, Boettiger et al. 2005, Yeung et al. 2005, Levental et al. 2009, Butcher et al. 2009, Lu et al. 2012) and cardiovascular diseases such as thoracic and abdominal aneurysms (Humphrey and Taylor 2008, Cyron et al. 2014, Humphrey et al. 2014b, Cyron et al. 2016, Humphrey and Tellides 2019). This results from mechanobiology being crucially involved in key cellular processes such as migration (Grinnell and Petroll 2010, Hall et al. 2016, Xie et al. 2017, Kim et al. 2020), differentiation (Chiquet et al. 2009, Mammoto et al. 2012, Zemel 2015), and even survival (Bates et al. 1995, Schwartz 1995, Zhu et al. 2001, Sukharev and Sachs 2012).

A central concept of mechanobiology is *mechanical homeostasis*, which describes the ability of cells to probe, interpret, and regulate the mechanical properties of soft tissues within a defined range around a preferred set-point (Fig. 1.1a and Fig. 1.2) (Cannon 1929, 1932, Brown et al. 1998, Humphrey et al. 2014a, Jansen et al. 2017). This ability enables tissues to restore their physical and mechanical properties back to normal in response to perturbations such as injury or disease using negative feedback mechanisms (Fig. 1.1b) (Cox and Erler 2011, Lu et al. 2011, Ross et al. 2013, Bonnans et al. 2014, Humphrey et al. 2014a). Paradoxically, despite the essential role of mechanical homeostasis for our well-being, its biophysical and micromechanical foundations remain largely elusive. It is not yet understood, how forces and mechanical cues are sensed by living biological systems, a process referred to as mechanosensing. The reciprocal process, referred to as mechanoregulation, is equally unexplored. Mechanoregulation describes how these systems actively adapt forces and regulate their mechanical properties on various scales of length – from the (sub-)cellular scale to the organ scale – and time – from minutes to years (Fig. 1.2, Humphrey et al. (2014a)).

Two scientific approaches have been proven particularly useful in the past to unravel the biophysical principles of mechanical homeostasis: experiments with cell-seeded tissue equivalents such as collagen gels (Eichinger et al. (2021b), Paper A) and computational modeling (Humphrey 2021). Although both concepts have contributed significantly to our current mechanobiological understanding, many key concepts are not yet understood, largely because of critical shortcomings of the available experimental and computational studies.

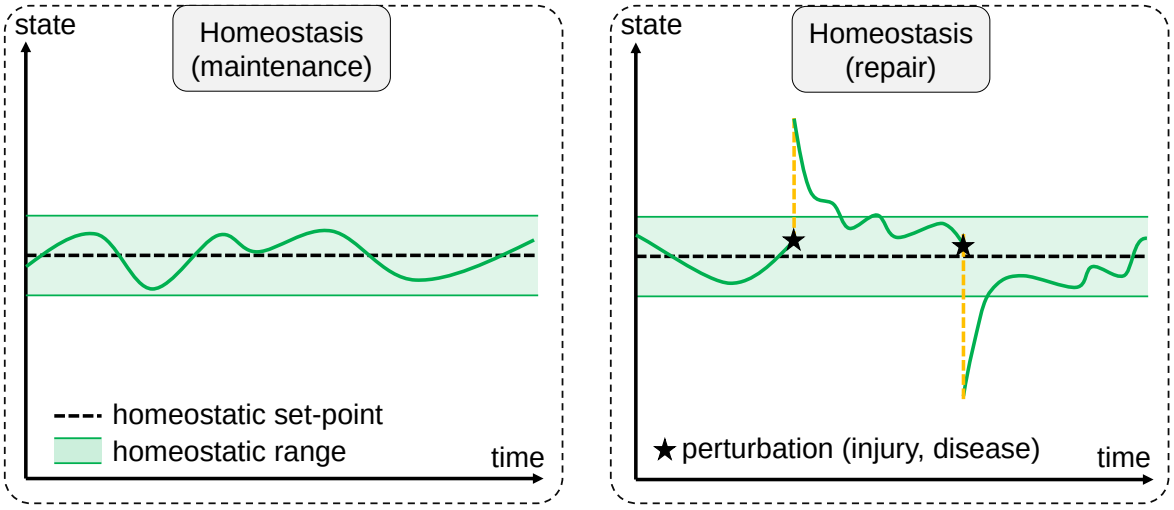

(a) (b)

Figure 1.1: A crucial process of mechanobiology is mechanical homeostasis, which describes the tendency of living soft tissues to maintain (a) and restore (b) specific mechanical variables within a tolerance around a specific set-point.

A major drawback of existing experimental studies is that they primarily focus on freely floating round gels (Bell et al. 1979, Simon et al. 2012, 2014) or uniaxially constrained gels (Kolodney and Wysolmerski 1992, Eastwood et al. 1994, Brown et al. 1998, 2002, Campbell et al. 2003, Marenzana et al. 2006, Ezra et al. 2010). This is, however, a severe simplification of the multiaxial loading present in most tissues *in vivo*. Therefore, a major achievement of this thesis is the development, validation, and application of the first biaxial bioreactor that can study the evolution and control of active tension in tissue equivalents under well-controlled *biaxial* loading conditions.

Although tissue culture experiments can significantly increase our understanding of mechanobiology, some essential concepts can hardly be unraveled with such studies alone. Mathematical and computational modeling of mechanobiology has thus attracted a lot of attention. Especially models on the continuum level were developed that helped tremendously in understanding mechanobiological principles (Holzapfel et al. 2000, Wakatsuki et al. 2000, Humphrey and Rajagopal 2002, Watton et al. 2004, Marquez et al. 2005, Cyron and Humphrey 2014, Cyron et al. 2014, Mauri et al. 2016, Loerakker et al. 2016, Cyron et al. 2016, Braeu et al. 2017). Yet, mechanobiological processes act on various scales of length ranging from molecules to cells to entire organs. To be able to understand mechanobiology of tissues, a crucial step is to understand which mechanisms act on the level of individual cells and fibers, especially at their interface, and how theses mechanisms superimpose to tissue-level phenomena (Humphrey et al. 2014a). For

this purpose, micromechanical modeling of the interaction of individual cells and matrix fibers can help to unveil the fundamental principles of mechanobiology and mechanical homeostasis by formulating them in mathematical or mechanical laws. Computational modeling on this level was, however, mostly done on decellularized ECM systems (Heussinger and Frey 2007, Mickel et al. 2008, Chatterjee 2010, Broedersz et al. 2011, Lang et al. 2013, Motte and Kaufman 2013, Jones et al. 2014, Lee et al. 2014, Müller et al. 2015, Ronceray et al. 2016, Mauri et al. 2016, Dong et al. 2017, Humphries et al. 2018, Zhou et al. 2018, Bircher et al. 2019, Domaschke et al. 2019) or suffers from severe limitations such as the restriction to two dimensions (Wang et al. 2014, Abhilash et al. 2014, Jones et al. 2014, Notbohm et al. 2015, Kim et al. 2017, Humphries et al. 2017, Grimmer and Notbohm 2017, Burkel et al. 2018). Therefore, a second major effort of this thesis is the development of a highly efficient microscale computational model that allows the simulation of multiple cells physically interacting with a three-dimensional fibrous matrix.

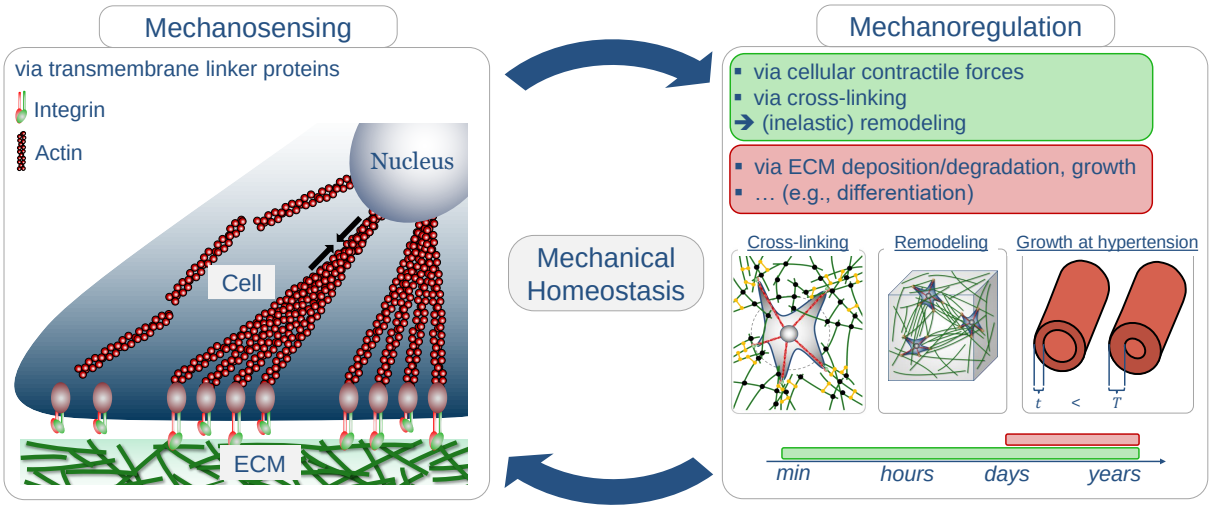

Figure 1.2: Control loop of mechanical homeostasis. Cells can sense altered mechanical loading or properties in their fibrous microenvironment via transmembrane integrins that connect intra- and extracellular structures (left). Having interpreted the mechanical condition, cells have multiple measures for control, such as adapting their contractile forces or cross-linking on short time scales, or adjusting mass turnover on longer time scales (right).

A special feature and the third major achievement of the presented thesis is that it combines micromechanical computer simulations and reliable quantitative experimental data with a thorough theoretical analysis. This allows a deeper understanding of the biophysical foundations of mechanobiology. This understanding is essential to advance in the emerging field of tissue engineering (Dzobo et al. 2018), i.e., the fabrication of tailor-made tissue substitutes, which can be expected to have major impact on biomedical engineering over the next decades, since it crucially relies on a precise understanding of the physical interactions of cells with their mechanical environment. Moreover, clinical practitioners could benefit from a better computer-aided diagnosis of certain diseases such as aneurysms using computational models to provide improved patient-specific therapies.

1.2 Contributions of this thesis

Tissue culture studies and computational modeling have been essential tools to decipher fundamental mechanobiological principles. Yet, many pressing questions still need to be answered, because a reliable experimental device especially for biaxial studies, a sophisticated computational microscale model of active soft tissues mechanics, and a comprehensive theoretical analysis are lacking. To this end, the following three major ***methodical contributions*** are achieved in this thesis.

A) Development and validation of the first biaxial bioreactor for cell-seeded tissue equivalents (Eichinger et al. (2021b, 2020, 2021c), Paper A, Paper B, Paper D):
This work presents the first biaxial bioreactor that allows the study of the development and control of active tension in cell-populated collagen gels over a period of up to two days. The custom-designed parts of the device can be found in Appendix F, and the respective experimental protocols in Appendix G. The newly developed device is used to quantify the impact of cell type, cell density, and collagen concentration, all of which vary in different tissues of the body, on homeostasis. Moreover, the influence of different external loads on homeostatic regulation is studied, and the first quantification of the homeostatic range is presented.

B) Development and validation of a highly efficient, micromechanical computational model for soft tissue mechanobiology (Eichinger et al. (2021a,c), Paper C, Paper D):
A novel, highly efficient computational framework based on the finite element method is introduced that models soft tissues on the scale of individual cells and fibers. It is constructed bottom-up, i.e., it models key mechanobiological processes and mechanisms such as actin stress fiber contractility and focal adhesion clutch behavior that are involved in the interaction of cells with the ECM. Its high efficiency allows the simulation of three-dimensional representative volume elements (RVEs) with physiologically reasonable values for both cell density and matrix fiber concentration. The framework is directly backed-up with experimental data gained using the novel biaxial testing device.

C) Development of a mechanical analog model for active soft tissue mechanics (Eichinger et al. (2021c), Paper D):
The thesis presents a simple mechanical analog model that contains all essential parts to reproduce how soft tissues develop and regulate a preferred mechanical state. Based on this analog model, various different hypotheses regarding the target quantity of cellular mechanoregulation are tested. Breaking down the complex mechanics to simple theoretical considerations allows an essential understanding of what can be regulated at the cell-matrix interface and how it translates to the macroscopic scale.

These novel methods are used to answer some of the most important open questions regarding mechanical homeostasis (as raised in Eichinger et al. (2021b), Paper A). In the following, these question are summarized, each of which is followed by respective novel contributions of this thesis to the ***biophysical understanding*** of mechanobiology.

1) **What is the micromechanical origin of mechanical homeostasis?**
So far, both *in vivo* (Wolinsky and Glagov 1967, Nakagawa et al. 1989, Matsumoto and Hayashi 1994, Shadwick 1999) and *in vitro* (Delvoye et al. 1991, Kolodney and Wysolmerski 1992, Brown et al. 1998, Ezra et al. 2010) experiments and observations have suggested the existence of mechanical homeostasis. However, it is not possible so far to name the exact mechanisms that exist at the cellular (Kong et al. 2009, Weng et al. 2016, Eloseguí-Artola et al. 2018) and single fiber (Bhole et al. 2009, Flynn et al. 2010) level, especially at their interface, so that homeostasis arises at tissue level. To understand homeostasis of entire tissues and organs, a prerequisite is to determine which quantity individual cells regulate and, subsequently, how such regulations on the scale of micrometers translate to phenomena observed on the scale of centimeters.

Contribution:
Combining the results from experiments and simulations with a thorough theoretical analysis based on a mechanical analog model allows this thesis to present cellular contractile forces as the most likely candidate for the target quantity of cellular mechanoregulation on short time scales. Other hypotheses regarding the cellular target are discussed and transparently ruled out (Eichinger et al. (2021c), Paper D).

2) **What are the target mechanical quantities and mechanisms that govern homeostasis on short and on long time scales?**
Existing experimental and computational studies agree that mechanical homeostasis acts on at least two time scales. On the first scale of minutes to days, mostly remodeling is relevant. On the second scale of days to years, also deposition and degradation of matrix fibers need to be considered (Wolinsky and Glagov 1967, Nakagawa et al. 1989, Matsumoto and Hayashi 1994, Brown et al. 1998, Ezra et al. 2010, Braeu et al. 2017, Latorre and Humphrey 2019). However, neither the precise target quantity of cellular mechanoregulation on short time scales nor a comprehensive set of required mechanisms for homeostasis on long time scales are available to date.

Contribution:
The short-term homeostatic response is shown to be explainable alone by cells regulating their focal adhesion stresses applied to the surrounding matrix. Other potential regulatory targets are excluded by examining them using a mechanical analog model, experimental data, and finite element simulations (Eichinger et al. (2021c), Paper D). Moreover, a quantitative study of how residual matrix tension (RMT) can arise, that is, how cell-mediated remodeling can be inelastic even on short time scales, is presented. Finally, for the first time, a sufficient set of mechanosensitive and -regulatory mechanisms on the microscale is proposed that is able to capture various phenomena related to mechanical homeostasis on long time scales such as growth and atrophy (Section 5.3).

3) **What is the tolerance at which the homeostatic steady state is restored?**
A major shortcoming of available studies that focus on the active control of tension in tissue equivalents facing external perturbations is the restriction of the observed relaxation intervals to one hour or less (Brown et al. 1998, Bisson et al. 2004, Ezra et al. 2010). In this

short time interval, no new steady state of tension can be reached in the gels. Therefore, these studies cannot reveal the tolerance within which the homeostatic state is actually restored after perturbations, i.e. a quantification of the homeostatic range is still lacking. Moreover, these studies could also not provide the information required to draw reliable conclusions regarding the exact quantity that is preserved by the cells exposed to such perturbations.

Contribution:
This thesis is the first to examine the mechanobiological behavior of cell-seeded gels for more than 15 hours after perturbations, that is, until a new steady state is reached. This study is thus the first to provide the data required to quantify the tolerance within which a prior state is recovered after perturbations. Therefore, it also allows conclusions about the target quantity preserved by cells facing perturbations (Eichinger et al. (2021c), Paper D). Answering these questions was a crucial step in understanding the principles underlying mechanical homeostasis on the tissue scale.

4) **What does homeostasis mean in multiaxial loading conditions?**
A severe limitation of available *in vitro* data is their restriction to simple boundary constraints such as traction-free boundary conditions in freely floating circular gels or uniaxial constraints in dog-bone-shaped gels (Eichinger et al. (2021b), Paper A). *In vivo* studies concentrated so far primarily on hoop stresses in blood vessels (Wolinsky and Glagov 1967, Shadwick 1999), which also do not allow to conclude what homeostasis exactly means in higher dimensional loading states.

Contribution:
This thesis exploits the possibility to extend allied methods such as tissue culture studies to multiple dimensions. It presents the first data of the evolution and regulation of tension in *biaxially* constrained and loaded tissue equivalents (Eichinger et al. (2020, 2021c), Paper B, Paper D). It is found that specimens show a higher homeostatic tension when being constrained biaxially compared to uniaxially. Moreover, the first data showing the effect of the type of boundary condition, e.g. equi-biaxial vs. strip-biaxial, and of the loading amplitude on the homeostatic behavior is presented in this thesis.

5) **How do different types of cells and cells from different tissue origins differ regarding the development and maintenance of the homeostatic state?**
Although different cell types and cells from different tissue origins have been tested in tissue culture studies, many cell and tissue types are missing. Therefore, conclusions on the precise role of cell type (such as fibroblasts and SMCs) and tissue origin (such as dermal, tendinous, or aortic) in mechanobiological homeostasis cannot be drawn yet. There is a pressing need for further (biaxial) tissue culture experiments to determine both quantitatively and qualitatively how cells of different type and origin generate and control a preferred mechanical state, and how long they remember their prior function when being transferred to an artificial environment.

Contribution:
NIH 3T3 fibroblasts, primary aortic fibroblasts, and primary aortic smooth muscle cells

(SMCs) are tested in this thesis with regard to their tendency to develop and maintain a preferred mechanical state. SMCs produced, ceteris paribus, the highest forces. Moreover, the influence of various factors such as cell and fiber density, medium composition, and the type of boundary condition is determined quantitatively (Eichinger et al. (2020, 2021c), Paper B, Paper D).

The following publications form the core of the presented work (in the order of presentation herein):

- Paper A (Eichinger et al. 2021b): J. F. Eichinger, L. J. Haeusel, D. Paukner, R. C. Aydin, J. D. Humphrey, and C. J. Cyron. Mechanical homeostasis in tissue equivalents - a review. Biomech. Model. Mechanobiol., 20(3):833–850, 2021b. DOI: 10.1007/s10237-021-01433-9.
- Paper B (Eichinger et al. 2020): J. F. Eichinger, D. Paukner, J. M. Szafron, R. C. Aydin, J. D. Humphrey, and C. J. Cyron. Computer-Controlled Biaxial Bioreactor for Investigating Cell-Mediated Homeostasis in Tissue Equivalents. J. Biomech. Eng., 142(7):1–22, 2020. DOI : 10.1115/1.4046201
- Paper C (Eichinger et al. 2021a): J. F. Eichinger, M. J. Grill, R. C. Aydin, W. A. Wall, J. D. Humphrey, and C. J. Cyron. A computational framework for modeling cell-matrix interactions in soft biological tissues. Biomech. Model. Mechanobiol., 20(5):1851–1870, 2021a. DOI: 10.1007/s10237-021-01480-2.
- Paper D (Eichinger et al. 2021c): J. F. Eichinger, D. Paukner, R. C. Aydin, W. A. Wall, J. D. Humphrey, and C. J. Cyron. What do cells regulate in soft tissues on short time scales? Acta Biomater., 134:348–356, 2021c. DOI: 10.1016/j.actbio.2021.07.054.

All computational methods have been implemented in the in-house finite element code BACI. Existing functionality, especially functionality that was implemented in the dissertations of Cyron (2011), Müller (2014), and Grill (2020), was reused. Parallel computing and linear solvers are taken from the open source project trilinos (Heroux and Willenbring 2012). Some experimental protocols developed in the dissertation of Simon (2014) were reused with slight modifications.

1.3 Outline

On an abstract level, this thesis is composed of three major complementary efforts which will be presented in Chapter 3, Chapter 4, and Chapter 5, respectively (Fig. 1.3). Before that, Chapter 2 gives a thorough introduction to the topic.

The first effort (Chapter 3, containing Paper A and Paper B) is the experimental investigation of mechanobiology in tissue equivalents, in particular in cell-seeded collagen or fibrin gels. To this end, Paper A gives a thorough review of the state of the art in this field. First, a descriptive history of mechanobiology, tissue homeostasis, and mechanical regulation is presented. Then, the various experimental methods and quantitative results are collected and compared, and the most relevant experimental observations are discussed. Motivated by the limitations of the

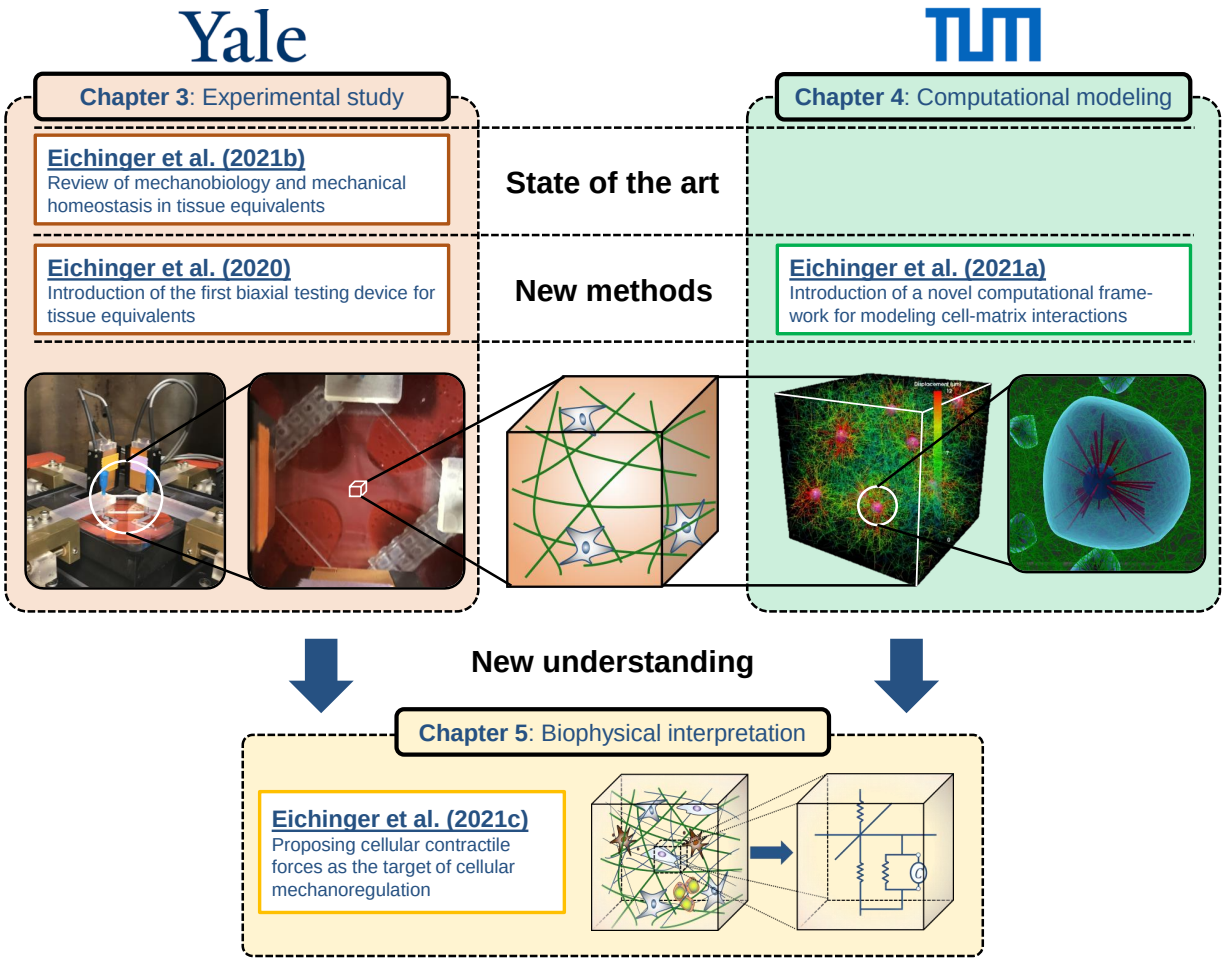

Figure 1.3: On an abstract level, the presented thesis pursues three major complementary goals: i) Chapter 3 is devoted to an experimental investigation of mechanobiology, consisting of a comprehensive review of existing techniques and results (Eichinger et al. (2021b), Paper A) and the development and use of the first biaxial testing device for the study of the evolution of tension in constrained tissue equivalents performed at Yale University (Eichinger et al. (2020), Paper B). ii) Chapter 4 presents a novel computational framework for the simulation of cell-matrix interactions in three-dimensional RVEs of soft tissues which was developed at TUM (Eichinger et al. (2021a), Paper C). iii) Chapter 5 combines results from the experimental and computational study with a theoretical analysis. This allows a novel bottom-up understanding of mechanobiology and homeostasis (Eichinger et al. (2021c), Paper D).

available studies, Paper B introduces the first computer-controlled, biaxial bioreactor especially designed to test cell-seeded delicate collagen or fibrin gels. After showing the validity of the new device using NIH 3T3 fibroblasts, novel observations regarding the development, maintenance, and re-establishment of the tensional state are presented.

The second effort (Chapter 4, consisting of Paper C) is the development of a novel, highly efficient computational framework based on the finite element method that allows detailed com-

puter simulations of the micromechanical processes during mechanoregulation in soft biological tissues. Paper C is dedicated to a detailed motivation and description of the various submodels of the framework. Subsequently, the ability of the chosen modeling approach to reproduce key experimental observations is shown by directly comparing simulation results with data gained in Paper B.

The third effort (Chapter 5, containing Paper D) combines experimental data and simulation results with a mathematical analysis to advance the current biophysical and micromechanical understanding of mechanobiology and homeostasis. This allows the identification of the cellular target of mechanical regulation on short times scales and the proposal of a set of microscopic mechanisms by which tissues can maintain their structural integrity despite continuous turnover of mass.

Finally, Chapter 6 discusses the main results and novelties of this thesis. Chapter 7 summarizes its efforts and ventures an outlook on how they can be exploited in future projects.

Chapter 2

Mechanobiology and mechanical homeostasis

This chapter is intended to give a comprehensive introduction to mechanobiology and mechanical homeostasis in particular, both from a biological and from a computational modeling perspective in the context of the respective methodical approaches chosen in this thesis. First, the chapter briefly reflects the history of mechanobiology and homeostasis. Subsequently, a physiological introduction to the current understanding of mechanical homeostasis is presented by shedding light on its key players. Finally, the chapter motivates and introduces the chosen methodical approaches for both the experimental and computational study presented in this thesis.

2.1 Origin and history

This section briefly recapitulates the milestones in the history of mechanobiology and homeostasis as portrayed in Eichinger et al. (2021b) (Paper A). Roughly four centuries ago, Galileo Galilei (1564–1641) and Giovanni Borelli (1608–1667) were the first to identify that physical stimuli such as changes in applied forces or displacements can alter cellular behavior. Yet, not until the mid 1800s, this ability of biological tissues to adapt in response to mechanical cues was put into a precise statement by the surgeon Henry Gassett Davis (1807–1896) (Davis 1867):

> "... soft tissue, when put under even a moderate degree of tension ... will elongate by the addition of new material; on the contrary, when ... soft tissues remain uninterruptedly in a loose or lax state, they will gradually shorten, as the effete material is removed ...".

About 25 years after Davis came up with his concept which is well-known today under Davis' law, the German anatomist and surgeon Julius Wolff (1836–1902) identified a similar relation for hard tissues (Wolff 1892):

> "... im Gefolge primärer Abänderungen der Form und Inanspruchnahme oder auch bloß der Inanspruchnahme der Knochen [sich] bestimmte, nach mathematischen Regeln eintretende Umwandlungen der inneren Architektur und ebenso bestimmte, denselben mathematischen

> Regeln folgende sekundäre Umwandlungen der äußeren Form der betreffenden Knochen vollziehen ...[1]".

Both Davis and Wolff can be entitled the prime fathers of modern mechanobiology as they identified the essential role of mechanically controlled processes for tissue health and disease.

Roughly another four decades later in the 1920s, Walter Cannon introduced the seminal concept of *homeostasis* (Cannon 1929, 1932), which he defined as "coordinated physiological reactions which maintain most of the steady states in the body". Based on various further computational and experimental studies such as the seminal work of Wolinsky and Glagov (1967), who showed that the tension per medial lamellar unit of the aorta is nearly the same for various mammals of largely differing sizes, the perception arose that soft tissue have the natural tendency to establish and subsequently maintain a preferred mechanical state. Building on this idea and on the concept proposed by Walter Cannon, Brown et al. (1998) introduced the term *tensional homeostasis* in a seminal paper on tissue equivalents about 20 years ago as

> "... the control mechanism by which fibroblasts establish a tension within their extracellular collagenous matrix and maintain its level against opposing influences of external loading."

They showed that cell-seeded collagen gels tend to counteract externally applied loads such that a specific tensional state is restored and therefore preferably maintained.

Since the latter definition already contains the assumption that tension is the target quantity of mechanoregulation, which is, however, not yet clear (e.g., also strain, force, or stiffness are possible candidates), the more general term *mechanical homeostasis* (Humphrey et al. 2014a) will be used within this thesis based on the following definition, which is similar to the one suggested in Eichinger et al. (2021b) (Paper A):

Definition 1

Mechanical homeostasis is an ubiquitous mechanobiological process acting on multiple scales of length and time by which living soft tissues seek to maintain key regulated mechanical variables within a defined tolerance around a preferred value, often called the homeostatic target or set-point.

This definition also accounts for the wise choice by Cannon (1929, 1932) of the prefix "homeo" (from the ancient Greek word "homoios" meaning "similar", thus allowing a tolerance) rather than "homo" (from the ancient Greek word "homos" meaning the "same", not allowing any variation). It is worth pointing out that also other terms such as allostasis (Romero et al. 2009, Evans and Barocas 2009) or rheostasis (Weng et al. 2016) are sometimes used (Eichinger et al. (2021b), Paper A).

As mentioned in the previous chapter, mechanical homeostasis is an essential process to preserve health and proper functionality of living soft tissues. Therefore, both the adaption of the homeostatic target (Fig. 2.1a) (Davies 2016) and its loss (Fig. 2.1b) are closely related to specific diseases (Chovatiya and Medzhitov 2014, Kotas and Medzhitov 2015). Importantly, this

[1] literally translated: "... as a consequence of primary changes in form and usage or even just usage of bones arise specific transformations of the inner architecture according to mathematical rules, and likewise certain secondary transformations of the outer form of the bones according to the same mathematical rules ..."

thesis focuses on mechanobiological regulation of modest perturbations from the normal state, and does not consider effects of emotional stress (McEwen and Wingfield 2010) or the immune system (Wynn et al. 2013, Okabe and Medzhitov 2016) on homeostasis.

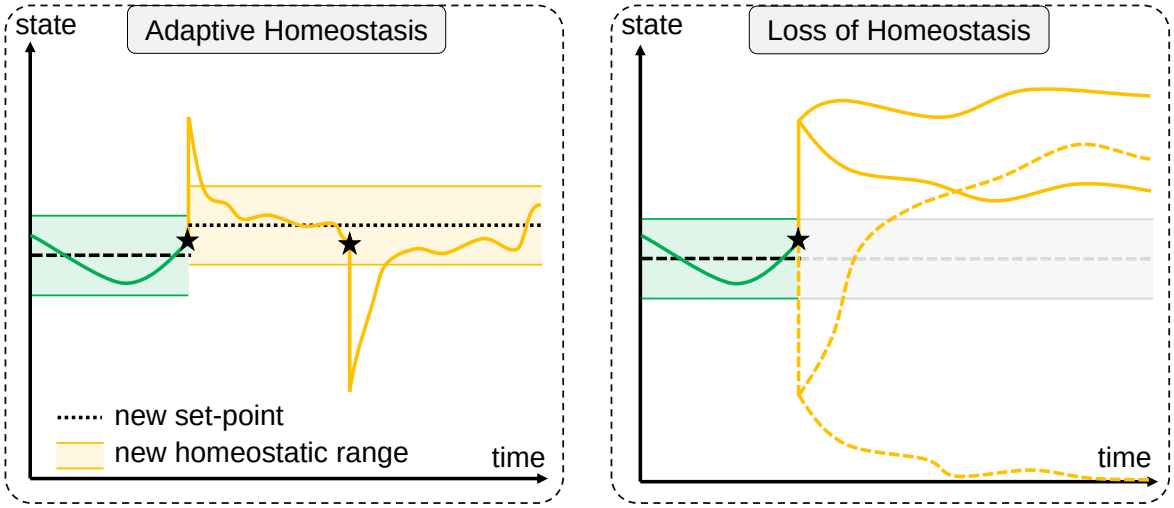

(a) (b)

Figure 2.1: Schematic of adaptive homeostasis (Davies 2016) (a) and loss of homeostasis (b), both being closely linked to specific diseases.

2.2 State of the art: key players in mechanical homeostasis

To be able to both sense mechanical signals and exert forces to control the mechanical properties, cells need to physically interact with their surrounding ECM. Transmembrane linker proteins, so-called integrins, connect the actin cytoskeleton inside the cell to extracellular filaments. These connections form the cornerstone for the control loop consisting of mechanosensing and mechanoregulation. This coupling is responsible for the effect that changes in the mechanical properties of the ECM have been shown to have on essential cellular processes such as cell migration (Grinnell and Petroll 2010, Hall et al. 2016, Xie et al. 2017, Kim et al. 2020), differentiation (Chiquet et al. 2009, Mammoto et al. 2012, Zemel 2015), and even survival (Bates et al. 1995, Schwartz 1995, Zhu et al. 2001, Sukharev and Sachs 2012). At the same time, this connection allows cells to actively regulate the surrounding ECM to maintain a preferred mechanical state within a specific range. The following sections introduce the key players in mechanical homeostasis, namely the ECM (transmitter), cells (effectors), and integrins (sensors) in more detail (Humphrey et al. (2014a), Fig. 2.2).

2.2.1 ECM as transmitter

In contrast to the former assumption that the only task of the ECM is to provide mechanical support, thus to preserve the shape of tissues against loads and offer structural support to the res-

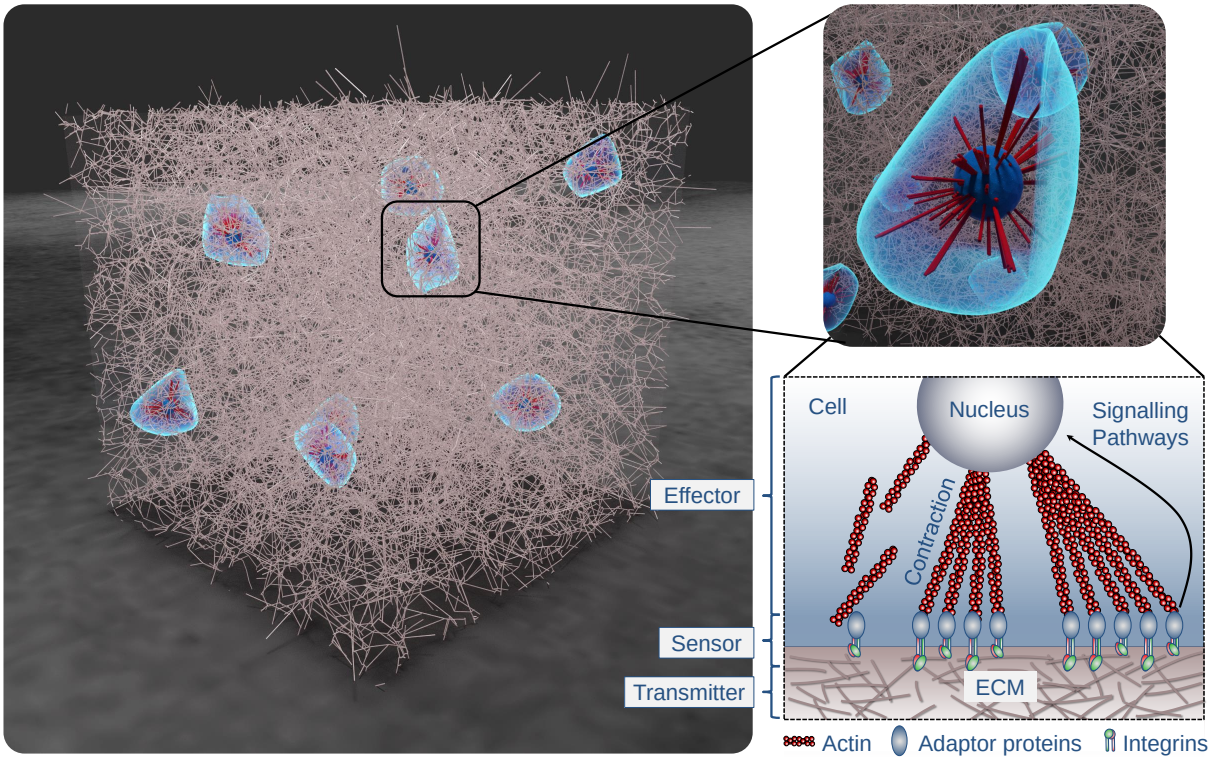

Figure 2.2: Schematic of the key players in mechanical homeostasis of living soft biological tissues: cells (effectors), integrins (the sensors), and the ECM (transmitter).

ident cells, it is known today that the ECM also provides biochemical and biomechanical cues which are essential for many cellular processes and mechanisms (Humphrey et al. 2014a). The ECM is a network of diverse interconnected macromolecules, whose exact composition depends on the specific type of tissue. Despite the large number of proteins which constitute the ECM, three components, namely collagen, elastin, and Glycosaminoglycans (GAGs), are primarily responsible for the ECM's integral mechanical and biomechanical role in mechanical homeostasis (Humphrey et al. 2014a, Theocharis et al. 2016). In the following, these three major components are characterized in more detail.

Collagens Collagen is the most abundant protein in the human body, making up around one third of its entire set of proteins. More than 25 different types have been identified so far, with fibrillar collagen types I and III being the most common (Gautieri et al. 2011, Marino 2016, Theocharis et al. 2016). Collagen fibers are built hierarchically: triple helical collagen molecules (1.5nm in diameter) are regularly staggered to from fibrils (12-500nm in diameter), which can in turn be chemically linked by cross-linking enzymes such as lysyl oxidase (LOX) to from collagen fibers (0.5-20μm in diameter) (Kadler et al. 2007, Humphrey et al. 2014a, Theocharis et al. 2016). Collagen fibrils and fibers provide the ECM with a high material stiffness and strength.

Collagen fibers have a relatively short half-life time of 1-3 month depending on the tissue, which means that extant material is continuously degraded while new fibers are deposited. Cells

(primarily fibroblasts) need to deposit fibers with a certain prestress to ensure tissue homeostasis and avert perturbance of the mechanical equilibrium which would result in an uncontrolled change of the geometry of tissues and therefore in a loss of proper functionality. Besides turnover, cells continuously remodel the collagenous matrix, by either reorienting it or changing the stress-free reference configuration by cross-linking (Humphrey et al. 2014a).

Importantly, collagen fibers have been shown to be mechanosensitive. Fibers that are loaded in tension are more stable against enzymatic degradation compared to fibers that are less loaded or unloaded, presumably due to a reorganization of the enzyme binding sites on stretched fibers (Bhole et al. 2009, Flynn et al. 2010, 2013).

Elastin Elastic fibers form large networks composed of two components: elastin, a cross-linked polymer of tropoelasin, and microfibrils. These networks provide extensibility (elastic fibers can extend up to 150% without failure) and recoil to tissues, both are required, e.g., in blood vessels, lung or heart tissues, because of their exposure to high dynamic stretching loads (Humphrey et al. 2014a). Elastic fibers are assembled and organized at young ages, having very long half-lives (up to 50-70 years in human arteries, Arribas et al. (2006)) and almost no turnover. Therefore, damages to elastic fibers in human adulthood cannot be repaired properly and can thus lead to irreversible mechanical failure and pathologies, such as wrinkles of the skin or stiffening of elastic arteries (Humphrey et al. 2014a, Theocharis et al. 2016).

GAGs GAGs are long, highly negatively charged polysaccharides of high-molecular weight. The exact composition of disaccharides in number and structure depends on the respective type of tissue in the body. GAGs and proteoglycans (PGs) are strongly involved in the maintenance and organization of the ECM since they interact (in complex, not yet understood ways) with various other ECM components such as growth factors, or with receptors on the cell surface via side chains. The latter makes them important players in many cellular processes such as cell signaling, migration and adhesion. Due to their high degree of hydration, they significantly contribute to the compressive stiffness of connective tissues (Humphrey et al. 2014a, Theocharis et al. 2016).

2.2.2 Cells as regulators

Fibroblasts are primarily responsible for maintaining the ECM; they produce elastin, collagen, GAGs, and cross-linking enzymes such as LOX and tissue transglutaminase (tTG), and help to coordinate the assembly of entire functional tissues. Notably, various other types of cells, such as SMCs or macrophages, are also involved in mechanical homeostasis (Humphrey et al. 2014a).

The physical interaction between cells and the ECM is based on the coupling between intracellular structures such as the actomyosin cytoskeleton and the surrounding ECM via transmembrane proteins such as integrins that cluster to form focal adhesions (Cavalcanti-Adam et al. 2007, Lerche et al. 2020). This coupling allows cells to receive mechanical cues from their environment, transduce these cues into intracellular signals, and react, for example, by adapting cellular stress and thereby also the stress of the surrounding ECM. On short time scales (hours to days), mechanical homeostasis is primarily controlled by cell-mediated remodeling, that is, reorganization by cellular contractile forces and cross-linking (Marenzana et al. 2006, Simon et al. 2014, Nam et al. 2016, Kim et al. 2017, Ban et al. 2019). On longer time scales (days to years),

mass turnover, that is degradation and deposition of matrix fibers, dominates connective tissue regulation (Nissen et al. 1978, Nakagawa et al. 1989, Matsumoto and Hayashi 1994, Gineyts et al. 2000).

Notably, the experimental investigation of mass turnover is very difficult, both *in vivo* and *in vitro*. However, at least some level of understanding of the involvement of mass turnover in mechanical homeostasis could be achieved using continuum computational modeling (Humphrey and Rajagopal 2002, Cyron et al. 2014). Crucial factors could be identified, such as the rates of ECM synthesis and removal, the mechanical properties of ECM constituents and the prestress with which these components are deposited (Humphrey et al. 2014a). Especially the latter point is known to be crucial to ensure tissue homeostasis. Yet, it is largely unknown to date how cells are able to deposit new fibers with exactly the right prestress.

2.2.3 Integrins as sensors

Cells can attach to their extracellular fibrous microenvironment via transmembrane linker proteins, the so-called integrins (Roca-Cusachs et al. 2012). These are in turn connected to the intracellular contractile apparatus consisting of actin and myosin, which enables cells to actively apply forces to their surrounding matrix. These connections are known as cell-matrix adhesion complexes or as *molecular clutch* systems (Mitchison and Kirschner 1988), and usually consist of (Elosegui-Artola et al. 2018)

1) actin filaments,
2) myosin motors, which can bind to actin fibers to form contractile stress fibers,
3) adaptor proteins (such as talin or vinculin),
4) transmembrane proteins such as integrins,
5) and binding sites/ligands on fibers of the ECM.

The lifetime of the bond between integrins and the ECM ligand has been shown to follow a catch-slip bond behavior, that is, an increasing force acting on such a bond first stabilizes the bond before destabilizing it when the pulling force exceeds a certain threshold (Kong et al. 2009, Chen et al. 2012).

The physical interaction between a cell and the surrounding ECM typically happens as follows. Integrins bind to the ECM with a certain probability. If some clutches are bound and actin stress fibers contract, the ECM, if compliant, is deformed. Depending on the stiffness of the ECM, the resulting forces acting on all engaged bonds influence their lifetime. Growing cellular contraction increases these forces, which eventually leads to the failure of some of them, which in turn can lead to a catastrophic event which quickly dissolves all bonds a the same time (Elosegui-Artola et al. 2018). A new cycle consisting of adhesion first, then contraction and finally disengagement can start, which has been shown experimentally in focal adhesions (Plotnikov et al. 2012) or leading edges of fibroblasts (Pontes et al. 2017).

The stiffness of the cellular microenvironment influences this process primarily by modifying the loading rate, i.e. the rate at which forces build in engaged clutches, which is therefore often designated as a driving factor for cellular clutch mechanosensitivity (Chan and Odde 2008, Elosegui-Artola et al. 2018). On substrates with a low stiffness, forces in engaged clutches build

up slower due to some form of buffering effect resulting from the deformation of the ECM, which decreases the loading rate, which may lead to disengagement of clutches before higher forces are achieved. At high substrate stiffnesses, clutch forces build up faster than new bonds can form. In this regime, which is often referred to as *frictional slippage*, unbinding rates become higher than binding rates, which also impedes the build-up of high focal adhesion forces (Fournier et al. 2010). Thus, there exists a regime in between these extremes in which force transmission is maximal (Bangasser et al. 2013).

In summary, the loading force sensitivity of integrins can be assumed as a key factor determining the response of a cell-matrix adhesion complex (Cui et al. 2015, Jiang et al. 2016, Nguyen et al. 2017). It is influenced by both external factors such as the ECM stiffness or ligand density and internal factors such as cellular contraction rate or integrin binding dynamics (Humphrey et al. 2014a, Elosegui-Artola et al. 2018).

Several further studies have analyzed the influence of mechanical cues and stimuli on the behavior of various cell types such as fibroblasts or SMCs. These cells have been shown to spread more, develop larger focal adhesions and higher traction forces on stiffer substrates compared to more compliant substrates (Elosegui-Artola et al. 2014, Zhu et al. 2016). Furthermore, adhesions based on integrins have been shown to strengthen and stabilize with force (Bershadsky et al. 2003, Moore et al. 2010). Moreover, it has been shown that there exists a certain range of the substrate stiffness in which cell migration is maximal, with lower migration speeds at both lower and higher stiffnesses, therefore describing a biphasic dependence on stiffness (Peyton and Putnam 2005, Bangasser et al. 2013). If cells are put in substrates that have a gradient in stiffness, cells tend to migrate towards the stiffer region (Lo et al. 2000).

The idea of molecular clutches controlling mechanical homeostasis is based on the assumption that changes in forces (or loading rates) alter protein confirmation or the kinetics of assembly and disassembly of complexes of proteins (Humphrey et al. 2014a). Experimental studies of single molecules have shown that e.g. talin unfolds under load, which allows the actin binding protein vinculin to anchor (Patel et al. 2006, del Rio et al. 2009), which in turn stabilizes the link between actin and integrins (Grashoff et al. 2010, Dumbauld et al. 2010).

It is worth mentioning that beside integrins, other proteins have been shown to play a role in cellular mechanosensing, such as the aforementioned talin and vinculin (Ziegler et al. 2008, Grashoff et al. 2010, Carisey et al. 2013, Dumbauld et al. 2013, Das et al. 2014, Yao et al. 2014, Austen et al. 2015, Davidson et al. 2015, Truong et al. 2015, Yao et al. 2016, Zhu et al. 2016, Ringer et al. 2017). Malfunction of just one of the participating components can lead to altered cellular sensing, which in turn can alter mechanical regulation and therefore often results in pathologies.

2.3 Experimental study

Although great advances have been made in the past decades that led to the understanding of mechanobiology and homeostasis as presented in the previous section, the biophysical and micromechanical principles are to a large extent still not understood (see Section 1 or Eichinger et al. (2021b), Paper A). As mentioned before, one major effort of this thesis is an experimental study with tissue equivalents. Since much more can be learned using such model systems, the presented thesis develops the first biaxial testing device for such tissue model systems (Eichinger

et al. (2020), Paper B). This device is then used to discuss biophysical conclusions that can be drawn from the newly obtained results. The following section introduces the chosen experimental approach and its respective methods.

2.3.1 Experimental approach

Since mechanobiology and homeostasis can only be observed in living biological system in which it is difficult to adjust and control specific parameters (such as cell and fiber density, the composition of different cell and fiber types, presence of growth factors), cell-seeded tissue equivalents have been used as simple but powerful living biological systems in which both biochemical and mechanical conditions can be precisely controlled. Tissue culture studies focusing on mechanobiology can be categorized by the mechanical boundary conditions that are applied to the gel samples during an experiment. With increasing complexity, free-floating (mostly circular) and uniaxially or biaxially constrained, extended, or released cell-seeded gels have been used in the past (Fig. 2.3). This section briefly summarizes the most important observations that were made in such experiments so far. A thorough review can be found in Eichinger et al. (2021b) (Paper A).

Since being the easiest to test, circular free-floating gels have been studied experimentally first (Bell et al. 1979). As elucidated in the previous section, cells attach to matrix fibers in their surrounding via transmembrane proteins such as integrins and probe the matrix by applying contractile forces. This behavior leads in unconstrained gels to a strong compaction over multiple days in culture (Fig. 2.3a, Simon et al. (2012, 2014)).

Studies of cell-seeded gels whose compaction is prevented in one (data available in the literature) or two (new data presented in this thesis) directions by boundary constraints (Fig 2.3b,c) typically show two very distinct phases regarding the tensile state that develops in the tested gels (and is typically measured by force transducers): First, tension in the gels rapidly increases to a specific value (phase I), the so-called homeostatic tension, at which it then remains largely constant (phase II) with neither further increase nor decrease (Fig. 2.4). Both the time at which the steady state is achieved and its level have been shown to be influenced by various factors, including the cell type, tissue type, and the presence of growth factor such as TGF-β1 (Brown et al. 1998, 2002, Sethi et al. 2002, Campbell et al. 2003, Dahlmann-Noor et al. 2007, Karamichos et al. 2007, Ezra et al. 2010, Courderot-Masuyer 2017).

To examine if and how mechanical homeostasis arises in tissue equivalents, gels were uniaxially perturbed from the steady state in phase II, for example, by an externally imposed deformation that was applied in a step-like manner to the ends of the gels. Interestingly, cells appeared to promote the restoration of the homeostatic state, both if gels were rapidly stretched or released (Fig. 2.5, Brown et al. (1998), Ezra et al. (2010)). However, the available data so far only allows a vague assessment if the state before the mechanical stimulus is restored, since no data are available of the new steady that eventually develops.

Finally, tissue culture experiments have shown that part of the cell-mediated matrix reorganization is inelastic, which means that a significant residual tension can be measured in the gels after active cellular forces are eliminated, e.g., by induced cell lysis (Fig. 2.6, Marenzana et al. (2006), Simon et al. (2012, 2014)). This tension is often referred to as residual matrix tension.

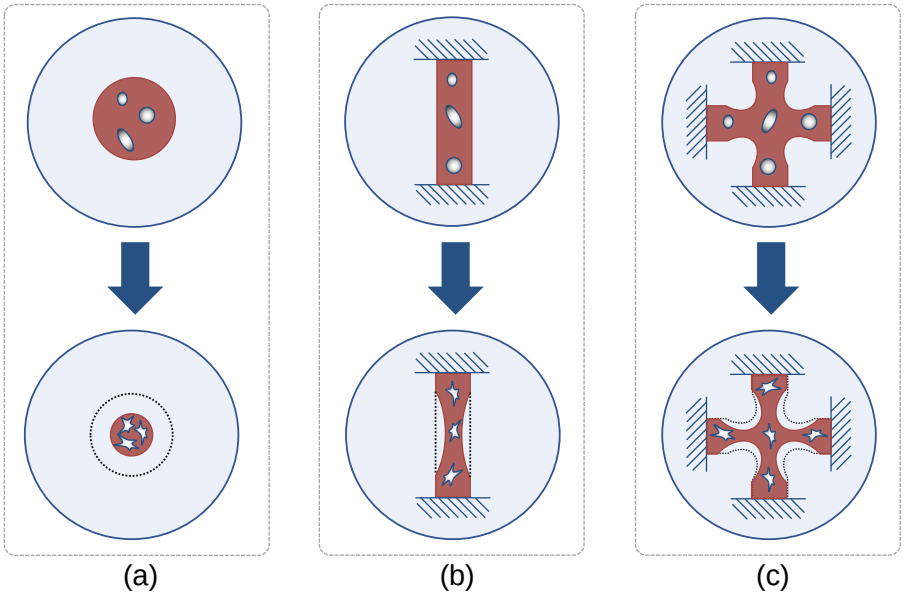

Figure 2.3: Schematic of cell-mediated matrix compaction in free-floating (a), unaxially constrained (b), and biaxially constrained (c) cell-seeded tissue equivalents. Starting from an initial geometry (top row), cells spread and attach to surrounding collagen fibers; cellular retraction leads to changes in the geometry of the observed sample (bottom row).

As mentioned before, a major contribution of this thesis is the introduction, validation and use of the first biaxial bioreactor for cell-seeded tissue equivalents. The following two sections introduce the corresponding experimental methods.

2.3.2 Cell culture

Before cells can be studied in tissue culture experiments, they need to be extracted and then cultured to reach a sufficiently large number. Depending on the type of cell that is used, different approaches need to be followed as presented in the following.

2.3.2.1 NIH/3T3 fibroblasts

NIH/3T3 cells stem from an immortalized cell line which was created in the 1960s from mouse embryo tissue. As cells from this line are simple to handle compared to primary cells, they represent a standard cell line used in many *in vitro* studies.

NIH/3T3 fibroblasts (ATCC) are cultured using a protocol modified from Simon et al. (2012, 2014). Briefly, after thawing, cells are maintained in T75 flasks (ThermoFisher) containing Dulbeccos modified Eagles medium (DMEM) (Gibco, Life Tech-nologies, D5796) substituted with 10% heat-inactivated fetal bovine serum (FBS) (Gibco, Life Technologies) and 1% penicillin-streptomycin (ThermoFisher). The flasks are placed inside a cell culture incubator at 37°C , 5% CO_2 and ∼95% humidity. Cells are passaged at 70-80% confluence. Medium is changed every other day. Passages 4 and 5 are used in experiments (Eichinger et al. (2020), Paper B).

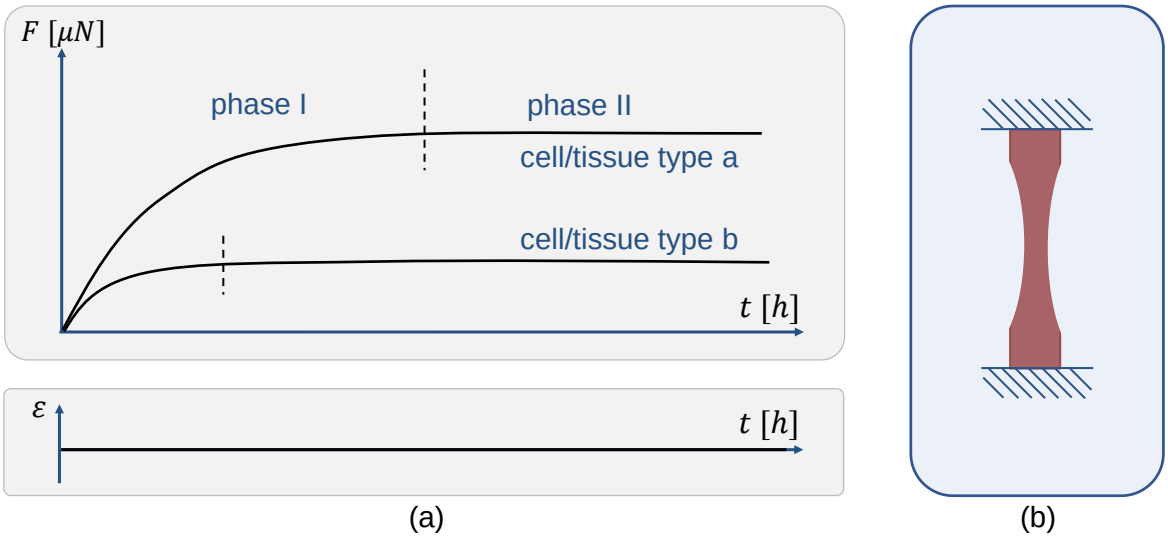

Figure 2.4: (a) Tension (in the range of 0-1000μN) establishes (within a couple of hours) in two characteristic phases in uniaxially constrained tissue equivalents (b): a steep increase (phase I) is followed by a plateau (phase II) (Brown et al. 1998, Ezra et al. 2010). Depending on the type of cell (e.g. fibroblast or smooth muscle cell) and the type of tissue the tested cells were extracted from, different levels of homeostatic tension are reached. Moreover, phase II is reached at different time points.

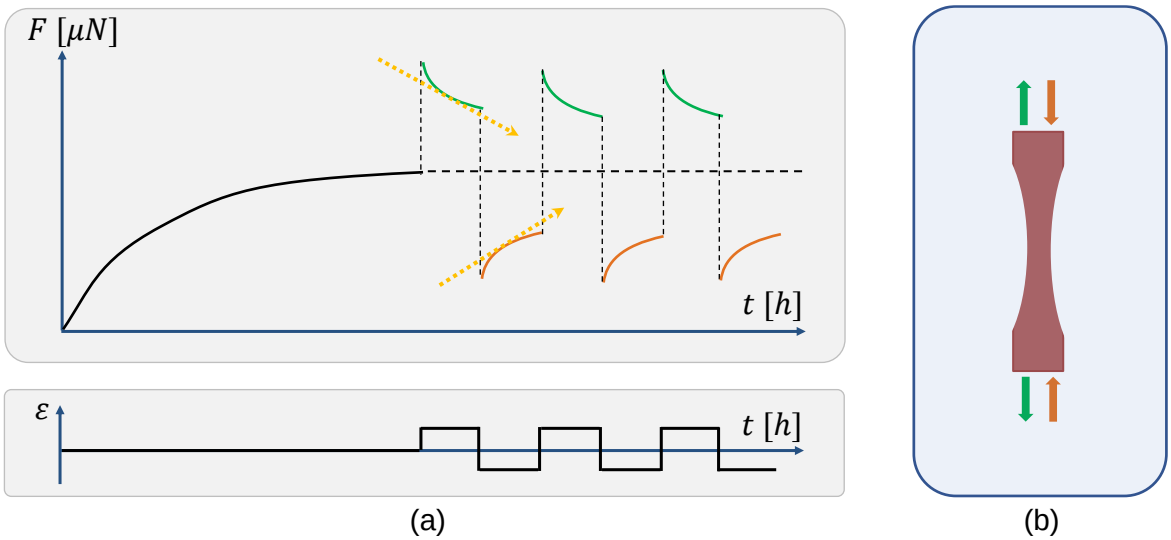

Figure 2.5: If a tissue equivalent is suddenly stretched or released (see positive and negative jump in force F in (a), respectively); the externally applied load is shown in the bottom row of (a). After having reached the homeostatic plateau state, tension in the gel returns toward its value prior to the perturbation. However, the range around the set-point to which the tension returns is unknown.

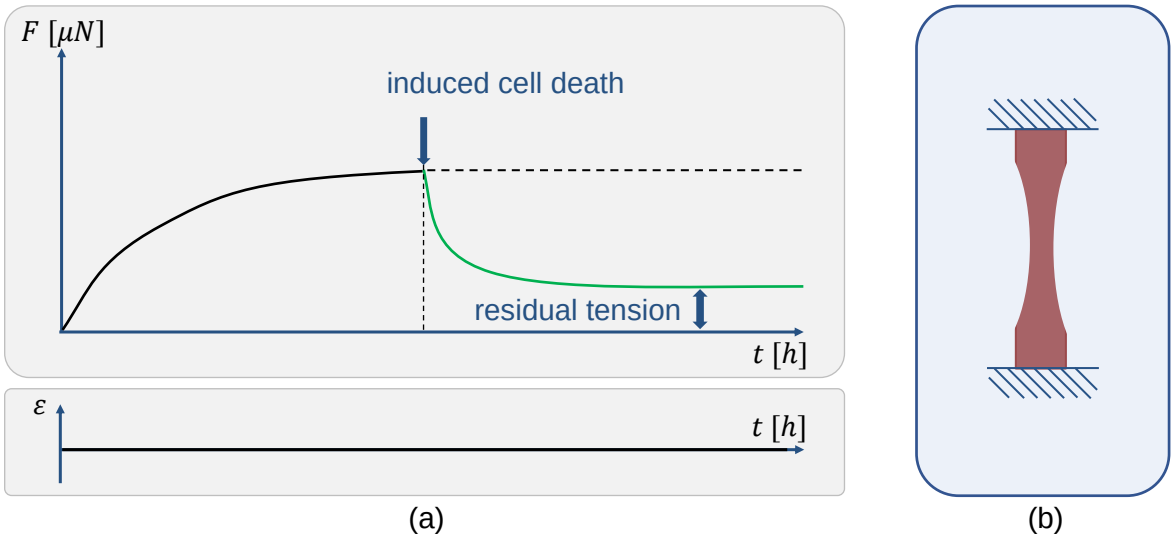

Figure 2.6: If active cellular forces are removed from uniaxially constrained gels (b), e.g., via cell lysis, a fraction of the homeostatic tension remains in the gel as a so-called RMT (Marenzana et al. 2006) (b). This implies that part of the cell-mediated matrix remodeling is inelastic.

2.3.2.2 Primary cells

Primary cells are isolated from 13-15 week old male C57BL/6 wild-type mouse aortas. Fig. 2.7 shows the process of the isolation of primary cells. Adventitia and media, two of the main layers of the aorta, are digested separately to isolate SMCs from the media and fibroblasts from the adventitia. Cells are extracted from the the descending, suprarenal, and infrarenal aorta because of their identical mesoderm embryonic lineage (Majesky 2007). Directly after cell extraction, cells are grown in one well of a 6-well plate before being transferred to a T25 flask in passage 1. In passages 2 and 3, cells are grown in T75 flasks. All flasks are coated with fibronectin or collagen prior seeding to facilitate cellular adhesion. The culture medium is changed every other day. Cells were passaged at 70-80% confluence roughly every 6 days.

SMCs are maintained in culture medium consisting of DMEM, 20% heat-inactivated FBS, and 1% penicillin-streptomycin in an incubator at $37°$C and 5% CO_2.

Fibroblasts are treated with the same medium, enriched, however, with fibroblast growth factor FGF-2 (Sigma, USA) owing to their poor proliferation rate. Concentrations of FGF-2 ranging from from 5-50ng/mL were tested. 15ng/mL was found to lead to similar proliferation rates between fibroblasts and SMCs and was therefore used.

As soon as cells have reached a sufficiently large number in passage 3, they are frozen in liquid nitrogen to preserve them for experiments at later points in time. To this end, they are re-suspended in medium containing 20% FBS substituted with 10% dimethylsulfoxid to inhibit the formation of ice crystals with a density of 2 million cells per ml. Cryovials containing 1ml of the resulting cell suspension are then first slowly cooled down to -80°C before being transferred to a liquid nitrogen container.

6 days prior to an experiment, 4 million cells are thawed and cultured in two T75 flasks coated with collagen type I (Corning, USA) instead of fibronectin to already accustom the cells to collagen. Culture medium containing 10% FBS is used for SMCs and medium with 10% FBS and 15ng/mL FGF-2 is used for fibroblasts. Passages 4 and 5 are used in all experiments. Cells are starved in medium containing 2.0% FBS for 24h prior to the experiments to inhibit proliferation during the experiments.

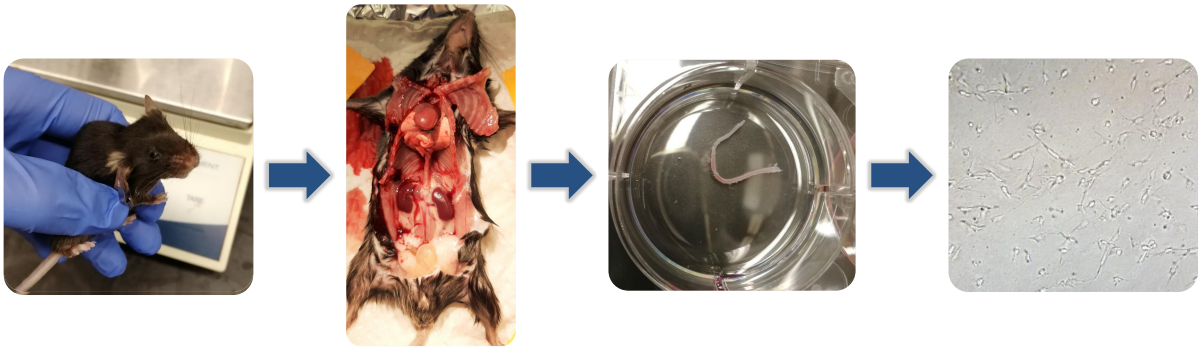

Figure 2.7: Consecutive steps performed during extraction of primary murine aortic fibroblasts and SMCs. First, mice are taken care of until they reach the desired age (13-15 weeks herein). They are then euthanized, cut open and dissected to extract the aorta. The aorta is then digested to isolate the cells.

2.3.3 Preparation of tissue equivalents

Cell-seeded collagen gels are prepared using a protocol modified from Simon et al. (2012, 2014). A detailed step by step instruction is given in Appendix G. Due to unavoidable changes in the concentration of the purchased collagen (range: 8-11mg/ml), the exact amount of each constituent of the gel needs to be adjusted to reach the same final concentration of collagen in each gel. To make 7.0ml of gel solution (volume of the biaxial mold is ∼6.5ml) with a final collagen concentration of 1.0 mg/ml and a cell density of 0.5×10^6 cells/ml assuming an initial concentration of 8.22mg/ml of type I rat tail collagen (Corning), 1.43ml of 5x DMEM, 0.68ml of a 10x reconstitution buffer (0.1N NaOH and 20mM HEPES; Sigma), and 0.79ml of type-I rat tail collagen need to be mixed with 4.1ml of experimental culture medium containing $3.5\cdot10^6$ cells. A Neubauer chamber in combination with trypan blue staining is used to count cells. The experimental culture medium consists of DMEM supplemented with 2.0% FBS and 1% penicillin-streptomycin (Eichinger et al. (2020, 2021c), Paper B, Paper D).

The final gel solution is pipetted into the uniaxial or biaxial mold that is already placed in the center of the bioreactor. After 30-45min in which the gel is allowed to set, the bath is filled with 80ml of the respective experimental culture medium. This leads to a detachment of the gel from the base of the bath. Subsequently, a time period of 15min needs to be awaited to allow the bioreactor to re-establish the required environmental conditions such as temperature and humidity, since the force transducers react to them very sensitively. The experiments can last up to 48h to ensure that enough nutrients are available at all times, and to avoid contamination, e.g., by bacteria or fungi.

2.4 Computational modeling

In addition to the experimental study, a second major effort of this thesis is the development, validation and application of a computational model that allows the simulation of mechanobiological processes in living soft tissues. In the following, the chosen modeling approach and the respective underlying methods are introduced.

2.4.1 Modeling approach

As mentioned before, there is a pressing need for a micromechanical computational framework that allows the simulation of three-dimensional cell-matrix interactions, because these build the cornerstone for mechanical homeostasis. Driven by the shortcomings of existing computational models, the following requirements were used to select an appropriate numerical model:

1) The computational framework should contain models for all key players in mechanical homeostasis as presented in Section 2.2, that is, for individual cells, fibers and integrins, especially considering that homeostasis fundamentally arises at the interface of cells and fibers.

2) Processes acting within a couple of seconds (such as binding and unbinding of integrins (Kong et al. 2009) should be resolved. Moreover, simulations of physical time intervals of a couple minutes should be possible within a reasonable amount of time.

3) The computational framework should allow the simulation of systems consisting of multiple cells interacting at the same time with a three-dimensional fibrous matrix.

Based on these requirements, a decision has to be made regarding the spatial resolution of the employed modeling approach, keeping in mind that spatial resolution and efficiency are competing parameters. Modeling the ECM on the level of single atoms or molecules using laws of quantum mechanics or molecular dynamics would predict the overall system behavior very well, is, however, unfeasible due to the resulting large system sizes (huge number of degrees of freedom). Since the length scale of fibers and cells is much larger than the one of single atoms, system sizes can be largely reduced by simply modeling these microstructural components of soft tissues as continua (Cyron 2011). Previous work on biopolymer networks has shown that their mechanical behavior can be modeled well when single fibers (typically a couple of microns in length) are modeled as continua (Lindström et al. 2010, Cyron and Wall 2012, Cyron et al. 2013a,b, Müller et al. 2014, 2015, Ban et al. 2019). Especially useful in this regard are one dimensional Cosserat continua in combination with classical beam models from structural mechanics. This is also the approach of this thesis (Fig. 2.8).

As shown in Section 2.2, the predominant protein in mammals is fibrillar collagen. Collagen fibrils are usually $\sim$10μm long with a diameter of 50-500nm. Using these values, a slenderness ratio of 10-100 can be computed. Therefore, individual fibers are discretized using geometrically exact beam finite elements based on the non-linear Simo-Reissner theory (Reissner 1981, Simo 1985, Simo and Vu-Quoc 1986, Jelenić and Crisfield 1999). This beam theory captures the modes of axial tension, torsion, bending, and shear deformation and is appropriate for large deformations (in contrast to simpler beam models such as the Euler-Bernoulli beam model or

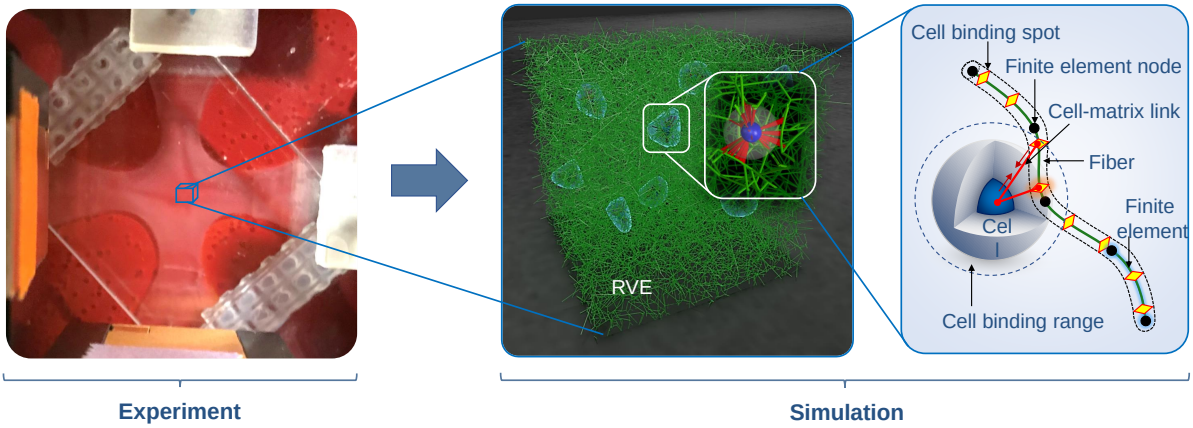

Figure 2.8: The cruciform-shaped cell-seeded collagen gels used in the experiments (left) build a fibrous microstructure in which the cells reside. The latter are attached to the fibers by focal adhesions via transmembrane receptors such as integrins (middle). Collagen fibers, cells and cell-fiber links are simulated using a discrete fiber network model based on the finite element method in a representative volume element (middle, right). Individual collagen fibers are modeled as one-dimensional Cosserat continua and discretized by geometrically exact beam finite elements based on the non-linear Simo-Reissner theory (right). Cells can form cell-matrix links to predefined binding spots on the matrix fibers.

Timoshenko beam model). Usually when modeling such slender structures, external forces and moments, stochastic forces and moments, and viscous forces and moments resulting from the viscous fluid need to be considered in addition to the internal, elastic forces and moments. When comparing the magnitude of stochastic stresses which is in the order of $0.01\text{pN}/\mu m^{-2}$ (Cyron and Wall 2012) with the magnitude of cellular contractile stresses which is in the order of $1000\text{pN}/\mu m^{-2}$ (Moore et al. 2010), it appears reasonable to neglect stochastic forces. Moreover, individual collagen fiber segments within a network are usually much smaller than their persistence length L_p=39μm (Grill et al. 2021).

2.4.2 Mechanical network model and discretization

As mentioned before, collagen fibers can be interpreted as rod-like slender continua, because their axial extension dominates over their lateral extension. This allows to assume the Bernoulli hypothesis, that is, to model the cross sections of these slender fibers as undeformable. Such continua can be mathematically described as one-dimensional Cosserat continua immersed in the three-dimensional space $\mathbb{R}^3$ (Cyron 2011). The following part is a brief recapitulation of the methods presented in Cyron (2011), Cyron and Wall (2012), Müller (2014), and Grill (2020) on which the novel computational framework presented in this thesis (Eichinger et al. (2021a), Paper C) builds upon. These references will not be named explicitly anymore in the following.

Every physically possible configuration of a slender body with length L at a certain point in time t can be uniquely described in $\mathbb{R}^3$ by the position of each point of the neutral line (which passes through the centroids of the cross sections of the body), and the orientation of the (plane) cross section corresponding to each of theses points. Therefore, at each point, three translational

and three rotational degrees of freedom are required and sufficient to uniquely describe a certain configuration of the slender continuum. If one assumes that the arc-length parameter $\xi \in [0; L]$ describes every point of the neutral line, also referred to as the centerline, then the deformation of this line in the time interval $[0; T]$ can be described by the function

$$\boldsymbol{r} : [0; L] \times [0; T] \to \mathbb{R}^3,\ (\xi, t) \mapsto \boldsymbol{r}(\xi, t), \tag{2.1}$$

in which $\boldsymbol{r}(\xi, t)$ maps ξ to the time-dependent position in $\mathbb{R}^3$. Analogously, a time dependent, vector-valued function can be defined that maps the orientation of the corresponding cross section to its time-dependent orientation:

$$\boldsymbol{\theta} : [0; L] \times [0; T] \to \mathbb{R}^3,\ (\xi, t) \mapsto \boldsymbol{\theta}(\xi, t). \tag{2.2}$$

Herein, the rotation $\boldsymbol{\theta}(\xi, t)$ represents a so-called pseudo-vector, whose orientation in $\mathbb{R}^3$ represents the axis of rotation, whereas its L^2-norm defines the angle of rotation. Importantly, two pseudo-vectors cannot be added such as normal vectors, which is to a great extent responsible for the inherent complexity when using geometrically exact beam theory.

To be able to describe the deformation and motion of a fiber, both boundary and initial data are required to be able to compute a unique solution of the corresponding initial boundary value problem. With sensible boundary conditions at $\xi = 0$ and $\xi = L$ and the initial, stress-free configuration at $t = 0$ being

$$\boldsymbol{r}^0 : [0; L] \times [0; T] \to \mathbb{R}^3,\ (\xi, t) \mapsto \boldsymbol{r}^0(\xi, 0), \tag{2.3}$$

$$\boldsymbol{\theta}^0 : [0; L] \times [0; T] \to \mathbb{R}^3,\ (\xi, t) \mapsto \boldsymbol{\theta}^0(\xi, 0), \tag{2.4}$$

both the translation $\boldsymbol{r}$ and the rotation $\boldsymbol{\theta}$ can be determined from the balance of linear and angular momentum, that is from

$$\boldsymbol{f}_{elastic}(\boldsymbol{r}, \boldsymbol{\theta}, \xi, t) + \boldsymbol{f}_{viscous}(\boldsymbol{r}, \boldsymbol{\theta}, \xi, t) = \boldsymbol{f}_{external}(\boldsymbol{r}, \boldsymbol{\theta}, \xi, t) \tag{2.5}$$

and

$$\boldsymbol{m}_{elastic}(\boldsymbol{r}, \boldsymbol{\theta}, \xi, t) + \boldsymbol{m}_{viscous}(\boldsymbol{r}, \boldsymbol{\theta}, \xi, t) = \boldsymbol{m}_{external}(\boldsymbol{r}, \boldsymbol{\theta}, \xi, t) + \boldsymbol{r}'(\xi, t) \times \boldsymbol{f}_s(\boldsymbol{R}.\boldsymbol{\theta}, \xi, t), \tag{2.6}$$

Herein, all quantities represent line loads, thus forces are forces per unit length, and moments are moments per unit length. The integral of the internal stresses defines the elastic section force $\boldsymbol{f}_s$ which results in a moment that can be computed using the tangent of the centerline $\boldsymbol{r}'(\xi, t) := \partial \boldsymbol{r}(\xi, t)/\partial \xi$.

It is worth mentioning again that both inertia and stochastic forces based on Brownian dynamics can be neglected for collagen fibers.

Elastic forces and moments As mentioned above, the vector $\boldsymbol{\theta}$ can be used to describe finite rotations in $\mathbb{R}^3$. As two consecutive rotations cannot be expressed by the addition of two of such vectors, they are usually referred to as *pseudo*-vectors. As an alternative, a corresponding

orthonormal rotation matrix $\boldsymbol{R}(\boldsymbol{\theta}) \in SO(3)$ can be used, which can be computed according to Rodrigues' formula

$$\boldsymbol{R}(\boldsymbol{\theta}) = \mathbf{1} + \frac{\sin\|\theta\|}{\|\theta\|}\boldsymbol{S}(\boldsymbol{\theta}) + \frac{1-\cos\|\theta\|}{\|\theta\|}\boldsymbol{S}(\boldsymbol{\theta})\boldsymbol{S}(\boldsymbol{\theta}) \tag{2.7}$$

with the skew-symmetric spin tensor

$$\boldsymbol{S}(\boldsymbol{\theta}) = \begin{pmatrix} 0 & -\theta_3 & \theta_2 \\ \theta_3 & 0 & -\theta_1 \\ -\theta_2 & \theta_1 & 0 \end{pmatrix}. \tag{2.8}$$

Importantly, the i-th column of $\boldsymbol{R}$ represents the i-th base vector of the triad field which corresponds to the principal directions of the respective cross section. The major advantage when using rotation matrices is the possibility to express two consecutive rotations by the product of two rotation matrices.

The elastic forces according to the three-dimensional beam equations of the Reissner theory can then be computed according to

$$\boldsymbol{f}_{elastic} = \frac{\partial}{\partial\xi}\left\{\boldsymbol{R}(\boldsymbol{\theta})\boldsymbol{C_F}\left[\boldsymbol{R}(\boldsymbol{\theta})^{\boldsymbol{T}}\boldsymbol{r'} - \boldsymbol{R}(\boldsymbol{\theta^0})^{\boldsymbol{T}}\boldsymbol{r'^0}\right]\right\}, \tag{2.9}$$

with

$$\boldsymbol{C_F} = \begin{pmatrix} EA & 0 & 0 \\ 0 & GA_2 & 0 \\ 0 & 0 & GA_3 \end{pmatrix}. \tag{2.10}$$

The elastic moments read

$$\boldsymbol{m}_{elastic} = \frac{\partial}{\partial\xi}\left\{\boldsymbol{R}(\boldsymbol{\theta})\boldsymbol{C_M}\left[\boldsymbol{\kappa}_{loc} - \boldsymbol{\kappa}^0_{loc}\right]\right\}, \tag{2.11}$$

with

$$\boldsymbol{C_M} = \begin{pmatrix} GI_r & 0 & 0 \\ 0 & EI_2 & 0 \\ 0 & 0 & EI_3 \end{pmatrix} \tag{2.12}$$

and

$$\boldsymbol{S}(\boldsymbol{\kappa_{loc}}) = \boldsymbol{R}(\boldsymbol{\theta})^T\boldsymbol{R}'(\boldsymbol{\theta}), \quad \boldsymbol{S}(\boldsymbol{\kappa}^0_{loc}) = \boldsymbol{R}(\boldsymbol{\theta}^0)^T\boldsymbol{R}'(\boldsymbol{\theta}^0). \tag{2.13}$$

$\boldsymbol{\kappa}_{loc}$ and $\boldsymbol{\kappa}^{\mathbf{0}}_{loc}$ are the curvature vectors in the current local coordinate system and in the reference configuration, respectively.

Values for the torsional rigidity GI_r, the bending rigidities EI_2 and EI_3, the axial rigidity EA, and the shear rigidities GA_2 and GA_3 can be either directly obtained from experimental studies, or computed from geometrical dimensions and constitutive parameters such as the Young's modulus E, the shear modulus G, and the Poisson's ratio ν. The cross sectional area is given by A, or when being multiplied with a shear correction factor for circular cross sections, $A_2 = A_3$.

Viscous forces and moments Collagen fibers are, *in vivo*, immersed in the extracellular fluid, which damps the motion of the filaments. This can be simply modeled by velocity-dependent drag-laws (Cyron and Wall 2012, Müller 2014):

$$\boldsymbol{f}_{viscous} = \boldsymbol{D}_t \dot{\boldsymbol{r}}, \tag{2.14}$$

$$\boldsymbol{m}_{viscous} = \boldsymbol{D}_r \dot{\boldsymbol{\theta}}. \tag{2.15}$$

$\boldsymbol{D}_t$ and $\boldsymbol{D}_r$ are the damping matrices for translational and rotational damping, respectively. These matrices can be expressed with respect to the principal axes of a segment according to

$$\boldsymbol{D}_{t,loc} = \begin{pmatrix} \gamma_\parallel & 0 & 0 \\ 0 & \gamma_\perp & 0 \\ 0 & 0 & \gamma_\perp \end{pmatrix}, \quad \boldsymbol{D}_{r,loc} = \begin{pmatrix} \gamma_a & 0 & 0 \\ 0 & 0 & 0 \\ 0 & 0 & 0 \end{pmatrix}. \tag{2.16}$$

Herein, the damping constants per unit length for translations perpendicular and parallel to the axis of a segment with a circular cross section of radius r, and for the rotation around the axis of a segment with a circular cross section of radius r are used. These are defined as follows:

$$\gamma_\perp = 4\pi\eta, \quad \gamma_\parallel = 2\pi\eta, \quad \gamma_a = 4\pi\eta r^2. \tag{2.17}$$

Considering the orientation of a segment in $\mathbb{R}^3$, the damping matrices can be computed according to

$$\boldsymbol{D}_t = \boldsymbol{R}\boldsymbol{D}_{t,loc}\boldsymbol{R}^T, \quad \boldsymbol{D}_r = \boldsymbol{R}\boldsymbol{D}_{r,loc}\boldsymbol{R}^T. \tag{2.18}$$

Weak form Finally, the weighted-residual forms of Eq. (2.5) and Eq. (2.6) for the finite element discretization can be given by

$$\int_0^L w_r \boldsymbol{f}_{elastic} d\xi + \int_0^L w_r \boldsymbol{f}_{viscous} d\xi = \int_0^L w_r \boldsymbol{f}_{external} d\xi, \tag{2.19}$$

$$\int_0^L w_\theta \boldsymbol{m}_{elastic} d\xi + \int_0^L w_\theta \boldsymbol{m}_{viscous} d\xi = \int_0^L w_\theta \boldsymbol{m}_{external} d\xi + \int_0^L w_\theta \boldsymbol{r}' \times \boldsymbol{f}_s d\xi. \tag{2.20}$$

Chapter 3

Experimental study

3.1 Introduction

Driven by the pressing need for a more detailed understanding of mechanobiology while at the same time considering the difficulties of *in vivo* experiments arising from the complex composition of native ECM (of various fiber types and substances), studies with gel-based tissue equivalents have been designed and improved over the past decades. These simple *in vitro* model systems – typically cell-seeded collagen or fibrin gels – have less degrees of freedom and therefore interdependencies, which makes them expedient for precise quantitative studies of mechanobiological processes arising at the interface of cells and ECM.

This chapter forms the first major effort of this thesis by investigating mechanical homeostasis experimentally using tissue equivalents. The chapter first reviews the state of the art in this field by summarizing observations made so far regarding the development and control of a preferred tensional state in tissue equivalents (Eichinger et al. (2021b), Paper A). Although the reviewed studies have significantly contributed to our current understanding of mechanobiology, they nevertheless suffer from severe shortcomings, such as the restriction to uniaxial loading cases only. Hence, a novel custom-built biaxial bioreactor is developed and presented next in this chapter (Eichinger et al. (2020), Paper B). The article contains a detailed description of the general set-up of the new device (also see Appendix F) and briefly highlights its most important features. Subsequently, some studies with NIH 3T3 fibroblasts are presented deemed for validation of the device. Finally, novel data regarding the active response of cell-seeded collagen gels subject to various multiaxial boundary conditions are provided.

Finally, this chapters presents a simple theoretical analysis on the quantitative differences between uniaxially and biaxially constrained gels and compares the behavior of gels seeded with either primary fibroblasts or primary SMCs.

3.2 Paper A: Mechanical homeostasis in tissue equivalents: a review

3.2.1 Summary

The origins of mechanobiology and thereby the perception that the physiology of living biological systems is to a large extent controlled by mechanical factors goes back roughly four centuries to the times of Galileo Galilei and Giovanni Borelli. A milestone in the history of mechanobiology was the pioneering work of Cannon (1929, 1932), who introduced the concept of homeostasis as "coordinated physiological reactions which maintain most of the steady states in the body". Driven by advances in the experimental techniques over the following decades, especially *in vitro* studies (Brown et al. 1998, Ezra et al. 2010) have contributed to the understanding that cells probe and regulate the mechanical properties of tissues around a preferred state when experiencing an external mechanical perturbation. This unique ability is nowadays often referred to as tensional or mechanical homeostasis. Since being more general, mechanical homeostasis is preferable, which this article defines as

> "a ubiquitous mechanobiological process by which soft tissues seek to maintain key regulated variables within a range near a preferred value, often called a homeostatic target or set-point."

Tissues that suffer from failures in the mechanosensitive or -regulatory process chains have been shown to be prone to diseases such as cancer or medical conditions of the cardiovascular system. Unfortunately, the biophysical foundations of soft tissue mechanical homeostasis remain poorly understood. Since studying select mechanisms of mechanobiology in native soft tissues is difficult, many novel findings have stemmed from tissue culture studies over the past decades due to their largely reduced number of degrees of freedom.

This article provides an in-depth review of mechanical homeostasis in three-dimensional cell-seeded hydrogel environments and discusses how it is impacted by various factors, including boundary conditions, cell and tissue type, cell density, and the mechanical and chemical composition of the matrix. The article focuses on studies in which the specimens were uniaxially or biaxially constrained, since these setups form simple boundary value problems that allow to quantitatively relate external mechanical loads to subsequent cellular reactions.

The major experimental observations made so far can be summarized as follows. Circular, cell-seeded free-floating collagen gels compact strongly over multiple days in culture due to cellular contractile forces. If gels are constrained by boundary conditions and are therefore not able to compact, a two-stage response of the tension inside the gel can be observed; first, cells rapidly built up a certain tension, which is then, secondly, maintained for a prolonged period. The level of this second phase appears to increase with both cell density and collagen concentration. Moreover, cells seem to pursue the re-establishment of this homeostatic state in response to mechanical perturbations. This homeostatic behavior appears to depend on the cell type and the exact experimental condition.

Besides gathering, comparing, and discussing the various observations that have been made so far, a further contribution of this article is the collection of available quantitative data regarding the homeostatic force level that was measured for various different cell and tissue types.

To this end, the available data was first processed and normalized to force per million cells to allow a comparison between the different studies. An important conclusion of the paper is that future studies in this field should provide values for both the cross-sectional area of the gel and its total volume. This would allow a more sensible normalization and therefore comparison between various studies which use slightly different setups. The supplementary material of the article presents two tables that contain the specific compositions of the gels that were used in the discussed studies.

After discussing the most important observations and categorizing the data, the article lists some limitations of the available studies. The two major shortcomings are the restriction of the available data describing the active evolution of gel tension to uniaxially constrained samples and the lack of data specifying how and which steady state develops in the gels after an external mechanical perturbation.

The article concludes with a brief discussion of remaining questions, many of which directly stem from the previously mentioned limitations. Most importantly, it is not yet known which mechanosensitive and -regulatory mechanisms work on and interact over multiple scales of length and time to lead to what is called homeostasis on the tissue level. Considering that most tissues are loaded in more than one direction *in vivo*, a crucial open issue is what mechanical homeostasis means in more than one dimension. Moreover, experiments that measure forces after perturbations until a new steady state is reached are required to determine the homeostatic range and discuss if and when homeostasis might become adaptive. Lastly, further studies with different cell types, including cells with induced defects, for example in integrin signaling, and cells from different tissue origins, are needed to investigate how that effects the homeostatic behavior.

3.2.2 Author contributions

JFE collected and categorized the articles that were included in the review. JFE primarily wrote the manuscript, with valuable contributions from LJH, DP, RCA, JDH, and CJC. LJH filtered and processed the quantitative data and created Tables 1 and 2. JFE created Fig. 1, 2, 3 and 4. All authors discussed the content.

3.3 Paper B: Computer-controlled biaxial bioreactor for investigating cell-mediated homeostasis in tissue equivalents

3.3.1 Summary

Only a few experimental studies exist so far that quantify the active development and maintenance of tension in tissue equivalents exposed to an external mechanical stimulus. Moreover, the available data suffer from an unsatisfactory limitation to uniaxially applied loads considering that most tissues *in vivo* are subject to multiaxial loading conditions (Eichinger et al. (2021b), Paper A). To close this gap, this article introduces the first computer-controlled biaxial bioreactor that can study how cell-seeded tissue equivalents develop and maintain a preferred tensional state. Moreover, it can examine how this unique behavior is impacted by various biochemical and mechanical parameters such as growth factors and boundary conditions, respectively.

The intention of the article is a detailed description of the design of the novel bioreactor. Briefly, a bath made of glass-filled polycarbonate forms the core of the device. The specimen is located in the center of the bath while being immersed in a special medium solution. Two of the four directions are equipped with a high-resolution force transducer attached to the sample to determine its tensile state. Each direction is connected to a stepper motor, which allows the application of diverse loading conditions (uniaxial, equi-biaxial, strip-biaxial) via a custom-written LabView interface. A lid made out of perspex protects the specimen from evaporation and contamination with bacteria and fungi. The entire device is placed in a cell culture incubator to provide the appropriate environmental conditions (37°C, 5% CO_2) and sterility needed for cell viability. A critical feature in mechanical testing of gel-based tissue equivalents is the connection between gel and testing device. Both the actual physical connection and the process of connecting need to be considered carefully since collagen gels are known to be extremely fragile. Various solutions have been proposed in the literature to attach the gel to the device, such as sutures, or porous polyethylene bars. This article presents a novel, advantageous design for 3D-printable porous insets which ensure a stable connection between gel and device and prevent problems such as tearing or separation at the interface which are known from other approaches. Regarding the process of connecting, every contact or movement of the gel bears the risk of damage. To eliminate such effects and ensure a high reproducibility of the experiments, the gel is made in place, i.e., already attached to the assembled device inside the cell culture incubator under sterile conditions without having to touch or move the gel after polymerization. Finally, to be able to investigate mechanical homeostasis in cell-seeded tissue equivalents, cellular contractile forces in the range of a few μN need to be measured over a long period of time in challenging environmental conditions stemming from the cell culture incubator. The chosen optical force transducers are shown to be able to measure such forces over multiple hours without loss in accuracy, with low noise, and low zero level drift despite the demanding environmental conditions.

Although the article focuses on describing the new device in detail rather than discussing biophysical conclusions that can be drawn from the obtained data, the results were interesting nevertheless. The level of homeostatic tension that developed within the gels over $\sim$20h was

shown to increase with both cell density and stiffness of the gel. Interestingly, the steady state tension achieved after ∼20h in biaxially constrained gels was ∼40% higher compared to uniaxially constrained gels. A further interesting finding of the article is the requirement to use either serum-starvation or treatment with mitomycin C to inhibit NIH/3T3 fibroblast proliferation during the experiments. Without one of these measures, the number of cells continuously increases, which also leads to a continuous increase in forces; that is, no steady state is reached. Finally, gels that were statically perturbed after the homeostatic state had been reached tended to re-establish the prior state within a certain tolerance. This tolerance depended on both the amplitude and direction of the applied load.

Although NIH/3T3 fibroblasts are very handy and could be used for further studies, they are of low biological interest due to genetic and phenotypic changes resulting from multiple years of culture. For this reason, the article suggest to use primary cells in future *in vitro* studies.

3.3.2 Author contributions

JFE came up with the central ideas for the device. JFE and DP were the lead designer. JFE primarily wrote the manuscript, with valuable contributions from DP, JMS, RCA, JDH, and CJC. DP conducted the experiments. All authors discussed the content.

3.4 Uniaxial versus biaxial

In contrast to previous work (Kolodney and Wysolmerski 1992, Eastwood et al. 1994, Brown et al. 1998, Marenzana et al. 2006, Ezra et al. 2010), the novel device presented in Eichinger et al. (2020) (Paper B) can subject tissue equivalents to biaxial stress or strain conditions by stretching or releasing the two arms of the cruciform-shape gel sample independently. To investigate how boundary conditions influence the level of homeostatic tension, experiments in uniaxial and biaxial protocols were, ceteris paribus, performed.

Interestingly, the homeostatic level of tension in uniaxially constrained gels was ∼40% lower than in biaxially constrained samples (Eichinger et al. (2020), Paper B). This might be explained by transverse contraction. Assuming that cells exert the same stress $\sigma_x = \sigma_y = \sigma_h$ in all directions and assuming linear elasticity with Young's modulus E, one can state for uniaxially tested tissue equivalents that are constrained in x-direction and free in y-direction

$$E\epsilon_y + \sigma_h = 0. \tag{3.1}$$

Any ϵ_y results in the transverse contraction

$$\epsilon_{x,trans} = -\nu\epsilon_y \tag{3.2}$$

with Poisson's ratio ν. As the gel is constrained in x-direction, a transverse contraction according to Eq. (3.2) leads to a change of stress in x-direction that is equal to

$$\sigma_{x,trans} = E\epsilon_{x,trans} = -E\nu\epsilon_y = -\nu\sigma_h. \tag{3.3}$$

Superposition of this elastic effect and the active cell stress in x-direction leads in a uniaxially constrained tissue equivalent to the overall stress in x-direction

$$\sigma_{x,total} = \sigma_h + \sigma_{x,trans} = \sigma_h(1-\nu). \tag{3.4}$$

In most random fiber networks the Poisson's ratio in the linear regime is around 0.25. The simple analysis presented above would lead to homeostatic stresses that are ∼25% lower in uniaxially tested tissue equivalents than in biaxially tested samples. Eichinger et al. (2020) (Paper B) showed that the homeostatic level of force is ∼40% lower. The discrepancy between 40% and 25% can have two reasons. First, ν = 0.25 is true in the load-free regime of random fiber networks, whereas in prestressed fibers networks ν is known to take on values slightly above 0.5 (Ban et al. 2018). Second, the cross section in uniaxially tested samples is smaller than in biaxially tested samples, which also explains why differences in forces are higher than in stresses. It seems therefore likely that transverse contraction can, ceteris paribus, explain the difference between the homeostatic level of tension in uni- and biaxially constrained tissue equivalents.

3.5 Primary cells

This section presents further results obtained with murine aortic cells.

3.5.1 Influence of FBS concentration on primary aortic fibroblasts

First, the influence of the concentration of FBS in the experimental medium was tested. Usually, this concentration is kept at a relatively low level to minimize parasitic effects resulting from fluctuations in the exact concentrations of FBS components that naturally appear between batches. To this end, three different concentrations, namely 2%, 10% and 20% FBS were tested (Fig. 3.1 and Fig. 3.2).

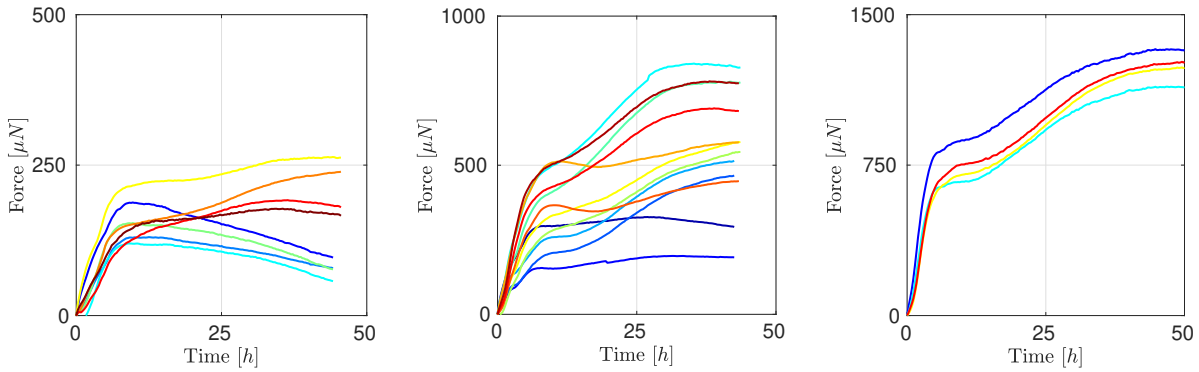

(a) (b) (c)

Figure 3.1: Impact of FBS concentration on the evolution of forces in fibroblast-seeded collagen gels. Three different concentrations were tested: (a) 2%, (b) 10%, and (c) 20%. Each line shows a different data set.

Interestingly, fibroblasts in medium containing 2% and 10% FBS developed inconsistent force patterns after the initial increase in force (Fig. 3.1a and Fig. 3.1b). This observation can have various reasons. First, the cells that were tested in different experiments stemmed from multiple mice. It is likely that this is at least partially responsible for the observed variations between experiments. Second, fibroblasts were extracted from the adventitia of the aorta via collagenase digestion as described in Section 2.3.2. In contrast to the media which consists almost exclusively of SMCs and is therefore well suited for the extraction of SMCs, the adventitia is made up of diverse cell types such as fibroblasts, myofibroblasts, macrophages, T cells and others (Majesky et al. 2011). When the fibroblast cultures were checked under the microscope, larger cells, probably macrophages, were detected. A mixture of different cells with different homeostatic force levels that are achieved at different rates could explain the observed two-phase characteristic. Third, contamination of the experimental medium could potentially be responsible for decaying force curves. This, however, was not relevant here. After each experiment the medium was checked under the microscope and no contamination was visible.

Gels that were tested in medium containing 10% and 20% FBS were characterized by a second phase of increasing forces. This phase started approximately after 10h (Fig. 3.1b and Fig. 3.1c). Similar behavior has been reported in the literature for gels seeded with human dermal or rat

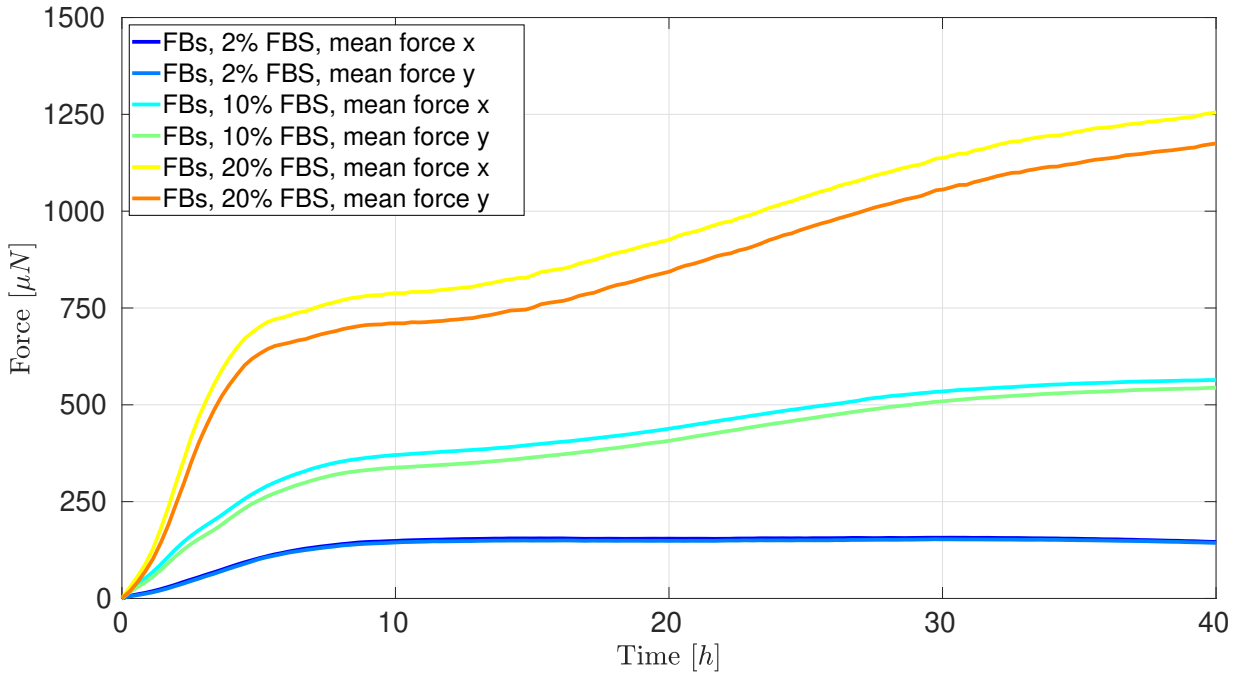

Figure 3.2: Direct comparison between gels immersed in medium with different FBS concentrations. Each line shows the mean of three identical experiments.

tendon fibroblasts (Eastwood et al. 1996, Brown et al. 2002, Marenzana et al. 2006). Based on the observations of Brown et al. (2002), a potential reason for the second increase in force could be the growth factors TGF-β1 and TGF-β3 which are also present in FBS. This assumption is corroborated by the observation that higher FBS concentrations led to a more pronounced second phase.

Moreover, as primary aortic fibroblasts barely proliferated in culture without the addition of 15–50ng/ml FGF-2 (which was not added to the experimental medium), it is very unlikely that cell proliferation is responsible for the second phase of increase in gel tension. This theory is supported by the observed plateau that is reached after the second phase, which would not arise if the number of cells would continuously rise.

3.5.2 Perturbation of SMC-seeded gels from homeostatic state

These results are presented in (Eichinger et al. (2021c), Paper D).

3.5.3 Comparison between fibroblasts and SMCs

It has been shown in the literature that the cell type strongly impacts the characteristics of the development of tension within constrained gels (Eichinger et al. (2021b), Paper A). When comparing murine aortic fibroblasts with murine aortic SMCs under identical experimental conditions, forces generated by SMCs are about five times higher. These results are important and new, since a direct comparison of fibroblasts and SMCs stemming from the same tissue origin (which also has a large impact, Eichinger et al. (2021b), Paper A) was lacking in the literature so far.

The difference in the level of tension between fibroblasts and SMCs might be explained by considering their respective functions in the aortic wall. While the main task of fibroblasts is the maintenance of the ECM (e.g. by depositing and degrading collagen fibers), SMCs are intended to contract tissues. Moreover, considering the composition of the aortic wall, the overall stresses acting within the media, in which SMCs are located, are higher than the stresses acting within the adventitia, in which fibroblasts reside (Gao et al. 2006). It seems therefore sensible that cells stemming from the media produce higher active forces.

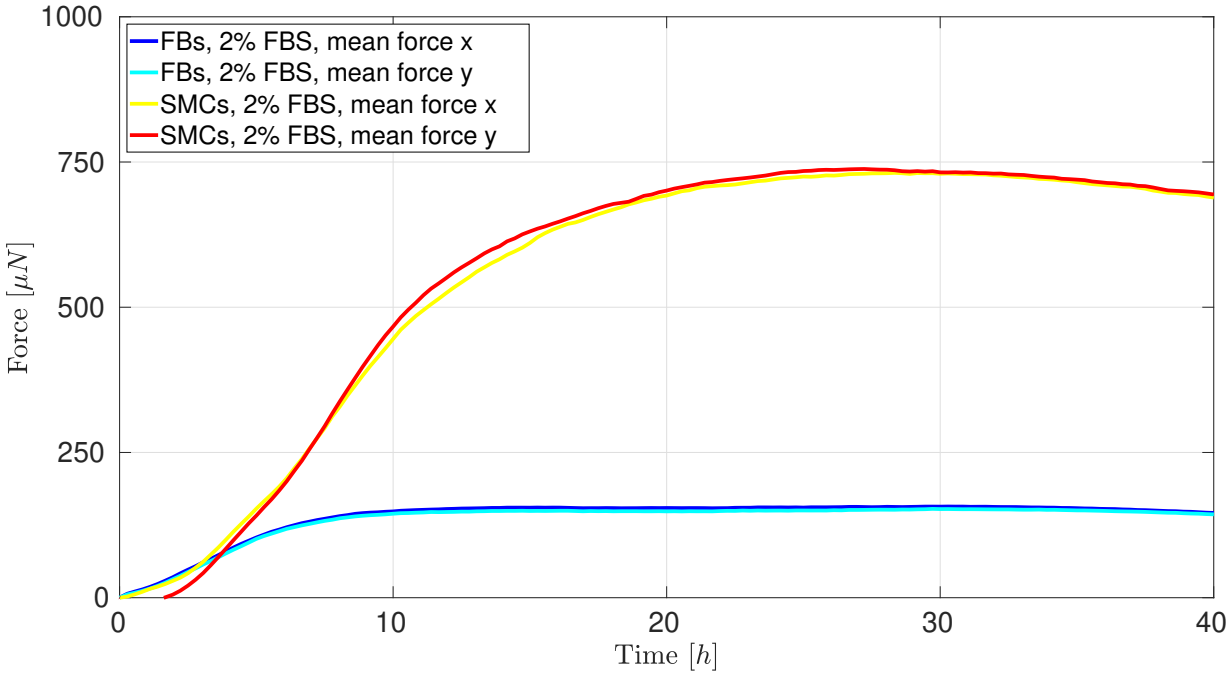

Figure 3.3: Comparison of the development of forces in gels seeded with fibroblasts and SMCs, respectively. Gels seeded with SMCs produce forces that are approximately five times higher. Each line represents the mean of three identical experiments.

Chapter 4

Computational modeling

4.1 Introduction

As shown in Eichinger et al. (2020, 2021b) (Paper A, Paper B), experiments with tissue equivalents are an essential tool to unravel the biophysical principles of mechanobiology. Yet, an endless series of undoubtedly interesting experiments is not practical, also considering that some of those would be barely feasible in practice. Thus, computational models are of tremendous importance to tackle the many open questions of mechanobiology. Especially helpful in this regard would be a micromechanical computational model which allows comprehensive studies of the complex three-dimensional interactions of cells with surrounding matrix fibers on the microscale. Elements of such a model could be directly related to specific micromechanical and molecular mechanisms.

However, computational modeling and studies on this length scale have been primarily done so far on decellularized ECM systems examining the physical and passive mechanical properties of fiber networks. Mathematical models accounting for cell-ECM interactions often suffer from an unsatisfactory experimental foundation. Moreover, most approaches that model soft tissues on the level of individual cells and fibers are restricted to two-dimensional studies and only consider a very low number of cells; however, two dimensional studies cannot adequately mimic the complexity of real three-dimensional tissue and are therefore of limited physiological relevance. Furthermore, the collagen networks in these models are often randomly created networks, thus, do not match specific microstructural characteristics such as the fiber length distribution or the average valency number of real collagen networks. Finally, especially models of the interaction of cells with ECM fibers rely in many crucial aspects on heuristic assumptions.

Driven by the aforementioned shortcomings and the great potential of a comprehensive microscale computational model of soft tissue mechanobiology, this chapter introduces a novel computational framework that overcomes the limitations known from many previous models (Eichinger et al. (2021a), Paper C). This forms the second major effort of this thesis.

4.2 Paper C: A computational framework for modeling cell-matrix interactions in soft biological tissues

4.2.1 Summary

Driven by the importance of mathematical modeling of mechanobiology and its current limitations, the present paper introduces a novel computational framework based on the finite element method that allows the simulation of mechanobiological processes in soft tissues on the level of individual cells and fibers. The proposed discrete fiber model captures single collagen fibers that are interconnected to form networks that match crucial micromechanical properties of collagen type I gels, namely the free fiber length, orientation, and valency distribution using stochastic optimization. Cells are represented by their transmembrane proteins, namely integrins, which act as molecular clutches and connect matrix fibers to intracellular structures, and the actin cytoskeleton, which is responsible for active cellular contraction. Dirichlet boundary conditions can be applied in a mathematically consistent manner in combination with periodic boundary conditions to externally perturb the system. The presented computational framework is implemented in an in-house C++ finite element code and allows, due to an efficient implementation based on parallel computing, the simulation of representative volume elements with physiological values for cell density and collagen concentration. A small C++ program that generates and transforms the networks to match the mentioned microstructural characteristics of collagen type I gels is provided online.

A set of computational examples demonstrated that the proposed framework is able to reproduce essential mechanobiological phenomena with regard to mechanical homeostasis. First, the chosen approach for constructing the fiber networks is validated, and it is shown that these artificial networks exhibit very similar mechanical properties compared to experimental data of collagen type I gels. Subsequently, it is demonstrated that simulations with higher cell densities and higher collagen concentrations lead to higher tissue tension, both being in accordance to experimental studies. The simulations also show that cells can mechanically interact with other cells over long ranges of a multiple of the cell diameter. A further contribution of the article is the quantitative analysis of how dynamic cross-linking influences inelastic matrix remodeling, that is, the permanent reorganization of the filamentous microstructure of the ECM. The presentation of specific values for on-rates and off-rates of the involved chemical bonds might be helpful for further modeling studies on various scales from molecular to continuum level.

Despite many advantages and its broad experimental foundation, the proposed computational model has some shortcomings. So far, mechanical homeostasis can only be simulated on short time scales, in which the deposition and degradation of collagen fibers can be largely neglected, since the latter is not yet part of the model. Moreover, it is well known that many different proteins are involved in the physical attachment of cells to the ECM, not just integrins. Especially the roles of talin and vinculin in the mechanics of focal adhesions were studied recently and could be included in the model. A further shortcoming is the very simple model for the cellular contractile apparatus. So far, a specific contraction rate is simply prescribed to the connections of cells and fibers. Including a more advanced model for the generation of forces within the cell might be worthwhile.

4.2.2 Author contributions

JFE designed the mathematical model. JFE and MJG designed the computational framework. JFE and MJG carried out the implementation. JFE, CJC, and JDH conceived and planned the numerical experiments. JFE carried out the simulations. JFE primarily wrote the manuscript, with valuable suggestions from MJG, IDK, RCA, WAW, JDH, and CJC. JFE prepared the figures. All authors discussed the content. JDH and CJC conceived the original idea and were in charge of overall direction and planning.

Chapter 5

Biophysical interpretation

5.1 Introduction

This chapter achieves to deepen our understanding of the governing biophysical and micromechanical principles of mechanical homeostasis in soft tissues by combining results from the conducted experimental study (Chapter 3) and results from simulations with the novel comprehensive computational model (Chapter 4) with a thorough theoretical analysis across the relevant scales of length and time.

To this end, the chapter first investigates the governing mechanisms of mechanoregulation of individual cells on short time scales (minutes to days). On this microscopic level, continuum quantities such as stress, strain, or metrics derived from them are not well defined. At this fundamental level, cells can presumably only sense and react to (changes of) forces or displacements in their environment. Nevertheless, on the scale of tissues and organs, this may render a phenomenon where cells effectively aim at maintaining a more abstract quantity known from continuum mechanics. Subsequently, the micromechanical principles governing the continuous turnover of tissue mass on long time scales (days to years) are discussed.

This chapter strives, in particular, to answer the following questions:

1) Which mechanical quantity can individual cells probe, interpret, and regulate in their extracellular microenvironment?

2) How do individual cellular reactions to altered mechanical loading superimpose to observations made on the tissue scale?

3) How do cells continuously remove old and incorporate new fibers of the ECM without the loss of the structural integrity of tissues?

5.2 Paper D: What do cells regulate in soft tissues on short time scales?

5.2.1 Summary

Two pressing questions in mechanobiology are, which mechanical quantity individual cells regulate on the microscale and how tension in the cytoskeleton of fibroblasts and smooth muscle cells translates into tissue tension. Answering these questions on short time scales (on which mass turnover can largely be neglected) is the intention of this article. To do so, experimental and computational results are combined with a theoretical analysis based on a simple mechanical analog model for soft tissue mechanics.

A major shortcoming of available experimental studies analyzing how tissue equivalents reestablish a preferred level of tension when facing an external perturbation is the restriction of the observed relaxation intervals to one hour or less. In these short time intervals, no new steady state of tension was reached in these gels. Therefore, these studies could not answer the question within which tolerance the homeostatic state is actually restored after perturbations. As a consequence, these studies could also not provide the information required to draw reliable conclusions regarding the quantity that is preserved by a cell facing a mechanical perturbation. This article presents the first study of the cellular behavior in such gels over more than 15h after the perturbation, that is, until a new steady state is reached, based on the device introduced in Eichinger et al. (2020) (Paper B). It thereby provides the required data to draw conclusions about the target quantity of cellular mechanosensing and -regulation.

These novel experimental results are used to test three different hypotheses regarding the cellular target of mechanoregulation on the microscale. Hypothesis I assumes that cells restore their own shape, or in other words, the displacements they apply to the surrounding matrix. Hypothesis II assumes that cells control the forces they apply to the ECM. Lastly, Hypothesis III assumes that cells regulate the strain in their surrounding matrix. Using a novel mechanical analog model for active and passive soft tissue mechanics, these competing hypotheses are discussed regarding their resulting behavior at tissue level, which is then compared to the experimental results.

The major finding of this article is that only Hypothesis II, thus the assumption that cells regulate the contractile forces they exert on their fibrous microenvironment rather than any tissue-intrinsic quantity is in agreement with experimental data. Notably, this conclusion is valid on short time scales, that is, in the absence of mass turnover.

Using the comprehensive finite element framework presented in Eichinger et al. (2021a) (Paper C), which contains a detailed model for the processes occurring at the interface of cells and fibers, thus, for focal adhesions dynamics, it is confirmed that catch-slip bond behavior of integrins gives cells the ability to regulate their contractile forces and therefore implement Hypothesis II. In general, catch-slip bonds have a specific optimal loading at which their lifetime is maximal; this optimal loading therefore determines the set-point around which cells regulate the forces they apply on the ECM, which is also in agreement with experimental data (Weng et al. 2016). Although the presented computations with the advanced computational model cannot evidence that molecular clutches and actin cytoskeleton contractility are the only mechanisms by which cells regulate their forces, they can, however, show that they are sufficient to do so.

5.2.2 Author contributions

JFE designed the mathematical analog model. JFE designed the computational framework. JFE carried out the implementation and the simulations. DP partially conducted and supervised the experiments. JFE primarily wrote the manuscript, with valuable suggestions from DP, RCA, WAW, JDH, and CJC. JFE prepared the figures. All authors discussed the content. JDH and CJC conceived the original idea and were in charge of overall direction and planning.

5.3 How do cells incorporate prestress in soft biological tissues on long time scales?

5.3.1 Motivation

Mechanosensing and mechanoregulation act on multiple scales of length and time ranging from molecules to cells to tissues and from minutes to hours to years, respectively. Eichinger et al. (2021c) (Paper D) concluded using mathematical modeling (Eichinger et al. (2021a), Paper C) and tissue culture experiments (Eichinger et al. (2020), Paper B) that on short time scales (less than 48h), mechanical homeostasis most likely primarily regulates the contractile forces exerted by cells on surrounding matrix fibers via integrins (Kong et al. 2009, Weng et al. 2016). On this time scale, the continuous deposition and degradation of matrix fibers, that is, mass turnover, can be neglected (Nissen et al. 1978, Nakagawa et al. 1989, Matsumoto and Hayashi 1994, Gineyts et al. 2000). On longer time scales of months to years, however, the continuous turnover of fibers is crucially involved in tissue homeostasis (Humphrey and Rajagopal 2002, Cyron et al. 2014).

Yet, very few is known about the microscopic processes that govern continuous mass-turnover on longer time scales. A crucial question is how newly deposited fibers are integrated with a precise prestress to maintain the structural integrity of loaded tissues. Previous studies have shown that matrix fibers degrade at a rate that depends on their respective tensile state. This endows tissues with a further mechanosensitive mechanism (Bhole et al. 2009, Flynn et al. 2010) in addition to the molecular clutches at the cell-matrix interface. Driven by this finding, both the ability and necessity of cells to neatly control the degradation and placement of each monomer with the exact prestress at all times during both morphogenesis and maintenance of load-bearing tissues can be questioned.

Both cells and matrix fibers have been shown to exhibit mechanosensitive mechanisms. However, a comprehensive microscale model that can explain tissue homeostasis on short and long time scales based on a fix set of microscopic mechanisms including matrix fiber deposition and degradation is still lacking. In addition, it is not yet understood what happens microscopically when tissue grows in case of prolonged overloading (Wolinsky 1971, Matsumoto and Hayashi 1994, 1996), shrinks in case of prolonged underloading (Nakagawa et al. 1989), and entrenches a residual tension as a result of inelastic, cell-mediated matrix remodeling (Marenzana et al. 2006, Simon et al. 2014). All of the aforementioned phenomena are intimately linked to mechanical homeostasis.

In this section, a set of microscopic mechanisms for cell-mediated fiber deposition, degradation, and remodeling is proposed, which is sufficient to explain how load-bearing soft tissues can be structurally maintained despite continuous turnover of collagen fibers. Furthermore, this set of mechanisms is shown to capture the phenomena of growth (in case of long-term increases in loading), shrinkage (in case of long-term decreases in loading), and residual matrix tension.

5.3.2 Discussion

In healthy tissues, deposition and degradation of collagen fibers (half-lives of ∼1-3 months, Humphrey et al. (2014a)) are in equilibrium, i.e., the form and mass of tissues are conserved. In diseased tissues, however, that are characterized by an altered mechanical environment, phenomena such as tissue growth (Wolinsky 1971, Matsumoto and Hayashi 1994, 1996) or shrinking (Nakagawa et al. 1989) may arise. Interestingly, both of the latter processes seem to stop as soon as a similar stress state compared to the state before the disease is re-established.

To maintain their structural integrity under normal conditions and to grow or shrink when facing altered mechanical loading for a prolonged time, tissues are equipped with two crucial processes. First, fibroblasts constantly produce synthetic and degradative ECM molecules to both deposit and degrade fibers (Parsons et al. 1999, Prajapati et al. 2000, Blain et al. 2001, Koskinen et al. 2004). Second, collagen fibers that are loaded in tension are more stable against enzymatic degradation compared to fibers that are less loaded or unloaded, presumably due to a reorganization of the enzyme binding sites on the fibers (Bhole et al. 2009, Flynn et al. 2010, 2013). This mechano-chemical relationship between fiber tension and reaction kinetics for degradation provides the missing mechanosensitive process for soft tissue mechanical homeostasis on long time scales. The following two paragraphs explain how the mentioned mechanisms interact on the microscale to allow both tissue maintenance and growth or shrinkage on the macroscale, respectively.

Maintenance A slightly extended version of the simple mechanical analog model proposed in Eichinger et al. (2021c) (Paper D) is used to elucidate how tissues can maintain their structural integrity in health despite continuous turnover of mass (Fig. 5.1). As demonstrated before, cells attach to a nearby collagen fiber via integrins (Fig. 5.1a), to then contract (Fig. 5.1b) until a specific preferred force F_c is reached (Weng et al. 2016). As region 2 in the analog model has always less tension compared to region 1, fibers in region 2 will slacken locally (if they are not compressed due to a strong external tensile load, they are at least always less loaded than fibers of region 1), which would cause them to be more susceptible to enzymatic breakdown. It can thus be concluded that fibers which are currently located in region 2 are degraded with a higher probably than fibers of region 1. If one assumes that cells place a new fiber at a position very similar to the old one, however, in a stress-free state (Fig. 5.1c), a subsequent detachment of the cell (focal adhesion lifetimes are in order of a few minutes, Stehbens and Wittmann (2014)) then leads to strain in the newly deposited matrix fiber. If both cellular forces and the external loading do not change and therefore introduce a constant amount of energy into the system, the aforementioned mechanism would lead to the maintenance of the structural integrity that is observed on the tissue level.

If tissue maintenance on long time scales is driven by the aforementioned mechanisms, the actual role of cells could be greatly simplified. They only need to supply synthetic and degradative ECM molecules and regulate the force they exert on surrounding matrix fibers rather than a tissue-intrinsic quantity (Eichinger et al. (2021c), Paper D, Fig. 5.1c). It is anyway hardly conceivable that cells can directly place each proteolytic enzyme and collagen monomer at an exact position at all times during maintenance of load-bearing ECM, especially considering that a cell is attached to multiple fibers in a three-dimensional fiber network.

Importantly, the proposed interaction of the mentioned processes can also explain the entrenchment of residual matrix tension and inelastic remodeling which has been shown both *in vivo* (Cardamone et al. 2009, Holzapfel and Ogden 2019) and *in vitro* (Marenzana et al. 2006, Simon et al. 2014). If cells attach, contract, and then substitute the fiber in region 2 with a new stress-free fiber, detachment of the cell or cell lysis would lead to $L_t > L_1 + L_2^*$, which explains why a residual tension can be measured even when active cellular forces are removed from the system (Fig. 5.1).

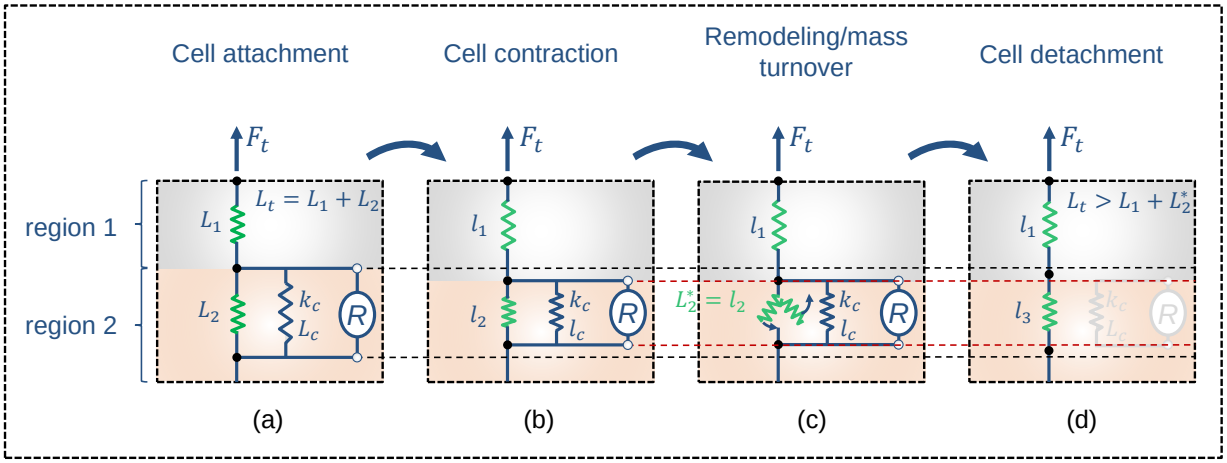

Figure 5.1: Schematic of tissue maintenance under constant mass turnover. Physical cell-matrix interactions usually consist of the following steps: cells first attach to a fiber (a), contract (b), degrade and deposit (c), and then detach (d). This process then starts anew. L_i define lengths in undeformed springs, l_i lengths in deformed springs.

Growth and atrophy The extended analog model can also be used to explain how growth and shrinkage of tissue can be driven by the processes introduced so far. To this end, an artery is considered that is exposed to hypertension for a prolonged period of time, analogously to the experimental study of Matsumoto and Hayashi (1994, 1996) (Fig. 5.2). As mentioned before, the deposition and degradation of collagen fibers are in equilibrium during tissue maintenance. Thus, no change of mass can be observed over time, yielding

$$\dot{m}(t, F_f) = \dot{m}_{deposition}(t) + \dot{m}_{degradation}(t, F_f) = 0. \tag{5.1}$$

The change of mass herein depends on the average force F_f that is acting on a single fiber, since the rate of degradation of a single fiber $\dot{m}_d(t, F_f)$ depends on its tension (Bhole et al. 2009, Flynn et al. 2010, 2013). The cellular deposition rate of collagen $\dot{m}_{deposition}(t)$ is thereby presumed to be independent of the loading state.

If the analyzed artery is assumed to be exposed to higher external loading for a longer period of time as a result of, e.g., hypertension (Fig. 5.2b), the average force per fiber F_f increases, which in turn decreases their turnover rate (Bhole et al. 2009, Flynn et al. 2010, 2013). If cells still produce the same amount of new ECM but with a decreased degradation rate, $\dot{m}(t, F_f) > 0$ holds true, i.e., growth arises. Deposition and degradation of fibers will be in a new equilibrium

as soon as the force F_f has decreased to its original value, since more fibers are available to carry the permanently excessive external load. Then, growth transforms back to maintenance as described before, now with more total mass resulting from the permanently elevated external loads. Therefore, the role of cells for growth can be confined to a supplier and degradator of ECM material, provided that cells apply the same contractile forces independently of the external loading (Eichinger et al. (2021c), Paper D).

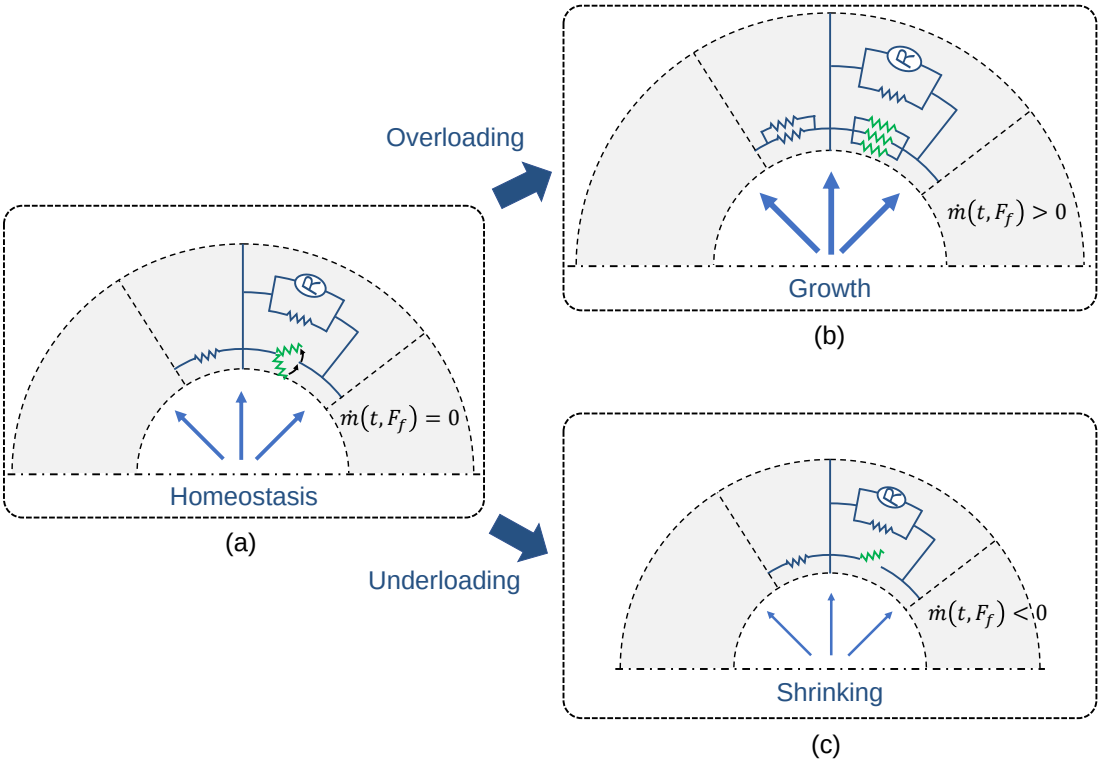

Figure 5.2: Schematic of an RVE within the cross section of an artery under normal conditions (a), hypertension (b), and underloading (c). Due to load dependent disassembly of matrix fibers, overloading leads to growth (production $>$ degradation) and underloading to shrinkage (production $<$ degradation) of tissue.

In analogy to the previous reflections on growth, tissue shrinkage or atrophy in case of underloading can be explained (Nakagawa et al. 1989). If a tissue is exposed to lower external forces for a prolonged period of time (Fig. 5.2c), the force F_f acting in each individual fiber decreases, making them more susceptible to degradation, yielding $\dot{m}(t, F_f) < 0$. This process stops as soon as enough fibers have been degraded so that the consisting fibers carry – on average – the same load as before, despite the permanently decreased external load. Then, atrophy stops and turns into maintenance of the new state.

One can therefore conclude that cells would not need to sense the intrinsic mechanical state of its surrounding, e.g., to up- or down-regulate the production of collagen to control the mechanical state of tissues. This control is rather achieved by the interaction of mechanosensitive phenomena of cells and the ECM.

In summary, one can conclude that maintenance and re-establishment (by growth or shrinkage) of a certain mechanical state in tissues on the long run can be achieved by the interaction of the following mechanisms (extended from Bhole et al. (2009)):

1) guided self-assembly of organized collagen networks from monomer solutions, which has been shown, e.g., in acellular collagen gels (Sun et al. 2015),

2) strain or tension dependent degradation of collagen fibers (Bhole et al. 2009, Flynn et al. 2010, 2013),

3) cellular production of both synthetic and degradative ECM molecules (Parsons et al. 1999, Prajapati et al. 2000, Blain et al. 2001, Koskinen et al. 2004) at constant rates, and

4) the regulation of cellular contractile forces exerted on the ECM (Eichinger et al. (2021c), Paper D).

In summary, Eichinger et al. (2021c) (Paper D) first studied the regulatory response of cells in statically perturbed fibrous networks on short time scales (seconds to hours). On this time scale, phenomena such as mass-turnover implying inelastic matrix deformations can be neglected. This allows the study of the isolated regulatory response of cells immersed in a purely elastic fiber network. It was found that cells most certainly control the forces they exert on the ECM via integrins rather than a tissue intrinsic quantity.

Subsequently, this chapter also considered the impact of inelastic remodeling and mass turnover on mechanical homeostasis on longer time scales (days to years). A set of four microscopic mechanisms was proposed that can sufficiently explain how tissue maintenance and growth or shrinkage can arise. A crucial next step is to validate the proposed set of mechanisms in the comprehensive three-dimensional fiber network model proposed in (Eichinger et al. (2021a), Paper C) by extending it with a model for force-dependent mass-turnover.

Chapter 6

Discussion

The ability of cells within living biological systems to sense, interpret, and subsequently regulate the mechanical properties is vital for human health. This unique feature of biological tissues is often referred to as tensional (Brown et al. 1998) or mechanical homeostasis (Humphrey et al. 2014a). Defects in this essential control loop manifest in unrestricted changes of the mechanical properties of affected tissues and organs, which ultimately results in a loss of functionality. Therefore, failure or loss of the ability to sense or regulate mechanics is directly related to many life-threatening diseases such as cancer (Weaver et al. 1997, Boettiger et al. 2005, Yeung et al. 2005, Levental et al. 2009, Butcher et al. 2009, Lu et al. 2012) or aneurysms (Humphrey and Taylor 2008, Humphrey et al. 2014b, Cyron et al. 2014, 2016, Humphrey and Tellides 2019).

Until now, the specific micromechanical and biophysical processes governing homeostasis and how they interact over various scales of length and time remained mostly unidentified (Eichinger et al. (2021b), Paper A). For example, a quantitative description, or rules, how individual cells dynamically retrieve their homeostatic conditions in response to altered mechanical loading, and how the individual responses of cells superimpose to render homeostasis on the tissue level could not be given. Moreover, referring to the original idea of Cannon (1929, 1932) who wisely chose the prefix "homeo" meaning "similar to" (and not "homo" meaning "the same"), a quantification of the homeostatic range within which a mechanical state is regulated as a function of the loading amplitude and time of exposure to an external loading did not exist due to shortcomings of the available studies (Brown et al. 1998, Bisson et al. 2009, Ezra et al. 2010). Finally, since being simpler to execute, experimental studies of cellular mechanoregulation have been performed so far exclusively under uniaxial loading conditions (Kolodney and Wysolmerski 1992, Eastwood et al. 1994, Brown et al. 1998, 2002, Campbell et al. 2003, Marenzana et al. 2006, Ezra et al. 2010), which is unsatisfactory given that loading *in vivo* is predominantly multidimensional.

Greater understanding of how homeostasis arises can have a tremendous impact on both diagnosis and therapy of various diseases (Ingber 2003), not to mention its importance for the promising field of tissue engineering (Dzobo et al. 2018). To contribute to this endeavor, the presented thesis employs three approaches: experiments with tissue equivalents, computational modeling based on the finite element method, and a profound theoretical analysis. In the past, experiments (Bell et al. 1979, Brown et al. 1998, Marenzana et al. 2006, Ezra et al. 2010, Simon

et al. 2014) and mathematical modeling (Holzapfel et al. 2000, Wakatsuki et al. 2000, Humphrey and Rajagopal 2002, Watton et al. 2004, Marquez et al. 2005, Mauri et al. 2016, Loerakker et al. 2016, Cyron et al. 2016, Ban et al. 2019, Domaschke et al. 2019) have been proven to be particularly helpful in this regard.

6.1 Experimental study

To understand if and how cells sense mechanical cues and regulate the mechanical properties of tissues, it is essential to trace which specific mechanical stimuli evoke which cellular actions. Therefore, both the cellular reaction and the mechanical stimulus need to be measurable (and the latter also controllable) precisely. Due to the high complexity of native tissue consisting of divers filamentous proteins, cell types, and substances, meaningful *in vivo* experiments are difficult to perform. Precise control of specific parameters like the composition of fiber and cell types, substrate stiffness, or growth factors is hardly possible, which impedes conclusions regarding selected mechanisms. Cell-seeded collagen or fibrin gels have been shown to be simple but powerful model systems to study active and passive mechanics of native soft tissues. A thorough review of the state of the art in this field can be found in Eichinger et al. (2021b) (Paper A).

A major limitation of available studies is the restriction to uniaxial tests, which are, e.g., insufficient to derive complete constitutive equations or explain what homeostasis means in higher dimensions. Biaxial testing devices can be a valuable tool in this regard (Humphrey et al. 2008). Eichinger et al. (2020) (Paper B) introduces such a device, thereby providing multiple novel opportunities for advanced tests such as equi-biaxial or non-equi-biaxial stretching (including strip-biaxial stretching). In a 0-2000μN range, the novel device can monitor forces stemming from active cellular contraction within collagen gels for up to two days. Despite the demanding environmental conditions required for cell culture, noise and drift of the implemented force transducers are almost non-existent in relevant time and force ranges.

In agreement with published data (Delvoye et al. 1991), experiments in the novel device with NIH 3T3 fibroblasts showed that the level of homeostatic tension depends linearly on the collagen concentration, which has been shown to directly correlate with the stiffness of the substrate (Alcaraz et al. 2011, Miroshnikova et al. 2011, Hall et al. 2016, Joshi et al. 2018). Therefore, the increased level of tension in stiffer gels may result from cells being more contractile in stiffer environments (Ghibaudo et al. 2008, Califano and Reinhart-King 2010, Schiller and Fässler 2013, Cheng et al. 2013, Elosegui-Artola et al. 2014, Zhu et al. 2016). Moreover, an increased gel tension was observed for higher cell densities which has been shown previously (Delvoye et al. 1991, Legant et al. 2009, Jin et al. 2015). An important novel finding of the presented study is that the stable homeostatic level of tension is, ceteris paribus, higher under biaxial compared to uniaxial constraints. A plausible explanation for this observation is transverse contraction (see Section 3.4). Furthermore, a steady state in force could only be achieved and maintained if cells were prevented from proliferating by either serum starvation or treatment with mitomycin C. This has to be considered in future studies and in the interpretation of previously published data based on this cell type. When gels seeded with NIH/3T3 fibroblasts were perturbed by 10-20% of the homeostatic force, the prior state was restored within a homeostatic range of $\sim$5%. This range depended both on the type and amplitude of the applied load. Remarkably, this is the first data quantifying this range and therefore allowing conclusions with regard to which mechanical

quantity is actually regulated in such systems. Previous data were restricted to relaxations times of less than 1h in which no new steady state of tension was achieved in the gels (Brown et al. 1998, Bisson et al. 2009, Ezra et al. 2010). Finally, if these gels are modeled as constrained mixtures (Cyron et al. 2016), two time constants differing by roughly two orders of magnitude are sufficient to describe the relaxation in such gels after perturbation, which is in agreement with previously published results (Cyron and Aydin 2017).

Although more can be learned from NIH/3T3 cells, their poor biological relevance may not be ignored. Therefore, further tests were performed with murine aortic smooth muscle cells (Eichinger et al. (2021c), Paper D). If gels seeded with such cells were perturbed with a step-like applied strain of 2% after 24h, the tensional state was restored with a 10-15% tolerance, both when gels were stretched or released by 2%.

The novel biaxial bioreactor can serve in the future as a valuable tool for further *in vitro* studies, including studies of cells with defects in the cytoskeletal structure or integrin signaling (both being key players in mechanical homeostasis) and studies of gels exposed to various types of cyclic loading (e.g., strip- and equi-biaxial).

6.2 Mathematical modeling

Mechanobiology and homeostasis is ultimately governed by the interaction of cells and fibers of the ECM, in particular, by processes taking place at their physical interface. Micromechanical models on this level can contribute tremendously to unraveling the fundamental biophysical mechanisms. However, computational modeling on this scale was so far primarily focused on fibrous networks without cells and the study of their passive mechanical properties (Heussinger and Frey 2007, Mickel et al. 2008, Chatterjee 2010, Lindström et al. 2010, Stein et al. 2010, Broedersz et al. 2011, Cyron and Wall 2012, Lang et al. 2013, Müller et al. 2014, Jones et al. 2014, Lee et al. 2014, Ronceray et al. 2016, Humphries et al. 2018, Zhou et al. 2018, Bircher et al. 2019, Domaschke et al. 2019). Models of cell-seeded fibrous matrices often suffered from unsatisfactory shortcomings such as the restriction to two dimensions considering that fiber networks behave differently in three dimensions (Baker and Chen 2012, Jansen et al. 2015, Duval et al. 2017), or the limitation to a small number of modeled cells (Wang et al. 2014, Abhilash et al. 2014, Notbohm et al. 2015, Kim et al. 2017, Humphries et al. 2017, Grimmer and Notbohm 2017, Burkel et al. 2018). Moreover, most cell-matrix interaction models were simplistic. Cell contraction was often described as displacement boundary conditions on certain points in the network around an imaginary round cell (Abhilash et al. 2014, Liang et al. 2016, Humphries et al. 2017), which per se excludes any influence of the mechanical properties of the ECM on the cellular behavior. Finally, most models were based on random fiber networks which do not match any microstructural characteristics of real collagen networks (Abhilash et al. 2014, Wang et al. 2014, Humphries et al. 2017, Kim et al. 2017).

Eichinger et al. (2021a) (Paper C) introduces a micromechanical computational model that overcomes the aforementioned shortcomings and limitations. Simulations are performed with networks that are constructed to match the distributions of the three most important microstructural descriptors (Davoodi-Kermani et al. 2021) of real collagen networks, namely the free fiber length, the orientation, and valency distribution using stochastic optimization. Single fibers are discretized using geometrically exact beam finite elements which ensure accurateness even un-

der large deformations. Cells are modeled as point like entities that can form elastic, contractile focal adhesion clutches to nearby matrix fibers. The physical connection of cells and fibers is modeled as multiple integrin cluster, each consisting of multiple integrins whose on- and off-rates were chosen to imitate their experimentally determined catch-slip bond behavior (Kong et al. 2009, Chen et al. 2012). This approach allows a control loop in which cellular contractile forces are indeed influenced by (changes of) the mechanical properties of the matrix. The model captures that the lifetime of single integrins are on the order of seconds, while the ones of entire focal adhesions are on the order of minutes (Stehbens and Wittmann 2014). Due to an efficient implementation of the presented framework in a C++ finite element code, systems with multiple contractile cells immersed in a three-dimensional fiber network can be simulated.

Some illustrative numerical examples validated that the micromechanical model is able to reproduce many experimental observations known from studies with tissue equivalents. The homeostatic behavior for both increasing cell densities (Legant et al. 2009, Jin et al. 2015) and increasing substrate stiffnesses (Eichinger et al. (2020), Paper B) is captured by the model, both qualitatively and quantitatively. Moreover, the phenomenon that cells can mechanically interact over distances that are a multiple of the cell diameter by building so-called force chains can be shown by the model (Shi et al. 2013, Wang et al. 2014, Baker et al. 2015, Mann et al. 2019). Finally, experimental studies have shown that part of the cell-driven reorganization of the matrix is inelastic, meaning that if active cellular forces are eliminated from the system, a residual tension remains resulting from an altered stress-free configuration (Marenzana et al. 2006, Simon et al. 2014). The presented framework allows precise quantitative studies of the influence of various parameters on this phenomenon. Such a study is presented for the characteristic determinants of the chemical bonds that newly form in between matrix fibers.

One shortcoming of the proposed model is that mass turnover, i.e. the deposition and degradation of matrix fibers, is not yet captured, which limits studies to short time scales. Thus, phenomena such as growth (Wolinsky 1971, Humphrey and Rajagopal 2002, Ambrosi et al. 2010, Cyron et al. 2016, Braeu et al. 2017, Cyron and Humphrey 2017) cannot yet be simulated. A second shortcoming is the chosen simplified approach for the intracellular contractile apparatus of cells. Advanced models could be included here (Mogilner and Oster 2003, Murtada et al. 2010, 2012).

In summary, the proposed computational model for the active and passive micromechanics of soft tissues can serve as a valuable *in silico* tool to study further phenomena such as cell migration (Yamada and Sixt 2019) that crucially rely on the physical interaction of cells and ECM .

6.3 Biophysical interpretation

Probably the most important question yet to answer was, which mechanical quantity individual cells actually regulate in response to altered mechanical loading (Eichinger et al. (2021b), Paper A). Although tissue-intrinsic continuum quantities such as strain/stress were often assumed to be controlled on tissue level, a comprehensive analysis of how such regulation can be achieved by superposition of individual cellular responses was lacking. To close this gap, Eichinger et al. (2021c) (Paper D) presents a profound theoretical analysis on what individuals cells actually regulate by discussing different hypotheses based on a novel mechanical analog for soft tissue mechanics, experimental data gained with the new biaxial device introduced in Eichinger et al.

(2020) (Paper B) and three-dimensional simulations with the model presented in Eichinger et al. (2021a) (Paper C).

A precondition to unravel how homeostasis arises are data that precisely quantify if and how the tensional state in tissues is restored when facing an external perturbation. As mentioned before, previous data so far lack relaxation times long enough for perturbed gels to reach a new steady state (Brown et al. 1998, Bisson et al. 2004, 2009, Ezra et al. 2010). Eichinger et al. (2021c) (Paper D) presents the first data of this kind, in particular of collagen gels seeded with primary aortic fibroblast. In response to a 2% externally applied strain (both when being stretched and released) after 24h, gels restored the tension within a couple of hours within a homeostatic range of 10-15%.

Three hypotheses regarding the cellular regulatory target are feasible to discuss, namely I) their own dimension, II) the contractile forces they exert on the ECM, and III) the strain in the surrounding tissue. A novel simple mechanical analog model can theoretically explain that only hypothesis II is consistent with the experimental findings mentioned above. One can therefore derive that cells presumably regulate the forces they transfer to the ECM via integrins rather than some tissue-intrinsic quantity such as strain. Importantly, previous experimental studies have shown that the force-sensitive catch-slip bond behavior of integrins endows cells with the ability to control the forces they exert on a substrate (Kong et al. 2009, Weng et al. 2016). The aforementioned conclusion is supported by simulations of RVEs of tissue equivalents performed with the computational framework presented in (Eichinger et al. (2021a), Paper C), which contains a detailed model for the dynamic relaxation of focal adhesions based on single integrin catch-slip-bond kinetics.

In summary, cells most likely regulate the contractile forces they transfer to the ECM via force-sensitive integrin bonds when facing altered mechanical conditions. Importantly, this conclusion can so far only be drawn for short time scales in which cell-mediated turnover of fibers can be neglected.

Chapter 7

Conclusions and outlook

This final chapter first briefly retells the story of this thesis. Subsequently, a brief outlook appraises past experience and ventures to cast a glance into worthwhile future research efforts.

7.1 Conclusions

The presented thesis pursued three major goals, driven by the gap that existed between the understanding of soft tissue mechanobiology and its important role in some of the most life-threatening medical conditions such as cardiovascular diseases or cancer.

The first goal was to advance currently available experimental techniques and data by studying mechanobiological processes in gel-based tissue equivalents. To this end, the first biaxial bioreactor for cell-seeded collagen gels was presented. This device was custom-designed and built for the examination of the evolution of the mechanical state in cruciform-shaped gel samples under divers multiaxial loading conditions for up to 48h. Using this device, the influence of multiple parameters such as cell density and type, substrate stiffness, and type of boundary condition – such as uniaxial, strip- and equi-biaxial – on the homeostatic behavior was studied. Moreover, the first quantitative data were presented for the tolerance at which cells restore the tensile state when being statically perturbed from the homeostatic steady state.

The second objective was the development of a highly efficient computational microscale framework based on the finite element method that resolves active and passive soft tissue mechanics on the level of individual cells and fibers while relying on a strong experimental foundation. As input to the simulations, artificial fiber networks are constructed to match the free fiber length, graph valency, and fiber orientation distributions to those of real collagen gels determined using confocal microscopy. Single collagen fibers are modeled as continua and are discretized with geometrically exact beam finite elements to represent their mechanical properties such as bending and extensional stiffness. Cells are modeled as point-like particles that can form contractile focal adhesion clutches to matrix fibers in their nearby surrounding, allowing for both mechanosensing and -regulation.

The computational framework has major improvements compared to available models from the literature. First, many approaches are limited to a two-dimensional problem formulation,

although it is well known that cell behavior in a three-dimensional matrix differs greatly from the two-dimensional case. Furthermore, tensional forces exerted by contracting cells are often modeled as prescribed displacements on certain points located in the neighborhood of fictitious cells. Changes in the mechanical properties of the surrounding matrix caused, for example, by cell-mediated remodeling, cannot influence cellular behavior in such an approach.

The last goal of the presented thesis was to combine the experimental study and numerical simulations with a profound theoretical analysis to tackle some of the fundamental open questions regarding the biophysical principles of mechanobiology and mechanical homeostasis. In doing so, cellular contractile forces were identified as the regulated quantity in tissue equivalents on short time scales, in which deposition and degradation of matrix fibers can be neglected. For longer times, on which the latter mechanisms play a vital role, the thesis proposed a comprehensive set of mechanisms acting on the microscale. These mechanisms can explain how phenomena such as growth or atrophy can arise macroscopically in tissues that are exposed to permanent changes in mechanical loading.

7.2 Outlook

This section collects some of the potential future extensions and applications of the experimental device and the computational model developed in this thesis. The following ideas and considerations are, however, not intended to represent a complete list, but rather to potentially inspire to worthwhile future research in this field.

Extensions to experiments One shortcoming of the presented biaxial bioreactor is its limitation to experiments that last less than 48h. To enable durations up to 7 days, the device would need to allow a change of the experimental medium every two days to ensure sufficient nutrient supply for cells and to avoid contamination with bacteria and fungi. This could be achieved by adding a tube to the bath that is connected to a small pump outside the incubator. Such an extension would allow to also study mass turnover, that is cell-mediated deposition and degradation of collagen fibers, which is negligible for experiments that run less than two days, but crucial to understand homeostasis on longer time scales. In this regard, it might also be worth considering the development of an experimental protocol that is based on fibrin gels rather than collagen gels to be able to easily track newly deposited collagen. Moreover, the effect of the cross-linking enzyme LOX could be studied quantitatively in case of extended experimental durations (Simon et al. 2014).

A second shortcoming of the presented device is that it is so far not possible to exactly determine the thickness and the cross-sectional area of a tested gel sample over time. This could be achieved by adding two cameras to the device, one from the the top and one from the side. Adding some form of markers or micro particles to the gel would additionally allow to track the deformation of the sample. These extensions are necessary for the calculation of important mechanical measures such as Cauchy stresses or the deformation gradient.

Extensions to simulations One major advantage of the computational framework presented in this thesis is its high computational efficiency, which enables the simulation of RVEs with multiple cells and high fiber densities. To be able to further reduce simulation time or scale up

the systems size even more, more suitable preconditioners and linear iterative solvers need to be developed. Despite the very efficient implementation of the required search algorithm, the current bottleneck with regard to realizable system sizes is given by GMRES and ILU (Heroux and Willenbring 2012) being the only selectable linear solver and preconditioner, respectively.

Similarly to the first shortcoming of the experimental device, the computational model currently is restricted to short times scales, that is, less than two day, because it does not capture mass turnover so far, i.e., the deposition and degradation of matrix fibers, which is, however, assumed to be crucial for mechanical homeostasis on longer time scales (Humphrey and Rajagopal 2002, Ambrosi et al. 2010, Cyron et al. 2016, Braeu et al. 2017, Cyron and Humphrey 2017).

Another important extension to the model would be the implementation of a novel form of boundary condition that allows a direct comparison between experimental data and simulation results. This is so far only partially possible, since tissue culture experiments have one traction-free boundary in case of biaxially tested gels and even two in uniaxially tested gels, which is neither mimicked correctly by periodic boundary conditions nor by a free boundary in an RVE in the respective direction. Eichinger et al. (2020) (Paper B) for example showed that the number of free boundaries has a significant impact on the homeostatic plateau value.

Finally, a very simple model for the contraction of cells is deliberately chosen so far. Yet, much research has been done on the actin cytoskeleton in both experimental and computational studies (Mogilner and Oster 2003, Lieleg et al. 2007, 2010, Murtada et al. 2010, Cyron and Wall 2012, Murtada et al. 2012, Müller et al. 2014). Results and models of theses studies could be included to endow this part of the framework with additional biological details.

Further applications of the experimental device Especially interesting and simple would be to rerun the experiments performed in this thesis but use cells with induced defects in cytoskeletal structure or integrin signaling to study the exact roles of specific components of the cellular control system that gives rise to mechanical homeostasis. Similarly, cell treatment with drugs that just target one specific mechanism could provide important insights. Moreover, comparing the behavior of cells stemming from healthy tissue with cells coming from diseased tissue, or testing cancer cells on their ability to sense and regulate matrix mechanics will be tremendously helpful to understand various diseases such as cancer or hypertension. Finally, the precise and quantitative role of important biochemical growth factors such as TGF-β could be studied in the future.

One of the crucial steps of mechanical homeostasis is mechanotransduction, i.e. the translation of mechanical signals at the cell-matrix interface into appropriate intracellular signals, which are then processed by cell-specific signaling pathways. Usually, these systems represent negative feedback loops that counteract changes of the mechanical environment to bring it back to normal. Disruption or malfunction of these internal pathways can, inter alia, lead to altered gene expression and thus a loss of homeostasis. The presented experimental device could be used to test the influence of various (biaxial, static or cyclic) boundary conditions on the expression of specific genes. For this purpose, the messenger RNA (mRNA) of cells could be isolated and reverse-transcribed to complementary DNA (cDNA) at the end of an experiment. Using quantitative-PCR (qPCR), relative changes in gene expression of selected targets including ECM-remodeling proteins such as collagen type 1 or matrix metalloproteinase-2 (MMP2), inflammatory markers, or negative feedback mechanisms regulating proteins such as regulator of G-protein signaling-2 (RGS2) could be studied.

A further worthwhile experimental study would be the investigation of the influence of pH-value and temperature on mechanobiological processes. Both of these parameters can be adjusted and controlled easily during the experiment and are of great importance for many pathological processes. They can, for example, be assumed to be abnormal in case of inflammation.

Further applications of the computational model Cell migration is a crucial mechanism in many (patho-)physiological processes, such as wound healing, or metastasis and cancer invasion, the extension of cancer cells into neighboring tissues. Multiple articles have been published discussing the migration of cells on flat, two-dimensional substrates, yet, the molecular and biophysical principles governing migration in three-dimensional environments remain mostly elusive (Yamada and Sixt 2019). Cells migrate by following a cycle consisting of focal adhesion generation, contraction of the actin-cytoskeleton, and release of the focal adhesion, all mechanisms that are covered by the presented computational model. It is therefore well suited to study how changes in the environmental conditions influence, for example, cell migration speed and direction (Bangasser et al. 2013, Elosegui-Artola and Oria 2020). Experimentally observed phenomena such as the random migration of cells (Wolf et al. 2013, Wu et al. 2014), durotaxis (cells tend to move toward stiffer regions of tissues (DuChez et al. 2019); preliminary simulations of durotaxis are shown in Fig. 7.1), haptotaxis (dependence on ligand concentration (Taraboletti et al. 1987)), and contact guidance (cells tend to move in the direction of aligned fibers (Weigelin et al. 2012, Sharma et al. 2012)) could all be investigated in detail. Moreover, the computational model is readily applicable to study the influence of ECM cross-linking (covalent vs. non-covalent) (Grossman et al. 2016), the presence and size of pores in the matrix (Wolf et al. 2013), and how multiple cells communicate mechanically with each other (Shi et al. 2013, Baker et al. 2015, Mann et al. 2019) and how this affects cell migration.

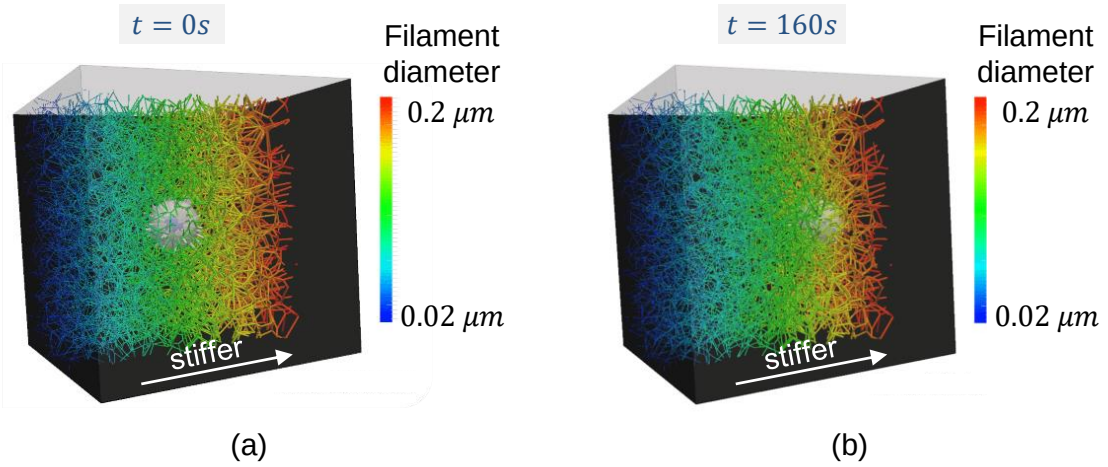

Figure 7.1: Simulated migration of a cell immersed in a fibrous collagen matrix with a linear stiffness gradient. Consistent with experimental observations, cells move toward higher stiffnesses.

Moreover, the simulated RVE could be made more realistic to real soft tissues by adding further fiber types such as elastin or GAGs (with largely differing mechanical properties), multiple

types of cells (e.g. characterized by different contraction rates), and multiple types of cross-linking enzymes. All of this could be done without further implementation and would be a logical next step. The possibility to account for the heterogeneity of soft tissues with respect to diverse types of filaments varying both in mechanical properties and cross-link affinity contribute to the generality of the developed framework.

Finally, daring to reflect on the big picture, the model will eventually be used by clinical practitioners, e.g., in the computer-aided diagnosis of aneurysms to provide improved patient-specific predictions for aneurysmal enlargement and rupture risk.

Appendices

Appendix A

Paper A

Mechanical homeostasis in tissue equivalents: a review

Jonas F. Eichinger, Lea J. Haeusel, Daniel Paukner, Roland C. Aydin, Jay D. Humphrey, Christian J. Cyron

published in

Biomechanics and Modeling in Mechanobiology, 10.1007/s10237-021-01433-9

Biomechanics and Modeling in Mechanobiology
https://doi.org/10.1007/s10237-021-01433-9

REVIEW PAPER

Mechanical homeostasis in tissue equivalents: a review

Jonas F. Eichinger[1,3] · Lea J. Haeusel[1] · Daniel Paukner[3,4] · Roland C. Aydin[4] · Jay D. Humphrey[2] · Christian J. Cyron[3,4]

Received: 12 October 2020 / Accepted: 4 February 2021

Abstract
There is substantial evidence that growth and remodeling of load bearing soft biological tissues is to a large extent controlled by mechanical factors. Mechanical homeostasis, which describes the natural tendency of such tissues to establish, maintain, or restore a preferred mechanical state, is thought to be one mechanism by which such control is achieved across multiple scales. Yet, many questions remain regarding what promotes or prevents homeostasis. Tissue equivalents, such as collagen gels seeded with living cells, have become an important tool to address these open questions under well-defined, though limited, conditions. This article briefly reviews the current state of research in this area. It summarizes, categorizes, and compares experimental observations from the literature that focus on the development of tension in tissue equivalents. It focuses primarily on uniaxial and biaxial experimental studies, which are well-suited for quantifying interactions between mechanics and biology. The article concludes with a brief discussion of key questions for future research in this field.

Keywords Mechanical homeostasis · Tensional homeostasis · Mechanobiology · Mechanoregulation · Mechanotransduction · Mechanosensation · Growth and remodeling

1 Introduction

The important role of mechanics in governing biological form and function has been known since the time of Galileo Galilei (1564–1641) and Giovanni Borelli (1608–1667), that is, for at least four centuries (Cyron and Humphrey 2017; Piolanti et al. 2018). Yet, it was only about a century ago that Henry Gassett Davis and Julius Wolff succeeded in condensing this general notion into two precise statements, Davis' law in 1867 and Wolff's law in 1892, which established relations between mechanical loading and growth and remodeling (G&R) in soft and hard tissues, respectively (Davis 1867; Wolff 1892). Building on the ideas of Claude Bernard in 1865 (Bernard 1865), Walter Cannon introduced the central concept of homeostasis in the 1920s (Cannon 1929), as summarized in the influential book "The Wisdom of the Body" in 1932 (Cannon 1932), which introduces the concept of homeostasis as "coordinated physiological reactions which maintain most of the steady states in the body". These laws and concepts can be considered as landmarks paving the way to modern mechanobiology by exposing the fundamental importance of mechanically regulated processes for tissue health and disease.

Due to rapidly improving experimental and computational techniques and technologies, substantial progress has been made in mechanobiology, especially since the mid-1970s. A corner stone of nearly all approaches is the hypothesis that there exists a preferred mechanical state—often referred to as homeostatic—toward which mechanobiological activity is targeted. This generally accepted assumption goes back at least to the mid-1960s and the seminal study of Wolinsky and Glagov (1967), which showed that the aorta in various mammals develops such that the tension per medial lamellar unit is nearly the same (~ 2 N/m), implying a "target" value of medial stress on the order of 10^2 kPa. Twenty years later, Bissel and Aggeler (1987) introduced the concept of dynamic reciprocity, presenting the idea of

✉ Christian J. Cyron
christian.cyron@tuhh.de

1 Institute for Computational Mechanics, Technical University of Munich, 85748 Munich, Germany

2 Department of Biomedical Engineering, Yale University, New Haven, CT 06520, USA

3 Institute of Continuum and Materials Mechanics, Hamburg University of Technology, 21073 Hamburg, Germany

4 Institute of Material Systems Modeling, Helmholtz-Zentrum Geesthacht, 21502 Geesthacht, Germany

Published online: 08 March 2021

dynamic feedback loops between cells and the surrounding extracellular matrix (ECM) that ensure that this target state is maintained within a certain tolerance. Since then, changes in the mechanical properties of the ECM have been shown to effect crucial cellular processes such as migration (Grinnell and Petroll 2010; Hall et al. 2016; Xie et al. 2017; Kim et al. 2019), differentiation (Chiquet et al. 2009; Mammoto et al. 2012; Zemel 2015), and even survival (Bates et al. 1995; Zhu et al. 2002; Schwartz 2002; Sukharev and Sachs 2012) (outside-in effect). Conversely, cells establish tissue form and function during development, maintain tissue integrity in health, and adapt tissue in response to perturbations such as injury or disease (Cox and Erler 2011; Lu et al. 2011; Ross et al. 2013; Bonnans et al. 2014; Humphrey et al. 2014a) (inside-out effect). In short, cells are equipped with the complementary processes of mechanosensation and mechanoregulation which are assumed to be crucially involved in the promotion of tissue health and proper functionality. Cells constantly perceive cues from their extracellular environment, transduce them into intracellular signals, and react, for example, by adapting their contractile state. Transmembrane receptors such as integrins physically connect the actin cytoskeleton inside the cell to fibers of the ECM and thus enable the transfer of mechanical loads (Jiang et al. 2006; Cavalcanti-Adam et al. 2007; Lerche et al. 2019).

Among the many different experimental approaches for studying the cell-matrix interactions that govern such biological form and function, tissue equivalents have emerged as particularly useful. Often formed as reconstituted collagen- or fibrin-based gels, cell-seeded tissue equivalents are typically meant to be simple in vitro model systems, not ex vivo tissue-engineered materials for implantation in regenerative medicine. Our focus is on the use of tissue equivalents for studying the underlying mechanobiology; we leave to others the review of tissue-engineered constructs, often beginning as cell-seeded polymeric scaffolds. We note, nonetheless, that some investigators use the term tissue-engineered to describe tissues fabricated for basic science studies, including via decellularization and subsequent cell-seeding, and that have revealed important mechanobiological effects, as, for example, that aberrant matrix can corrupt the behavior of otherwise normal cells (Sewanan et al. 2019).

In a seminal paper on tissue equivalents, Brown et al. (1998) wrote: "We would define tensional homeostasis as the control mechanism by which fibroblasts establish a tension within their extracellular collagenous matrix and maintain its level against opposing influences of external loading." This definition reflected well their specific observations in fibroblast-seeded collagen gels under particular conditions and further highlighted the importance of homeostasis in mechanobiology. With an additional twenty-plus years of hindsight, Stamenović and Smith (2020) wrote, "we define tensional homeostasis as the ability to maintain a consistent level of tension, with a low variability around a set point, across multiple length scales." This latter definition is closer in concept to that put forth by Cannon (1929, 1932) who introduced the word homeostasis, noting his careful choice of the prefix "homeo" (derived from the ancient Greek "homoios" meaning "similar", thus allowing some variation) rather than "homo" (derived from the ancient Greek "homos" meaning the "same", implying rigid constancy). Some accounts in the literature appear to misinterpret data within this framework by ignoring the possibility of maintaining a steady state within a range, perhaps in part because the allowable extent of such a range is not easily known. We emphasize, further, that it is not yet clear what the cells sense (force, extension, stiffness, compliance, etc.), though it is clear that some cells are more responsive to shearing loads (endothelial), some to tensile loads (fibroblasts), and some to compressive loads (chondrocytes). Hence, we suggest that "tensional homeostasis" is too narrow of a definition, with possible further ambiguities arising due to individual interpretations of what a tension is: a tensile force (units of N), an actual tension (units of N/m, as in surface tension), or a tensile stress (units of N/m^2). For these and other reasons, we prefer "mechanical homeostasis" as a more general term to encompass different responses by different cell types under different conditions and to acknowledge that we as a community continue to seek what cells sense and regulate. One can thus define mechanical homeostasis broadly as a ubiquitous mechanobiological process by which soft tissues seek to maintain key regulated variables within a range near a preferred value, often called a homeostatic target or set-point. Importantly, homeostatic targets or ranges adapt in some cases (Davies 2016) and additional terms, including allostasis and rheostasis, have been used in such cases in different fields, including those focusing on different types of stressors (e.g., emotional stress; McEwen and Wingfield 2010). Alternatively, homeostatic targets or ranges can be overridden in other cases, including chronic inflammation (Chovatiya and Medzhitov 2014). Indeed, it has been suggested that it is the very adaptivity of homeostatic targets that renders particular biological systems susceptible to override and thus to particular diseases (Kotas and Medzhitov 2015). Notwithstanding the important roles of the immune system in promoting or preventing mechanical homeostasis, particularly by macrophages (Wynn et al. 2013; Okabe and Medzhitov 2016), we focus herein on mechanobiological responses over modest ranges from normal by cells such as fibroblasts, which have primary responsibility for establishing, maintaining, remodeling, and repairing extracellular matrix (Tomasek et al. 2002).

Awareness of the importance of mechanobiology and in particular mechanical homeostasis continues to grow in medicine and biomedical engineering. Some of the most important causes of mortality and morbidity in

industrialized countries are closely linked to mechanobiology. These include diverse cardiovascular diseases and cancer (Weaver et al. 1997; Boettiger et al. 2005; Yeung et al. 2005; Weninger et al. 2009; Butcher et al. 2009; Lu et al. 2012). For example, thoracic aortic aneurysms appear to arise in part from dysfunctional mechanosensing or mechanoregulation of the ECM (Humphrey et al. 2014b), whereas abdominal aortic aneurysms (AAAs) (Fig. 1a, b) may experience continued enlargement due to mechanobiological instabilities (Cyron and Humphrey 2014; Cyron et al. 2014). While advances in medical imaging have increased the number of diagnosed aneurysms, a comprehensive understanding of their initiation and natural history, ranging from the sub-cellular to the organ scale, still remains elusive. There exists, therefore, a considerable opportunity to use allied methods, including in vitro studies of tissue equivalents (Fig. 1). Model systems—typically cell-seeded fibrin (Sander et al. 2011) or collagen (Sander and Barocas 2008) gels—are much simpler and therefore suitable for precise quantitative in vitro studies of cell-matrix interactions due to a greatly reduced number of confounding factors and interdependencies (Fig. 1c, d).

In this article, we review the current understanding of mechanical homeostasis in three-dimensional, gel-based tissue equivalents by summarizing and comparing results gained in different types of tissue culture experiments. Finally, we discuss limitations of the available data, raise open questions, and consider future directions of this emerging field of research.

2 Using tissue equivalents to study mechanical homeostasis in soft tissues

Mechanobiology focuses on understanding effects of mechanical stimuli on particular cellular actions. To study this, both the stimulus and the response need to be measurable and controllable; in other words, it is best to design experiments representing simple boundary and initial value problems that simplify data analysis and interpretation. Toward this end, in vitro studies using planar (rectangular or annular) or cylindrical tissue equivalents have been preferred. It is worth highlighting that cells in three-dimensional in vitro environments such as collagen or fibrin gels behave differently compared to those exposed to two-dimensional in vitro environments. The latter include micro-patterned substrates such as petri dishes made of plastic or glass coated with collagen or fibronectin. While such two-dimensional setups are simple, they cannot adequately mimic several important factors of the physiological environment in vivo. In fact, the dimensionality of the substrate interacting with cells has been shown to crucially influence

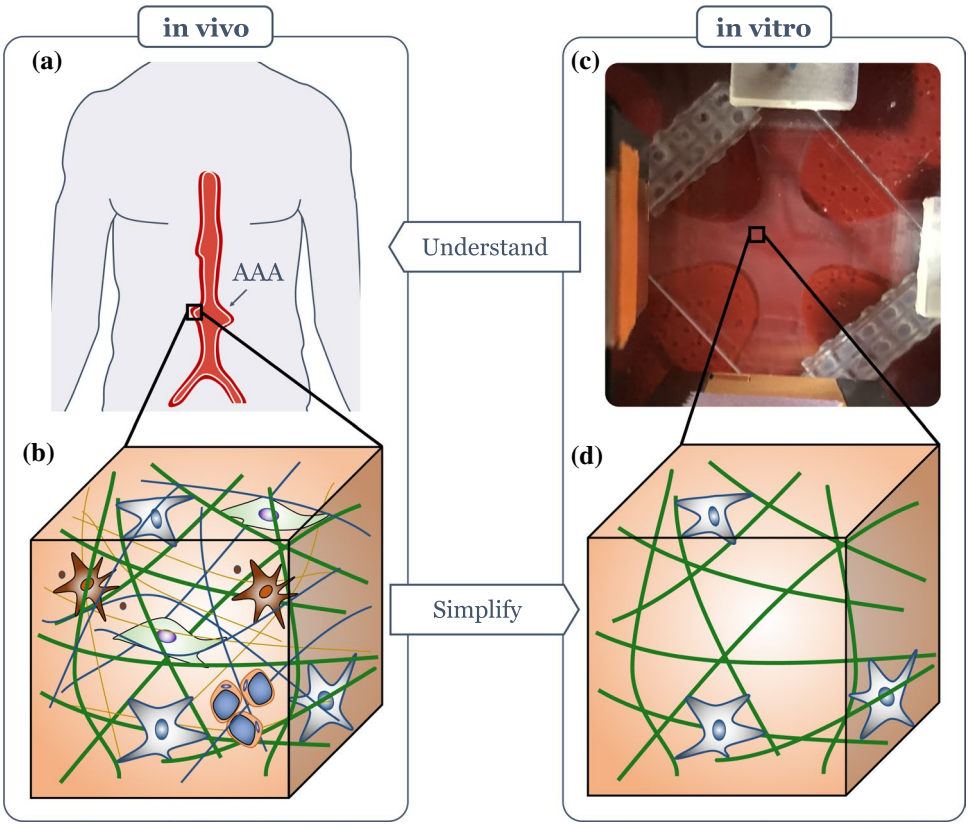

Fig. 1 Cell-seeded collagen gels as tissue equivalents can provide information relevant to mechanical homeostasis of soft tissues. **a** Illustration of a patient with a local dilatation of the aorta (i.e., an aneurysm); due to ill-controlled mechanobiological processes; such aneurysms can continue to grow over years and often finally rupture, resulting in high mortality and morbidity; **b** in vivo studies often cannot provide the fine control needed to assess the cell-ECM interactions that are fundamental to promoting or preventing homeostasis, and thus understanding disease progression. **c** Cell-seeded collagen or fibrin gels have proven to be simple but powerful model systems to study soft tissue mechanobiology. **d** The much lower complexity of cell-seeded collagen gels compared to native ECM makes them useful for studying the fundamental cell-matrix interactions, often one cell type at a time

cellular processes such as cell proliferation, survival, differentiation, and migration; see Baker and Chen (2012), Friedl et al. (2012), and Bonnier et al. (2015). For a review of two-dimensional versus three-dimensional culture environments, see Baker and Chen (2012) and Duval et al. (2017). The studies with three-dimensional tissue equivalents can be classified further by the mechanical boundary conditions imposed experimentally. So far, free-floating (mostly circular), uniaxially constrained or extended, and biaxially constrained or extended cell-seeded gels have been used in most experiments (Fig. 2). Cylindrical tissue equivalents that generate hoop stresses and circumferential fiber alignment if set around a non-adhesive mandrel have been used similarly (Barocas et al. 1998; Isenberg et al. 2006), but are less common and are not discussed in detail here. In most cases, cylindrical geometries are motivated by tissue engineering applications, including vascular grafts.

2.1 Circular free-floating tissue equivalents

First, free-floating collagen discs were introduced by Bell et al. (1979), who showed that the gels compact significantly (~ 90% Fig. 2a) due to cellular mechanobiological activity over a period of days. Free-floating discs are experimentally simple to create and handle and thus are favorable for qualitative studies (Steinberg et al. 1980; Buttle and Ehrlich 1983; Grinnell and Lamke 1984; Ehrlich et al. 1986; Woodley et al. 1991; Schiro et al. 1991; Kelynack et al. 2000; Ehrlich and Rittenberg 2000; Grinnell 2000; Grinnell and Ho 2002; Redden and Doolin 2003; Orlandi et al. 2005; Stevenson et al. 2010; Grinnell and Petroll 2010). Nevertheless, due to the relatively complex residual stress fields that develop (Simon et al. 2012, 2014), it can be challenging to determine key parameters or mechanisms of soft tissue mechanobiology quantitatively from experiments with free-floating discs. For example, as mentioned before, one key question is how mechanical stimuli are transduced and then drive cellular actions via corresponding signaling pathways. To obtain a quantitative understanding of this problem, experiments are required where both the mechanical loads and the subsequent cellular responses can be quantified accurately. Given that prior studies using free-floating gels have not interpreted regional cellular responses in terms of the complex inhomogenous stress field (compressive and tensile stresses, which induce regional anisotropies), this review focuses instead on uniaxial and biaxial testing studies, which were introduced several decades after the first free-floating gels were studied, in part, to overcome limitations of the latter. For a review of free-floating collagen gels, see Dallon and Ehrlich (2008) and Simon and Humphrey (2014). Here, therefore, we turn our attention to uniaxial and biaxial studies wherein stress/strain fields can be homogeneous if studied sufficiently far from the end-effects at the boundaries.

2.2 Uniaxially constrained tissue equivalents

General setup For quantitative studies of how cells respond to external mechanical loading, uniaxially constrained or extended tissue equivalents (Fig. 2b) were developed. Unlike free-floating gels, uniaxial setups exhibit a largely homogeneous tension field (within the central region), with measurements of the net uniaxial loading straightforward.

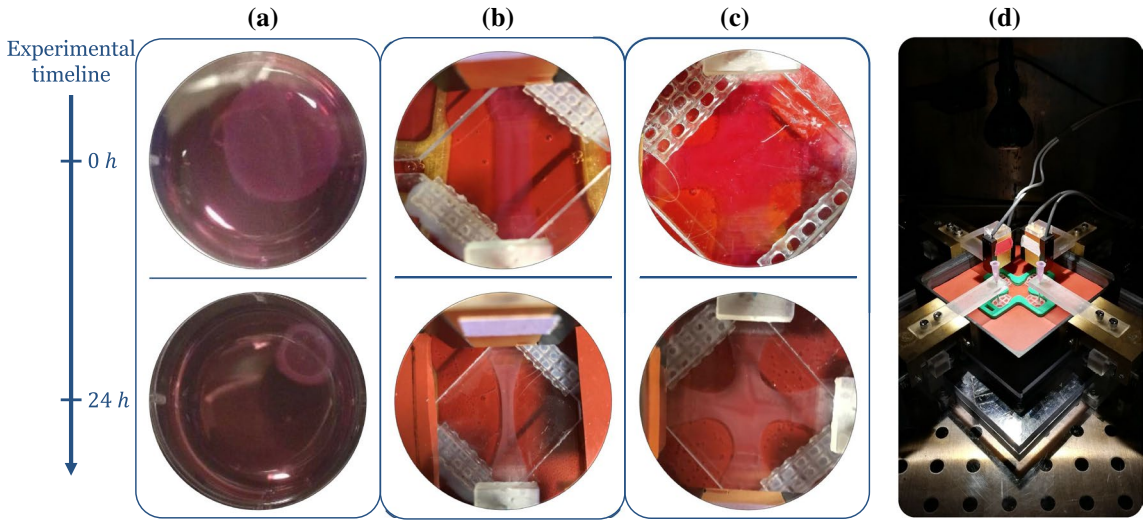

Fig. 2 Free-floating (**a**), uniaxially constrained (**b**), and biaxially constrained (**c**) fibroblast-seeded collagen gels (i.e., tissue equivalents) are observed to contract substantially over the first hours to days. Cells residing in the gel initially spread and attach to surrounding collagen fibers. Cellular contraction then compacts the surrounding matrix thus stressing the fibers. **d** Biaxial testing device reported in Eichinger et al. (2020). Sensors are installed along two axes to record the development of tension in a cruciform gel

This makes it easier to quantify how a certain mechanical target state evolves over time, and if and how it is restored after perturbations. Most uniaxial experiments with tissue equivalents follow a similar approach. First, a gel is fabricated by combining collagen, cells, Dulbecco's modified Eagle's medium (DMEM), a buffer, and an antibiotic (for more details, see supplementary Tables S1 and S2). The collagen solution is then cast into a rectangular mold within a device where it sets around two insets, one of which can be connected to a motor that can impose uniaxial strain. The other inset, residing on the opposite side of the gel, is connected to a force transducer such that forces imposed on or generated within the gel can be measured. Typically, the gel is initially free of mechanical load. If, however, the total length of the gel is kept constant by the device, one observes that a substantial tension builds up over a period of several hours due to cell-mediated contraction of the gel (phase I), often reaching a steady state (phase II) (Fig. 3). This steady state is often referred to as a homeostatic state—thus reflecting Brown's tensional homeostasis. As the tissue evolves, the initial rectangular shape of the gel typically changes to a more dog-bone like shape because cell-mediated contraction acts not only along the gel axis, but also transversely, where it is not impeded as the lateral surface remains traction-free (Fig. 2b). Studies with tissue equivalents in such a uniaxial setting have addressed in particular the following aspects so far.

Mechanical homeostasis In contrast to classical engineering materials, living soft tissues apparently seek to establish and maintain a preferred mechanical state that is not stress-free. Delvoye et al. (1991) were the first to show that uniaxially constrained collagen gels seeded with dermal fibroblasts exhibit a characteristic behavior with the aforementioned two distinct stages. During the first 6 – 12 h, a tensile force increases rapidly (phase I) before entering a steady state ('homeostatic state') with neither further increase nor decrease (phase II). When this tension is perturbed by slightly stretching or releasing a gel that has already reached phase II, tension returns toward the prior level within around 1 h. To date, it remains controversial within what tolerance the prior level is restored, mainly or only to some extent, but we must recall here Cannon's particular choice of the prefix homeo, meaning "similar", not "the same". The two stages observed by Delvoye et al. (1991) were confirmed by Eastwood et al. (1994, 1996), who found that even cell-free constrained collagen gels tend to build up some tension during the first few hours of maturation, presumably due to entanglement and cross-linking of fibers in the gel. As noted earlier, it was a few years later that this group coined the terminology "tensional homeostasis" to describe their observations in these uniaxially constrained, fibroblast-populated gels under particular fabrication and culture conditions. Namely, they examined cell-populated collagen-glycosaminoglycan sponges subjected to different loading protocols, including cyclical over- and underloading, cyclical median loading, and cyclical incremental loading, to study reactions of the gels triggered by these diverse external stimuli. When gels were subjected to a sudden stretch or release, gels were observed to return toward their prior tension level in the following 15 min. Especially

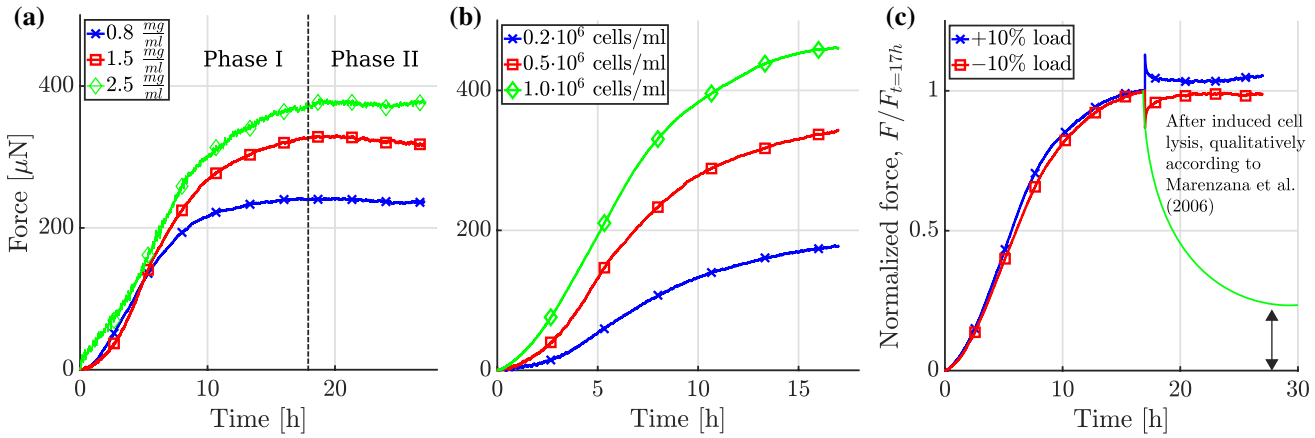

Fig. 3 In uniaxially constrained tissue equivalents, the measured tensile force evolves in two characteristic phases: a steep increase (phase I) followed by a plateau (phase II). Here, we show experimental data from Eichinger et al. (2020). Each curve is an average of three identical experiments. **a** Dependence of the plateau value of tension on collagen concentration in the gel with a constant cell density of $0.5 \cdot 10^6$cells/ml. Higher collagen concentrations lead to higher steady state values. **b** Influence of cell density for a collagen concentration of 1.5 mg/ml : Higher cell densities lead to both a steeper initial increase and a higher plateau value of the measured force. **c** If the tissue equivalent (collagen concentration 1.5 mg/ml , cell density $1.0 \cdot 10^6$ cells/ml) is suddenly stretched or released after having reached the plateau state, force returns toward its value prior to this perturbation. The monotonically decreasing force qualitatively illustrates the expected evolution in case of cell lysis according to Marenzana et al. (2006); the fraction of the tensile force remaining in the gel has been called residual matrix tension (RMT)

notable is that the tension in the gels was observed to re-increase immediately after release, which led the authors to the conclusion that viscoelastic effects alone are not sufficient to explain the observed behavior.

The two characteristic stages of this so-called tensional homeostasis and the tendency of tissue equivalents to restore their prior tension level after perturbation were confirmed by Ezra et al. (2010). They observed the homeostatic state to arise during the first 8 h. When this state was perturbed by a series of alternate stretch and release steps every 30 min, tension was observed to return toward the prior value during the 30 min between two consecutive perturbation steps. However, the 30 min relaxation periods between two subsequent perturbations were too short to answer the question within which tolerance the homeostatic state is restored after a perturbation. Generally, Ezra et al. (2010) found that gels reacted more strongly to perturbations if their amplitude was higher. Very similar results were reported by Bisson et al. (2009), where gels were observed to counteract uniaxially applied loads. In cases of reduced loading, gels reacted by increasing tension; in cases of increased loading, gels reacted by decreasing tension. Furthermore, it was observed that fibroblasts from diseased fibrotic tissue did not replicate the aforementioned characteristic two-stage behavior—steep increase of tissue tension (phase I) followed by a plateau (phase II), because they failed to reach the second stage characterized by steady state at least within the same time interval.

The observations summarized above were further supported by Marenzana et al. (2006), who studied the effect of cytochalasin D. This agent disrupts the actin cytoskeleton and thereby eliminates active cellular contraction from the gel. When added to the culture medium after 24 h, when the homeostatic state had been reached, it induced a rapid and total decline of the tension in gels populated with human dermal fibroblasts. No residual matrix tension (RMT) was measured in this case. Interestingly, in gels populated with fibroblasts from rat tendon, a substantial residual tension was observed even 12 h after treatment with cytochalasin D. Hypo-osmotic cell lysis via replacement of the culture medium with distilled water gave similar results regarding the measurable RMT. When comparing the results of adding cytochalasin D after 4 h and after 60 h in culture, RMT seemed to increase linearly with time in culture, making up a growing fraction of the tension before treatment. RMT was also higher when gels had been exposed to cyclical loading. Moreover, it was shown that cell-seeded collagen gels after 24 h had a significantly higher stiffness than cell-free gels after the same time in culture. Collectively, these observations suggest that at least certain types of fibroblasts, such as the ones from rat tendon, remodel the matrix surrounding them in a way that is not purely elastic (Yamato et al. 1995; Sawhney and Howard 2002). Such cells rather appear to start by elastically contracting their surrounding gel; subsequently, they seem to entrench an increasing fraction of this tension, possibly because this is energetically more favorable than maintaining it over a prolonged time by active cellular tension. It remains an open question why cyclical loading increases RMT. It is noteworthy that Kolodney and Wysolmerski (1992) did not observe any RMT for chick embryo fibroblasts or endothelial cells, despite following an approach very similar to the one of Marenzana et al. (2006). This further supports the hypothesis that the entrenchment of matrix tension—perhaps via physical entanglements, but also via matrix cross-linking via transglutaminases (when remodeled) or lysyl oxidases (when synthesized) as noted before (Simon et al. 2014)—depends on the cell type and experimental conditions, including the type of matrix used to constitute the gel and the culture media (e.g., whether containing copper or not, noting that enzymes such as lysyl oxidase are copper dependent).

Influence of cell density and matrix composition on tension When using both calf skin fibroblasts (Delvoye et al. 1991) and NIH 3T3 fibroblasts (Eichinger et al. 2020), tension in the homeostatic state of uniaxial tissue equivalents increases linearly with collagen concentration. Notably, Eichinger et al. (2020) demonstrated that higher collagen concentrations increase the steady state tension but not the rate at which tension is built up initially. Moreover, tissue tension increases with cell density, either linearly (Delvoye et al. 1991; Eichinger et al. 2020) or nonlinearly (Legant et al. 2009; Jin et al. 2015) depending on the experimental conditions.

Increasing the collagen concentration also increases the gel stiffness (Alcaraz et al. 2011; Miroshnikova et al. 2011; Hall et al. 2016; Joshi et al. 2018). Therefore, one may hypothesize that the reason for the effect of the collagen concentration on the homeostatic tension is that cells often tend to respond more to a stiffer mechanical environment by increasing contraction (Ghibaudo et al. 2008; Califano and Reinhart-King 2010; Schiller and Fässler 2013; Cheng et al. 2013; Oria et al. 2014; Zhu et al. 2016). This hypothesis is supported by observations of Zhao (2014), who statically prestretched microtissues, which increased their stiffness, and subsequently observed higher cell-mediated tissue tension. It is interesting to note that the alignment of fibers and cells by static loading can reorganize the tissue, which can increase its anisotropic strength, stiffness, and ability to contract (Grenier et al. 2005). In general, mechanical homeostasis is promoted by the cells not only under static but also under dynamic loading (Walker et al. 2020), which can thus also be used to alter tissue stiffness.

It is noteworthy that Karamichos et al. (2007) reported that human dermal fibroblasts produced a much lower homeostatic tension and also a much slower development of the homeostatic tension plateau if exposed to an initially

prestretched matrix. This effect was the more pronounced the higher the initial prestretch. Given that prestretch stiffens the collagen matrix, these observations may seem at first glance a contradiction to the ones of Delvoye et al. (1991), Zhao (2014), and Eichinger et al. (2020). Yet, both may be brought into agreement by noting that cells have been found to respond to changes in stiffness in a biphasic manner (Chan and Odde 2008), that is, there may exist a certain regime where cellular tension increases with the stiffness of the mechanical environment and another regime where the opposite is true. A similar phenomenon is also known for cell migration (Bangasser et al. 2017).

It has been shown that the effective stiffness that is sensed by the cells and that is determined by the matrix stiffness and the stiffness of the boundary (noting that stress and stiffness fields can often be computed away from the end effects, but cells near the boundaries yet sense and respond to their local environment) needs be considered for mechanoregulation (Kural and Billiar 2016). In particular, Legant et al. (2009) observed that both a higher gel stiffness and a stiffer fixation of the tissue at the boundary led to a higher cell-mediated tension in the tissue.

Role of cell type and tissue origin Multiple studies have shown that both the type of the cells used in tissue equivalents as well as the type of tissue from which they have been extracted affect the homeostatic tension. Delvoye et al. (1991) reported that calf dermal fibroblasts produced higher tension than human dermal fibroblasts. Active tension generated by chick embryo fibroblasts was found to be higher than that generated by a monolayer of human umbilical vein endothelial cells (Kolodney and Wysolmerski 1992). It is possible that the latter is not a consequence of the different cell type but rather because the endothelial cells were seeded on the surface of pre-polymerized gels, not embedded within the gel. On the other hand, it is also noteworthy that the endothelial cells reached their homeostatic state only after 4–5 days, whereas the fibroblasts did so in less than 24 h, which may indicate a more pronounced contractile activity of the fibroblasts. Interestingly, neither the chick embryo fibroblasts nor the endothelial cells entrenched any RMT, proven by a rapid decay of the tension to zero after addition of Cytochalasin D. By contrast, Marenzana et al. (2006) reported RMT for rat tendon fibroblasts as mentioned above, which suggests that generation of RMT may depend on factors not yet fully understood. Also Eastwood et al. (1996) demonstrated considerable dependency on the cell type and cell line for both the level of homeostatic tension and the rate at which it is built up initially. Rabbit tendon fibroblasts, for example, only started contracting after 14 h in culture and produced much less tension than human dermal fibroblasts. It was also found that there is a difference in homeostatic tension between human dermal fibroblasts from the same tissue sample depending on whether the fibroblasts were grown by explant migration or extracted by bacterial collagenase digestion. Fibroblasts grown from explants generated a tension approximately 60% higher than the one generated by fibroblasts extracted with collagenase. This effect was attributed to a natural selection bias. The cells that migrated most strongly were favored by the explant growth extraction process so that this process selected a sub-population of cells that distinguished itself by unusually strong cellular contractility. Note that Ezra et al. (2010) studied mechanical homeostasis with occular fibroblasts from individuals with and without floppy eyelid syndrome. The latter is associated with a reduced stiffness of the tarsal plate and thus a supposedly higher (dynamic) tension in vivo. Interestingly, fibroblasts from individuals with floppy eyelid syndrome were also observed to establish a higher homoestatic tension when extracted from their natural environment and studied in vitro. A possible explanation for this is that cells may alter their homeostatic target state when exposed to altered mechanical or possibly biochemical conditions over a prolonged period. Such a possibility is consistent with a generalized concept of adaptive homeostasis (Davies 2016).

Porcine smooth muscle cells from different layers of the pulmonary artery were found to establish (within around one day) a homeostatic tension at different speeds and with different magnitudes. Both were higher for cells from the outer medial layer than for cells from the inner medial layer (Hall et al. 2007). The tension generated by fibroblasts from different regions of the human eye were studied by Dahlmann-Noor et al. (2007). Corneal fibroblasts established a much higher tension than fibroblasts from Tenon's layer. The tension generated by scleral fibroblasts was barely measurable. Notably, fibroblasts from the same organ differ significantly in their ability to generate tension. The authors also determined the intrinsic cellular tension of each fibroblast type, which was defined as the plateau tension divided by the mean cell volume. When comparing intrinsic tension with the ones measured during the experiment, the intrinsic cellular tension was at least of a similar order of magnitude. Cell size could therefore be an important factor influencing the homeostatic plateau level of tension. It is worth mentioning that Bisson et al. (2004, 2009) observed for Dupuytren's fibroblasts a significantly higher tension than for control fibroblasts but no plateau of tension. A likely explanation for the latter phenomenon is that for these cells the time to reach the homeostatic state was simply longer than the period for which the experiments were run. Another possible explanation would be the loss of the ability of these fibroblasts to control the mechanical state of their surrounding tissue. Interestingly, they also found that these cells reacted after the first of four consecutive uniaxial overloading events with a further increase in contraction, that is, not following the concept of homeostasis which would suggest a reduced contraction so that the gel tension returns toward the preferred

plateau value. An uncontrolled contraction of fibroblasts in Dupuytren's tissue, regardless of the mechanical stimulus, could explain why patients stretching their fingers to overcome the disease particularly suffer from severe disease. Finally, Sawadkar et al. (2020) found that tendon fibroblasts produced lower tension with an increasing passage number.

Role of growth factors As reported by Brown et al. (2002), TGF-β1 elevates both the rate and extent of cellular tension generation, although only up to a certain saturation value. TGF-β1 increases cell tension and this may trigger integrin expression and contractile protein expression, and thereby enable higher tissue tension (Ignotz and Massague 1986; Brown et al. 2002). Note that Bisson et al. (2009) demonstrated that both the early contraction rate after 2 h and the rate after 20 h of Dupuytren's fibroblasts was significantly increased when stimulated with TGF-β1. Notably, TGF-β1 seems to affect also the cells' response to external mechanical loads. If a tissue equivalent in its homeostatic state is stretched, mechanical homeostasis typically ensures a subsequent decay of the tension back toward the homeostatic level, which naturally requires a decrease in the contractile activity of the cells in the tissue equivalent. However, when the TGF-β1 treated cell-seeded gels were exposed in Bisson et al. (2009) to four consecutive uniaxial overloading events by rapidly increasing the length of the gel, a further increase was observed during the first three of these load steps. This suggests that the nodule and cord fibroblasts used in this experiment responded to the external stretch not by a decrease but rather by an increase of their contractile activity.

TGF-β1 also appears to affect inelastic matrix remodeling. TGF-β1 increases not only the overall tension generation by the cells, but also the mean RMT measurable after addition of Cytochalasin D (Marenzana et al. 2006). However, the ratio of RMT after addition of Cytochalasin D and the tension prior to the addition of Cytochalasin D was much smaller for TGF-β1 treated cells compared to cultures without TGF-β1, indicating that a lower percentage of tension is entrenched in the matrix.

Brown et al. (2002) also investigated effects of the concentration of fetal bovine serum (FBS) in the experimental culture medium. They found that in a medium with a concentration of 2%, the tension rose more slowly and to a lower homeostatic value compared to a medium with a concentration of 10% FBS. The use of experimental medium without any FBS resulted in no tension generation. An increase in total tension generation for increasing concentrations of FBS was shown by Delvoye et al. (1991).

Cell-matrix interactions Cell-matrix interactions rely on the proper interplay of multiple components and substances. Kolodney and Wysolmerski (1992) studied the role of different parts of the cytoskeleton by treating the gels with drugs that selectively deactivated or disrupted particular constituents or interactions within the cytoskeleton. When Cytochalasin D—causing the disruption of actin filaments—was added to the culture medium after the plateau state had been reached, the entire tension disappeared rapidly for both chick embryo fibroblasts and human vein endothelial cells. These findings highlight that actin filaments are essential for mechanical homeostasis, both sensing and regulating the matrix. Conversely, treatment with the microtubule-disrupting drug nocodazole increased gel tension roughly by a factor of 2. Intact microtubules support cell shape and act against the tension of the actin cytoskeleton. Therefore, their disintegration may be expected to increase the contractile tension exerted by the cell on the surrounding tissue. Sethi et al. (2002) found on the basis of cell-populated glycosaminoglycan sponges that cells use their distinct receptor-ligand systems in a sequential order to exert tension on the surrounding matrix. Cells first attach through their fibronectin receptors, followed by their vitronectin receptors, and finally through their collagen receptors. It appears that if one of these stages is left out, cells can no longer generate the full tension through normal collagen attachment.

2.3 Biaxially constrained tissue equivalents

The inability of uniaxially constrained tissue equivalents to reproduce bi- or triaxial stress or strain states, which prevail in vivo, motivated the development of biaxial testing devices in the 2000s (Fig. 2d) (Knezevic et al. 2002; Thomopoulos et al. 2005, 2007; Humphrey et al. 2008; Sander et al. 2009; Hu et al. 2009, 2013; Lee et al. 2018; Eichinger et al. 2020). In many cases, however, biaxial settings have been used mainly for fairly general studies of fiber alignment and mechanical properties. Biaxial setups usually follow an approach very similar to the one of uniaxial ones. A premixed matrix solution containing a prescribed number of cells is cast into a biaxial mold (mostly square-shaped or cruciform-shaped (Fig. 2c)) and is then allowed to set for some time. Insets are used on four sides so that weights or motors can be connected to the gel to apply external loading, or to constrain the gel in two directions to study cell-mediated compaction and the associated generation of tension. The following section briefly reviews key findings from biaxial experiments with tissue equivalents.

Fiber alignment One drawback of uniaxial collagen gels compared to biaxial gels is that, due to the experimental setup itself, a strong structural and therefore mechanical anisotropy arises. This anisotropy is characterized by an alignment of collagen fibers and therefore a stiffening in the constrained direction. Interestingly, it was shown that the intensity of the anisotropy induced this way by the boundary conditions was the same for tendon and cardiac fibroblasts (Thomopoulos et al. 2005). Conversely, fibers in cruciform-shaped biaxial gels were found to be

randomly oriented in the central region, suggesting an isotropic response, whereas in the arms, uniaxial conditions induced a fiber alignment parallel to the axis of the arms (Hu et al. 2009). Also, the influence of external loading on fiber orientation was studied. If cruciform gels seeded with dermal fibroblasts were loaded in only one direction, fibers in the gel appeared to align in this direction also in the central region of the gel. If these gels were subsequently unloaded and then loaded orthogonally to the first loading direction, cells were found to remodel the fibers in the central region of the gel such that they first became randomly distributed again. After prolonged loading, finally, an anisotropic fiber alignment in the new loading direction was observed (Lee et al. 2008).

Mechanical properties The influence of static and cyclic equibiaxial stretching on the mechanical properties of fibroblast-seeded collagen gels has been studied over multiple days (Chen et al. (2018)). Lee et al. (2018) observed that cyclic loading increased the stiffness more than static loading. Interestingly, the increased stiffness could be maintained even after cell lysis, again supporting the concept of inelastic cell-mediated matrix remodeling known already from uniaxial experiments (Marenzana et al. 2006). Based on second harmonic generation images, the enhancement of the mechanical properties was explained by thickening of collagen fibers in case of cyclic stretching (Lee et al. 2018).

Mechanical homeostasis in higher dimensions Regulation of matrix tension has only recently been studied in a fully controllable biaxial setup (Eichinger et al. 2020). In this study, NIH 3T3 fibroblasts were used (Fig 2c, d). Homeostatic tension in the biaxial setting was found to be higher and to be reached faster compared to a uniaxial setting (under otherwise identical conditions). Perturbations of the homeostatic state were studied under both equi-biaxial and strip-biaxial loading conditions. Notably, this was the first experiment to study relaxation after perturbation for up to 10 h (compared to less than 60 min in similar studies (Brown et al. 1998; Ezra et al. 2010)). This provided valuable information about whether the homeostatic state is fully or only partially restored after perturbations. When gels were released, gel tension was observed to increase above the prior level. By contrast, in case of a stretch perturbation, only a $\sim 5\%$ offset was observed to remain compared to the prior tension. So far, it is not yet clear how these observations can be understood and to which extent they reflect general properties of mechanical homeostasis and tissue equivalents, e.g., considering that NIH 3T3 fibroblasts were used.

In an even more recent study, the mechanosensitive response of collagen gels seeded with primary aortic smooth muscle cells to a step-wise stretch was studied (Eichinger et al. 2021a). Both for release and extension by 1%, which corresponded to a perturbation of $\sim 25\%$ of the homeostatic state force, the gel tension returned toward the prior step within a tolerance of $\sim 10\%$.

3 Discussion and conclusion

Studies with tissue equivalents have significantly increased our understanding of mechanobiology over the past few decades. Tissue equivalents represent controllable experimental model systems to study the evolution of biomechanical properties and mechanobiological responses of native tissues and tissue-engineered constructs with resident cells in a mechanically and chemically controlled three-dimensional matrix environment. Circular, cell-seeded free-floating collagen gels compact strongly over multiple days due to cell contraction (Simon et al. 2012, 2014). If similar gels are constrained in a uni- or biaxial setting at the boundaries and are therefore not able to deform the gel in the direction of loading, a two-stage response is generally observed: first, cells rapidly build up a certain level of tension (phase I), which is subsequently maintained (phase II) for a prolonged period (Brown et al. 1998; Jenkins et al. 1999; Brown et al. 2002; Sethi et al. 2002; Campbell et al. 2003; Marenzana et al. 2006; Karamichos et al. 2007; Dahlmann-Noor et al. 2007; Ezra et al. 2010; Courderot-masuyer 2017; Eichinger et al. 2020). The level of homeostatic tension appears to increase with both collagen concentration and cell density. By contrast, the rate of change leading to the homeostatic plateau tension seems to depend on the cell density but not on the collagen density. When the homeostatic state is perturbed mechanically, it appears that tissue equivalents work to re-establish the prior state within a particular range or tolerance. The exact response tends to depend, however, on the cell type and experimental conditions, including the presence of exogenous growth factors and ions that support different types of cellular activities, including matrix cross-linking (Brown et al. 1998; Ezra et al. 2010; Simon et al. 2014; Eichinger et al. 2020) (see Tables 1 and 2 for a collection of data from the literature and Fig. 4 for an overview).

Despite the impact of the aforementioned studies on our understanding of mechanobiology, many available experimental data are subject to at least one of the following three drawbacks (most drawbacks (i) and (ii)):

(i) Gels were subjected to uniaxial loading only, although most soft tissues are subjected to multiaxial mechanical states in vivo, with notable exceptions being tendons and some ligaments.
(ii) Relaxation intervals following external mechanical perturbations were often restricted to one hour or less, not allowing a definite answer within which tolerance the homeostatic state is restored after perturbations.

Table 1 Overview of experimental methods and results related to uniaxially constrained tissue equivalents seeded with human dermal fibroblasts (FB)

Cell type	Force ($\frac{\mu N}{10^6 \text{ cells}}$)	Cell density ($\frac{10^6 \, cells}{\text{ml}}$)	Collagen concentration ($\frac{mg}{ml}$)	Annotations	References
Human dermal FB	2522 (Max.)	0.20	0.46		Delvoye et al. (1991)
	2377 (Max.)	0.40			
Human dermal FB	126 (Plat.)	1.10	1.00		Eastwood et al. (1994)
Human dermal FB	260-609 (Max.)	Unknown	0.80	Different cell lines	Eastwood et al. (1996)
	333 (Plat.)			Extraction by collagenase digestion	
	516 (Plat.)			Extraction by explant growth	
Human dermal FB	355 (Max.)	1.00	1.50	No mAb 4B4 (β1-blocking antibody)	Jenkins et al. (1999)
	252 (Max.)			1 µg/ml mAb 4B4	
	218 (Max.)			2 µg/ml mAb 4B4	
Human dermal FB	−54 (Plat.) 342 (Max.) 629 (Plat.)	1.00	1.70	0% FBS 2% FBS 10% FBS } Matched cell line and Passage number (∗)	Brown et al. (2002)
	334 (Max.) 254 (Max.) 544 (Max.) 515 (Max.) 82 (Max.)			2% FBS, no TGF − β1 2% FBS, 2.5 ng/ml TGF − β1 2% FBS, 7.5 ng/ml TGF − β1 2% FBS, 15.0 ng/ml TGF − β1 2% FBS, 30.0 ng/ml TGF − β1 } ∗	
	80 (Max.) 258 (Plat.) 381 (Max.) 118 (Max.)			2% FBS, 2.5 ng/ml TGF − β3 2% FBS, 7.5 ng/ml TGF − β3 2% FBS, 15.0 ng/ml TGF − β3 2% FBS, 30.0ng/ml TGF − β3 } ∗	
	199 (Max.) 623 (Plat.)			2% FBS, no TGF − β1 *or* − β3 2% FBS, 12.5 ng/ml TGF − β1 2%FBS, 15.0 ng/ml TGF − β3 } ∗	
Human dermal FB	159 (Plat.)	0.29	1.83		Campbell et al. (2003)
	182 (Max.)				
Human dermal FB	129 (Plat.)	1.00	Unknown	0% prestrain, FBS addition after 0 h	Karamichos et al. (2007)
	17 (Max.)			5% prestrain, FBS addition after 0 h	
	34 (Max.)			10% prestrain, FBS addition after 0 h	
	179 (Plat.)			0% prestrain, FBS addition after 1 h	
	78 (Plat.)			5% prestrain, FBS addition after 1 h	
	15 (Plat.)			10% prestrain, FBS addition after 1 h	

Forces refer to experiments without (or before) any external strain applied. The culture medium contained 10% FBS unless indicated differently. Maximal forces (Max.) and plateau forces (Plat.) are normalized by the number of cells used in the experiment. Due to missing data, the possibly more suitable normalization (force/cross-sectional area)/(number of cells/gel volume) was not possible. Therefore, information about the dimensions of the tissue equivalents (cross-sectional area, length, volume) in future studies would facilitate the comparison between experiments

(iii) Gels were seeded with cells from an immortalized line; thus, they are of little biological interest due to genetic and phenotypic changes resulting from multiple years of culture.

Besides these limitations, one must remember that in vivo conditions are necessarily much more complex than either in vitro or ex vivo conditions. Cells reside in vivo within a complex extracellular matrix consisting of myriad proteins, glycoproteins, and glycosaminoglycans, subject to complex aperiodic mechanical loading and influenced by paracrine signaling from multiple cell types, including inflammatory. Nevertheless, much has been learned and much can yet be learned with simple model systems. In the following, we summarize some of the most pressing remaining questions.

How does mechanical homeostasis arise? Probably the most important question yet to be answered is: which mechanosensitive mechanisms and processes at the level

Table 2 Overview of experimental methods and results related to tissue equivalents seeded with cells other than human dermal fibroblasts (FB)

Cell type	Force ($\frac{\mu N}{10^6\ cells}$)	Cell density ($\frac{10^6\ cells}{ml}$)	Collagen concentration($\frac{mg}{ml}$)	Annotations	References
Human osteosarcoma FB	221 (Max.)	1.00	1.50	Without $\alpha 2\beta 2$ integrins	Jenkins et al. (1999)
	318 (Max.)			With $\alpha 2\beta 2$ integrins	
Human ocular FB	18 (Plat.)	7.00	1.50	Human scleral FB	Dahlmann-Noor et al. (2007)
	208 (Plat.)	1.00		FB human Tenon's	
	311 (Plat.)	1.00		Human corneal FB	
Human tarsal plate FB	162 (Plat.)	1.00	1.58	Healthy upper eyelid FB	Ezra et al. (2010)
	437 (Plat.)			Floppy eyelid syndrome FB	
Human fascial tissue FB	80 (Max.)	1.00	1.88	Healthy carpal ligament (HCL)	Bisson et al. (2004)
	219 (Max.)			Dupuytren's cord (DC)	
	290 (Max.)			Dupuytren's nodule (DN)	
Human fascial tissue FB	91 (Max.)	1.00	1.88	HCL FB, without TGF-$\beta 1$	Bisson et al. (2009)
	234 (Max.)			DC FB, without TGF-$\beta 1$	
	262 (Max.)			DN FB, without TGF-$\beta 1$	
	330 (Max.)			HCL FB, 2 ng/ml TGF-$\beta 1$	
	428 (Max.)			DC FB, 2 ng/ml TGF-$\beta 1$	
	560 (Max.)			DN FB, 2 ng/ml TGF-$\beta 1$	
Calf dermal FB	5623 (Plat.)	0.20	0.46		Delvoye et al. (1991)
Chick embryo FB	585 (Plat.)	0.77	0.87		Kolodney and Wysolmerski (1992)
Rabbit tendon FB	124 (Max.)	Unknown	0.80	Endotenon FB	Eastwood et al. (1996)
	172 (Max.)			Sheath FB	
Rabbit tendon FB	168 (Plat.)	1.00	Unknown	P0, P = passage number	Sawadkar et al. (2020)
	126 (Max.)			P1	
	90 (Max.)			P3	
	51 (Max.)			P6	
Rat tendon FB	197 (Max.)	1.00	1.70	Without TGF-$\beta 1$	Marenzana et al. (2006)
				RMT = 53 $\mu N/10^6$ cells	
	456 (Max.)			15.0 ng/ml TGF-$\beta 1$	
				RMT = 40 $\mu N/10^6$ cells	
NIH 3T3 FB	255(Plat.)	0.20	1.50	Uniaxially constrained	Eichinger et al. (2020)
	213 (Plat.)	0.50	2.50	Uniaxially constrained	
	187 (Plat.)	0.50	1.50	Uniaxially constrained	
	135 (Plat.)	0.50	0.80	Uniaxially constrained	
	128 (Plat.)	1.00	1.50	Uniaxially constrained	
	138 (Plat.)	1.00	1.50	Biaxially constrained x-direction	
	142 (Plat.)			Biaxially constrained y-direction	
Porcine pulmonary arterial smooth muscle cell	759 (Plat.)	1.00	1.00	Inner 25% of artery, healthy	Hall et al. (2007)
	1119 (Plat.)			Outer 50% of artery, healthy	
	524 (Plat.)			Inner 25% of artery, hypoxic	
	228 (Plat.)			Outer 50% of artery, hypoxic	

Experiments were conducted in a uniaxial setup with medium containing 10% FBS unless indicated differently. Forces refer to experiments without (or before) any external strain applied. The RMT was obtained 12 h after addition of the actin cytoskeleton disrupting agent cytochalasin D after 24 h in culture. Maximal forces (Max.) and plateau forces (Plat.) are normalized by the number of cells used in the experiment. Analogously to the studies with dermal fibroblast, the possibly more suitable normalization (force/cross-sectional area)/(number of cells/gel volume) was not possible due to a lack of data, again suggesting a need to provide information about the cross-sectional area in future studies

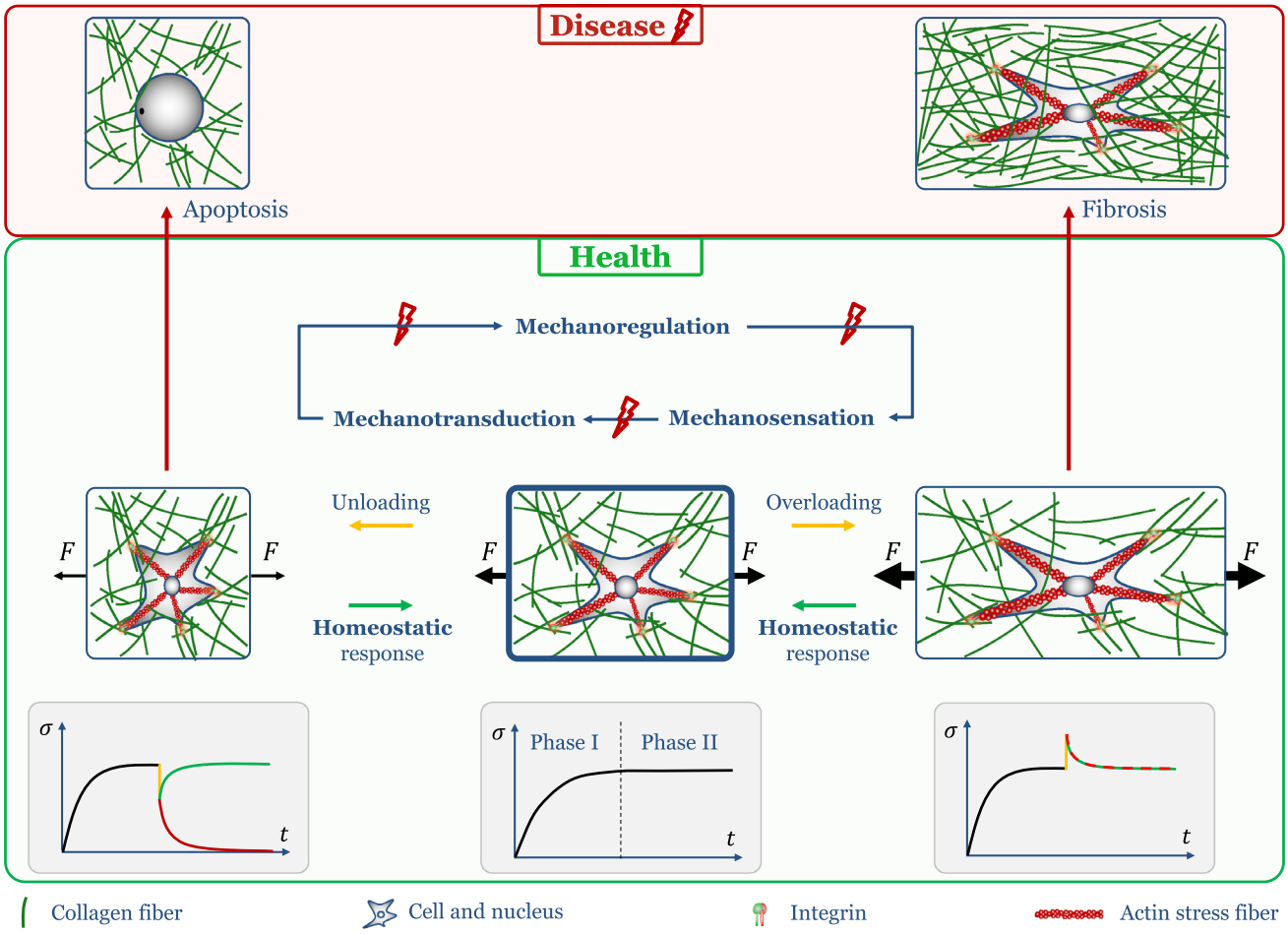

Fig. 4 Schematic drawing of cell-matrix interactions in health and disease. Center: cell in normal conditions interacting via integrins with surrounding ECM, which in vivo typically exhibits some tension. Bottom row shows typical behavior of tissue equivalents developing a homeostatic nonzero plateau of tension over time. Right: In case of further increases in tension, i.e., overloading, healthy tissue seeks to restore the prior mechanical state due to a homeostatic feedback loop consisting of mechanosensation, mechanotransduction, and mechanoregulation. If this feedback loop is compromised, pathological signaling can lead to a fibrotic response (top right). In general, both the healthy and the fibrotic reaction may help to restore the preferred mechanical state (bottom right). Left: in case of decreases in tension, i.e., under-loading, e.g., due to injury, homeostatic feedback loops can lead to re-establishment of a homeostatic state. By contrast, pathological mechanosensitivity of tissues can lead to apoptosis (top row). The homeostatic feedback loop aims at restoring the homeostatic state, whereas apoptosis may lead to tissue failure (bottom row)

of the cell (Weng et al. 2016) and of the tissue (Bhole et al. 2009; Flynn et al. 2010) together give rise to what we call mechanical homeostasis on the macroscale? One key need in this regard is to identify which mechanical quantity the individual cells can sense in their micro-environment and how their response is translated to the macroscopic organ level. On the microscopic level, where cells and tissue fibers appear as discrete objects, continuum-scale quantities such as stress or strain, or quantities derived from them, are not well-defined. Thus, on this scale, cells can probably only sense and react to (changes of) forces or displacements (Humphrey 2001). On the tissue and organ scale, this microscale behavior may give rise to an emergent behavior where continuum quantities such as stress or strain are effectively regulated. The micro-biomechanical and biochemical mechanisms of cellular mechano-sensing, transduction of cues into cellular regulative reactions via intracellular signaling pathways, and the controlled production, prestressing and degradation of extracellular matrix remain poorly understood. Tissue culture experiments are simple systems where accurately controlled stress and strain states can be imposed to study cellular responses. Especially interesting would be the use of cells with induced defects to study exact roles of specific components of the intracellular control system that gives rise to mechanical homeostasis. Similarly, cell treatment with drugs that just target one specific mechanism could provide important insights.

Which regulatory processes govern mechanical homeostasis on short and long time scales? In addition to different spatial scales, different time scales also need to be considered. Mechanical homeostasis is closely related to growth and remodeling. The latter refers to the inelastic reorganization of the microstructure of tissues, whereas growth describes the process of production and removal of tissue mass. This implies that mechanical homeostasis probably involves at least two very different biophysical processes, which can be expected to evolve in general at different time scales. Remodeling appears to regulate the mechanical state on the time scale of hours to days. Structurally significant mass turnover, that is, production and removal of tissue mass, most likely evolves over days to weeks (Nakagawa et al. 1989; Matsumoto and Hayashi 1994), and over such prolonged periods, mechanical homeostasis has not yet been studied using tissue equivalents given the challenges with long-term culture.

What is the target of mechanical homeostasis? So far, it remains controversial which mechanical quantity might be the target of mechanical homeostasis. There is evidence that it may be closely linked to tension in particular tissues because a wide range of different animal species, differing in size and body weight over multiple orders of magnitude, develop nearly the same tension per medial lamellar unit (or wall stress) in the aorta (Wolinsky and Glagov 1967). Indeed, externally perturbed tissue equivalents appear to restore their tension toward the level prior to the perturbation (Delvoye et al. 1991; Brown et al. 1998; Ezra et al. 2010). Yet, other equally striking studies report that wall stiffness at mean blood pressure also tends to be nearly the same in the aorta across various invertebrates and vertebrates (Shadwick 1999). Könnig et al. (2018) yet reported that fibroblast-populated biomaterial scaffolds reacted differently when subjected to environments with different stiffnesses. In a 2-week period, compaction was significantly less and tension higher with stiffer surroundings. Other recent investigations suggest loading rate as a crucial parameter for mechanobiological homeostasis on the cellular scale (Zhu et al. 2016; Eloseguí-Artola et al. 2018). This leaves open the key question which target quantity is governing mechanical homeostasis at the tissue and organ level: is it strain, tension/stress, stiffness, stress or strain rate, or some other more complex quantity? To answer this and other related questions, it could, for example, be helpful to develop tissue culture experiments where such quantities can be controlled independently for prolonged periods.

What is the homeostatic range and when does homeostasis become adaptive? Most in vitro studies of mechanical homeostasis in tissue equivalents are restricted to periods within which it is often hard to decide at which tolerance mechanical homeostasis aims to restore a certain target state. Moreover, it still remains unclear how and when the homeostatic target value or the tolerance around it change, following the concept of adaptive homeostasis (Davies 2016).

What does mechanical homeostasis mean in higher dimensions? In vivo observations so far focused on the component of tension in the circumferential direction of blood vessels (Wolinsky and Glagov 1967; Shadwick 1999), not allowing a generalization of the concept of mechanobiological homeostasis to higher dimensions. Similarly, in tissue cultures, quantitative studies of the homeostatic plateau tension have been performed almost exclusively in uniaxial settings. This is a major concern noting that in vivo, living tissues are predominantly subjected to complex multiaxial loading. To close the resulting gap in our understanding of mechanical homeostasis, there is a pressing need for more studies in multiaxial settings, with coordinate invariant mechanical metrics important to consider (e.g., although stress may be uniaxial with respect to the long-axis of a uniaxially loaded sample, shear stress yet exists relative to other coordinate systems, hence even in simple cases, we do not really know what component or collection of components of stress the cells may respond to). Additional studies and concepts will be needed to answer the question what mechanical homeostasis exactly means in higher dimensions.

What are the different targets of different cell types and what is the influence of tissue origin? So far, limited knowledge is available on how cell type and tissue origin influence mechanical homeostasis in tissue equivalents. In vivo, cells from different tissues have been exposed to different loading and different environments, which in general can be expected to affect cell function (Sewanan et al. 2019). A key question in this regard is how and for how long do cells remember their specific prior function when transferred to an artificial environment in vitro. Moreover, given that a basic tenet of experimentation is to keep everything the same except the one variable of interest, the question is how to quantify and assess the prior function and environment of cells used in tissue culture experiments. Alternatively, one may think about more complex ex vivo experimental devices and strategies, but matrix complexity remains complicated. In this regard, using matrices from decellularized tissues (as in tissue engineering) needs further attention.

As mentioned before, a major limitation of many available studies is the use of immortalized cell lines, or the frequent use of fibroblasts in cases of primary cells. The extension of these studies to other differentiated cells, stem cells (Butler et al. 2010; Leong et al. 2010), and cells stemming from diseased, for example, fibrotic or aneurysmal tissues, with possible defects that may, for example, affect cell-matrix interactions, will be helpful to further understand mechanical homeostasis in health and disease.

Importantly, to allow better comparisons across studies, more consistent experimental guidelines should be adopted.

Such is difficult, however, given the many different methods, cell types, tissue types, species, ages, disease conditions, and so forth. At the minimum, there is a need for more precise reporting. It may be reported that vascular smooth muscle cells were harvested from the aorta, for example, yet these cells arise from different embryonic origins when contrasting the aortic root, ascending aorta, and abdominal aorta. Site-specific differences may be critical determinants of findings in culture. One can also read that dermal fibroblasts were used; from where on the body were these cells taken, however, and what was the age and sex of the donor are often undocumented pieces of information that may be critical in comparing results. For example, it was even shown that human ocular fibroblasts from different regions of the eye produce significantly different tension (Dahlmann-Noor et al. 2007). Of course, precise information on culture medium and gel constituents or gel preparation time should be given since they influence the behavior of cells with respect to mechanical homeostasis. Similarly, also cell passage number (Sawadkar et al. 2020) and isolation process (Eastwood et al. 1996) have a major impact. Finally, normalization of the measured data could prove useful, as, for example, a normalized force F_n,

$$F_n = \frac{\text{force/cross-sectional area}}{\text{number of cells/gel volume}}, \tag{1}$$

would allow a better comparison between different studies, although information about the dimensions of the tissue equivalents (cross-sectional area, length, volume) remains indispensable. By including this information in future reports, it may be possible to develop dimensionless quantities characterizing the mechanobiological properties of tissue equivalents, following the example of fluid mechanics where dimensionless quantities such as the Reynolds or Stokes number have greatly contributed to our understanding of complex physical systems.

Summing up, experiments with tissue equivalents have contributed significantly to our understanding of mechanobiology. Nevertheless, many key questions have not yet been addressed, or at least not fully. Mathematical modeling of mechanobiology is a fast growing field and could help tremendously in understanding the foundations of mechanical homeostasis (Holzapfel et al. 2000; Wakatsuki et al. 2000; Humphrey and Rajagopal 2002; Watton et al. 2004; Marquez et al. 2005; Mauri et al. 2016; Loerakker et al. 2016; Cyron et al. 2016; Braeu et al. 2017; Ban et al. 2019; Domaschke et al. 2019; Eichinger et al. 2021a, b). To support mathematical modeling, it will be particularly important to collect larger sets of reliable quantitative experimental data, especially about bi- or triaxial mechanical states. Understanding the exact mechanisms by which cells sense and regulate their mechanical microenvironment and how these mechanisms macroscopically affect tissues will be key for the development of therapies against numerous diseases such as aneurysms or cancer. Moreover, it will be of great importance for future regenerative medicine in general.

Supplementary Information The online version contains supplementary material available at https://doi.org/10.1007/s10237-021-01433-9.

Acknowledgements We thank Dr. Jason Szafron, Ms. Isabella Jennings, and Ms. Lydia Ehmer for technical assistance and thoughtful discussions.

Funding Open Access funding enabled and organized by Projekt DEAL. Funded by the Deutsche Forschungsgemeinschaft (DFG, German Research Foundation)-Projektnummer 257981274, Projektnummer 386349077. The authors also gratefully acknowledge financial support by the International Graduate School of Science and Engineering (IGSSE) of Technical University of Munich, Germany.

Compliance with ethical standards

Conflicts of interest The authors declare that they have no conflict of interests.

References

Alcaraz J, Mori H, Ghajar CM, Brownfield D, Galgoczy R, Bissell MJ (2011) Collective epithelial cell invasion overcomes mechanical barriers of collagenous extracellular matrix by a narrow tube-like geometry and MMP14-dependent local softening. Integr Biol 3(12):1153–1166

Baker BM, Chen CS (2012) Deconstructing the third dimension-how 3D culture microenvironments alter cellular cues. J Cell Sci 125(13):3015–3024

Ban E, Wang H, Franklin JM, Liphardt JT, Janmey PA, Shenoy VB (2019) Strong triaxial coupling and anomalous Poisson effect in collagen networks. In: Proceedings of the National Academy of Sciences of the United States of America, pp 201815659

Bangasser BL, Shamsan GA, Chan CE, Opoku KN, Tuezel E, Schlichtmann BW, Kasim JA, Fuller BJ, McCullough BR, Rosenfeld SS, Odde DJ (2017) Shifting the optimal stiffness for cell migration. Nat Commun 8(1):1–10

Barocas VH, Girton TS, Tranquillo RT (1998) Engineered alignment in media equivalents: magnetic preaiignment and mandrel compaction. J Biomech Eng 120(5):660–666

Bates RC, Lincz LF, Burns GF (1995) Involvement of integrins in cell survival. Cancer Metastasis Rev 14(3):191–203

Bell E, Ivarsson B, Merrill C (1979) Production of a tissue-like structure by contraction of collagen lattices by human fibroblasts of different proliferative potential in vitro. Proc Natl Acad Sci U S A 76(3):1274–8

Bernard C (1865) An introduction to the study of experimental medicine. Dover Pubn Inc, New York

Bhole AP, Flynn BP, Liles M, Saeidi N, Dimarzio CA, Ruberti JW (2009) Mechanical strain enhances survivability of collagen micronetworks in the presence of collagenase: implications for load-bearing matrix growth and stability. Philos Trans R Soc A Math Phys Eng Sci 367(1902):3339–3362

Bissel MJ, Aggeler J (1987) Dynamic reciprocity: How do extracellular matrix and hormones direct gene expression? Prog Clin Biol Res 249:251–262

Bisson MA, Beckett KS, McGrouther DA, Grobbelaar AO, Mudera V (2009) Transforming growth factor-β1 stimulation enhances Dupuytren's fibroblast contraction in response to uniaxial mechanical load within a 3-dimensional collagen gel. J Hand Surg Am 34(6):1102–1110

Bisson MA, Mudera V, McGrouther DA, Grobbelaar AO (2004) The contractile properties and responses to tensional loading of Dupuytren's disease-derived fibroblasts are altered: A cause of the contracture? Plast Reconstr Surg 113(2):611–621

Boettiger D, Hammer DA, Rozenberg GI, Johnson KR, Margulies SS, Weaver VM, Dembo M, Reinhart-King CA, Gefen A, Lakins JN, Zahir N, Paszek MJ (2005) Tensional homeostasis and the malignant phenotype. Cancer Cell 8(3):241–254

Bonnans C, Chou J, Werb Z (2014) Remodelling the extracellular matrix in development and disease. Nat Rev Mol Cell Biol 15(12):786–801

Bonnier F, Keating ME, Wróbel TP, Majzner K, Baranska M, Garcia-Munoz A, Blanco A, Byrne HJ (2015) Cell viability assessment using the Alamar blue assay: A comparison of 2D and 3D cell culture models. Toxicol Vitr 29(1):124–131

Braeu FA, Seitz A, Aydin RC, Cyron CJ (2017) Homogenized constrained mixture models for anisotropic volumetric growth and remodeling. Biomech Model Mechanobiol 16(3):889–906

Brown RA, Prajapati R, McGrouther DA, Yannas IV, Eastwood M (1998) Tensional homeostasis in dermal fibroblasts: Mechanical responses to mechanical loading in three-dimensional substrates. J Cell Physiol 175(3):323–332

Brown RA, Sethi KK, Gwanmesia I, Raemdonck D, Eastwood M, Mudera V (2002) Enhanced fibroblast contraction of 3D collagen lattices and integrin expression by TGF-β1 and -β3: Mechanoregulatory growth factors? Exp Cell Res 274(2):310–322

Butcher DT, Alliston T, Weaver VM (2009) A tense situation: forcing tumour progression. Nat Rev Cancer 9(2):108–122

Butler DL, Gooch C, Kinneberg KR, Boivin GP, Galloway MT, Nirmalanandhan VS, Shearn JT, Dyment NA, Juncosa-Melvin N (2010) The use of mesenchymal stem cells in collagen-based scaffolds for tissue-engineered repair of tendons. Nat Protoc 5(5):849–863

Buttle DJ, Ehrlich HP (1983) Comparative studies of collagen lattice contraction utilizing a normal and a transformed cell line. J Cell Physiol 116(2):159–166

Califano JP, Reinhart-King CA (2010) Substrate stiffness and cell area predict cellular traction stresses in single cells and cells in contact. Cell Mol Bioeng 3(1):68–75

Campbell BH, Clark WW, Wang JHC (2003) A multi-station culture force monitor system to study cellular contractility. J Biomech 36(1):137–140

Cannon WB (1929) Reviews 1929. Physiol Rev 9(3):399–431

Cannon WB (1932) The Wisdom of the Body. W.W Norton, Incorporated, New York

Cavalcanti-Adam EA, Micoulet A, Volberg T, Geiger B, Spatz JP, Kessler H (2007) Cell spreading and focal adhesion dynamics are regulated by spacing of integrin ligands. Biophys J 92(8):2964–2974

Chan CE, Odde DJ (2008) Traction dynamics of filopodia on compliant substrates. Science (80-) 322(5908):1687–1691

Chen K, Vigliotti A, Bacca M, McMeeking RM, Deshpande VS, Holmes JW (2018) Role of boundary conditions in determining cell alignment in response to stretch. Proc Natl Acad Sci U S A 115(5):986–991

Cheng Q, Sun Z, Meininger G, Almasri M (2013) PDMS elastic micropost arrays for studying vascular smooth muscle cells. Sensors Actuators B Chem 188:1055–1063

Chiquet M, Gelman L, Lutz R, Maier S (2009) From mechanotransduction to extracellular matrix gene expression in fibroblasts. Biochim Biophys Acta Mol Cell Res 1793(5):911–920

Chovatiya R, Medzhitov R (2014) Stress, inflammation, and defense of homeostasis. Mol Cell 54(2):281–288

Courderot-masuyer C (2017) Mechanical Properties of Fibroblasts. Agache's Meas. Ski

Cox TR, Erler JT (2011) Remodeling and homeostasis of the extracellular matrix: implications for fibrotic diseases and cancer. Dis Model Mech 4(2):165–178

Cyron CJ, Aydin RC, Humphrey JD (2016) A homogenized constrained mixture (and mechanical analog) model for growth and remodeling of soft tissue. Biomech Model Mechanobiol 15(6):1389–1403

Cyron CJ, Humphrey JD (2014) Vascular homeostasis and the concept of mechanobiological stability. Int J Eng Sci 85:203–223

Cyron CJ, Humphrey JD (2017) Growth and remodeling of load-bearing biological soft tissues. Meccanica 52(3):645–664

Cyron CJ, Wilson JS, Humphrey JD (2014) Mechanobiological stability: A new paradigm to understand the enlargement of aneurysms? J R Soc Interface 11(100):20140680

Dahlmann-Noor AH, Martin-Martin B, Eastwood M, Khaw PT, Bailly M (2007) Dynamic protrusive cell behaviour generates force and drives early matrix contraction by fibroblasts. Exp Cell Res 313(20):4158–4169

Dallon JC, Ehrlich HP (2008) A review of fibroblast-populated collagen lattices. Wound Repair Regen 16(4):472–479

Davies KJA (2016) Adaptive homeostasis. Mol Aspects Med 49:1–7

Davis H (1867) Conservative surgery. Appleton & Co., New York

Delvoye P, Wiliquet P, Levêque J-L, Nusgens BV, Lapière CM (1991) Measurement of mechanical forces generated by skin fibroblasts embedded in a three-dimensional collagen gel. J Invest Dermatol 97(5):898–902

Domaschke S, Morel A, Fortunato G, Ehret AE (2019) Random auxetics from buckling fibre networks. Nat Commun 10(1):1–8

Duval K, Grover H, Han LH, Mou Y, Pegoraro AF, Fredberg J, Chen Z (2017) Modeling physiological events in 2D vs 3D cell culture. Physiology 32(4):266–277

Eastwood M, McGrouther DA, Brown RA (1994) A culture force monitor for measurement of contraction forces generated in human dermal fibroblast cultures: evidence for cell-matrix mechanical signalling. BBA - Gen Subj 1201(2):186–192

Eastwood M, Porter R, Khan U, McGrouther G, Brown R (1996) Quantitative analysis of collagen gel contractile forces generated by dermal fibroblasts and the relationship to cell morphology. J Cell Physiol 166(1):33–42

Ehrlich HP, Griswold TR, Rajaratnam JB (1986) Studies on vascular smooth muscle cells and dermal fibroblasts in collagen matrices. Effects Heparin Exp Cell Res 164(1):154–162

Ehrlich HP, Rittenberg T (2000) Differences in the mechanism for high-versus moderate-density fibroblast-populated collagen lattice contraction. J Cell Physiol 185(February):432–439

Eichinger JF, Aydin RC, Wall WA, Humphrey JD, Cyron CJ (2021a) What do cells regulate in soft tissues on short time scales? *to be submitted*

Eichinger JF, Grill MJ, Aydin RC, Wall WA, Humphrey JD, Cyron CJ (2021b) A computational framework for modeling cell-matrix interactions in soft biological tissues. *to be submitted*

Eichinger JF, Paukner D, Szafron JM, Aydin RC, Humphrey JD, Cyron CJ (2020) Computer-controlled biaxial bioreactor for investigating cell-mediated homeostasis in tissue equivalents. J Biomech Eng 142(c):1–22

Elosegui-Artola A, Trepat X, Roca-Cusachs P (2018) Control of mechanotransduction by molecular clutch dynamics. Trends Cell Biol 28(5):356–367

Ezra DG, Ellis JS, Beaconsfield M, Collin R, Bailly M (2010) Changes in fibroblast mechanostat set point and mechanosensitivity: an adaptive response to mechanical stress in floppy eyelid syndrome. Investig Ophthalmol Vis Sci 51(8):3853–3863

Flynn BP, Bhole AP, Saeidi N, Liles M, Dimarzio CA, Ruberti JW (2010) Mechanical strain stabilizes reconstituted collagen fibrils against enzymatic degradation by mammalian collagenase matrix metalloproteinase 8 (MMP-8). PLoS ONE 5(8):21–23

Friedl P, Sahai E, Weiss S, Yamada KM (2012) New dimensions in cell migration. Nat Rev Mol Cell Biol 13(11):743–747

Ghibaudo M, Saez A, Trichet L, Xayaphoummine A, Browaeys J, Silberzan P, Buguin A, Ladoux B (2008) Traction forces and rigidity sensing regulate cell functions. Soft Matter 4(9):1836–1843

Grenier G, Rémy-Zolghadri M, Larouche D, Gauvin R, Baker K, Bergeron F, Dupuis D, Langelier E, Rancourt D, Auger FA, Germain L (2005) Tissue reorganization in response to mechanical load increases functionality. Tissue Eng 11(1–2):90–100

Grinnell F (2000) Fibroblast-collagen-matrix contraction: growth-factor signalling and mechanical loading. Trends Cell Biol 10(9):362–365

Grinnell F, Ho CH (2002) Transforming growth factor β stimulates fibroblast-collagen matrix contraction by different mechanisms in mechanically loaded and unloaded matrices. Exp Cell Res 273(2):248–255

Grinnell F, Lamke CR (1984) Reorganization of hydrated collagen lattices by human skin fibroblasts. J Cell Sci 66:51–63

Grinnell F, Petroll WM (2010) Cell Motility and Mechanics in Three-Dimensional Collagen Matrices. Annu Rev Cell Dev Biol 26(1):335–361

Hall MS, Alisafaei F, Ban E, Feng X, Hui C-Y, Shenoy VB, Wu M (2016) Fibrous nonlinear elasticity enables positive mechanical feedback between cells and ECMs. Proc Natl Acad Sci 113(49):14043–14048

Hall SM, Soueid A, Smith T, Brown RA, Haworth SG, Mudera V (2007) Spatial differences of cellular origins and in vivo hypoxia modify contractile properties of pulmonary artery smooth muscle cells: lessons for arterial tissue engineering S. J Tissue Eng Regen Med 1:287–295

Holzapfel GA, Gasser TC, Ogden RW (2000) A new constitutive framework for arterial wall mechanics and a comparative study of material models. J Elast 61(1–3):1–48

Hu J-J, Humphrey JD, Yeh AT (2009) Characterization of engineered tissue development under biaxial stretch using nonlinear optical microscopy. Tissue Eng Part A 15(7):1553–1564

Hu JJ, Liu YC, Chen GW, Wang MX, Lee PY (2013) Development of fibroblast-seeded collagen gels under planar biaxial mechanical constraints: A biomechanical study. Biomech Model Mechanobiol 12(5):849–868

Humphrey JD (2001) Stress, strain, and mechanotransduction in cells. J Biomech Eng 123(6):638–641

Humphrey JD, Dufresne ER, Schwartz MA (2014a) Mechanotransduction and extracellular matrix homeostasis. Nat Rev Mol Cell Biol 15(12):802–812

Humphrey JD, Milewicz DM, Tellides G, Schwartz MA (2014b) Dysfunctional mechanosensing in aneurysms. Science 344(6183):477–479

Humphrey JD, Rajagopal KR (2002) A constrained mixture model for growth and remodeling of soft tissues. Math Model Methods Appl Sci 12(3):407–430

Humphrey JD, Wells PB, Baek S, Hu J-J, McLeroy K, Yeh AT (2008) A theoretically-motivated biaxial tissue culture system with intravital microscopy. Biomech Model Mechanobiol 7(4):323–34

Ignotz RA, Massague J (1986) Transforming growth factor-β stimulates the expression of fibronectin and collagen and their incorporation into the extracellular matrix. J Biol Chem 261(9):4337–4345

Isenberg BC, Williams C, Tranquillo RT (2006) Small-diameter artificial arteries engineered in vitro. Circ Res 98(1):25–35

Jenkins G, Redwood KL, Meadows L, Green MR (1999) Effect of gel re-organization and tensional forces on alpha2beta1 integrin levels in dermal fibroblasts. Eur J Biochem 263(1):93–103

Jiang G, Huang AH, Cai Y, Tanase M, Sheetz MP (2006) Rigidity sensing at the leading edge through \textalpha v \textbeta 3 integrins and RPTP\textalpha. Biophys J 90(5):1804–1809

Jin T, Li L, Siow RCMM, Liu K-KK (2015) A novel collagen gel-based measurement technique for quantitation of cell contraction force. J R Soc Interface 12(106):20141365

Joshi J, Mahajan G, Kothapalli CR (2018) Three-dimensional collagenous niche and azacytidine selectively promote time-dependent cardiomyogenesis from human bone marrow-derived MSC spheroids. Biotechnol Bioeng 115(8):2013–2026

Karamichos D, Brown RA, Mudera V (2007) Collagen stiffness regulates cellular contraction and matrix remodeling gene expression. J Biomed Mater Res, Part A 83A(3):887–894

Kelynack KJ, Hewitson TD, Nicholls KM, Darby I, Becker GJ (2000) Nephrology dialysis transplantation human renal fibroblast contraction of collagen I lattices is an integrin- mediated process. Nephrol Dial Transplanat 15:1766–1772

Kim J, Zheng Y, Alobaidi AA, Nan H, Tian J, Jiao Y, Sun B (2019) Collective ECM remodeling organizes 3D collective cancer invasion. pp 1–6

Knezevic V, Sim AJ, Borg TK, Holmes JW (2002) Isotonic biaxial loading of fibroblast-populated collagen gels: a versatile, low-cost system for the study of mechanobiology. Biomech Model Mechanobiol 1(1):59–67

Kolodney MS, Wysolmerski RB (1992) Isometric contraction by fibroblasts and endothelial cells in tissue culture?: A quantitative study. J Cell Biol 117(1):73–82

Könnig D, Herrera A, Duda GN, Petersen A (2018) Mechanosensation across borders: fibroblasts inside a macroporous scaffold sense and respond to the mechanical environment beyond the scaffold walls. J Tissue Eng Regen Med 12(1):265–275

Kotas ME, Medzhitov R (2015) Homeostasis, inflammation, and disease susceptibility. Cell 160(5):816–827

Kural MH, Billiar KL (2016) Myofibroblast persistence with real-time changes in boundary stiffness. Acta Biomater 32:223–230

Lee EJ, Holmes JW, Costa KD (2008) Remodeling of engineered tissue anisotropy in response to altered loading conditions. Ann Biomed Eng 36(8):1322–1334

Lee PY, Liu YC, Wang MX, Hu JJ (2018) Fibroblast-seeded collagen gels in response to dynamic equibiaxial mechanical stimuli: a biomechanical study. J Biomech 78:134–142

Legant WR, Pathak A, Yang MT, Deshpande VS, McMeeking RM, Chen CS (2009) Microfabricated tissue gauges to measure and manipulate forces from 3D microtissues. Proc Natl Acad Sci U S A 106(25):10097–10102

Leong WS, Tay CY, Yu H, Li A, Wu SC, Duc DH, Lim CT, Tan LP (2010) Thickness sensing of hMSCs on collagen gel directs stem cell fate. Biochem Biophys Res Commun 401(2):287–292

Lerche M, Elosegui-Artola A, Guzmán C, Georgiadou M, Kechagia JZ, Gulberg D, Roca-Cusachs P, Peuhu E, Ivaska J (2019) Integrin binding dynamics modulate ligand-specific mechanosensing in mammary gland fibroblasts. bioRxiv, pages 1–27

Loerakker S, Ristori T, Baaijens FP (2016) A computational analysis of cell-mediated compaction and collagen remodeling in tissue-engineered heart valves. J Mech Behav Biomed Mater 58:173–187

Lu P, Takai K, Weaver VM, Werb Z (2011) Extracellular Matrix degradation and remodeling in development and disease. Cold Spring Harb Perspect Biol 3(12):1–24

Lu P, Weaver VM, Werb Z (2012) The extracellular matrix: a dynamic niche in cancer progression. J Cell Biol 196(4):395–406

Mammoto A, Mammoto T, Ingber DE (2012) Mechanosensitive mechanisms in transcriptional regulation. J Cell Sci 125(13):3061–3073

Marenzana M, Wilson-Jones N, Mudera V, Brown RA (2006) The origins and regulation of tissue tension: identification of collagen tension-fixation process in vitro. Exp Cell Res 312(4):423–433

Marquez JP, Genin GM, Zahalak GI, Elson EL (2005) Thin bio-artificial tissues in plane stress: the relationship between cell and tissue strain, and an improved constitutive model. Biophys J 88(2):765–777

Matsumoto T, Hayashi K (1994) Mechanical and dimensional adaptation of rat aorta to hypertension. J Biomech Eng 116(3):278–283

Mauri A, Hopf R, Ehret AE, Picu CR, Mazza E (2016) A discrete network model to represent the deformation behavior of human amnion. J Mech Behav Biomed Mater 58:45–56

McEwen BS, Wingfield JC (2010) What is in a name? Integrating homeostasis, allostasis and stress. Horm Behav 57(2):105–111

Miroshnikova YA, Jorgens DM, Spirio L, Auer M, Sarang-Sieminski AL, Weaver VM (2011) Engineering strategies to recapitulate epithelial morphogenesis within synthetic three-dimensional extracellular matrix with tunable mechanical properties. Phys Biol 8(2):026013

Nakagawa Y, Totsuka M, Sato T, Fukuda Y, Hirota K (1989) Effect of disuse on the ultrastructure of the achilles tendon in rats. Eur J Appl Physiol Occup Physiol 59(3):239–242

Okabe Y, Medzhitov R (2016) Tissue biology perspective on macrophages. Nat Immunol 17(1):9–17

Oria R, Sunyer R, Trepat X, Jones JL, Allen MD, Elosegui-Artola A, Marshall JF, Andreu I, Bazellières E, Gomm JJ, Roca-Cusachs P (2014) Rigidity sensing and adaptation through regulation of integrin types. Nat Mater 13(6):631–637

Orlandi A, Ferlosio A, Gabbiani G, Spagnoli LG, Ehrlich PH (2005) Phenotypic heterogeneity influences the behavior of rat aortic smooth muscle cells in collagen lattice. Exp Cell Res 311(2):317–327

Piolanti N, Polloni S, Bonicoli E, Giuntoli M, Scaglione M, Indelli PF (2018) Giovanni alfonso borelli: the precursor of medial pivot concept in knee biomechanics. Joints 6(3):167–172

Redden RA, Doolin EJ (2003) Collagen crosslinking and cell density have distinct effects on fibroblast-mediated contraction of collagen gels. Skin Res. Technol. 9(3):290–293

Ross TD, Coon BG, Yun S, Baeyens N, Tanaka K, Ouyang M, Schwartz MA (2013) Integrins in mechanotransduction. Curr Opin Cell Biol 25(5):613–618

Sander EA, Barocas VH (2008) Biomimetic collagen tissues: collagenous tissue engineering and other applications. Collagen Struct Mech, pp 475–504

Sander EA, Barocas VH, Tranquillo RT (2011) Initial fiber alignment pattern alters extracellular matrix synthesis in fibroblast-populated fibrin gel cruciforms and correlates with predicted tension. Ann Biomed Eng 39(2):714–729

Sander EA, Stylianopoulos T, Tranquillo RT, Barocas VH (2009) Image-based multiscale modeling predicts tissue-level and network-level fiber reorganization in stretched cell-compacted collagen gels. Proc Natl Acad Sci U S A 106(42):17675–17680

Sawadkar P, Player D, Bozec L, Mudera V (2020) The mechanobiology of tendon fibroblasts under static and uniaxial cyclic load in a 3D tissue engineered model mimicking native extracellular matrix. J Tissue Eng Regen Med 14(1):135–146

Sawhney RK, Howard J (2002) Slow local movements of collagen fibers by fibroblasts drive the rapid global self-organization of collagen gels. J Cell Biol 157(6):1083–1091

Schiller HB, Fässler R (2013) Mechanosensitivity and compositional dynamics of cell-matrix adhesions. EMBO Rep 14(6):509–519

Schiro JA, Chan BMC, Roswit WT, Kassner PD, Pentland AP, Hemler ME, Eisen AZ, Kupper TS (1991) Integrin alpha 2 beta 1 (VLA-2) mediates reorganization and contraction of collagen matrices by human cells. Cell 67(2):403–410

Schwartz MA (2002) Integrins: emerging paradigms of signal transduction. Annu Rev Cell Dev Biol 11(1):549–599

Sethi KK, Yannas IV, Mudera V, Eastwood M, McFarland C, Brown RA (2002) Evidence for sequential utilization of fibronectin, vitronectin, and collagen during fibroblast-mediated collagen contraction. Wound Repair Regen 10(6):397–408

Sewanan LR, Schwan J, Kluger J, Park J, Jacoby DL, Qyang Y, Campbell SG (2019) Extracellular matrix from hypertrophic myocardium provokes impaired twitch dynamics in healthy cardiomyocytes. JACC Basic to Transl Sci 4(4):495–505

Shadwick RE (1999) Mechanical design in arteries. J Exp Biol 202(Pt 23):3305–3313

Simon DD, Horgan CO, Humphrey JD (2012) Mechanical restrictions on biological responses by adherent cells within collagen gels. J Mech Behav Biomed Mater 14:216–226

Simon DD, Humphrey JD (2014) Learning from tissue equivalents: biomechanics and mechanobiology. Bio-inspired Mater. Biomed. Eng. 9781118369:281–308

Simon DD, Niklason LE, Humphrey JD (2014) Tissue transglutaminase, not Lysyl oxidase, dominates early calcium-dependent remodeling of fibroblast-populated collagen lattices. Cells Tissues Organs 200(2):104–117

Stamenović D, Smith ML (2020) Tensional homeostasis at different length scales. Soft Matter 16(30):6946–6963

Steinberg BM, Smith K, Colozzo M, Pollack R (1980) Establishment and transformation diminish the ability of fibroblasts to contract a native collagen gel. J Cell Biol 87(1):304–308

Stevenson MD, Sieminski AL, McLeod CM, Byfield FJ, Barocas VH, Gooch KJ (2010) Pericellular conditions regulate extent of cell-mediated compaction of collagen gels. Biophys J 99(1):19–28

Sukharev S, Sachs F (2012) Molecular force transduction by ion channels-diversity and unifying principles. J Cell Sci 125(13):3075–3083

Thomopoulos S, Fomovsky GM, Chandran PL, Holmes JW (2007) Collagen fiber alignment does not explain mechanical anisotropy in fibroblast populated collagen gels. J Biomech Eng 129(5):642–650

Thomopoulos S, Fomovsky GM, Holmes JW (2005) The development of structural and mechanical anisotropy in fibroblast populated collagen gels. J Biomech Eng 127(5):742–750

Tomasek JJ, Gabbiani G, Hinz B, Chaponnier C, Brown RA (2002) Myofibroblasts and mechano: Regulation of connective tissue remodelling. Nat Rev Mol Cell Biol 3(5):349–363

Wakatsuki T, Kolodney MS, Zahalak GI, Elson EL (2000) Cell mechanics studied by a reconstituted model tissue. Biophys J 79(5):2353–2368

Walker M, Rizzuto P, Godin M, Pelling AE (2020) Structural and mechanical remodeling of the cytoskeleton maintains tensional homeostasis in 3D microtissues under acute dynamic stretch. Sci Rep 10(1):1–16

Watton PN, Hill NA, Heil M (2004) A mathematical model for the growth of the abdominal aortic aneurysm. Biomech Model Mechanobiol 3(2):98–113

Weaver VM, Petersen OW, Wang F, Larabell CA, Briand P, Damsky C, Bissell MJ (1997) Reversion of the malignant phenotype of human breast cells in three- dimensional culture and in vivo by integrin blocking antibodies. J Cell Biol 137(1):231–245

Weng S, Shao Y, Chen W, Fu J (2016) Mechanosensitive subcellular rheostasis drives emergent single-cell mechanical homeostasis. Nat Mater 15(9):961–967

Weninger W, Csiszar K, Kass L, Erler JT, Yu H, Weaver VM, Yamauchi M, Levental KR, Gasser DL, Fong SFT, Lakins JN, Giaccia A, Egeblad M (2009) Matrix crosslinking forces tumor progression by enhancing integrin signaling. Cell 139(5):891–906

Wolff J (1892) Das Gesetz der Transformation der Knochen. august hirschwald

Wolinsky H, Glagov S (1967) A lamellar unit of aortic medial structure and function in mammals. Circ Res 20(1):99–111

Woodley DT, Yamauchi M, Wynn KC, Mechanic G, Briggaman RA (1991) Collagen telopeptides (cross-linking sites) play a role in collagen gel lattice contraction

Wynn TA, Chawla A, Pollard JW (2013) Macrophage biology in development, homeostasis and disease. Nature 496(7446):445–455

Xie J, Bao M, Bruekers SMC, Huck WTS (2017) Collagen gels with different fibrillar microarchitectures elicit different cellular responses. ACS Appl Mater Interfaces 9(23):19630–19637

Yamato M, Adachi E, Yamamoto K, Hayashi T (1995) Condensation of collagen fibrils to the direct vicinity of fibroblasts as a cause of gel contraction. J Biochem 117(5):940–946

Yeung T, Georges PC, Flanagan LA, Marg B, Ortiz M, Funaki M, Zahir N, Ming W, Weaver V, Janmey PA (2005) Effects of substrate stiffness on cell morphology, cytoskeletal structure, and adhesion. Cell Motil Cytoskeleton 60(1):24–34

Zemel A (2015) Active mechanical coupling between the nucleus, cytoskeleton and the extracellular matrix, and the implications for perinuclear actomyosin organization. Soft Matter 11(12):2353–2363

Zhao X (2014) Multi-scale multi-mechanism design of tough hydrogels: building dissipation into stretchy networks. Soft Matter 10(5):672–687

Zhu C, Pérez-González C, Trepat X, Chen Y, Castro N, Oria R, Roca-Cusachs P, Elosegui-Artola A, Kosmalska A (2016) Mechanical regulation of a molecular clutch defines force transmission and transduction in response to matrix rigidity. Nat Cell Biol 18(5):540–548

Zhu YK, Umino T, Liu XD, Wang HJ, Romberger DJ, Spurzem JR, Rennard SI (2002) Contraction of fibroblast-containing collagen gels: initial collagen concentration regulates the degree of contraction and cell survival. Vitr Cell Dev Biol - Anim 37(1):10

Appendix B

Paper B

Computer-controlled biaxial bioreactor for investigating cell-mediated homeostasis in tissue equivalents

Jonas F. Eichinger, Daniel Paukner, Jason M. Szafron, Roland C. Aydin, Jay D. Humphrey, Christian J. Cyron

published in

Journal of Biomechanical Engineering, 10.1115/1.4046201

Order Date	15-Jun-2021	**Type of Use**	Republish in a thesis/dissertation
Order License ID	1125943-1		
ISSN	0148-0731	**Publisher**	AMERICAN SOCIETY OF MECHANICAL ENGINEERS,
		Portion	Chapter/article

LICENSED CONTENT

Publication Title	Journal of biomechanical engineering	**Country**	United States of America
		Rightsholder	American Society of Mechanical Engineers ASME
Article Title	Computer-Controlled Biaxial Bioreactor for Investigating Cell-Mediated Homeostasis in Tissue Equivalents.	**Publication Type**	Journal
		Issue	7
Author/Editor	AMERICAN SOCIETY OF MECHANICAL ENGINEERS.	**Volume**	142
Date	01/01/1977		
Language	English		

REQUEST DETAILS

Portion Type	Chapter/article	**Rights Requested**	Main product
Page range(s)	1-8	**Distribution**	Worldwide
Total number of pages	8	**Translation**	Original language of publication
Format (select all that apply)	Print, Electronic	**Copies for the disabled?**	No
Who will republish the content?	Academic institution	**Minor editing privileges?**	No
Duration of Use	Life of current and all future editions	**Incidental promotional use?**	No
		Currency	EUR
Lifetime Unit Quantity	Up to 499		

NEW WORK DETAILS

Title	Micromechancial Foundations of Mechanobiology in Soft Tissues	**Institution name**	Technical University of Munich
		Expected presentation date	2021-10-01
Instructor name	Ph.D.		

ADDITIONAL DETAILS

Order reference number	N/A	**The requesting person / organization to appear on the license**	Jonas F. Eichinger

REUSE CONTENT DETAILS

Title, description or numeric reference of the portion(s)	Computer-Controlled Biaxial Bioreactor for Investigating Cell-Mediated Homeostasis in Tissue Equivalents.	**Title of the article/chapter the portion is from**	Computer-Controlled Biaxial Bioreactor for Investigating Cell-Mediated Homeostasis in Tissue Equivalents.
Editor of portion(s)	Eichinger, Jonas F.; Paukner, Daniel; Szafron, Jason M; Aydin, Roland C.; Humphrey, Jay; Cyron, Christian	**Author of portion(s)**	Eichinger, Jonas F.; Paukner, Daniel; Szafron, Jason M; Aydin, Roland C.; Humphrey, Jay; Cyron, Christian
Volume of serial or monograph	142	**Issue, if republishing an article from a serial**	7
Page or page range of portion	1-8	**Publication date of portion**	2020-07-01

SPECIAL RIGHTSHOLDER TERMS AND CONDITIONS

Permission is granted for the specific use of the ASME paper as stated herein and does not permit further use of the materials without proper authorization. As is customary, we request that you ensure proper acknowledgment of the exact sources of this material, the authors, and ASME as original publisher.

CCC Terms and Conditions

1. Description of Service; Defined Terms. This Republication License enables the User to obtain licenses for republication of one or more copyrighted works as described in detail on the relevant Order Confirmation (the "Work(s)"). Copyright Clearance Center, Inc. ("CCC") grants licenses through the Service on behalf of the rightsholder identified on the Order Confirmation (the "Rightsholder"). "Republication", as used herein, generally means the inclusion of a Work, in whole or in part, in a new work or works, also as described on the Order Confirmation. "User", as used herein, means the person or entity making such republication.

2. The terms set forth in the relevant Order Confirmation, and any terms set by the Rightsholder with respect to a particular Work, govern the terms of use of Works in connection with the Service. By using the Service, the person transacting for a republication license on behalf of the User represents and warrants that he/she/it (a) has been duly authorized by the User to accept, and hereby does accept, all such terms and conditions on behalf of User, and (b) shall inform User of all such terms and conditions. In the event such person is a "freelancer" or other third party independent of User and CCC, such party shall be deemed jointly a "User" for purposes of these terms and conditions. In any event, User shall be deemed to have accepted and agreed to all such terms and conditions if User republishes the Work in any fashion.

3. Scope of License; Limitations and Obligations.

    3.1. All Works and all rights therein, including copyright rights, remain the sole and exclusive property of the Rightsholder. The license created by the exchange of an Order Confirmation (and/or any invoice) and payment by User of the full amount set forth on that document includes only those rights expressly set forth in the Order Confirmation and in these terms and conditions, and conveys no other rights in the Work(s) to User. All rights not expressly granted are hereby reserved.

    3.2. General Payment Terms: You may pay by credit card or through an account with us payable at the end of the month. If you and we agree that you may establish a standing account with CCC, then the following terms apply: Remit Payment to: Copyright Clearance Center, 29118 Network Place, Chicago, IL 60673-1291. Payments Due: Invoices are payable upon their delivery to you (or upon our notice to you that they are available to you for downloading). After 30 days, outstanding amounts will be subject to a service charge of 1-1/2% per month or, if less, the maximum rate allowed by applicable law. Unless otherwise specifically set forth in the Order Confirmation or in a separate written agreement signed by CCC, invoices are due and payable on "net 30" terms. While User may exercise the rights licensed immediately upon issuance of the Order Confirmation, the license is automatically revoked and is null and void, as if it had never been issued, if complete payment for the license is not received on a timely basis either from User directly or through a payment agent, such as a credit card company.

    3.3. Unless otherwise provided in the Order Confirmation, any grant of rights to User (i) is "one-time" (including the editions and product family specified in the license), (ii) is non-exclusive and non-transferable and (iii) is subject to any and all limitations and restrictions (such as, but not limited to, limitations on duration of use or circulation) included in the Order Confirmation or invoice and/or in these terms and conditions. Upon

completion of the licensed use, User shall either secure a new permission for further use of the Work(s) or immediately cease any new use of the Work(s) and shall render inaccessible (such as by deleting or by removing or severing links or other locators) any further copies of the Work (except for copies printed on paper in accordance with this license and still in User's stock at the end of such period).

3.4. In the event that the material for which a republication license is sought includes third party materials (such as photographs, illustrations, graphs, inserts and similar materials) which are identified in such material as having been used by permission, User is responsible for identifying, and seeking separate licenses (under this Service or otherwise) for, any of such third party materials; without a separate license, such third party materials may not be used.

3.5. Use of proper copyright notice for a Work is required as a condition of any license granted under the Service. Unless otherwise provided in the Order Confirmation, a proper copyright notice will read substantially as follows: "Republished with permission of [Rightsholder's name], from [Work's title, author, volume, edition number and year of copyright]; permission conveyed through Copyright Clearance Center, Inc. " Such notice must be provided in a reasonably legible font size and must be placed either immediately adjacent to the Work as used (for example, as part of a by-line or footnote but not as a separate electronic link) or in the place where substantially all other credits or notices for the new work containing the republished Work are located. Failure to include the required notice results in loss to the Rightsholder and CCC, and the User shall be liable to pay liquidated damages for each such failure equal to twice the use fee specified in the Order Confirmation, in addition to the use fee itself and any other fees and charges specified.

3.6. User may only make alterations to the Work if and as expressly set forth in the Order Confirmation. No Work may be used in any way that is defamatory, violates the rights of third parties (including such third parties' rights of copyright, privacy, publicity, or other tangible or intangible property), or is otherwise illegal, sexually explicit or obscene. In addition, User may not conjoin a Work with any other material that may result in damage to the reputation of the Rightsholder. User agrees to inform CCC if it becomes aware of any infringement of any rights in a Work and to cooperate with any reasonable request of CCC or the Rightsholder in connection therewith.

4. Indemnity. User hereby indemnifies and agrees to defend the Rightsholder and CCC, and their respective employees and directors, against all claims, liability, damages, costs and expenses, including legal fees and expenses, arising out of any use of a Work beyond the scope of the rights granted herein, or any use of a Work which has been altered in any unauthorized way by User, including claims of defamation or infringement of rights of copyright, publicity, privacy or other tangible or intangible property.

5. Limitation of Liability. UNDER NO CIRCUMSTANCES WILL CCC OR THE RIGHTSHOLDER BE LIABLE FOR ANY DIRECT, INDIRECT, CONSEQUENTIAL OR INCIDENTAL DAMAGES (INCLUDING WITHOUT LIMITATION DAMAGES FOR LOSS OF BUSINESS PROFITS OR INFORMATION, OR FOR BUSINESS INTERRUPTION) ARISING OUT OF THE USE OR INABILITY TO USE A WORK, EVEN IF ONE OF THEM HAS BEEN ADVISED OF THE POSSIBILITY OF SUCH DAMAGES. In any event, the total liability of the Rightsholder and CCC (including their respective employees and directors) shall not exceed the total amount actually paid by User for this license. User assumes full liability for the actions and omissions of its principals, employees, agents, affiliates, successors and assigns.

6. Limited Warranties. THE WORK(S) AND RIGHT(S) ARE PROVIDED "AS IS". CCC HAS THE RIGHT TO GRANT TO USER THE RIGHTS GRANTED IN THE ORDER CONFIRMATION DOCUMENT. CCC AND THE RIGHTSHOLDER DISCLAIM ALL OTHER WARRANTIES RELATING TO THE WORK(S) AND RIGHT(S), EITHER EXPRESS OR IMPLIED, INCLUDING WITHOUT LIMITATION IMPLIED WARRANTIES OF MERCHANTABILITY OR FITNESS FOR A PARTICULAR PURPOSE. ADDITIONAL RIGHTS MAY BE REQUIRED TO USE ILLUSTRATIONS, GRAPHS, PHOTOGRAPHS, ABSTRACTS, INSERTS OR OTHER PORTIONS OF THE WORK (AS OPPOSED TO THE ENTIRE WORK) IN A MANNER CONTEMPLATED BY USER; USER UNDERSTANDS AND AGREES THAT NEITHER CCC NOR THE RIGHTSHOLDER MAY HAVE SUCH ADDITIONAL RIGHTS TO GRANT.

7. Effect of Breach. Any failure by User to pay any amount when due, or any use by User of a Work beyond the scope of the license set forth in the Order Confirmation and/or these terms and conditions, shall be a material breach of the license created by the Order Confirmation and these terms and conditions. Any breach not cured within 30 days of written notice thereof shall result in immediate termination of such license without further notice. Any unauthorized (but licensable) use of a Work that is terminated immediately upon notice thereof may be liquidated by payment of the Rightsholder's ordinary license price therefor; any unauthorized (and unlicensable) use that is not terminated immediately for any reason (including, for example, because materials containing the Work cannot reasonably be recalled) will be subject to all remedies available at law or in equity, but in no event to a payment of

less than three times the Rightsholder's ordinary license price for the most closely analogous licensable use plus Rightsholder's and/or CCC's costs and expenses incurred in collecting such payment.

8. Miscellaneous.

    8.1. User acknowledges that CCC may, from time to time, make changes or additions to the Service or to these terms and conditions, and CCC reserves the right to send notice to the User by electronic mail or otherwise for the purposes of notifying User of such changes or additions; provided that any such changes or additions shall not apply to permissions already secured and paid for.

    8.2. Use of User-related information collected through the Service is governed by CCC's privacy policy, available online here:https://marketplace.copyright.com/rs-ui-web/mp/privacy-policy

    8.3. The licensing transaction described in the Order Confirmation is personal to User. Therefore, User may not assign or transfer to any other person (whether a natural person or an organization of any kind) the license created by the Order Confirmation and these terms and conditions or any rights granted hereunder; provided, however, that User may assign such license in its entirety on written notice to CCC in the event of a transfer of all or substantially all of User's rights in the new material which includes the Work(s) licensed under this Service.

    8.4. No amendment or waiver of any terms is binding unless set forth in writing and signed by the parties. The Rightsholder and CCC hereby object to any terms contained in any writing prepared by the User or its principals, employees, agents or affiliates and purporting to govern or otherwise relate to the licensing transaction described in the Order Confirmation, which terms are in any way inconsistent with any terms set forth in the Order Confirmation and/or in these terms and conditions or CCC's standard operating procedures, whether such writing is prepared prior to, simultaneously with or subsequent to the Order Confirmation, and whether such writing appears on a copy of the Order Confirmation or in a separate instrument.

    8.5. The licensing transaction described in the Order Confirmation document shall be governed by and construed under the law of the State of New York, USA, without regard to the principles thereof of conflicts of law. Any case, controversy, suit, action, or proceeding arising out of, in connection with, or related to such licensing transaction shall be brought, at CCC's sole discretion, in any federal or state court located in the County of New York, State of New York, USA, or in any federal or state court whose geographical jurisdiction covers the location of the Rightsholder set forth in the Order Confirmation. The parties expressly submit to the personal jurisdiction and venue of each such federal or state court.If you have any comments or questions about the Service or Copyright Clearance Center, please contact us at 978-750-8400 or send an e-mail to support@copyright.com.

v 1.1

J. F. Eichinger[1]
Department of Mechanical Engineering,
Institute for Computational Mechanics,
Technical University of Munich,
Boltzmannstrasse 15,
Garching 85748, Germany;
Department of Mechanical Engineering,
Institute of Continuum and Materials Mechanics,
Hamburg University of Technology,
Eissendorfer Strasse 42,
Hamburg 21073, Germany
e-mail: eichinger@lnm.mw.tum.de

D. Paukner[1]
Department of Biomedical Engineering,
Yale University,
55 Prospect Street,
New Haven, CT 06511
e-mail: daniel.paukner@yale.edu

J. M. Szafron
Department of Biomedical Engineering,
Yale University,
55 Prospect Street,
New Haven, CT 06511
e-mail: jason.szafron@yale.edu

R. C. Aydin
Department for Simulation of
Solids and Structures,
Materials Mechanics,
Institute of Materials Research,
Helmholtz-Zentrum Geesthacht,
Max-Planck-Strasse 1,
Geesthacht 21502, Germany
e-mail: roland.aydin@hzg.de

J. D. Humphrey
Department of Biomedical Engineering,
Yale University,
55 Prospect Street,
New Haven, CT 06511
e-mail: jay.humphrey@yale.edu

C. J. Cyron
Department of Mechanical Engineering,
Institute of Continuum and Materials Mechanics,
Hamburg University of Technology,
Eissendorfer Strasse 42,
Hamburg 21073, Germany;
Department for Simulation of
Solids and Structures,
Materials Mechanics,
Institute of Materials Research,
Helmholtz-Zentrum Geesthacht,
Max-Planck-Strasse 1,
Geesthacht 21502, Germany
e-mail: christian.cyron@tuhh.de

Computer-Controlled Biaxial Bioreactor for Investigating Cell-Mediated Homeostasis in Tissue Equivalents

Soft biological tissues consist of cells and extracellular matrix (ECM), a network of diverse proteins, glycoproteins, and glycosaminoglycans that surround the cells. The cells actively sense the surrounding ECM and regulate its mechanical state. Cell-seeded collagen or fibrin gels, so-called tissue equivalents, are simple but powerful model systems to study this phenomenon. Nevertheless, few quantitative studies document the stresses that cells establish and maintain in such gels; moreover, most prior data were collected via uniaxial experiments whereas soft tissues are mainly subject to multiaxial loading in vivo. To begin to close this gap between existing experimental data and in vivo conditions, we describe here a computer-controlled bioreactor that enables accurate measurements of the evolution of mechanical tension and deformation of tissue equivalents under well-controlled biaxial loads. This device allows diverse studies, including how cells establish a homeostatic state of biaxial stress and if they maintain it in response to mechanical perturbations. It similarly allows, for example, studies of the impact of cell and matrix density, exogenous growth factors and cytokines, and different types of loading conditions (uniaxial, strip-biaxial, and biaxial) on these processes. As illustrative results, we show that NIH/3T3 fibroblasts establish a homeostatic mechanical state that depends on cell density and collagen concentration. Following perturbations from this homeostatic state, the cells were able to recover biaxial loading similar to homeostatic. Depending on the precise loads, however, they were not always able to fully maintain that state. [DOI: 10.1115/1.4046201]

1 Introduction

Living soft tissues consist of cells embedded within an extracellular matrix (ECM). The ECM consists of a network of diverse proteins, often collagen and elastic fibers, as well as glycoproteins and glycosaminoglycans that together provide mechanical support and biological cues to the resident cells. Cells and ECM interact closely, and these interactions have a crucial impact on tissue health and disease [1–5]. Changes in matrix properties affect, for example, cell migration [6–8], differentiation [9–11], and survival [12–15]. At the same time, cells actively sense and regulate their surrounding ECM to establish or maintain a preferred (so-called

[1]These authors contributed equally.

Manuscript received July 4, 2019; final manuscript received January 11, 2020; published online April 8, 2020. Assoc. Editor: Nathan Sniadecki.

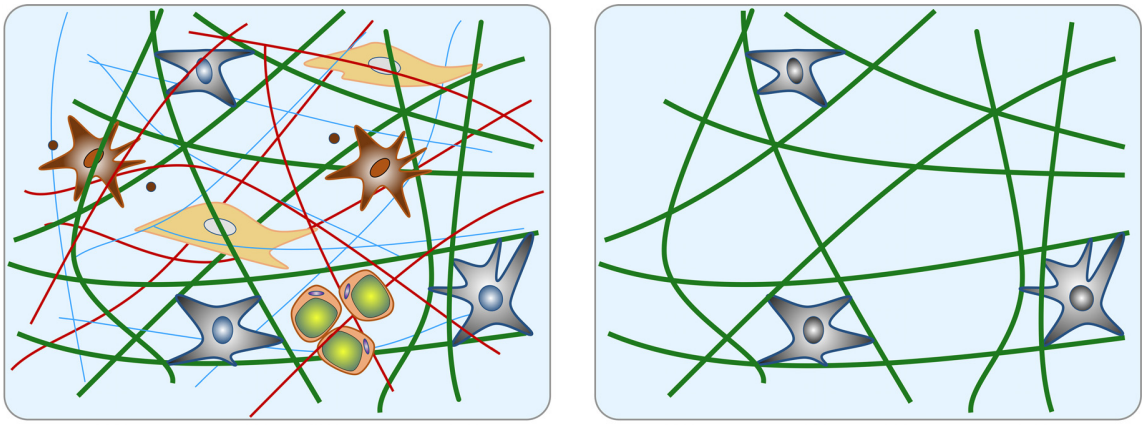

(*a*) (*b*)

Fig. 1 Schematic of native tissue consisting of various fiber and cell types, as well as additional constituents (*a*); cell-seeded collagen (Fig. 5(*b*)) gel as a simplified model system to study cell–matric interactions (*b*). In both cases, we emphasize the typical multiaxial geometry and loading that is important for in vivo relevance.

homeostatic) state [16–18]. Understanding feedback mechanisms between cells and ECM is critical to advancing our understanding of mechanobiology.

Native ECM is a highly complex mixture of diverse fiber types and substances. To reduce parameters and interdependencies and focus on select mechanisms, cell-seeded collagen or fibrin gels, so-called tissue equivalents, often serve as simplified model systems for studying cell-matrix interactions (see Fig. 1). Most studies focus on free-floating gels [18,19] or the tension imposed on or developed within tissue equivalents in uniaxial settings [16,17,20–24]. Yet, in vivo most soft tissues are neither free from external loads nor subjected to simple uniaxial loading. Rather, most experience complex multiaxial loading. While some studies have examined biaxial loading cases, they have tended to focus on the analysis of fiber (re)orientation or passive mechanical properties [25–27], not cell-driven evolution of tension or deformation [28]. As demonstrated in computational studies [29,30], cell-mediated maintenance, adaptation, and repair of soft tissues in response to changes in mechanical environment over hours to days is critical for promoting both mechanobiological equilibrium and mechanobiological stability. A key reason why cell–matrix interactions have been studied in simple settings, such as free-floating or uniaxial gels, is the technical challenge associated with designing bioreactors for biaxial studies.

There is, therefore, a pressing need for a device that allows one to study cell-mediated changes in matrix, which give rise to stress–strain responses that characterize tissue behavior under loading conditions of interest and relevant time scales. Herein, we describe the development of such a device using paired high sensitivity, low drift force transducers and precision motors to allow diverse testing conditions, including static and cyclic uniaxial, strip-biaxial, and biaxial. Moreover, we report illustrative results obtained with this device, in particular, relations between cell density, matrix density, and loading state with a focus on the homeostatic stress level that is established and maintained in tissue equivalents in response to various perturbations in loading.

2 Design of Biaxial Culture Force Monitoring System

To mimic the multidimensional loading experienced by tissues in vivo, we designed a computer-controlled bioreactor for cell-seeded tissue equivalents capable of measuring mechanical metrics under a range of long-term (>24 h) biaxial stress/strain conditions. Here, we first overview the structure of the device before discussing its key features separately.

2.1 Overview. An image of the custom device as well as a schematic drawing of its most important parts can be seen in

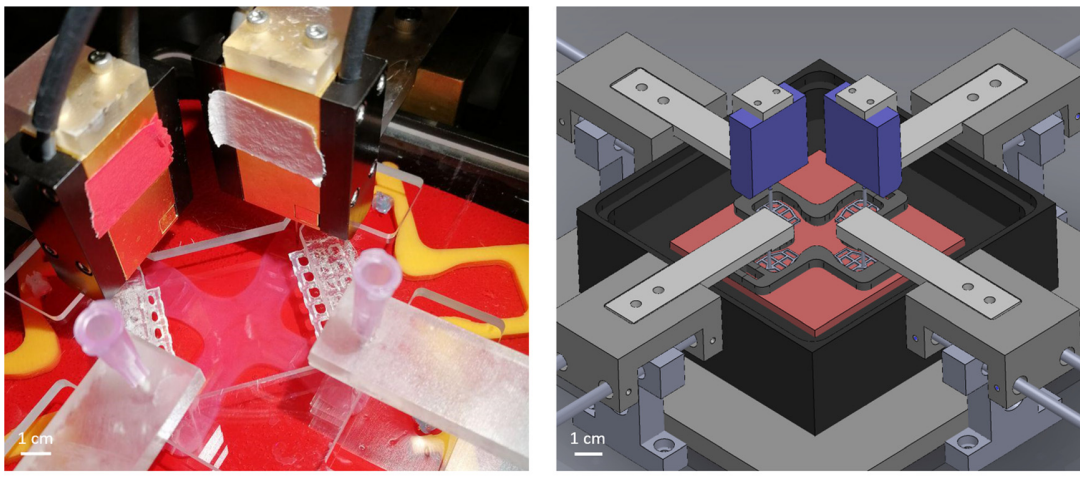

(*a*) (*b*)

Fig. 2 (*a*) Biaxial bioreactor and mechanical testing device with attached sample and (*b*) schematic drawing showing the inside of the bath chamber and the load cells mounted from above

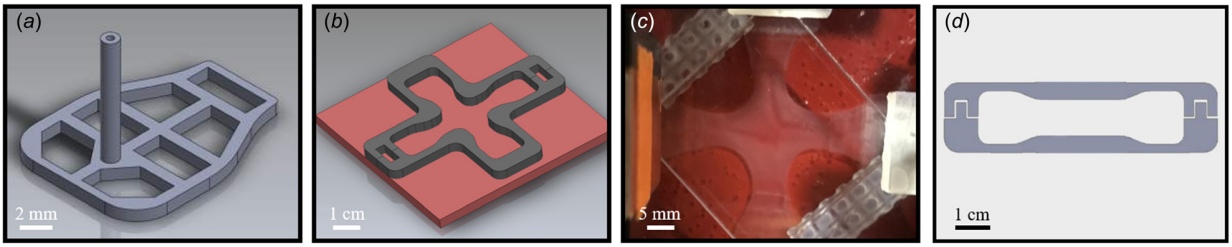

Fig. 3 (*a*) A porous insert for attaching a gel to the testing device; (*b*) two-part mold having a cruciform shape to form gels; (*c*) floated cruciform gel attached to testing device; and (*d*) dog-bone shape mold for uniaxial experiments

Fig. 2. The core of the bioreactor is a square sample chamber ($130 \times 130 \times 46$ mm) made of glass-filled polycarbonate with a removable lid made of clear polycarbonate that prevents evaporation of culture medium and contamination of the sample during experiments. The samples are placed in the central region of the bath and attached to arms printed with a Form 2 printer (Formlabs, Somerville, MA). Both the *x*- and *y*-axes are equipped with high-resolution force transducers to allow accurate time-dependent measurements of force. A stepper motor (Advanced Micro-Systems, Liberty Hill, TX) is attached to each arm via a brass sled and stainless steel rods. The four motors, in combination with lead screws, have a resolution less than 1.0 μm, thus enabling precise loading (e.g., uniaxial, strip-biaxial, equi-biaxial, or non-equi-biaxial) of the gel sample. Each motor can be operated independently using a LabVIEW interface, allowing static or cyclic loading during load- or displacement-controlled tests while recording position and force. All components are attached to a polycarbonate base platform placed within a custom incubator (NU-5820, NuAire, Plymouth, MN, with sealed side ports for exteriorizing electrical cables) to provide appropriate environmental conditions (37 °C, 5% CO_2) and sterility for cell viability. A camera (V4K, IPEVO, Sunnyvale, CA) is mounted onto the base plate to image the specimens during testing.

2.2 Sample Preparation, Geometry, and Attachment. A challenging step in the mechanical testing of collagen gels is their attachment to the testing device. Due to their fragility, every movement of the gel risks damage. Several approaches have been proposed for this coupling, including using sutures [31], wires [32], and by placing porous polyethylene bars in the mold before adding the gel solution so that the fiber network forming during gelation naturally surrounds and connects to these bars [28,33,34]. To ensure a simple mount and stable connection of the gel to the high-resolution force transducers, we developed a new design (Fig. 3(*a*)). Porous inserts stabilize the connection between the gel and device, avoiding problems like tearing at the transition between the holder and gel. These embedded inserts are 3D-printed using a Form 2 printer (Formlabs, Somerville, MA).

Cruciform-shaped molds (Fig. 3(*b*)) are used to form the gels (Fig. 3(*c*)). Other shapes, including square or rectangular as widely used in testing native tissues, are more difficult to secure to the device when highly compliant as for collagen gels. The cruciform molds are 3D-printed from polylactide using a MakerBot Replicator+. To avoid stress concentrations, sharp edges in the molds were smoothed with filets. For a uniaxial setting, the cruciform mold can simply be replaced with a traditional "dog-bone" shaped mold (Fig. 3(*d*)) with analogously smoothed edges. A silicon rubber pad is used as a base for the mold to avoid leakage of the gel during gelation (Fig. 3(*b*)).

To avoid damage during experimental setup as well as to increase reproducibility and enable testing of delicate gels with low collagen concentrations (<1 mg/mL), the gel is set in the sample chamber, at the start of an experiment, already attached to the completely assembled testing frame while inside the incubator under sterile conditions (Fig. 2). This procedure also ensures a reproducible, stress-free configuration at the beginning of all experiments. To this end, a two-part cruciform mold (Fig. 3(*b*)) is placed inside the sample chamber and followed by a complete assembly of the testing device. Subsequently, the gel solution is prepared within a laminar flow hood and then transferred to the mold inside the chamber. After gelation for 30–45 min, the samples are floated with culture medium and the mold is detached from the gel with the help of four narrow slits in the chamber lid (Fig. 2(*a*)). The experiment starts directly after the mold is removed from the gel without the need for any relocation or attachment steps, which minimizes the probability of sample damage.

2.3 Force Measurement. Cell-mediated forces acting within the gels tend to be low, in the order of 200 μN/million cells [16,17,20,21,22]. These small forces must be resolved by the transducer and measured accurately for long durations (e.g., 48 h) in a high humidity, 37 °C environment with negligible drift and a reasonable signal-to-noise ratio. We use two SI-H KG7 force transducers from World Precision Instruments (Sarasota, FL). These transducers detect force by optically measuring the deflection of a stiff beam, which limits the potential for damage from overloading as in traditional capacitive transducers. They have a

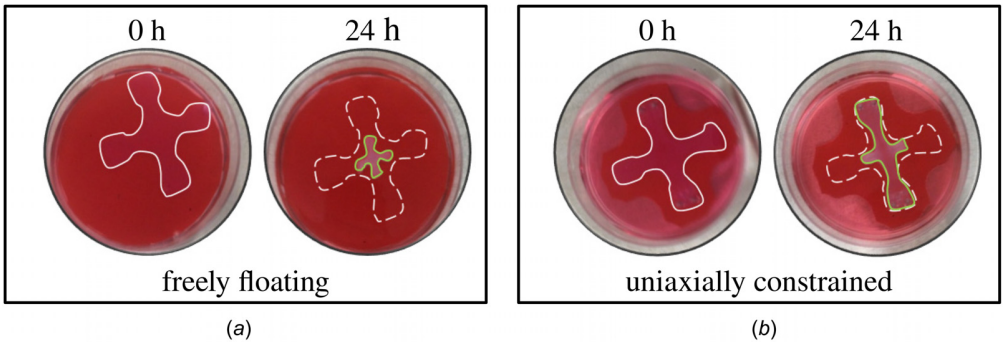

Fig. 4 Compaction of a cruciform gel from an initial configuration (solid line at 0 h) to a deformed contour (solid line at 24 h) due to contractile forces imposed by resident cells (dashed line at 24 h indicates initial configuration): (*a*) freely floating gel and (*b*) uniaxially constrained gel

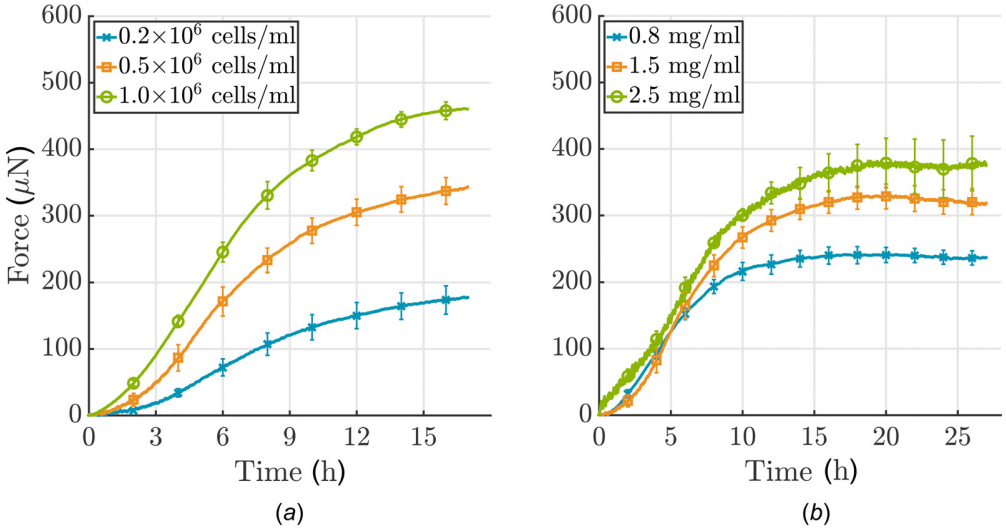

Fig. 5 (*a*) Influence of cell density and (*b*) collagen concentration on force development in a uniaxial setting (cells were serum-starved; each curve shows the mean ± SEM for three identical experiments). (*a*) Note that force development depends nonlinearly on cell density: more cells/mL lead to higher forces; (*b*) force development depends nearly linearly on collagen concentration, higher concentrations lead to higher force.

force range of 0–5 mN (also allowing passive material tests of tissue equivalents) with noise less than 0.2 μN. These transducers demonstrated excellent performance with respect to physical as well as environmental requirements as described earlier. High accuracy, low noise, and low zero-level drift could be maintained up to the prescribed 40 h (Fig. S1 available in the Supplemental Materials on the ASME Digital Collection).

3 Materials and Methods

3.1 Cell Culture. For illustrative purposes, NIH/3T3 fibroblasts (ATCC, Gaithersburg, MD) were maintained in culture medium consisting of Dulbecco's modified Eagle's medium (DMEM), 10% heat-inactivated fetal bovine serum (FBS) (Life Technologies, Carlsbad, CA), and 1% penicillin-streptomycin (ThermoFisher, Waltham, MA) in an incubator at 37 °C and 5% CO_2. Cells were grown in T75 flasks (ThermoFisher, Waltham, MA) and passaged at 70–80% confluence. Passages 4 and 5 were used in all experiments.

3.2 Cell Proliferation. Pilot studies showed that NIH/3T3 fibroblasts have a tendency to proliferate strongly within the collagen gel, leading to a continuous increase in force rather than a force that tended to steady-state (Fig. S2(*a*) blue curve available in the Supplemental Materials on the ASME Digital Collection). To minimize cell proliferation, we used serum-starvation or treatment with Mitomycin C (Sigma, St. Louis, MO) to inhibit cell cycle progression (Fig. S2(*a*) available in the Supplemental Materials on the ASME Digital Collection). In the former, cells were starved in medium containing 0.5% FBS for 18 h prior to the experiment; in the latter, 0.12 mL of Mitomycin C (0.4 mg/mL, diluted in PBS, giving a final concentration of 4 μg/mL) was added to the cell culture flasks 2.5 h prior to the experiment. The influence of both treatments on cell number and force development was analyzed (Figs. S2(*a*) and S2(*b*) available in the Supplemental Materials on the ASME Digital Collection).

3.3 Collagen Gel Preparation. Cell-seeded collagen gels were prepared on ice following a protocol modified slightly from Ref. [19]. Briefly, for 7.0 mL of gel solution (volume of the biaxial mold was ~6.5 mL), 1.31 mL of 5× DMEM, 0.63 mL of a 10× reconstitution buffer (0.1 N NaOH and 20 mM HEPES; Sigma, St. Louis, MO), and 1.28 mL of high concentration, type I rat tail collagen (8.22 mg/mL; Corning, Corning, NY) were mixed with 3.78 mL of an experimental culture medium containing 7.0×10^6 cells (a Neubauer chamber in combination with Trypan blue staining was used to count cells), giving a final collagen concentration of 1.5 mg/mL and a cell density of 1.0×10^6 cells/mL. The experimental culture medium consisted of DMEM supplemented with 10% FBS, 10% porcine serum (Life Technologies, Carlsbad, CA), 1% penicillin-streptomycin, and 1% antibiotic/antimycotic (ThermoFisher, Waltham, MA). Acellular gels were prepared using the same protocol but omitting the cells.

The final gel solution was then pipetted into a uniaxial or biaxial mold placed within the bioreactor. The mold was removed after 30–45 min of gelation and the bath was filled with 100 ml of the experimental culture medium. This led to a detachment of the gel from the base of the bath, allowing it to float freely.

4 Results

Cells can sense and regulate their mechanical environment by, among other things, applying forces to the surrounding matrix.

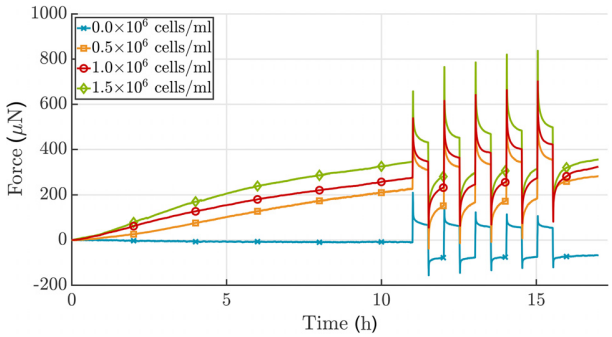

Fig. 6 Analysis of the effect of 3T3 cell density on force development in case of a ±2.0% stretch alternating every 30 min after an initial 11 h culture period in uniaxial setting. The total force increases when the number of cells increases. Additionally, the amplitude of the resulting force perturbation due to applied stretch is higher for a larger number of cells. Since cells were not treated to prevent proliferation, no plateau in force was reached. The acellular gel shows typical viscoelastic relaxation behavior (collagen concentration 1.5 mg/mL), which differs dramatically from the active relaxation/recovery achieved via cell-mediation. Shown is one experiment for each cell density.

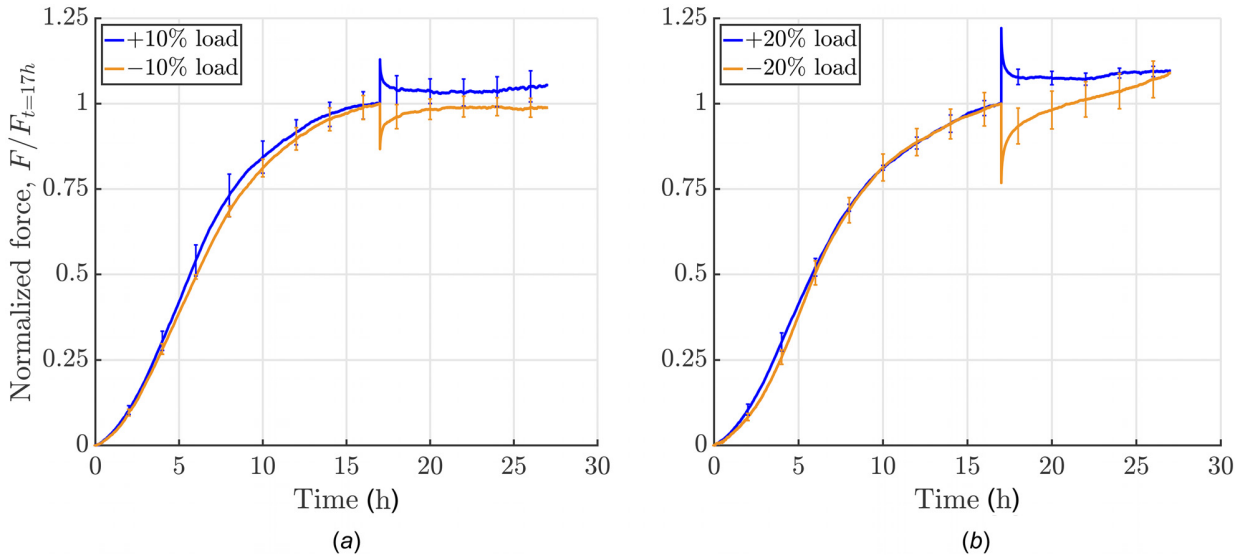

Fig. 7 Influence of amplitude and direction of perturbation: force development was measured for 10 h following a perturbation in loading (uniaxial setting, cells were serum-starved; experiments were force-controlled: 10% load means application of a force that equals 10% of the homeostatic force; each curve shows the mean ± SEM of three identical experiments). (*a*) Increasing or releasing the load by 10%: a positive perturbation elicited a cell-mediated relaxation toward the prior steady-state force with a small residual offset whereas a negative perturbation resulted in a recovery of the homeostatic force. (*b*) Conversely increasing load by 20% led to a notable offset from homeostatic force after 10 h of cell-mediated relaxation whereas decreasing load by 20% led to a continuous increase in force, with a new plateau not reached over the subsequent 10 h.

When cells are embedded in free-floating collagen gels, a strong compaction of the gel can be observed over multiple days [18,19] (Fig. 4). If gel compaction is prevented by uniaxial constraints, one observes a two-stage response consisting, first, of a steep increase in tension and, second, a near-constant tension in the gel [17,22,24,35]. Similar to prior uniaxial studies, our device allows one to study parameters such as cell density, collagen concentration, boundary conditions, and load amplitudes and directions on this general phenomenon.

4.1 Influence of Cell Density and Collagen Concentration Under Uniaxial Constraint. To confirm the influence of the number of cells/mL of gel on force buildup, three different cell densities, 0.2, 0.5 and 1.0×10^6 cells/mL, were tested in a uniaxial setting for 17 h. As expected, a higher number of cells led to a steeper increase in force and thus a higher homeostatic force (Fig. 5(*a*)). However, the time needed to reach a steady-state was similar for the three cell densities. The relationship between cell density and steady-state force was nonlinear. Furthermore, the amplitude of the resulting force perturbation due to applied stretch is higher for a larger number of cells. The acellular gel shows typical viscoelastic relaxation behavior, which differs dramatically from the active relaxation/recovery mediated by cells (Fig. 6).

Analogously, force development was measured for 27 h in gels with three different collagen concentrations, namely, 0.8, 1.5, and 2.5 mg/mL. A higher concentration of collagen also leads to a higher plateau of force (Fig. 5(*b*)). Force development depends nearly linearly on collagen concentration. The steady-state level, with neither a further increase nor decrease of force, was reached earlier for lower collagen concentrations. Interestingly, the gradient of force increase was similar for these three concentrations, unlike the case of varying cell densities.

4.2 Influence of Load Amplitude Under Uniaxial Constraint. As shown above, cells embedded in a collagen gel build up a certain force, often called homeostatic, which is then maintained for a prolonged period. It was shown previously that cells appear to seek to re-establish this state following mechanical perturbations [16,17]. However, prior data were restricted to 30 min relaxation intervals following such perturbations, not allowing confirmation of whether the force actually re-established completely or just partially. Our device allows measurements over extended relaxation times (e.g., 10+ h as shown in Figs. 7 and 8) when studying force development following mechanical perturbations (e.g., 10% and 20%, positive and negative perturbations in force) from the steady-state. We ran our experiments as semiforce controlled, that is, gels were stretched until force was perturbed by 10% or 20% with respect to the homeostatic value that had been reached. Subsequently, the stretch was fixed. The force recovery of the gels was dependent on the sign of the perturbation when gels were loaded to an extent corresponding to 10% of the steady-state level of force (Fig. 7(*a*)). For an increase in force caused by an increase in stretch, an offset remained after 10 h. When the force was decreased by a decrease in the stretch, the homeostatic state was re-established and then maintained. Our gels had an initial stiffness, that is Young's modulus, of about 10 kPa.

To understand the effects of differing loads, we increased the magnitude of the applied force to 20% of the homeostatic value (Fig. 7(*b*)). Similar to the 10% perturbation, a notable offset to the prior steady-state value of force remained after 17 h. In contrast, if gels were released such that their internal force decreased by 20%, an increase in force above the value prior to load application was seen over the subsequent 17 h. This might be because cells in these experiments were only serum-starved prior to the experiment and cells may re-enter the cell cycle after 20 h in the apparatus, possibly triggered by external loading if a certain threshold is exceeded. An increased number of cells would then explain higher forces as shown before (Fig. 5(*a*)). This behavior could be prevented by treating cells with Mitomycin C, see Sec. 4.3. It is also worth noting that changes in the gel mechanical state are likely due to active tension generated by the cells. As there is a limit to the amount of tension generated by cells, it may be that longer time periods that allow for the production and degradation of extracellular matrix components are required to fully recover the basal state.

4.3 Influence of Boundary Conditions. As described in Sec. 3, and in contrast to previous work by others [16,17,20,21,22], our new device can subject tissue equivalents to complex biaxial

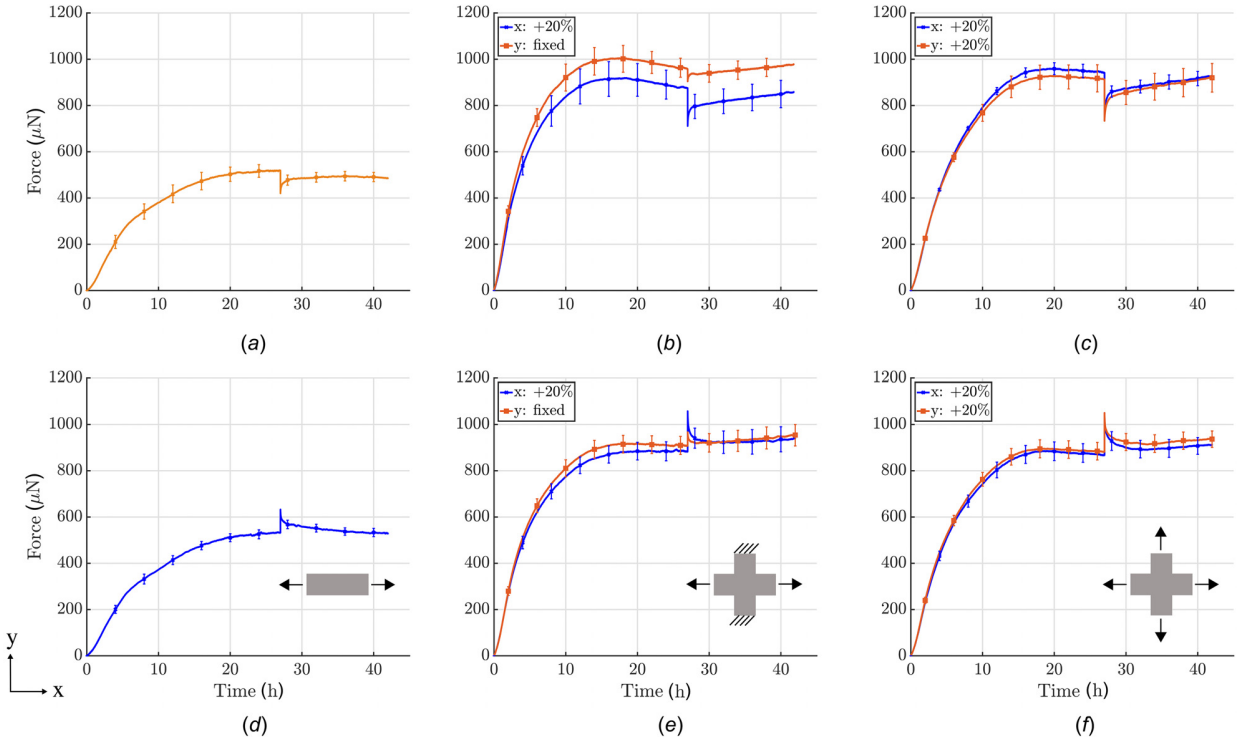

Fig. 8 Influence of boundary conditions on force development prior to and after perturbing the load from steady-state (cells treated with Mitomycin C to minimize cell proliferation during testing; each curve shows the mean±SEM of three identical experiments). First row: 20% reduction in load after an initial 27 h culture period under uniaxial, strip-biaxial, or equi-biaxial ((*a*)–(*c*)) conditions. Second row: 20% increase in load after 27 h in uniaxial, strip-biaxial, and equi-biaxial ((*d*)–(*f*)) conditions.

stress or strain conditions by stretching or releasing the two arms of the cruciform gel independently. To the best of our knowledge, the following results represent the first quantitative data of tension produced by cells within a collagen gel in a biaxial setting. For comparison, we performed experiments in uniaxial, strip-biaxial, and equi-biaxial protocols, with a ±20% perturbation of force after the homeostatic state was reached (Fig. 8). All experiments were performed with equal cell densities of 1.0×10^6/mL and equal collagen concentrations of 1.5 mg/mL. As we suspected proliferation in the gels after 20% load perturbations prevented reestablishment of the homeostatic state, we used Mitomycin C to completely prevent cells from duplicating.

Due to in-plane coupling, homeostatic forces were approximately 1.8-times higher in both biaxial protocols than in the uniaxial protocols. Additionally, the rate of force increase was higher in the biaxial setting and homeostatic forces were reached almost 10 h earlier, after 17 h. In the strip-biaxial setup, the *y*-direction of the cruciform gel was kept at constant length while the *x*-direction was stretched or released (Figs. 8(*b*) and 8(*e*), also see Fig. S3 available in the Supplemental Materials on the ASME Digital Collection), again with a ±20% perturbation in force. Due to the in-plane coupling of the two directions, a small perturbation emerged in the *y*-direction (roughly one-third of the load perturbation in *x*-direction) even though stretch was applied in *x*-direction alone. In the direction of load perturbation (*x*-direction), force returned to a steady-state but with an offset of approximately 4–5% of the homeostatic force. The *y*-direction increased slowly without reaching a steady-state during the 15 h recovery period. A similar continuous increase was observed for both the *x*- and *y*-directions in the release case (Fig. 8(*b*))). In the equi-biaxial case, equal loading perturbations were applied in the *x*- and *y*-directions (Figs. 8(*c*) and 8(*f*)). This condition led to a compensatory response from the gel that depended on the sign of the perturbation: if gels were stretched, forces actively relaxed almost back to the homeostatic value, but a small offset remained in both directions; if gels were released, both directions showed an active restoration of force without reaching a steady-state within the considered period.

4.4 Identification of Relaxation Constants. Following our previous work [36], a collagen gel can be modeled as a constrained mixture consisting of n collagen fiber families that can differ in their decay time constants T^i. Assuming the same homeostatic stress σ_c for all fiber families and a nearly constant cross section over the considered 10 h time period, we can describe the recovery of the total Cauchy stress $\sigma(t)$ within the gel as a sum of relaxation processes

$$\sigma(t) - \sigma_c = \sum_{i=1}^{n} \varphi^i \exp\left[-\frac{t-t_p}{T^i}\right]\left[\sigma\left(t_p^+\right) - \sigma_c\right] \text{ for } t > t_P \quad (1)$$

Table 1 Volume fractions φ^i, time constants T^i and L_2-errors for the best fit of Eq. (1) to experimental data shown in Fig. 8

		Uniaxial	Strip-biaxial		Equi-biaxial	
		x	x	y	x	y
Negative change in load	φ^1	0.58	0.41	0.34	0.46	0.48
	φ^2	0.42	0.59	0.66	0.54	0.52
	T^1 (h)	0.19	0.18	0.08	0.23	0.24
	T^2 (h)	14.11	13.00	5.95	11.41	7.12
	L_2-error (%)	14.86	9.44	26.30	8.62	8.04
Positive change in load	φ^1	0.54	0.67	0.53	0.70	0.64
	φ^2	0.46	0.33	0.47	0.30	0.36
	T^1 (h)	0.11	0.00	0.00	0.36	0.31
	T^2 (h)	7.18	4.2×10^{15}	2.5×10^4	14.98	22.60
	L_2-error (%)	18.60	14.80	40.31	12.83	10.90

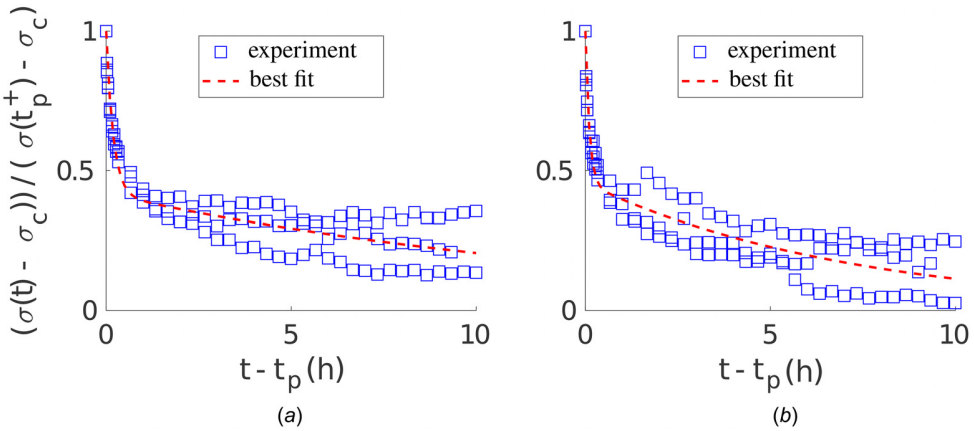

Fig. 9 Best fit of Eq. (1) with $n = 2$ exponentials to stress recovery data (hours 27–37) of uniaxial experiments shown in Figs. 8(*a*) and 8(*d*). (*a*) Decreased load perturbation from the homeostatic state according to Fig. 8(*a*); (*b*) increased load perturbation from homeostatic state according to Fig. 8(*d*).

where φ^i is the volume fraction of the ith fiber family, with $\sum_{i=1}^{n} \varphi^i = 1$. σ_c describes the value of homeostatic stress and $\sigma\left(t_p^+\right)$ the stress immediately after the perturbation at time t_p when external loading is applied.

We used a sum of $n = 2$ exponentials to fit the superimposed stress recovery data (hours 27–37) of three replicates of experiments that were performed for each setup shown in Fig. 8. The respective stress–time curves were normalized with respect to the initial perturbation from the homeostatic stress value $[\sigma(t_p^+) - \sigma_c]$ and the respective time t_p when external loading was applied. Figure 9 shows the best fit of Eq. (1) to both negative and positive recovery in the uniaxial setup, that is, to data in Figs. 8(*a*) and 8(*d*), respectively. Also, see Fig. S4 available in the Supplemental Materials on the ASME Digital Collection for the best fit of Eq. (1) to a strip-biaxial setup and Fig. S5 available in the Supplemental Materials on the ASME Digital Collection for the best fit of Eq. (1) to an equi-biaxial setup.

Table 1 lists volume fractions φ^i, time constants T^i, and L_2-errors for the respective best fits of Eq. (1) to the experimental data in Fig. 8. The computed L_2-errors are ~15% (besides strip-biaxial), which was considered satisfactory given the standard error of the mean of the experimental data of ~10%. Interestingly, as noted in Refs. [36] and [37], two relaxation time constants differing by about two orders of magnitude were needed for all fitted setups (besides for positive change in load in strip-biaxial setup due to re-increase in force after relaxation), thus suggesting two independently acting remodeling mechanisms within the gel.

5 Discussion

To date, the fundamental mechanisms underlying mechanobiological feedback loops between cells and ECM that ensure the viability and mechanical integrity of soft biological tissues remain poorly understood. In particular, few quantitative experimental data have been available that describe the cell-regulated evolution of stress and strain in soft tissues in response to perturbing forces. Moreover, the available data have also been restricted largely to free-floating gels or gels subjected to uniaxial loading. Because most soft tissues are subjected to multidimensional loads in vivo, we developed a computer-controlled biaxial bioreactor to create testing environments for both dogbone-shaped and cruciform-shaped tissue equivalents subjected to well-controlled uniaxial, strip-biaxial, or biaxial stress and strain states.

We demonstrated that our new device can measure forces produced by cells within collagen gels for up to 2 days within a 0–2000 μN range. Noise and drift were negligible (Fig. S1 available in the Supplemental Materials on the ASME Digital Collection). Although our device enables tests under load or stretch control, either statically or dynamically (Fig. S6 available in the Supplemental Materials on the ASME Digital Collection), we illustrated its utility via a subset of tests. One advantage of the cruciform-shaped samples is that they experience nearly homogeneous stress and strain fields in a central region under biaxial loads, with the added advantage that the cruciform arms of the sample also represent uniaxially loaded configurations. Another advantage of biaxial tests is that the effects of stresses can be studied in the absence of strains in the strip-biaxial test [31].

Our new device enables studies in a biaxial setting that focus on how cells establish a so-called homeostatic state within an initially stress-free gel and how they respond to perturbations to this state. Of course, one can study the effects of many parameters, including the impact of cell and fiber density, effects of exogenous cytokines and growth factors, and diverse loading conditions—uniaxial, strip-biaxial, equi-biaxial, and non-equi-biaxial—under static or dynamic stretching (see Fig. S6 available in the Supplemental Materials on the ASME Digital Collection). We emphasize, however, that the objective of this article was to present a new bioreactor design and to illustrate its utility, not to provide comprehensive data on the effects of one or more parameters.

Nonetheless, some of the illustrative gel results were provocative. When unperturbed, NIH/3T3 fibroblasts established and maintained a homeostatic state that depended on cell density, collagen concentration, and mechanical loading. Importantly, this stable homeostatic state was characterized by higher forces under biaxial conditions and it could only be maintained if cell proliferation was inhibited by either serum-starvation or treatment with Mitomycin C. In these cases, the cells were able to re-establish a force close to the preferred homeostatic state after a (single) step increase or decrease load perturbation, though, depending on the applied load, they were not fully able to maintain a stable state during the remaining course of the experiments. Although much more could be learned with the NIH/3T3 cells, there is a need to use cells that are of more interest biologically, including those with defects in cytoskeletal structure or integrin signaling, which would be expected to affect cell–matrix interactions dramatically.

In summary, this new biaxial bioreactor enables novel studies of cell–ECM interactions. It should help answer questions like: What does mechanical homeostasis mean in higher dimensions? What are cells sensing and how do they regulate their environment on the tissue scale? How does cell tension translate into tissue tension? How do cell–matrix interactions differ across different cell types on the tissue scale? Answering these and other

key questions will help us to develop a rigorous theoretical foundation for understanding principles governing soft tissue mechanobiology.

Funding Data

- Deutsche Forschungsgemeinschaft (DFG, German Research Foundation)—(Projektnummer 257981274; Projektnummer 386349077; Funder ID: 10.13039/501100001659).
- International Graduate School of Science and Engineering (IGSSE) of Technical University of Munich, Germany (Funder ID: 10.13039/501100005713).
- US National Science Foundation (Grant No. NSF DGE1122492; Funder ID: 10.13039/100000001).
- US National Institutes of Health (Grant No. P01 HL134605; Funder ID: 10.13039/100000002).

References

[1] Lu, P., Takai, K., Weaver, V. M., and Werb, Z., 2011, "Extracellular Matrix Degradation and Remodeling in Development and Disease," Cold Spring Harb. Perspect. Biol., **3**(12), pp. 1–24.

[2] Humphrey, J. D., Dufresne, E. R., and Schwartz, M. A., 2014, "Mechanotransduction and Extracellular Matrix Homeostasis," Nat. Rev. Mol. Cell Biol., **15**(12), pp. 802–812.

[3] Ross, T. D., Coon, B. G., Yun, S., Baeyens, N., Tanaka, K., Ouyang, M., and Schwartz, M. A., 2013, "Integrins in Mechanotransduction," Curr. Opin. Cell Biol., **25**(5), pp. 613–618.

[4] Cox, T. R., and Erler, J. T., 2011, "Remodeling and Homeostasis of the Extracellular Matrix: Implications for Fibrotic Diseases and Cancer," Dis. Model. Mech., **4**(2), pp. 165–178.

[5] Bonnans, C., Chou, J., and Werb, Z., 2014, "Remodelling the Extracellular Matrix in Development and Disease," Nat. Rev. Mol. Cell Biol., **15**(12), pp. 786–801.

[6] Xie, J., Bao, M., Bruekers, S. M. C., and Huck, W. T. S., 2017, "Collagen Gels With Different Fibrillar Microarchitectures Elicit Different Cellular Responses," ACS Appl. Mater. Interfaces, **9**(23), pp. 19630–19637.

[7] Hall, M. S., Alisafaei, F., Ban, E., Feng, X., Hui, C.-Y., Shenoy, V. B., and Wu, M., 2016, "Fibrous Nonlinear Elasticity Enables Positive Mechanical Feedback Between Cells and ECMs," Proc. Natl. Acad. Sci. U. S. A., **113**(49), pp. 14043–14048.

[8] Grinnell, F., and Petroll, W. M., 2010, "Cell Motility and Mechanics in Three-Dimensional Collagen Matrices," Annu. Rev. Cell Dev. Biol., **26**(1), pp. 335–361.

[9] Chiquet, M., Gelman, L., Lutz, R., and Maier, S., 2009, "From Mechanotransduction to Extracellular Matrix Gene Expression in Fibroblasts," Biochim. Biophys. Acta Mol. Cell Res., **1793**(5), pp. 911–920.

[10] Mammoto, A., Mammoto, T., and Ingber, D. E., 2012, "Mechanosensitive Mechanisms in Transcriptional Regulation," J. Cell Sci., **125**(13), pp. 3061–3073.

[11] Zemel, A., 2015, "Active Mechanical Coupling Between the Nucleus, Cytoskeleton and the Extracellular Matrix, and the Implications for Perinuclear Actomyosin Organization," Soft Matter, **11**(12), pp. 2353–2363.

[12] Bates, R. C., Lincz, L. F., and Burns, G. F., 1995, "Involvement of Integrins in Cell Survival," Cancer Metastasis Rev., **14**(3), pp. 191–203.

[13] Zhu, Y. K., Umino, T., Liu, X. D., Wang, H. J., Romberger, D. J., Spurzem, J. R., and Rennard, S. I., 2001, "Contraction of Fibroblast-Containing Collagen Gels: Initial Collagen Concentration Regulates the Degree of Contraction and Cell Survival," In Vitro Cell. Dev. Biol. Anim., **37**(1), pp. 10–16.

[14] Sukharev, S., and Sachs, F., 2012, "Molecular Force Transduction by Ion Channels—Diversity and Unifying Principles," J. Cell Sci., **125**(13), pp. 3075–3083.

[15] Schwartz, M. A., Schaller, M. D., and Ginsberg, M. H., 1995, "Integrins: Emerging Paradigms of Signal Transduction," Annu. Rev. Cell Dev. Biol., **11**(1), pp. 549–599.

[16] Brown, R. A., Prajapati, R., McGrouther, D. A., Yannas, I. V., and Eastwood, M., 1998, "Tensional Homeostasis in Dermal Fibroblasts: Mechanical Responses to Mechanical Loading in Three-Dimensional Substrates," J. Cell. Physiol., **175**(3), pp. 323–332.

[17] Ezra, D. G., Ellis, J. S., Beaconsfield, M., Collin, R., and Bailly, M., 2010, "Changes in Fibroblast Mechanostat Set Point and Mechanosensitivity: An Adaptive Response to Mechanical Stress in Floppy Eyelid Syndrome," Invest. Ophthalmol. Visual Sci., **51**(8), pp. 3853–3863.

[18] Simon, D. D., Niklason, L. E., and Humphrey, J. D., 2014, "Tissue Transglutaminase, Not Lysyl Oxidase, Dominates Early Calcium-Dependent Remodeling of Fibroblast-Populated Collagen Lattices," Cells Tissues Organs, **200**(2), pp. 104–117.

[19] Simon, D. D., Horgan, C. O., and Humphrey, J. D., 2012, "Mechanical Restrictions on Biological Responses by Adherent Cells Within Collagen Gels," J. Mech. Behav. Biomed. Mater., **14**, pp. 216–226.

[20] Kolodney, M. S., and Wysolmerski, R. B., 1992, "Isometric Contraction by Fibroblasts and Endothelial Cells in Tissue Culture: A Quantitative Study," J. Cell Biol., **117**(1), pp. 73–82.

[21] Eastwood, M., McGrouther, D. A., and Brown, R. A., 1994, "A Culture Force Monitor for Measurement of Contraction Forces Generated in Human Dermal Fibroblast Cultures: Evidence for Cell-Matrix Mechanical Signalling," BBA Gen. Subj., **1201**(2), pp. 186–192.

[22] Marenzana, M., Wilson-Jones, N., Mudera, V., and Brown, R. A., 2006, "The Origins and Regulation of Tissue Tension: Identification of Collagen Tension-Fixation Process In Vitro," Exp. Cell Res., **312**(4), pp. 423–433.

[23] Campbell, B. H., Clark, W. W., and Wang, J. H. C., 2003, "A Multi-Station Culture Force Monitor System to Study Cellular Contractility," J. Biomech., **36**(1), pp. 137–140.

[24] Brown, R. A., Sethi, K. K., Gwanmesia, I., Raemdonck, D., Eastwood, M., and Mudera, V., 2002, "Enhanced Fibroblast Contraction of 3D Collagen Lattices and Integrin Expression by TGF-B1 and -B3: Mechanoregulatory Growth Factors?," Exp. Cell Res., **274**(2), pp. 310–322.

[25] Hu, J.-J., Humphrey, J. D., and Yeh, A. T., 2009, "Characterization of Engineered Tissue Development Under Biaxial Stretch Using Nonlinear Optical Microscopy," Tissue Eng. Part A, **15**(7), pp. 1553–1564.

[26] Thomopoulos, S., Fomovsky, G. M., and Holmes, J. W., 2005, "The Development of Structural and Mechanical Anisotropy in Fibroblast Populated Collagen Gels," ASME J. Biomech. Eng., **127**(5), pp. 742–750.

[27] Thomopoulos, S., Fomovsky, G. M., Chandran, P. L., and Holmes, J. W., 2007, "Collagen Fiber Alignment Does Not Explain Mechanical Anisotropy in Fibroblast Populated Collagen Gels," ASME J. Biomech. Eng., **129**(5), pp. 642–650.

[28] Lee, P. Y., Liu, Y. C., Wang, M. X., and Hu, J. J., 2018, "Fibroblast-Seeded Collagen Gels in Response to Dynamic Equibiaxial Mechanical Stimuli: A Biomechanical Study," J. Biomech., **78**, pp. 134–142.

[29] Latorre, M., and Humphrey, J. D., 2019, "Mechanobiological Stability of Biological Soft Tissues," J. Mech. Phys. Solids, **125**, pp. 298–325.

[30] Braeu, F. A., Seitz, A., Aydin, R. C., and Cyron, C. J., 2017, "Homogenized Constrained Mixture Models for Anisotropic Volumetric Growth and Remodeling," Biomech. Model. Mechanobiol., **16**(3), pp. 889–906.

[31] Humphrey, J. D., Wells, P. B., Baek, S., Hu, J.-J., McLeroy, K., and Yeh, A. T., 2008, "A Theoretically-Motivated Biaxial Tissue Culture System With Intravital Microscopy," Biomech. Model. Mechanobiol., **7**(4), pp. 323–334.

[32] Aydin, R. C., Brandstaeter, S., Braeu, F. A., Steigenberger, M., Marcus, R. P., Nikolaou, K., Notohamiprodjo, M., and Cyron, C. J., 2017, "Experimental Characterization of the Biaxial Mechanical Properties of Porcine Gastric Tissue," J. Mech. Behav. Biomed. Mater., **74**, pp. 499–506.

[33] Hu, J. J., Liu, Y. C., Chen, G. W., Wang, M. X., and Lee, P. Y., 2013, "Development of Fibroblast-Seeded Collagen Gels Under Planar Biaxial Mechanical Constraints: A Biomechanical Study," Biomech. Model. Mechanobiol., **12**(5), pp. 849–868.

[34] Knezevic, V., Sim, A. J., Borg, T. K., and Holmes, J. W., 2002, "Isotonic Biaxial Loading of Fibroblast-Populated Collagen Gels: A Versatile, Low-Cost System for the Study of Mechanobiology," Biomech. Model. Mechanobiol., **1**(1), pp. 59–67.

[35] Eastwood, M., Mudera, V. C., McGrouther, D. A., and Brown, R. A., 1998, "Effect of Precise Mechanical Loading on Fibroblast Populated Collagen Lattices: Morphological Changes," Cell Motil. Cytoskeleton, **40**(1), pp. 13–21.

[36] Cyron, C. J., Aydin, R. C., and Humphrey, J. D., 2016, "A Homogenized Constrained Mixture (and Mechanical Analog) Model for Growth and Remodeling of Soft Tissue," Biomech. Model. Mechanobiol., **15**(6), pp. 1389–1403.

[37] Cyron, C. J., and Aydin, R. C., 2017, "Mechanobiological Free Energy: A Variational Approach to Tensional Homeostasis in Tissue Equivalents," Z. Angew. Math. Mech., **97**(9), pp. 1011–1019.

Appendix C

Paper C

A computational framework for modeling cell-matrix interactions in soft biological tissues

Jonas F. Eichinger, Maximilian J. Grill, Iman Davoodi Kermani, Roland C. Aydin, Wolfgang A. Wall, Jay D. Humphrey, Christian J. Cyron

published in

Biomechanics and Modeling in Mechanobiology, 10.1007/s10237-021-01480-2

Biomechanics and Modeling in Mechanobiology
https://doi.org/10.1007/s10237-021-01480-2

ORIGINAL PAPER

A computational framework for modeling cell–matrix interactions in soft biological tissues

Jonas F. Eichinger[1,2] · Maximilian J. Grill[1] · Iman Davoodi Kermani[1] · Roland C. Aydin[4] · Wolfgang A. Wall[1] · Jay D. Humphrey[3] · Christian J. Cyron[2,4]

Received: 25 March 2021 / Accepted: 8 June 2021

Abstract
Living soft tissues appear to promote the development and maintenance of a preferred mechanical state within a defined tolerance around a so-called set point. This phenomenon is often referred to as mechanical homeostasis. In contradiction to the prominent role of mechanical homeostasis in various (patho)physiological processes, its underlying micromechanical mechanisms acting on the level of individual cells and fibers remain poorly understood, especially how these mechanisms on the microscale lead to what we macroscopically call mechanical homeostasis. Here, we present a novel computational framework based on the finite element method that is constructed bottom up, that is, it models key mechanobiological mechanisms such as actin cytoskeleton contraction and molecular clutch behavior of individual cells interacting with a reconstructed three-dimensional extracellular fiber matrix. The framework reproduces many experimental observations regarding mechanical homeostasis on short time scales (hours), in which the deposition and degradation of extracellular matrix can largely be neglected. This model can serve as a systematic tool for future *in silico* studies of the origin of the numerous still unexplained experimental observations about mechanical homeostasis.

Keywords mechanical homeostasis · growth and remodeling · cell–extracellular matrix interaction · discrete fiber model · finite element method

1 Introduction

Living soft tissues, in contrast to classical engineering materials, usually seek to establish and maintain a mechanical state that is not stress-free. This behavior of living soft tissues is often referred to as *mechanical homeostasis*, and it plays a key role in the control of form and function in health and disease (Lu et al. 2011; Cox and Erler 2011; Ross et al. 2013; Humphrey et al. 2014; Bonnans et al. 2014). Intra cellular structures such as the actomyosin cytoskeleton are physically coupled to the surrounding extracellular matrix (ECM) via transmembrane protein complexes such as integrins that can cluster to form focal adhesions (Cavalcanti-Adam et al. 2007; Lerche et al. 2019). This coupling allows cells to receive mechanical cues from their environment, transduce these cues into intracellular signals, and react, for example, by adapting cellular stress and thereby also the stress of the surrounding ECM. Physical interactions between cells and ECM have been shown to control various processes on the cellular scale such as cell migration (Grinnell and Petroll 2010; Xie et al. 2017; Hall et al. 2016; Kim et al. 2020), differentiation (Chiquet et al. 2009; Mammoto et al. 2012; Zemel 2015; Seo et al. 2020), and survival (Bates et al. 1995; Schwartz 1995; Zhu et al. 2001; Sukharev and Sachs 2012) and are therefore fundamental for health and in disease of entire tissues and organs.

To study the micromechanical foundations of mechanical homeostasis experimentally, tissue culture studies with cell-seeded collagen or fibrin gels have attracted increasing interest over the past decades (Eichinger et al. 2021). Circular free-floating gels, when seeded with fibroblasts,

✉ Christian J. Cyron
christian.cyron@tuhh.edu

1 Institute for Computational Mechanics, Technical University of Munich, Garching 85748, Germany

2 Institute for Continuum and Materials Mechanics, Hamburg University of Technology, Hamburg 21073, Germany

3 Department of Biomedical Engineering, Yale University, New Haven, CT 06520, USA

4 Institute of Material Systems Modeling, Helmholtz-Zentrum Hereon, Geesthacht 21502, Germany

Published online: 25 June 2021

exhibit a strong compaction over multiple days in culture due to cellular contractile forces (Simon et al. 2012, 2014). Studies of such gels whose compaction is prevented by boundary constraints typically show a two-phase response. First, tension in the gels rapidly increases to a specific value, the so-called homeostatic tension (phase I), and then remains largely constant (phase II) for the rest of the experiment (Brown et al. 1998, 2002; Sethi et al. 2002; Campbell et al. 2003; Marenzana et al. 2006; Dahlmann-Noor et al. 2007; Karamichos et al. 2007; Ezra et al. 2010; Courderot-Masuyer 2017; Eichinger et al. 2020). If the gel is perturbed in phase II, for example, by an externally imposed deformation, cells appear to promote a restoration of the homeostatic state (Brown et al. 1998; Ezra et al. 2010). Despite substantial research efforts over decades, the exact interplay between cells and surrounding tissue that is crucial for mechanical homeostasis and other related phenomena such as durotaxis still remains poorly understood (Eichinger et al. 2021).

Computational studies in this field have focused primarily on decellularized ECM systems to study the micromechanical and physical properties of networks of fibers (Heussinger and Frey 2007; Mickel et al. 2008; Lindström et al. 2010; Chatterjee 2010; Broedersz et al. 2011; Stein et al. 2010; Cyron and Wall 2012; Cyron et al. 2013b, a; Lang et al. 2013; Motte and Kaufman 2013; Müller et al. 2014; Jones et al. 2014; Lee et al. 2014; Müller et al. 2015; Ronceray et al. 2016; Mauri et al. 2016; Dong et al. 2017; Humphries et al. 2018; Zhou et al. 2018; Bircher et al. 2019; Domaschke et al. 2019, 2020). Current computational models of cell–ECM interactions often suffer from shortcomings—most are limited to two dimensions and just one or two cells (Wang et al. 2014; Abhilash et al. 2014; Notbohm et al. 2015; Jones et al. 2015; Kim et al. 2017; Humphries et al. 2017; Grimmer and Notbohm 2017; Burkel et al. 2018). The importance of the third dimension for the physics of fiber networks is well known (Cukierman et al. 2002; Baker and Chen 2012; Jansen et al. 2015; Duval et al. 2017), and it can be assumed that collective interactions between more than just two cells play important roles in mechanical homeostasis. Moreover, current models typically rely in many crucial aspects on heuristic assumptions (Nan et al. 2018; Zheng et al. 2019) and almost all of them assume simple random fiber networks (e.g., based on Voronoi tessellations) that do not match the specific microstructural characteristics of actual collagen gels or tissues. What remains wanting is a robust, computationally efficient three-dimensional model of cell–fiber interactions, where the microstructure of the fiber network realistically resembles real collagen gels and tissues and which is efficient enough to enable simulations with several cells. Such a computational model can be expected to help unravel the micromechanical and molecular foundations of mechanical homeostasis.

In this paper, we introduce such a computational model. It is based on the finite element method and relies on a strong experimental foundation. It can be used to test various hypotheses with regard to the micromechanical principles of mechanical homeostasis. It can also help to identify promising future experiments. The model focuses on mechanical aspects of homeostasis by concentrating on the physical interactions of cells with surrounding matrix fibers and thus neglects direct modeling of biochemical phenomena. The paper focuses on a detailed description of the computational framework, but examples are used to demonstrate the physical validity of this framework and to illustrate the opportunities it will open up. It will be seen that this framework captures well key observations from experiments on short time scales (in which deposition and degradation of tissue fibers can be neglected), thus helping to explain the underlying physics.

2 Models and methods

To study the physical foundations of mechanical homeostasis in soft biological tissues on short time scales (hours), our framework models (i) interlinked ECM-like fiber networks whose microstructure closely resembles that of actual collagen gels, (ii) transmembrane proteins such as integrins which connect extra- to intracellular structures, and (iii) the contractile activity of the cytoskeleton. In the following, we describe the mathematical and computational details of our model.

2.1 Construction of representative volume elements (RVEs)

Computational modeling of soft tissues on the level of discrete fibers and individual cells remains intractable for large tissue volumes, noting that 1 ml of ECM may contain over one million cells. Therefore, we use RVEs as structurally typical samples of the considered tissue (Fig. 1a). Building on our previous work on biopolymer networks (Cyron and Wall 2012; Cyron et al. 2013a, b; Grill et al. 2021), we constructed physically realistic three-dimensional fiber networks from confocal microscope images of actual collagen gels (Fig. 1a). Following Lindström et al. (2010) and Davoodi-Kermani et al. (2021), we assumed that the mechanical properties of collagen fiber networks are predominantly governed by three descriptors, namely the valency (number of fibers connected to a network node, referred to by some as *connectivity*), the free-fiber lengths between adjacent nodes (herein also referred to as fiber length), and the angles between the fibers joining at the nodes (which can be quantified by the cosine of the angles between any pair of fibers joining at a node). These descriptors vary in the network across the

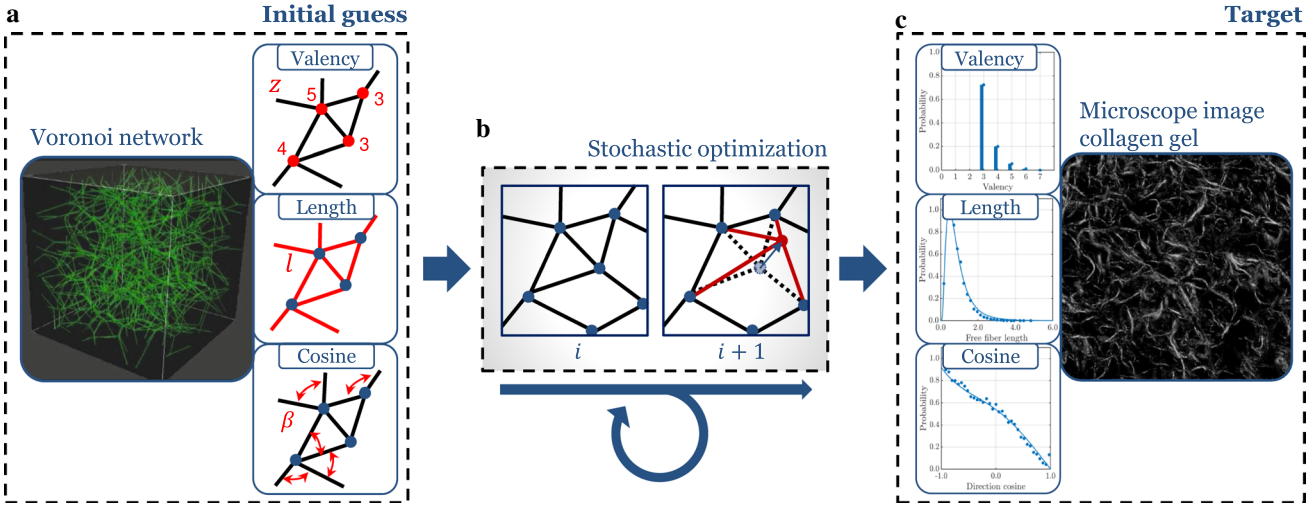

Fig. 1 Schematic of the network construction process. **a** Random fiber network geometries based on Voronoi tessellation are used as the initial configuration. Valency, length, and cosine distribution are used as descriptors of the network geometry for which target distributions are given. **b** By iterative random displacements of arbitrary nodes in the network and accepting these displacements based on their impact on the system energy, which penalizes deviations of the geometric descriptors from their target distributions, one arrives after a number of stochastic steps at a configuration with the desired distribution of the geometric descriptors of interest. **c** Microscope images of collagen gels are used to determine the target distributions for the descriptors of the network

fibers and nodes by following certain statistical distributions. Using the computational procedure described in Appendix A1, which is motivated by Yeong and Torquato (1998) and Lindström et al. (2010), and briefly illustrated in Fig. 1, we ensured that the statistical distributions of valency, free-fiber length, and inter-fiber cosines closely matched those of actual collagen fiber networks. The computational procedure to produce such networks has been implemented in a short C++ program which is available under the BSD 3-Clause License as the repository BioNetGen hosted at https://github.com/bionetgen/bionetgen.

2.2 Mechanical network model

We used the finite element method to model the mechanics of our fibrous RVEs. Individual fibers were modeled as geometrically exact beam finite elements based on the nonlinear Simo–Reissner theory (Reissner 1981; Simo 1985; Simo and Vu-Quoc 1986) and a hyperelastic material law. This beam theory captures the modes of axial tension, torsion, bending, and shear deformation and is appropriate for large deformations. Thus, our finite element model of the fiber network can capture all essential modes of mechanical deformation. If not stated otherwise, covalent bonds between fibers were modeled as rigid joints coupling both translations and rotations. We chose the dimensional and constitutive parameters to mimic collagen type I fibers as the most abundant structural protein of the ECM. Fibers are assumed to have circular cross sections with a diameter of $D_f = 180$ nm (Van Der Rijt et al. 2006) and elastic moduli of $E_f = 1.1$ MPa (Jansen et al. 2018). Assuming curvilinear fibers with circular cross section of diameter D_f, the average mass density of collagen ρ_c in the network RVE was calculated as

$$\rho_c = \frac{L_{tot} {D_f}^2 \pi}{V_{\mathrm{RVE}} v_c} \tag{1}$$

according to Stein et al. (2008), where L_{tot} is the sum of all individual fiber lengths, V_{RVE} the volume of the RVE, and $v_c = 0.73$ ml/g the specific volume of collagen fibers (Hulmes 1979).

2.3 Fiber to fiber cross-linking

A native ECM consists of myriad structural constituents, including collagen and elastin, which usually form networks to provide mechanical support to the resident cells. To form these networks, covalent cross-links are formed via the action of enzymes such as lysyl oxidase and transglutaminase, which can be produced by the cells (Simon et al. 2014). In addition to covalent bonds, transient hydrogen bonds or van der Waals bonds contribute further to the mechanical integrity of the ECM (Kim et al. 2017; Ban et al. 2018).

To model initially existing covalent bonds between fibers, we permanently connect individual fibers joining at nodes of our initially generated network by rigid joints. To model the formation of additional transient and covalent bonds, we define so-called binding spots on all fibers (Fig. 2). If during the simulation it happens that the distance between two binding spots on distinct filaments falls within a certain critical

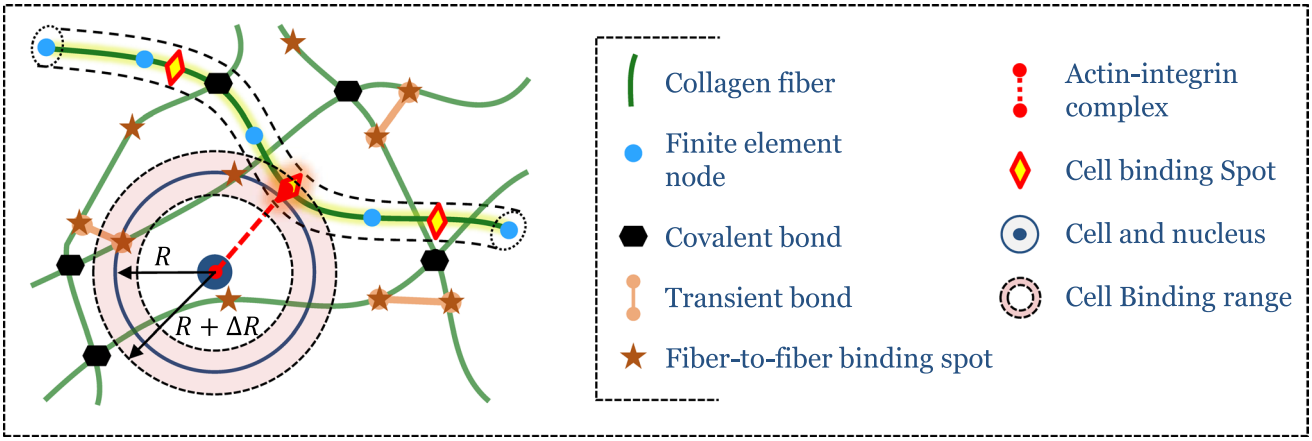

Fig. 2 Fiber network model: collagen fibers are modeled as beam-like mechanical continua discretized by beam finite elements. Nearby collagen fibers are connected by permanent (covalent) chemical bonds modeled as rigid joints. During the simulation, additional transient bonds may stochastically form and dissolve between nearby binding partners on the fibers. These bonds are also modeled by short beam elements transmitting forces and moments. Cells of radius R can attach to nearby collagen fibers if certain predefined cell binding locations on the surrounding fibers are within $R - \Delta R$ and $R + \Delta R$ around the cell

interval, a new bond between the two filaments is established according to a Poisson process with an on-rate k_{on}^{f-f}. That is, within a subsequent time step Δt, a bond is assumed to form with the probability

$$p_{on}^{f-f} = 1 - \exp\left(-k_{on}^{f-f}\Delta t\right). \tag{2}$$

Newly established bonds are modeled by initially stress-free beam elements. Bonds established this way during the simulation can also dissolve. This process is again modeled by a Poisson process with an off-rate k_{off}^{f-f}, yielding in each time step Δt an unbinding probability

$$p_{off}^{f-f}(F) = 1 - \exp\left(-k_{off}^{f-f}(F)\Delta t\right). \tag{3}$$

The off-rate is in general affected by the force F acting on the bond because transient chemical bonds under mechanical loading are typically less (though in certain regimes more) stable than load-free bonds (Bell 1980). This phenomenon can be modeled by a force-dependent off-rate

$$k_{off}^{f-f}(F) = k_{off,0}^{f-f}\ \exp\left(\frac{F\Delta x}{k_B T}\right), \tag{4}$$

with Δx a characteristic distance, k_B the Boltzmann constant, and T the absolute temperature (Bell 1980). $\Delta x > 0$ was chosen so that the bond weakens under tension, a bond behavior that is often referred to as slip-bond behavior. By choosing $k_{off,0}^{f-f} = 0$, we can model new covalent bonds formed during our simulations, whereas $k_{off,0}^{f-f} > 0$ mimics transient bonds.

2.4 Cell–ECM interaction

Cells in soft tissues can mechanically connect to surrounding fibers by integrins and exert stress on them via focal adhesions. A focal adhesion usually includes an actin stress fiber bundle in the cytoskeleton that connects the nucleus of the cell with the integrins of a cluster and can actively contract. Based on experimental observations, we restricted the maximal number of focal adhesions per cell to $N_{FA,max} = 65$ (Kim and Wirtz 2013; Horzum et al. 2014; Mason et al. 2019). Figure 3b on the left shows three focal adhesions. It has been shown experimentally that roughly $N_{i,FA,max} = 1000$ integrins are involved in one focal adhesion (Wiseman 2004; Elosegui-Artola et al. 2014). These integrins are organized in so-called integrin clusters of roughly $20 - 50$ integrins (Changede et al. 2015; Cheng et al. 2020) (Fig. 3c). We thus assume for each focal adhesion 50 integrin clusters containing a maximum of $N_{i,ic,max} = 20$ integrins each.

To model cell-mediated active mechanical processes in soft tissues, we model the cell centers as point-like particles. When these particles approach predefined integrin binding partners (with a distance of $d^{i-f} = 50$ nm to each other; López-García et al. 2010) on the fibers within $\pm\Delta R$ around the cell radius R, a physical connection between cells and fibers is assumed to form by a Poisson process similar to the one in Eq. (2), but with a specific on-rate k_{on}^{c-f} (see also Fig. 3a). The actin stress fibers connecting the cell nucleus with the fibers surrounding the cells are modeled as elastic springs (Fig. 3b, c) whose stress-free length evolves at some predefined rate $\dot{c}$ that can be calculated to match experimental data of different cell types. These stress fibers contract at a rate of $\dot{c} = 0.1$ μm/s (Choquet et al. 1997; Moore et al.

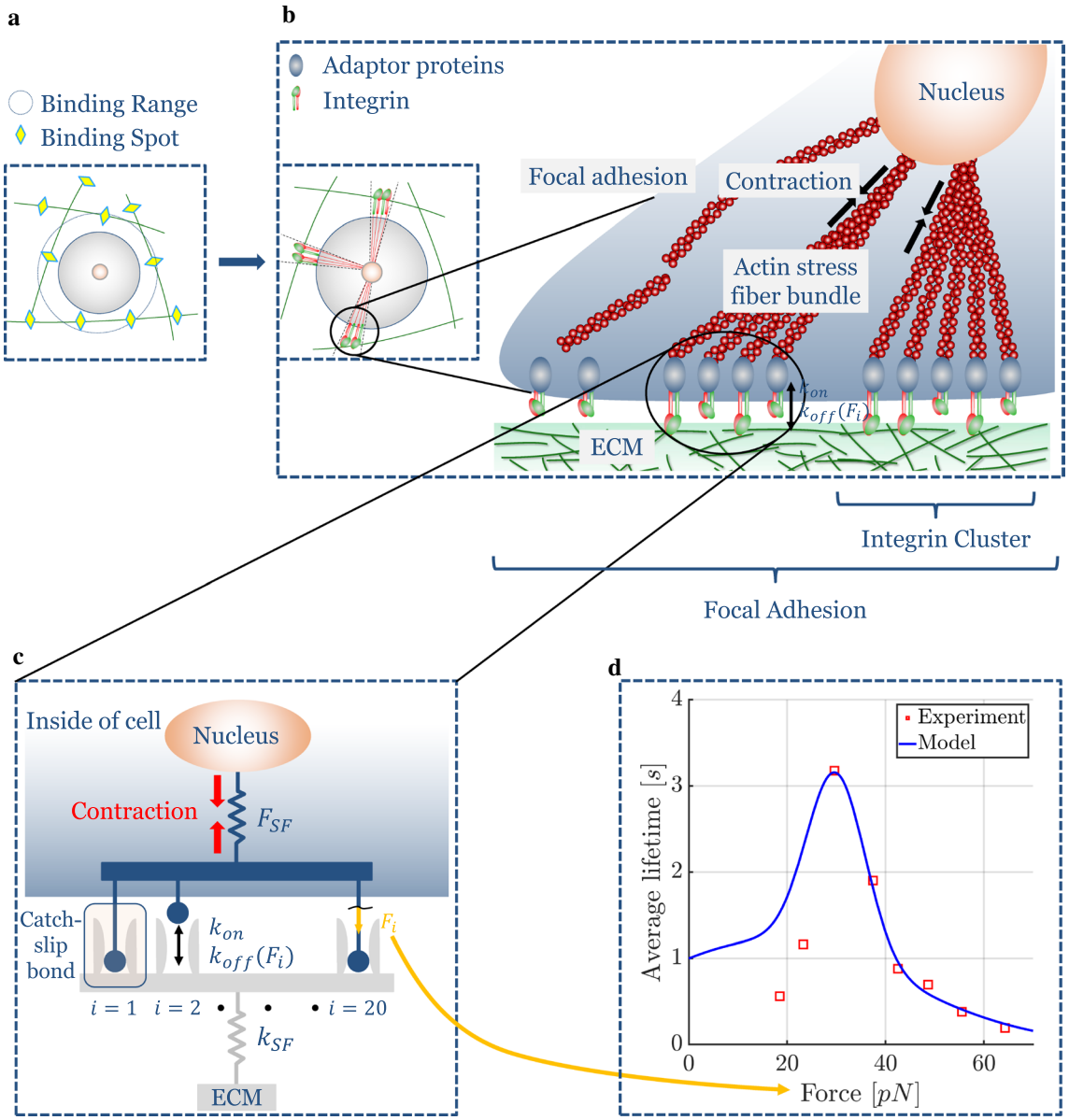

Fig. 3 **a** If cells lie within a certain distance from integrin binding spots on fibers, a focal adhesion can from with a certain probability. **b** A focal adhesion consists of around 1000 integrins connecting the intracellular actin cytoskeleton to the ECM fibers. Actin stress fibers connect the cell nucleus to the focal adhesions and are modeled as elastic springs that contract over time. **c** Each focal adhesion consists of numerous so-called integrin clusters, each formed by 20 – 50 integrins. We assume that each integrin cluster is connected to one actin stress fiber. Integrins are modeled as molecular clutches, i.e., they bind and unbind according to specific binding kinetics. **d** Experiments have determined a catch–slip bond behavior for single integrins where the lifetime does not monotonically decrease with the mechanical force transmitted through the bonds but where there exists a regime where increasing forces increase the average lifetime of the bond. To avoid infinite off-rates in case of low forces, we chose a slightly higher lifetime for low forces compared to the experimental data of Kong et al. (2009)

2010). The force acting on a single integrin F_i can be computed according to

$$F_i = \frac{F_{SF}}{N_{i,bonded}}, \tag{5}$$

with F_{SF} the force acting in the respective stress fiber and $N_{i,bonded}$ the number of currently bound integrins in the integrin cluster associated with the respective stress fiber.

In contrast to many previous approaches in which displacements have been prescribed in the neighborhood of cells to model their contraction, we are able to model a true two-way feedback loop between cell and ECM. Integrins

have been shown experimentally to exhibit a so-called catch–slip bond behavior (Kong et al. 2009) whose unbinding can be modeled by a Poisson process with a force-dependent off-rate

$$k_{off}^{c-f}(F) = a_1 \exp\left(-\left(\frac{F-b_1}{c_1}\right)^2\right) + a_2 \exp\left(-\left(\frac{F-b_2}{c_2}\right)^2\right) \tag{6}$$

whose parameters were determined via fits to the experimental data (Kong et al. 2009; Weng et al. 2016) as shown in Fig. 3d and in Table 2. While the average lifetime of most chemical bonds decreases monotonically with increasing force transmitted by the bond, catch-slip bonds exhibit a regime where the bond stabilizes as the force increases. As illustrated in Fig. 3d, this makes integrin bonds particularly stable for values of F_i in a range around 30 pN. Recall that we model an integrin cluster as a system of 20 parallel integrins whose bonds form and dissolve according to the above specified on- and off-rates (Fig. 3c). If at a certain point all bonds happen to have broken at the same time, the related integrin cluster is assumed to dissolve. It may, however, reform on the basis of a new (not yet contracted) stress fiber shortly thereafter with a binding rate k_{on}^{c-f}. If all clusters of a certain focal adhesion happen to dissolve at the same time, the focal adhesion as a whole is dissolved.

This model implies that many binding and unbinding events of integrins occur during the lifetime of a focal adhesion. This way, our model captures the chemical dynamics of the connection between cells and ECM fibers on different scales ranging from individual integrins to whole focal adhesions (Stehbens and Wittmann 2014). Thereby, our model both captures typical lifetimes of focal adhesions on the order of minutes and turnover rates of most proteins involved in the adhesion complex on the order of seconds.

2.5 Boundary conditions

As mentioned before, simulations of complete tissues on the *cm*-scale are computationally expensive with discrete fiber models; hence, we study RVEs. A major challenge in the context of discrete fiber simulations is the imposition of deformations on the RVE to study its response to certain strains. To this end, most previous work by others requires that the nodes of the finite elements used to discretize fibers are located exactly on the boundary surfaces of the RVE where displacements are prescribed (Stein et al. 2010; Abhilash et al. 2014; Liang et al. 2016; Humphries et al. 2018; Burkel et al. 2018; Ban et al. 2018, 2019). Other approaches prescribe the displacements of nodes close to these surfaces (Lee et al. 2014). These methods share the problem that they do not ensure full periodicity across the boundaries where displacements are prescribed. To overcome this limitation, we developed a novel form of fully periodic boundary conditions for fiber networks that allows imposition of complex multiaxial loading states. This approach ensures full periodicity across all surfaces of the RVE and thereby minimizes computational artifacts due to finite-volume effects. The computational details of our algorithm are summarized in Appendix A1. Briefly, every point on a fiber that would reside outside of the RVE in the i-th coordinate direction is shifted back in by the length of the RVE in the respective direction L_i (Fig. 11a). In this way, Dirichlet boundary conditions can be applied by simply stretching the RVE as a whole, as this results in a strain in each fiber that is cut by the boundary in the direction of the applied load due to a change in the shifting factor (Fig. 11c, d).

2.6 Search algorithm and parallel computing

To yield meaningful computational results, the RVEs have to be much larger than the characteristic microstructural features such as the free-fiber length between adjacent nodes. Using values for the cell density and collagen concentration in a physiologically reasonable range typically leads to a system size of the RVE that can be solved only by parallel computing, including an efficient parallel search algorithm for the evaluation of all interactions between cells and fibers. We implemented such a search algorithm based on a geometrical decomposition of the computational domain in uniform cubic subdomains. The computational details of our parallelization are summarized in Appendix A2. Importantly, our approach does not require any fully redundant information on all processes, which enables a highly efficient parallelization on even a very large number of processors.

3 Results and discussion

The presented computational framework was implemented in our in-house research finite element code BACI 2021. To ensure robustness, scalability, and especially validity, we performed various computational simulations and compared the results with available experimental data. The default parameters used in our simulations are listed in Table 2.

3.1 Network construction

We first validated the network generation method described in Sect. 2. To this end, we created networks with different collagen concentrations and target descriptor distributions as observed by confocal microscopy in tissue culture experiments with collagen type I gels (Lindström et al. 2010; Nan

et al. 2018). As shown in Fig. 4, our stochastic optimization method successfully generates networks with the desired distributions of valency, free-fiber length, and cosine. Figure 5a demonstrates that our simulated annealing converged well toward the desired network (Fig. 5b) with an increasing number of random iteration steps.

3.2 Passive mechanical properties: stiffness

Next, we verified that our constructed, still acellular, networks have similar mechanical properties as actual collagen networks. To this end, we simulated simple uniaxial tensile tests with different collagen concentrations and compared the resulting values for the stiffness with values that have been collected in uniaxial experiments with collagen type I gels (Alcaraz et al. 2011; Miroshnikova et al. 2011; Joshi et al. 2018). We stretched a cubic simulation box with edge length $L = 245$ μm in one direction by applying displacement boundary conditions as described in Appendix A1 at a slow loading rate of 0.01 μm/s up to a strain of 1.0%; strains around 1% have been shown to be the relevant range when studying active, cell-mediated force development (Eichinger et al. 2020). Figure 5c demonstrates that the Young's moduli of the constructed networks match well with the values observed in tissue culture experiments. In our artificial RVEs, we found a power law dependence between

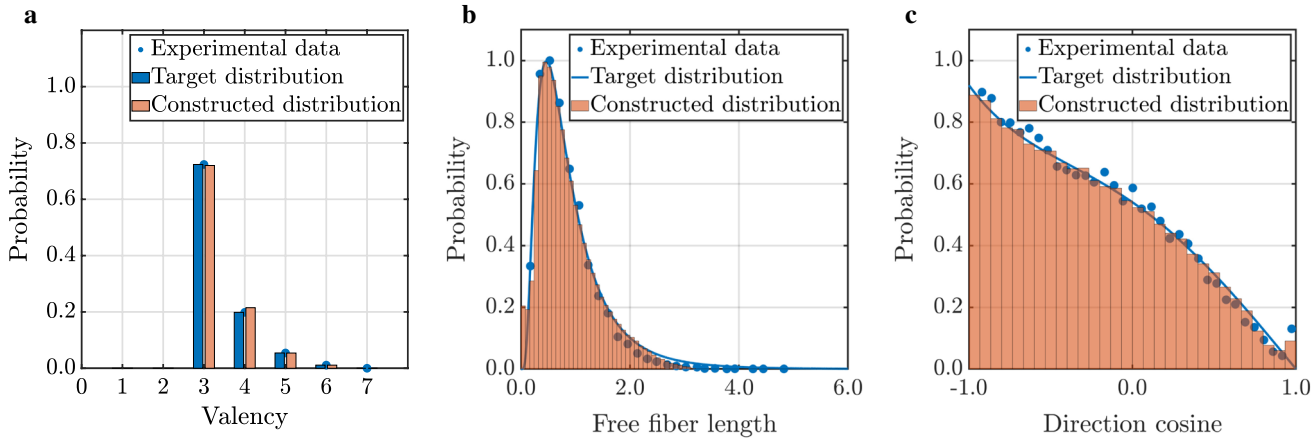

Fig. 4 Results of the network construction process for a collagen concentration of 2.5 mg/ml. **a** valency distribution, **b** free-fiber length distribution and **c** cosine distribution fit well the target distributions defined on the basis of experimental data taken from Nan et al. (2018) in **a** and from Lindström et al. (2010) in **b** and **c**

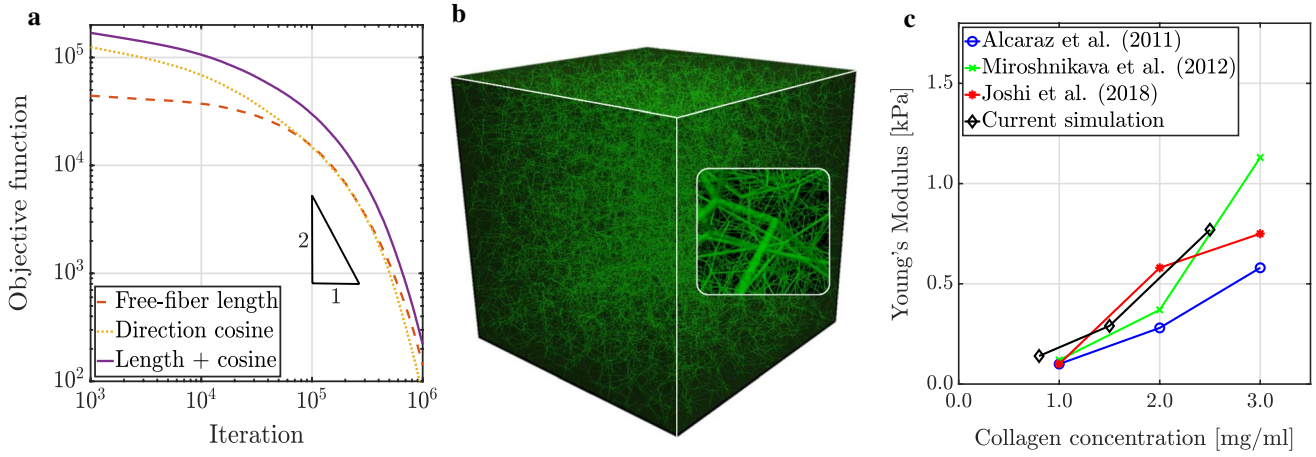

Fig. 5 **a** In the stochastic network construction with a collagen concentration of 0.8 mg/ml in a cube of edge length 245 μm, the energy-type objective function according to Eq. (11) is reduced during simulated annealing (in the studied range even superquadratically) by multiple orders of magnitude; **b** this optimization process yields RVEs with a desired microstructure; **c** the effective Young's moduli at strains < 1% of RVEs constructed this way match well with the ones observed in experiments (Alcaraz et al. 2011; Miroshnikova et al. 2011; Joshi et al. 2018)

the Young's modulus and the collagen concentration with an exponent of 1.33, similar to the exponent of 1.22 found experimentally (Joshi et al. 2018).

3.3 Active mechanical properties: homeostatic tension

In this section, we consider cell-seeded fiber networks to study the *active* mechanics of soft tissues. The tension that develops in constrained gels stems from the contractile forces exerted by the cells on the surrounding fibers. In initially stress-free collagen gels seeded with fibroblasts, the tension builds up over a few hours until it has reached a plateau value, the so-called homeostatic value (Brown et al. 1998, 2002; Sethi et al. 2002; Campbell et al. 2003; Marenzana et al. 2006; Dahlmann-Noor et al. 2007; Karamichos et al. 2007; Ezra et al. 2010; Courderot-Masuyer 2017; Eichinger et al. 2020). Tissue culture experiments (Delvoye et al. 1991; Eichinger et al. 2020) have shown that the homeostatic tension depends on both cell and collagen concentration in the gel. We used this observation to validate our computational model. We created RVEs with an edge length of $L = 245\ \mu$m and three different cell densities and collagen concentrations as studied experimentally in Eichinger et al. (2020). To increase the complexity of the RVE only gradually by adding cells, we still solely considered covalent bonds between matrix fibers. We then compared the cell-mediated active tension over time of our simulations to the one observed experimentally.

It is important to note that a direct (quantitative) comparison between experimental data and simulation results is difficult due to differing boundary conditions. Tissue culture experiments have at least one traction-free boundary (uniaxial gels have two, circular discs three), while we performed our simulations with RVEs with periodic boundary conditions applied in all directions. Note also that a free boundary in a microscopic RVE would not resemble a free boundary of a macroscopic specimen. It has been shown, however, that the number of fixed boundaries has a crucial impact on the homeostatic plateau value (Eichinger et al. 2020). In the following, we compare the first Piola–Kirchhoff stresses as the thickness of the gel samples over time is unknown. An initial thickness of the gel of $t_{initial} = 1.6$ mm (knowing it to be between 1.0 mm and 3.0 mm) is assumed to fit best to the simulation data presented in the following. The initial width of the undeformed gel is 10 mm. The stresses for the RVEs were quantified as the sum of all fiber tractions across a boundary divided by the respective cross-sectional area.

3.3.1 Variation of cell density

In this section, we consider gels with a constant collagen density of 1.5 mg/ml. Cell densities of $0.2 \cdot 10^6$ cells/ml, $0.5 \cdot 10^6$ cells/ml , and $1.0 \cdot 10^6$ cells/ml studied in Eichinger et al. (2020) translate in our simulations into 3, 8, and 15 cells per RVE, respectively. Figure 6a shows the evolution of first Piola–Kirchhoff stress (true force/original area) generated in uniaxially constrained, dog-bone-shaped collagen gels as observed experimentally. The gradient during the first 10 h of the experiment and the homeostatic plateau level of stress increase with cell density. Both features are observed in our simulations and fit quantitatively well (Fig. 6b, c). We can therefore conclude that actin cytoskeleton contraction and the focal adhesion dynamics described

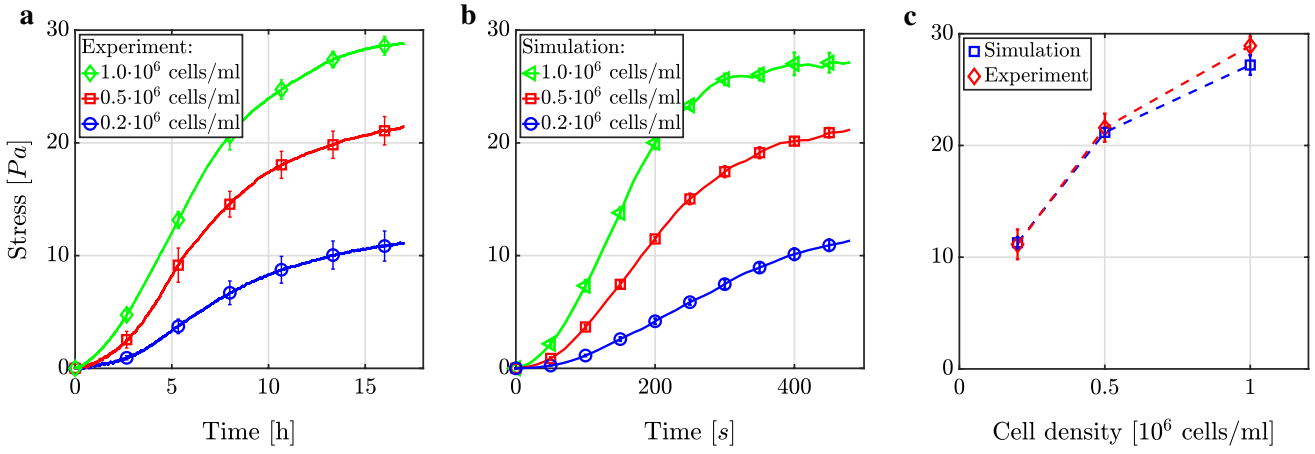

Fig. 6 For a collagen concentration of 1.5 mg/ml, we compare the development of first Piola–Kirchhoff stress in **a** experiments (Eichinger et al. 2020) and **b** simulations. A good semiquantitative agreement of the expected cell-mediated steady state with nonzero tension (last data points of **a** and **b**) is observed **c**, however, also a significant difference of the time scales. All lines show the mean ± standard error of the mean (SEM) of three identical experiments in **a** and **c** and of three simulations with different random network geometries in **b** and **c**

in Sect. 2.4 are sufficient mechanisms to reproduce this non-trivial relationship.

A crucial difference between experiments and simulations is the time scale. Whereas mechanical homeostasis develops over a couple of hours in the experiments, it does so within a couple of minutes in the simulation. Interestingly, this time scale of our simulations agrees well with that for which single cells in experiments on purely elastic substrates reach a homeostatic state (Weng et al. 2016; Hippler et al. 2020). Thus, a possible explanation for the difference between our simulations and the experimental data from Eichinger et al. (2020) may be that in tissues with numerous cells, complex interactions between the cells substantially delay the homeostatic state. Such interactions remain poorly understood and are not yet accounted for in our computational framework. Another possible explanation for the different time scales in Fig. 6a, b may be viscoelasticity due to collagen fibers moving within culture media, which is not included in our model in detail, and due to an increasing stiffness of the gel due to progressed polymerization when being placed in an incubator at 37°C for longer times. Finally, subtle aspects on the subcellular scale that are not included in our model may affect the time to reach the homeostatic state substantially because it is well known that this time differs considerably for different cell types (Eichinger et al. 2021).

Figure 7a shows that the deformation of the matrix fibers around the cells in our simulations is on the order of 10 μm, which agrees well with experiments (Notbohm et al. 2015; Malandrino et al. 2019). Our simulation framework also reproduces the ability of cells to communicate via long-range mechanical interactions over several cell diameters (Fig. 7b), which has also been observed experimentally (Ma et al. 2013; Shi et al. 2013; Baker et al. 2015; Kim et al. 2017; Mann et al. 2019).

3.3.2 Variation of collagen concentration

It is well known that interactions between cells and their environment crucially depend on the stiffness of the environment. This holds in particular for the proliferation, survival, migration, and differentiation of cells (Wang et al. 2012; Nguyen et al. 2018; Balcioglu et al. 2020). A simple way of testing the impact of stiffness on cellular behavior in tissue culture studies is to change the collagen concentration of the tested gels (Alcaraz et al. 2011; Miroshnikova et al. 2011; Hall et al. 2016; Joshi et al. 2018). As shown in Fig. 8a, tissue culture studies with a cell density of $0.5 \cdot 10^6$ cells/ml revealed that the cell-mediated first Piola–Kirchhoff stress increases in collagen gels with the collagen concentration (Delvoye et al. 1991; Eichinger et al. 2020). This behavior is both qualitatively and quantitatively reproduced well by our simulations as shown in Fig. 8b. Interestingly, both experiments and simulations exhibit a nearly linear relation (with a slope of $\sim 9/2$) between collagen concentration and the homeostatic stress (Fig. 8c). Moreover, the slope of the increase in stress up to the homeostatic stress was largely independent of the collagen concentration compared to the cell density in both the experiments and our simulations. We know from our simulations that an increased fiber density in cases of higher collagen concentrations in combination

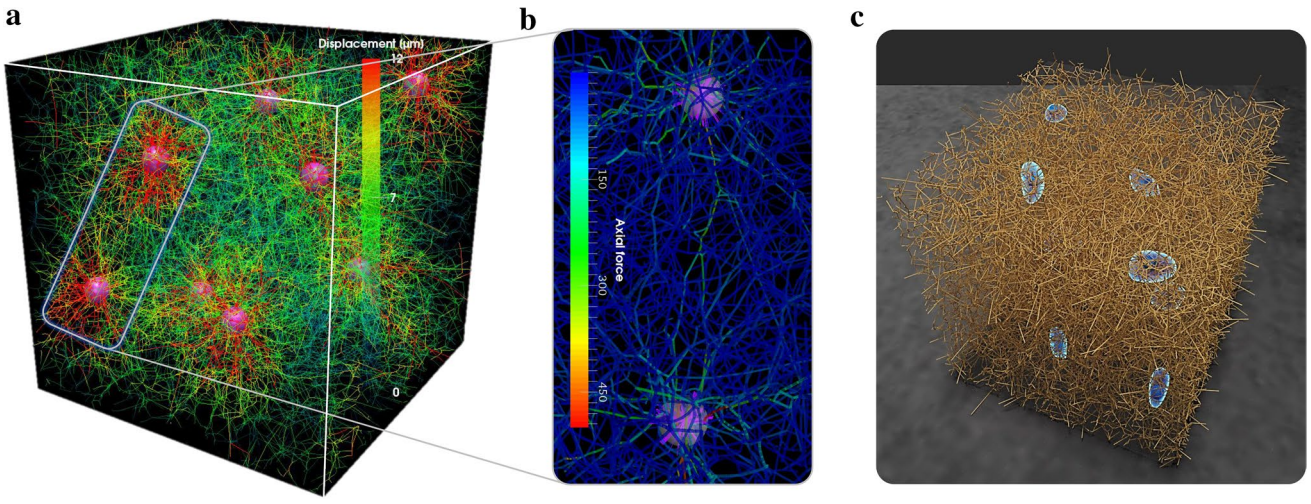

Fig. 7 Cells mechanically interact with surrounding matrix fibers. **a** Cells attach to nearby fibers, contract, and thereby deform the matrix. The simulated, cell-mediated matrix displacements are in a realistic range when compared to experimental data (Notbohm et al. 2015; Malandrino et al. 2019). **b** Contracting cells can mechanically interact with other cells over a distance of several cell diameters via long-range mechanical signaling through matrix fibers, a phenomenon observed also in experiments (Ma et al. 2013; Shi et al. 2013; Baker et al. 2015; Kim et al. 2017; Mann et al. 2019). **c** Cells, visualized with reconstructed cell membrane around stress fibers, develop different shapes when pulling on the ECM

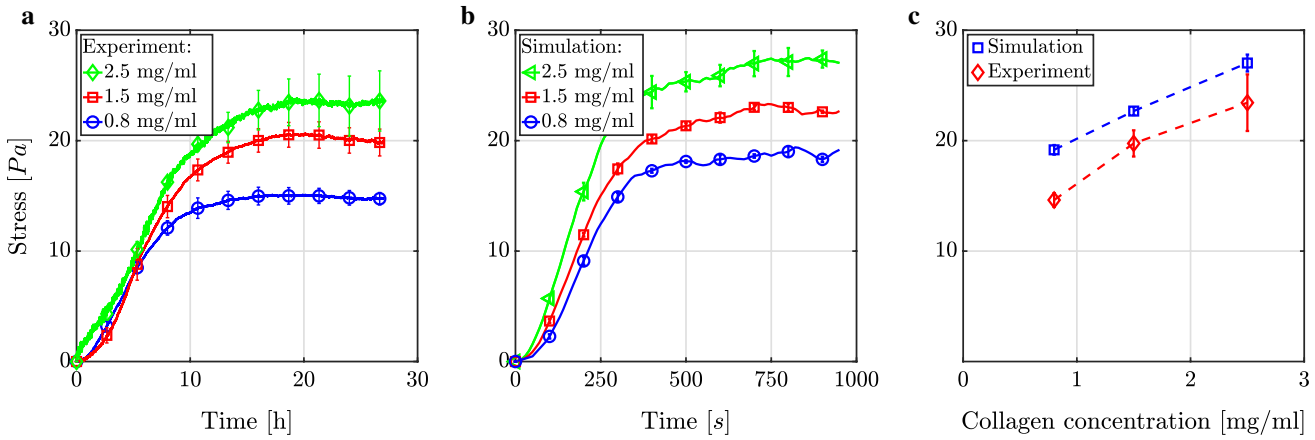

Fig. 8 Mechanical homeostasis for a cell concentration of $0.5 \cdot 10^6$ cells/ml and different collagen concentrations in **a** experiments (Eichinger et al. 2020) and **b** our simulations. **c** In both cases, the relation between homeostatic first Piola–Kirchhoff stress (last data points were taken, respectively) and collagen concentration is approximately linear. All lines show the mean ± SEM of three identical experiments in **a** and **c** and of three simulations with different random network geometries in **b** and **c**

with a constant distance between integrin binding spots on fibers of 50 nm (López-García et al. 2010) leads to more cell–matrix links per cell over time (data not shown) even when considering only the mechanisms presented in Sect.2. If one assumes that a cell stresses fibers one by one up to a certain level, this process takes longer if more fibers are present and can explain the observed nearly linear relationship between homeostatic stress and collagen concentration as well as the similar initial slope for all three collagen concentrations.

3.4 Residual matrix tension

Mechanical homeostasis in soft tissues is closely linked to growth (changes in mass) and remodeling (changes in microstructure) (Cyron and Humphrey 2017). In particular, a reorganization of the microstructure of tissues includes a change in the mechanical links between tissue fibers and of the constituent-specific natural (stress-free) configurations. Experimental studies have revealed that remodeling of collagen gels induced by cellular forces is time dependent and inelastic (Kim et al. 2017; Ban et al. 2018). Recent computational work suggested that the inelastic nature of cell-mediated remodeling is induced by force-dependent breaking of weak inter-fiber connections followed by the formation of bonds in new configurations leading to altered connections between tissue fibers (Nam et al. 2016; Kim et al. 2017; Ban et al. 2019; Cao et al. 2017) (Fig. 9a). This implies that after cell-mediated remodeling, a part of the matrix tension remains in the tissue even after the elimination of all active cellular forces (e.g., by disrupting the actomyosin apparatus via addition of cytochalasin D or by cell lysis). This remodeling is often referred to as residual matrix tension (RMT) (Marenzana et al. 2006; Simon et al. 2014).

To date, our quantitative understanding of how an altered state of the matrix is entrenched during remodeling and how RMT develops is limited. Even the exact kind of cross-linking which occurs when matrix tension is entrenched is unknown. An inelastic change of the stress-free configuration of the tissue could emerge from newly formed, transient bonds between collagen fibers (such as hydrogen bonds or van der Waals forces) as a result of fiber accumulation in the surroundings of contractile cells (Kim et al. 2017; Ban et al. 2018). However, RMT could also be entrenched by cells producing covalent cross-links via the actions of tissue transglutaminase, which can also form new bonds between deformed matrix fibers. The impact of these enzymes on matrix remodeling has been shown experimentally in free-floating collagen gels (Simon et al. 2014). To study RMT, we simulated the experimental protocol presented in Marenzana et al. (2006) and eliminated active cellular forces from the simulated system in the homeostatic state by dissolving all existing cell–ECM bonds at a certain time (by setting $k_{on}^{c-f} = 0$, which led to a rapid dissolution of the remaining bonds). We then tracked tension over time in the RVE.

We first studied RMT in a purely covalently cross-linked network, implying that all existing bonds between fibers remained stable and no new bonds were formed during the simulation. After deactivating active cellular forces, we observed a (viscoelastic) decline of tension to zero in the RVE (Fig. 9b, bottom curve). This finding suggested that networks that lack the ability to form new, at least temporary stable, bonds cannot entrench a residual tension in the matrix, which was observed in the aforementioned experimental studies (Marenzana et al. 2006; Simon et al. 2014).

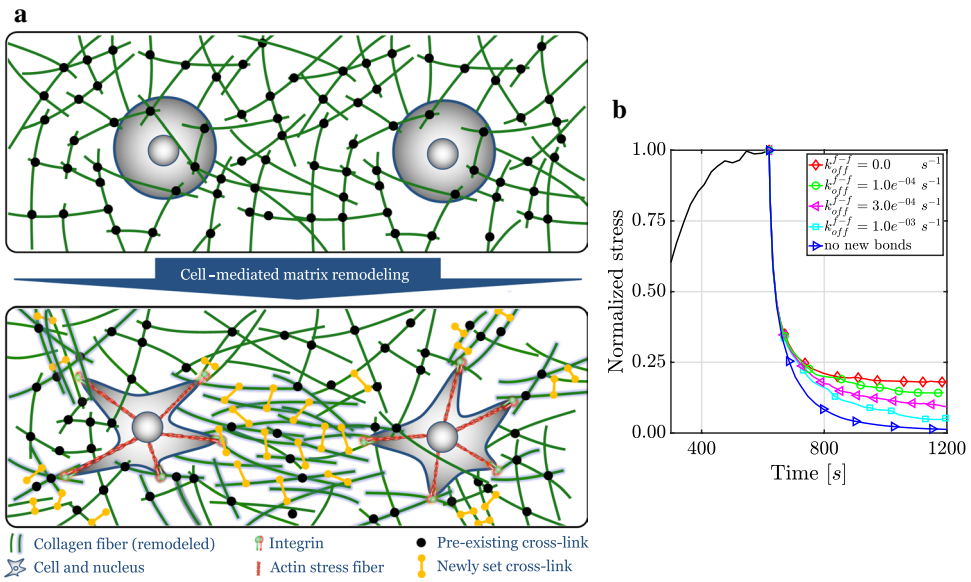

Fig. 9 **a** Cells actively permanently remodel their surrounding by reorganizing the network and establishing new cross-links. This way, cell-mediated tension can be entrenched in the network. **b** When removing active cellular forces suddenly, the matrix tension quickly drops. However, if cells have entrenched their reorganization of the network structure by permanent (covalent) cross-links (i.e., with $k_{off}^{f-f} = 0.0$), a residual tension persists in the network. By setting transient cross-links with a sufficiently low off-rate, the cells can ensure an RMT at least over the periods considered

In a second step, transient linkers (which could, for example, be interpreted as un-bonded, freely floating collagen molecules or hydrogen bonds) were allowed to form between fiber to fiber binding spots with a certain on-rate k_{on}^{f-f}; they were able to be dissolved with a certain off-rate k_{off}^{f-f}. If two binding spots of two nearby fibers resided at some point in close proximity to each other, a new, initially tension-free bond was formed according to Eq. (2). We found that introduction of newly formed, transient bonds enables the entrenchment of matrix remodeling and thus some RMT (Fig. 9b, $k_{off}^{f-f} = 1.0e^{-04}\ s^{-1}$, $k_{off}^{f-f} = 3.0e^{-04}\ s^{-1}$, $k_{off}^{f-f} = 1.0e^{-03}\ s^{-1}$) at least for a prolonged period. The transient nature of the cross-links between the fibers resulted, however, in a slow decrease in RMT over time. This decrease happened faster the higher the off-rate k_{off}^{f-f} (Fig. 9b). If k_{off}^{f-f} was chosen above a certain threshold, we did not observe any RMT.

In a third study, we allowed covalent cross-linker molecules to form between two nearby collagen fibers when they were within a certain distance to each other and Eq. (2) was fulfilled. By setting $k_{off}^{f-f} = 0$, a newly set bond could not be dissolved and was therefore covalent (permanent). In this case, we observed a substantial RMT that apparently did not decrease over time (Fig. 9b, $k_{off}^{f-f} = 0.0\ s^{-1}$).

It thus appears that both transient and covalent cross-links play roles in inelastic matrix remodeling. Our study suggests that RMT crucially depends on the ability of cells to entrench the deformation they impose on their neighborhood by covalent, permanent cross-links. Such a permanent entrenchment appears energetically favorable because it releases cells from the necessity of maintaining matrix tension over prolonged periods by active contractile forces, which consume considerable energy.

4 Conclusion

To date, our understanding of the governing principles of mechanical homeostasis in soft tissues on short time spans especially on the scale of individual cells remains limited (Eichinger et al. 2021). To address some of the many open questions in this area, we developed a novel computational framework for modeling cell–ECM interactions in three-dimensional RVEs of soft tissues. Our computational framework generates random fiber networks whose geometric characteristics resemble those of actual collagen type I gels, that is, they exhibit a similar distribution of valency, free-fiber length, and orientation correlation (cosine) between adjacent fibers. These microstructural characteristics have been shown to be the primary determinants of the mechanical properties of fiber networks (Davoodi-Kermani et al. 2021). To model the mechanics of the collagen fibers in the network, our framework discretizes these fibers with geometrically exact nonlinear beam finite elements, which are shown in Sect. 3 to reproduce the elastic properties of collagen fiber networks. Our framework enables efficient parallel computing and can thus be used to simulate RVEs of tissues with realistic collagen concentrations and cell densities.

The physical interactions of cells with surrounding fibers through stress fibers in the cytoskeleton and transmembrane proteins (integrins) are modeled by contractile elastic springs whose binding and unbinding dynamics closely resemble the situation in focal adhesions. We used the non-trivial, experimentally determined relations of both cell density and collagen concentration to the homeostatic stress to show that the mechanisms accounted for in our computational framework are sufficient to capture these relationships. We also demonstrated how our framework can help to (quantitatively) examine the micromechanical

foundations of inelastic cell-mediated matrix remodeling and RMT, which persists in the tissue even after active cellular forces have been removed.

Despite its advantages and broad experimental foundation, the proposed computational framework has some limitations that remain to be addressed. First, our model does not yet capture mass turnover, that is, the deposition and degradation of fibers, which are assumed to be crucial for mechanical homeostasis on long time scales (Humphrey and Rajagopal 2002; Ambrosi et al. 2011; Cyron et al. 2016; Braeu et al. 2017; Cyron and Humphrey 2017). Moreover, it models integrins but not associated proteins that also play a key role in the interactions between cells and surrounding matrix such as talin and vinculin (Ziegler et al. 2008; Grashoff et al. 2010; Carisey et al. 2013; Dumbauld et al. 2013; Das et al. 2014; Yao et al. 2014; Austen et al. 2015; Truong et al. 2015; Davidson et al. 2015; Zhu et al. 2016; Yao et al. 2016; Ringer et al. 2017). Also the model of cellular contractility is simplistic and should be endowed with additional biological details (Mogilner and Oster 2003; Murtada et al. 2010, 2012). Finally, we did not consider contact forces between fibers or between cells and fibers (assuming that cells and fibers mainly interact via integrins). While this reduces the computational cost substantially, a comprehensive incorporation of contact mechanics could also help to make our computational framework more realistic.

An important field of application for our computational framework will be *in silico* studies in which one can test step by step which additional features have to be incorporated in the framework to capture more and more phenomena observed *in vitro* and *in vivo*. In this way, it may contribute to uncovering the micromechanical foundations of mechanical homeostasis on the level of individual cells and fibers and help to understand how these microscopic processes lead to what we call mechanical homeostasis on the macroscale.

Appendix

A1 Construction of random fiber networks by simulated annealing

In this appendix, we present the computational details of the algorithm we used for constructing network RVEs as an input for our simulations. Our algorithm closely follows the approach of Lindström et al. (2010), using the stochastic optimization method of simulated annealing for constructing random heterogeneous media introduced by Yeong and Torquato (1998). Thereby, one assumes that the geometry of a fiber network can be characterized by some descriptors $\boldsymbol{x}_i$, with $i \in \{l, c\}$, in our case representing the fiber length and the direction cosine, respectively. These descriptors can be understood as random variables taking on specific values at certain nodes or fibers and characterize the network microstructure. The descriptors are assumed to follow some statistical distribution $P^i(x_i)$ across the different fibers and nodes. These distributions can be determined, for example, from confocal microscopy images of real networks (see also Fig. 10). According to Lindström et al. (2010), this yields for collagen type-I networks

$$P^l(l) = \frac{1}{l\sigma\sqrt{2\pi}} \exp\left(-\frac{[\mu - \ln(l)]^2}{2\sigma^2}\right), \tag{7}$$

where l denotes the fiber length normalized by $(N/V_{RVE})^{\frac{1}{3}}$, with V_{RVE} being the volume of the RVE and N representing the total number of network nodes in it. The parameters σ and μ denote a standard deviation and mean value that may vary from network to network. Typical parameters are given

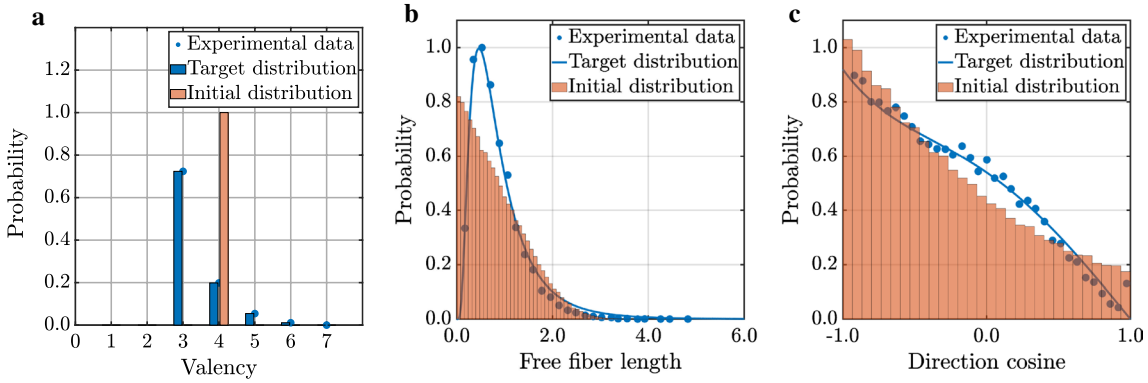

Fig. 10 Random initial descriptor distributions in a network generated by Voronoi tessellation vs. target distributions fitted by Lindström et al. (2010) and Nan et al. (2018) to experimental data (collagen concentration 2.5 mg/ml). Simulated annealing alters the initial network until its descriptor distributions match the required target distributions

Table 1 Parameters for length, valency, and cosine distribution functions according to Lindström et al. (2010) and parameters used for simulated annealing process

Parameter	Description	Value [–]
w_l	Weight for free-fiber length distribution in Eq. (11)	1.0
w_c	Weight for direction cosine distribution in Eq. (11)	1.0
μ	Mean in Eqs. (7) and (8)	−0.3000
σ	Standard deviation in Eqs. (7) and (8)	0.6008
b_1	Parameter for truncated power series in Eqs. (9) and (10)	0.6467
b_2	Parameter for truncated power series in Eqs. (9) and (10)	−0.1267
b_3	Parameter for truncated power series in Eqs. (9) and (10)	0.0200
b_l	Number of bins for free-fiber length distribution in Eq. (13)	1000
b_c	Number of bins for direction cosine distribution in Eq. (13)	1000
T_0	Initial temperature	0.05
–	Resulting average of nodal valency of constructed networks	3.3

in Table 1. The cumulative probability distribution associated with $P^l(l)$ is given by

$$C^l(l) = \frac{1}{2} + \frac{1}{2}\,\mathrm{erf}\left(\frac{\ln(x) - \mu}{\sqrt{2}\sigma}\right) \tag{8}$$

and will be used in Eq. (13).

The distribution of the direction cosine β of fibers adjacent to the same node has been described by Lindström et al. (2010) by a truncated power series

$$P^c(\beta) = \sum_{k=1}^{3} b_k (1-\beta)^{2k-1}, \tag{9}$$

with the associated cumulative distribution function

$$C^c(\beta) = 1 + \sum_{k=1}^{3} -\frac{b_k}{2k}(1-\beta)^{2k-1}. \tag{10}$$

Again, typical values for the parameters b_k are given in Table 1. To describe the valency distribution of the networks, we relied on the data reported in Nan et al. (2018).

Our target was to construct artificial random fiber networks as an input for our simulations whose descriptor distributions matched the ones defined above. To this end, we started from some random initial network. This network was then evolved in a number of discrete random steps according to the concept of simulated annealing (Kirkpatrick et al. 1983), until the descriptor distributions matched the desired target distributions.

To define the random initial configuration, we started by generating networks based on three-dimensional Voronoi tessellations (Rycroft 2009) with periodic boundary conditions applied in all directions. Subsequently, we randomly removed and added fibers until the valency distribution matched its target distribution. Only then we started the actual simulated annealing, where only fiber length and direction cosine distributions still had to be matched to their target distributions. The simulated annealing was performed following the concept introduced by Kirkpatrick et al. (1983). The idea is to iteratively select random nodes in the network and apply random displacements to them (Fig. 1b). In this way, the length of all fibers attached to the respective node and the angles between these fibers change. Importantly, only movements of nodes are accepted which do not lead to fiber lengths larger than one-third of the smallest edge length of the RVE to ensure that it stays *representative*. Note that a movement of a node does not affect its connectivity, which ensures that the initially created valency distribution remains unaffected during the whole simulated annealing.

For stochastic optimization according to the simulated annealing concept, it is helpful to define an objective (energy-type) function E

$$E = w_l \cdot E^l + w_c \cdot E^c, \tag{11}$$

where the E^l and E^c become minimal if the length and direction cosine distribution exactly match their target distributions and where the $w_i > 0$ are weights that can be adapted to tune the importance of a specific distribution function. Having defined the objective function E, simulated annealing can be understood as a stochastic minimization of E. Once the minimum is found, E^l and E^c must be minimal and thus the length and direction cosine distributions match their target distributions. To perform a stochastic minimization of E, a Metropolis algorithm is applied during the simulated annealing. It consists of a sequence of random steps. For each of these steps, the associated change of E is computed, that is, ΔE. Then, the step is actually performed only with a likelihood

$$p_{accept}(\Delta E) = \begin{cases} 1, & \Delta E \leq 0 \\ \exp(-\frac{\Delta E}{T}), & \Delta E > 0, \end{cases} \tag{12}$$

where T denotes a temperature-like parameter (having units of energy). In our simulated annealing, we slowly decreased

T as the number random steps increased, using at the annealing step k the value $T = 0.95^k \cdot T_0$ (according to Nan et al. (2018)). We chose T_0 such that the probability for accepting a random step with $\Delta E > 0$ was approximately 0.5 in the beginning. In practice, the simulated annealing was stopped if either the total energy of the system was below a predefined threshold or a maximal number of iterations were reached.

Remark A1 It is worth noting that for constructing RVEs with different collagen concentrations, we assumed the same target distributions for the valency, direction cosine and normalized fiber length. Only the normalization factor of the fiber length was changed. Moreover, an increased collagen concentration automatically also implies a higher number N of network nodes in the RVE.

Remark A2 While there exists a variety of simple and obvious choices for the E^i in Eq. (11), these mostly suffer from a computational cost on the order of $\mathcal{O}(n_i)$ with n_i the number of instances of a descriptor. This makes the generation of large random networks practically infeasible. To overcome this problem, we adopted the idea of Lindström et al. (2010) to use a binning algorithm and define the E^i as Cramer–von Mises test statistics, which reduces the computational cost to the order of $\mathcal{O}(b)$ with b the number of bins. To this end, we divided the range of $\boldsymbol{x_i}$ in b_i disjoint intervals (bins) and assigned each instance of a descriptor at a fiber or node of a random network to its associated bin. The resulting histogram is a discrete approximation of $P^i(x_i)$. The center of the j-th bin is denoted by x_{ij}. The number of instances of descriptor x_i assigned to the j-th bin is m_{ij}. The Cramer–von Mises test statistics can then be computed as

$$E^i = \frac{1}{n_i^2} \sum_{j=1}^{b_i} m_{ij} \left[\frac{1}{6}(m_{ij} + 1)(6S_{ij} + 2m_{ij} + 1) + S_{ij}^2 \right], \tag{13}$$

with $S_{ij} = M_{i(j-1)} - nC^i(x_{ij}) - \frac{1}{2}$, $M_{ij} = \sum_{k=1}^{j} m_{ik}$, and C^i the cumulative distribution of x_i.

A2 Boundary conditions

Here, we summarize how we applied fully periodic boundary conditions to our simulation domains. Let these domains be cuboids with edge length L_i in the i-th coordinate direction. In a fully periodic network, the part of a fiber sticking out across one periodic boundary must have a counterpart entering the RVE at the opposing side (Fig. 11a). One can interpret the element part sticking out of the domain at one boundary and the element part entering the RVE at the opposing boundary also as a fictitious single element (Fig. 11b, state II) cut into two parts (Fig. 11b, state I). Thereby, state I as delineated in Fig. 11b can be used to evaluate interactions with other fibers or cells, and state II for evaluating strains and stresses on element level. If the element is cutting through a boundary in the i-th coordinate direction, the i-th coordinate of the nodal positions in states I and II is shifted by L_i relative to each other. Importantly, only the translational degrees of freedom of the beam finite element nodes are affected by the periodic boundaries, rotational degrees of freedom remain unaffected.

It is a major challenge to impose periodic Dirichlet boundary conditions on fiber networks in a manner that is fully periodic. Most of the literature (Stein et al. 2010; Lee et al. 2014; Abhilash et al. 2014; Liang et al. 2016; Humphries et al. 2018; Burkel et al. 2018; Ban et al. 2018, 2019) bypasses this difficulty by fixing nodes on or close to the periodic boundary in a manner that unfortunately cannot ensure periodicity in a rigorous manner. To overcome this deficiency, we used the following approach. Dirichlet boundary conditions on RVEs can be represented by normal or shear strains. These strains can be converted into a relative displacement of opposing periodic boundaries by components Δd_j in the j-th coordinate direction. We accounted for this displacement by stretching (Fig. 11c) or shearing (Fig. 11d) the RVE as a whole. The nodal positions in states I and II were then no longer converted into each other in the above described simple manner, that is, by a relative shift by L_i in the i-the direction. Rather, all coordinates of the nodal positions were additionally shifted relative to each other by the components Δd_j. Note that this approach can account for complex multi-axial loading by applying the described procedure at all periodic boundaries. Moreover, this approach can account for large strains.

A3 Search algorithm and parallel computing

Here, we describe how we ensured efficient parallel computing for the presented modeling framework in our in-house finite element solver BACI 2021. Parallelization of the finite element discretization of the fibers can be handled with standard libraries such as the Trilinos libraries that form the basis of our in-house code. Therefore, we focus on the parallelization of cell–fiber interactions and chemical bonds between fibers; both require search algorithms to identify cell–fiber or fiber pairs that may interact at a certain point in time. We implemented a search algorithm based on a geometrical decomposition of the computational domain (RVE) in uniform cubic containers. For simplicity, these were aligned with the axes of our coordinate system (Fig. 12). Cells and finite beam elements are assigned to all containers with which they overlap. We chose the minimal size of the containers such that all possible interaction partners were certainly located within one layer of neighboring containers.

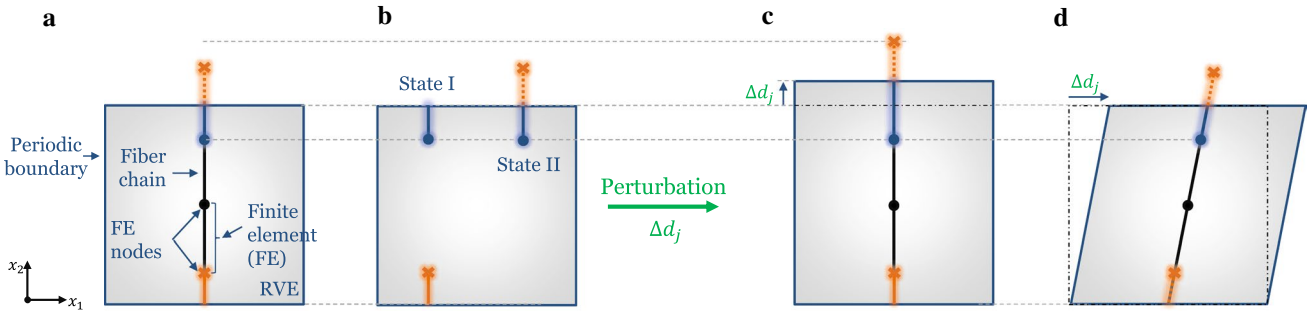

Fig. 11 Illustration of periodic boundary conditions using the example of a single fiber in a network: **a** any fraction of an element sticking out of a periodic boundary must have a counterpart entering at the opposing side; **b** both element fractions together define what is physically present within the RVE (state I). To compute strains and stresses in both element fractions, it is convenient to use a fictitious state II (shifted rightward in the figure for illustration purposes only), which represents the part of the cut element within the simulated RVE and the part located in an adjacent domain periodically continuing the RVE; **c** application of fully periodic normal strain boundary condition in vertical direction; **d** application of fully periodic shear strain boundary condition in the drawing plane

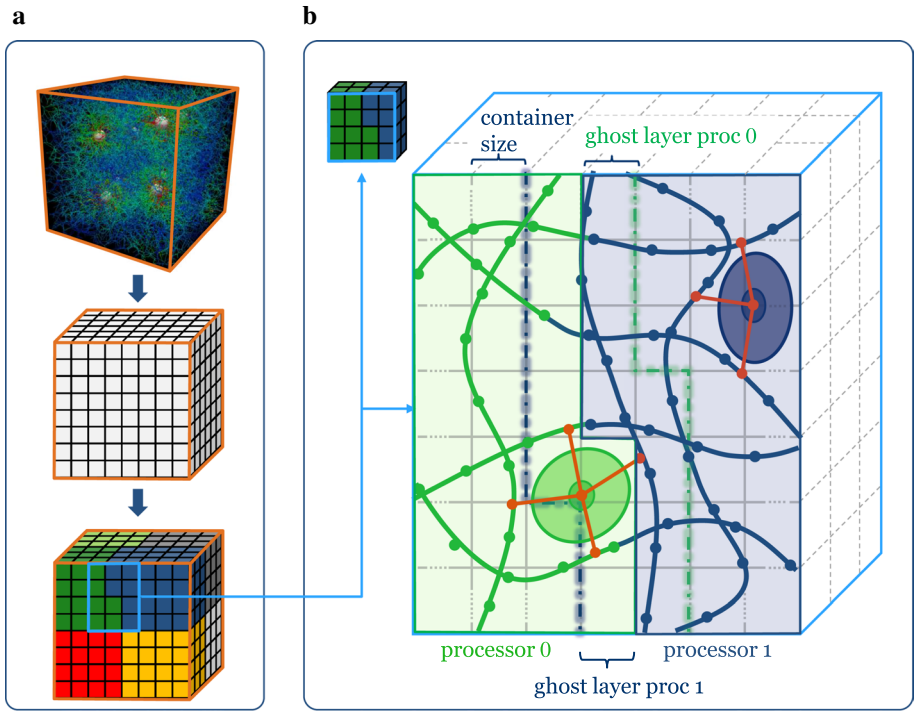

Fig. 12 **a** Our computational domain (top) was divided into a large number of cubic containers (middle). Sets of numerous such containers (highlighted by different colors, bottom) were distributed to different processors. **b** All fibers discretized by beam finite elements as well as all cells were assigned to all containers with which they overlapped. Each processor was provided information not only about its own containers but also about a layer of ghost containers elements with which the elements in its own container may interact

Hence, evaluating the possible interactions of a single cell or beam finite element simply required searching within one layer of containers around the containers to which the cell or element was assigned.

The content of the containers had to be updated over time as cells and matrix fibers moved during our simulations. Depending on the time step size of our simulations, container size and effective physical interaction distance, it was feasible to update our containers only every n-th time step.

The potentially large domain considered in our simulations typically required a distribution of the above described containers on several processors. To this end, each processor was assigned a set of containers forming a connected subdomain. In addition to these containers, each processor was also provided full information about one layer of so-called ghost containers surrounding its specific subdomain (Fig. 12b). The computational cost of sharing the information about ghost containers was negligible compared to the overall computational cost of our simulations.

To enable an effective search algorithm based on a rectangular Cartesian domain, we used a coordinate transformation to the undeformed domain in case boundary conditions imposing a deformation of the computational domain.

It is worth mentioning that in our parallelization framework, no data (except some uncritical parameters such as the current time step) need to be stored fully redundantly on all processors, which would drastically limit the problem sizes.

A4 Simulation parameters

Table 2 List of parameters and default values of computational model

Parameter	Description	Value	References
a_1	Integrin catch–slip bond parameter	2.2	To fit data of Kong et al. (2009)
b_1	Integrin catch–slip bond parameter	29.9	To fit data of Kong et al. (2009)
c_1	Integrin catchslip bond parameter	8.4	To fit data of Kong et al. (2009)
a_2	Integrin catch–slip bond parameter	1.2	To fit data of Kong et al. (2009)
b_2	Integrin catch–slip bond parameter	16.2	To fit data of Kong et al. (2009)
c_3	Integrin catch–slip bond parameter	37.8	To fit data of Kong et al. (2009)
R	Cell radius	12 µm	Typical value
ΔR	Linking range around cell	±3 µm	–
D_f	Diameter of collagen fibers	180 nm	Van Der Rijt et al. (2006)
E_f	Young's modulus of collagen fibers	1.1 MPa	Jansen et al. (2018)
$\dot{c}$	Contraction rate of stress fibers	$0.1\frac{\mu\,\mathrm{m}}{\mathrm{s}}$	Choquet et al. (1997); Moore et al. (2010)
k_BT	Thermal energy	$4.28 \cdot 10^{-3}$ aJ	at 37° C
L_i	RVE edge length in i-th coordinate direction	$245\mu m$	–
k_{on}^{f-f}	Chemical association rate for fiber linker	$0.0001 s^{-1}$	–
k_{off}^{f-f}	Chemical dissociation rate for fiber linker	$0.0001\mathrm{s}^{-1}$	–
Δx	Bell parameter	0.5 nm	–
$N_{FA,max}$	Maximal number of focal adhesions per cell	65	Kim and Wirtz (2013); Horzum et al. (2014); Mason et al. (2019)
$N_{i,FA,max}$	Maximal number of integrins per focal adhesion	1000	Wiseman (2004); Elosegui-Artola et al. (2014)
$N_{i,ic,max}$	Maximal number of integrins per cluster	20	Changede et al. (2015); Cheng et al. (2020)
k_{on}^{c-f}	Chemical association rate for integrin	$0.1\ s^{-1}$	slightly modified Zhu et al. (2016)
d^{i-f}	Distance between binding spots for integrinfiber links	50 nm	López-García et al. (2010)

Acknowledgements We gratefully thank Diane Tchibozo and Lisa Pretsch for their contributions to Fig. 7c. We thank Jonas Koban for his contributions to the development of the code that generated the fiber networks as input to our simulations.

Funding Open Access funding enabled and organized by Projekt DEAL. This study was funded by the Deutsche Forschungsgemeinschaft (DFG, German Research Foundation)—Projektnummer 257981274, Projektnummer 386349077. The authors also gratefully acknowledge financial support by the International Graduate School of Science and Engineering (IGSSE) of Technical University of Munich, Germany.

Code availability https://github.com/bionetgen/bionetgen.

Declaration

Conflict of interest The authors declare no conflicts, financial, or otherwise.

References

Abhilash AS, Baker BM, Trappmann B, Chen CS, Shenoy VB (2014) Remodeling of fibrous extracellular matrices by contractile cells: Predictions from discrete fiber network simulations. Biophys J 107(8):1829–1840

Alcaraz J, Mori H, Ghajar CM, Brownfield D, Galgoczy R, Bissell MJ (2011) Collective epithelial cell invasion overcomes mechanical barriers of collagenous extracellular matrix by a narrow tube-like geometry and MMP14-dependent local softening. Integr Biol 3(12):1153–1166

Ambrosi D, Ateshian G, Arruda E, Cowin S, Dumais J, Goriely A, Holzapfel G, Humphrey J, Kemkemer R, Kuhl E, Olberding J, Taber L, Garikipati K (2011) Perspectives on biological growth and remodeling. J Mech Phys Solids 59(4):863–883

Austen K, Ringer P, Mehlich A, Chrostek-grashoff A, Kluger C, Klingner C, Sabass B, Zent R, Rief M, Grashoff C (2015) Extracellular rigidity sensing by talin isoform-specific mechanical linkages. Nat Cell Biol 17(12):1597–1606

BACI: A Comprehensive Multi-Physics Simulation Framework (2021) https://baci.pages.gitlab.lrz.de/website. Accessed 21 June 2021

Cukierman E, Pankov R, Yamada KM (2002) Cell interactions with three-dimensional matrices. Curr Opin Cell Biol 14(5):633–639

Baker BM, Chen CS (2012) Deconstructing the third dimension-how 3D culture microenvironments alter cellular cues. J Cell Sci 125(13):3015–3024

Baker BM, Trappmann B, Wang WY, Sakar MS, Kim IL, Shenoy VB, Burdick JA, Chen CS (2015) Cell-mediated fibre recruitment drives extracellular matrix mechanosensing in engineered fibrillar microenvironments. Nat Mater 14(12):1262–1268

Balcioglu HE, Balasubramaniam L, Stirbat TV, Doss BL, Fardin MA, Mège RM, Ladoux B (2020) A subtle relationship between substrate stiffness and collective migration of cell clusters. Soft Matter 16(7):1825–1839

Ban E, Franklin JM, Nam S, Smith LR, Wang H, Wells RG, Chaudhuri O, Liphardt JT, Shenoy VB (2018) Mechanisms of Plastic Deformation in Collagen Networks Induced by Cellular Forces. Biophys J 114(2):450–461

Ban E, Wang H, Franklin JM, Liphardt JT, Janmey PA, Shenoy VB (2019) Strong triaxial coupling and anomalous Poisson effect in collagen networks. Proc Natl Acad Sci 116(14):6790–6799

Bates RC, Lincz LF, Burns GF (1995) Involvement of integrins in cell survival. Cancer Metastasis Rev 14(3):191–203

Bell GI (1980) Theoretical models for the specific adhesion of cells to cells or to surfaces. Adv Appl Probab 12(03):566–567

Bircher K, Zündel M, Pensalfini M, Ehret AE, Mazza E (2019) Tear resistance of soft collagenous tissues. Nat Commun 10(1):1–13

Bonnans C, Chou J, Werb Z (2014) Remodelling the extracellular matrix in development and disease. Nat Rev Mol Cell Biol 15(12):786–801

Braeu FA, Seitz A, Aydin RC, Cyron CJ (2017) Homogenized constrained mixture models for anisotropic volumetric growth and remodeling. Biomech Model Mechanobiol 16(3):889–906

Broedersz CP, Mao X, Lubensky TC, Mackintosh FC (2011) Criticality and isostaticity in fibre networks. Nat Phys 7(12):983–988

Brown RA, Prajapati R, McGrouther DA, Yannas IV, Eastwood M (1998) Tensional homeostasis in dermal fibroblasts: Mechanical responses to mechanical loading in three-dimensional substrates. J Cell Physiol 175(3):323–332

Brown RA, Sethi KK, Gwanmesia I, Raemdonck D, Eastwood M, Mudera V (2002) Enhanced fibroblast contraction of 3D collagen lattices and integrin expression by TGF-β1 and -β3: Mechanoregulatory growth factors? Exp Cell Res 274(2):310–322

Burkel B, Proestaki M, Tyznik S, Notbohm J (2018) Heterogeneity and nonaffinity of cell-induced matrix displacements. Phys Rev E 98(5):1–13

Campbell BH, Clark WW, Wang JHC (2003) A multi-station culture force monitor system to study cellular contractility. J Biomech 36(1):137–140

Cao X, Ban E, Baker BM, Lin Y, Burdick JA, Chen CS, Shenoy VB (2017) Multiscale model predicts increasing focal adhesion size with decreasing stiffness in fibrous matrices. Proc Natl Acad Sci 114(23):E4549–E4555

Carisey A, Tsang R, Greiner AM, Nijenhuis N, Heath N, Nazgiewicz A, Kemkemer R, Derby B, Spatz J, Ballestrem C (2013) Vinculin regulates the recruitment and release of core focal adhesion proteins in a force-dependent manner. Curr Biol 23(4):271–281

Cavalcanti-Adam EA, Volberg T, Micoulet A, Kessler H, Geiger B, Spatz JP (2007) Cell Spreading and Focal Adhesion Dynamics Are Regulated by Spacing of Integrin Ligands. Biophys J 92(8):2964–2974

Changede R, Xu X, Margadant F, Sheetz MP (2015) Nascent Integrin Adhesions Form on All Matrix Rigidities after Integrin Activation. Dev Cell 35(5):614–621

Chatterjee AP (2010) Nonuniform fiber networks and fiber-based composites: Pore size distributions and elastic moduli. J Appl Phys 108(6):063513

Cheng B, Wan W, Huang G, Li Y, Genin GM, Mofrad MR, Lu TJ, Xu F, Lin M (2020) Nanoscale integrin cluster dynamics controls cellular mechanosensing via FAKY397 phosphorylation. Sci Adv 6(10):eaax1909

Chiquet M, Gelman L, Lutz R, Maier S (2009) From mechanotransduction to extracellular matrix gene expression in fibroblasts. Biochim Biophys Acta 1793(5):911–920

Choquet D, Felsenfeld DP, Sheetz MP, Carolina N (1997) Extracellular Matrix Rigidity Causes Strengthening of Integrin - Cytoskeleton Linkages. Cell 88(1):39–48

Courderot-Masuyer C (2017) Mechanical Properties of Fibroblasts. In: Humbert P, Fanian F, Maibach H, Agache P (eds) Agache's Measuring the Skin. Springer, pp 903–909

Cox TR, Erler JT (2011) Remodeling and homeostasis of the extracellular matrix: implications for fibrotic diseases and cancer. Dis Model Mech 4(2):165–178

Cyron CJ, Wall WA (2012) Numerical method for the simulation of the Brownian dynamics of rod-like microstructures with three-dimensional nonlinear beam elements. Int J Numer Method Biomed Eng 90:955-987

Cyron CJ, Aydin RC, Humphrey JD (2016) A homogenized constrained mixture (and mechanical analog) model for growth and remodeling of soft tissue. Biomech Model Mechanobiol 15(6):1389–1403

Cyron CJ, Humphrey JD (2017) Growth and remodeling of load-bearing biological soft tissues. Meccanica 52(3):645–664

Cyron CJ, Müller KW, Bausch AR, Wall WA (2013a) Micromechanical simulations of biopolymer networks with finite elements. J Comput Phys 244:236–251

Cyron CJ, Müller KW, Schmoller KM, Bausch AR, Wall WA, Bruinsma RF (2013b) Equilibrium phase diagram of semi-flexible polymer networks with linkers. Epl 102(3):38003

Dahlmann-Noor AH, Martin-Martin B, Eastwood M, Khaw PT, Bailly M (2007) Dynamic protrusive cell behaviour generates force and drives early matrix contraction by fibroblasts. Exp Cell Res 313(20):4158–4169

Das M, Subbayya Ithychanda S, Qin J, Plow EF (2014) Mechanisms of talin-dependent integrin signaling and crosstalk. Biochim Biophys Acta 1838(2):579–588

Davidson MW, Ruehland S, Baird MA, Teo S, Bate N, Kanchanawong P, Goh WI, Wang Y, Goh H, Critchley DR, Liu J (2015) Talin determines the nanoscale architecture of focal adhesions. Proc Natl Acad Sci 112(35):E4864–E4873

Davoodi-Kermani I, Schmitter M, Eichinger JF, Aydin RC, Cyron CJ (2021) Computational study of the geometric properties governing the linear mechanical behavior of fiber networks (submitted)

Delvoye P, Wiliquet P, Levêque J-L, Nusgens BV, Lapière CM (1991) Measurement of Mechanical Forces Generated by Skin Fibroblasts Embedded in a Three-Dimensional Collagen Gel. J Invest Dermatol 97(5):898–902

Domaschke S, Morel A, Fortunato G, Ehret AE (2019) Random auxetics from buckling fibre networks. Nat Commun 10(1):1–8

Domaschke S, Morel A, Kaufmann R, Hofmann J, Rossi RM, Mazza E, Fortunato G, Ehret AE (2020) Predicting the macroscopic response of electrospun membranes based on microstructure and single fibre properties. J Mech Behav Biomed Mater 104:103634

Dong S, Huang Z, Tang L, Zhang X, Zhang Y, Jiang Y (2017) A three-dimensional collagen-fiber network model of the extracellular matrix for the simulation of the mechanical behaviors and micro structures. Comput Methods Biomech Biomed Engin 20(9):991–1003

Dumbauld DW, Lee TT, Singh A, Scrimgeour J, Gersbach CA, Zamir EA, Fu J, Chen CS, Curtis JE, Craig SW (2013) How vinculin regulates force transmission. Proc Natl Acad Sci 110(24):9788–9793

Duval K, Grover H, Han LH, Mou Y, Pegoraro AF, Fredberg J, Chen Z (2017) Modeling physiological events in 2D vs. 3D cell culture. Physiology 32(4):266–277

Eichinger JF, Paukner D, Szafron JM, Aydin RC, Humphrey JD, Cyron CJ (2020) Computer-Controlled Biaxial Bioreactor for Investigating Cell-Mediated Homeostasis in Tissue Equivalents. J Biomech Eng 142(7):1–22

Eichinger JF, Haeusel LJ, Paukner D, Aydin RC, Humphrey JD, Cyron CJ (2021) Mechanical homeostasis in tissue equivalents: a review. Biomech Model Mechanobiol 20:833–850

Elosegui-Artola A, Bazellières E, Allen MD, Andreu I, Oria R, Sunyer R, Gomm JJ, Marshall JF, Jones JL, Trepat X, Roca-Cusachs P (2014) Rigidity sensing and adaptation through regulation of integrin types. Nat Mater 13(6):631–637

Ezra DG, Ellis JS, Beaconsfield M, Collin R, Bailly M (2010) Changes in fibroblast mechanostat set point and mechanosensitivity: An adaptive response to mechanical stress in floppy eyelid syndrome. Investig Ophthalmol Vis Sci 51(8):3853–3863

Grashoff C, Hoffman BD, Brenner MD, Zhou R, Parsons M, Yang MT, McLean MA, Sligar SG, Chen CS, Ha T, Schwartz MA (2010) Measuring mechanical tension across vinculin reveals regulation of focal adhesion dynamics. Nature 466(7303):263–266

Grill MJ, Eichinger JF, Koban J, Meier C, Lieleg O, Wall WA (2021) Modeling and Simulation of the Hindered Mobility of Charged Particles in Biological Hydrogel. Proc R Soc A 477(2249):20210039

Grimmer P, Notbohm J (2017) Displacement Propagation in Fibrous Networks Due to Local Contraction. J Biomech Eng 140(4):1–11

Grinnell F, Petroll WM (2010) Cell Motility and Mechanics in Three-Dimensional Collagen Matrices. Annu Rev Cell Dev Biol 26(1):335–361

Hall MS, Alisafaei F, Ban E, Feng X, Hui C-Y, Shenoy VB, Wu M (2016) Fibrous nonlinear elasticity enables positive mechanical feedback between cells and ECMs. Proc Natl Acad Sci 113(49):14043–14048

Heussinger C, Frey E (2007) Force distributions and force chains in random stiff fiber networks. Eur Phys J E 24(1):47–53

Hippler M, Weißenbruch K, Richler K, Lemma ED, Nakahata M, Richter B, Barner-kowollik C, Takashima Y, Harada A, Blasco E, Wegener M, Tanaka M, Bastmeyer M (2020) Mechanical stimulation of single cells by reversible host-guest interactions in 3D microscaffolds. Sci Adv 6(39):eabc2648

Horzum U, Ozdil B, Pesen-Okvur D (2014) Step-by-step quantitative analysis of focal adhesions. MethodsX 1(1):56–59

Hulmes DJ (1979) Quasi-hexagonal molecular packing in collagen fibrils. Nature 282(5741):878–880

Humphrey JD, Dufresne ER, Schwartz MA (2014) Mechanotransduction and extracellular matrix homeostasis. Nat Rev Mol Cell Biol 15(12):802–812

Humphrey JD, Rajagopal KR (2002) A constrained mixture model for growth and remodeling of soft tissues. Math Model Methods Appl Sci 12(3):407–430

Humphries DL, Grogan JA, Gaffney EA (2018) The mechanics of phantom Mikado networks. J Phys Commun 2(5):055015

Humphries DL, Grogan JA, Gaffney EA (2017) Mechanical Cell-Cell Communication in Fibrous Networks: The Importance of Network Geometry. Bull Math Biol 79(3):498–524

Jansen KA, Donato DM, Balcioglu HE, Schmidt T, Danen EHJ, Koenderink GH (2015) A guide to mechanobiology: Where biology and physics meet. Biochim Biophys Acta 1853(11):3043–3052

Jansen KA, Licup AJ, Sharma A, Rens R, MacKintosh FC, Koenderink GH (2018) The Role of Network Architecture in Collagen Mechanics. Biophys J 114(11):2665–2678

Jones CAR, Cibula M, Feng J, Krnacik EA, McIntyre DH, Levine H, Sun B (2015) Micromechanics of cellularized biopolymer networks. Proc Natl Acad Sci 112(37):E5117–E5122

Jones CAR, Liang L, Lin D, Jiao Y, Sun B (2014) The spatial-temporal characteristics of type I collagen-based extracellular matrix. Soft Matter 10(44):8855–8863

Joshi J, Mahajan G, Kothapalli CR (2018) Three-dimensional collagenous niche and azacytidine selectively promote time-dependent cardiomyogenesis from human bone marrow-derived MSC spheroids. Biotechnol Bioeng 115(8):2013–2026

Karamichos D, Brown RA, Mudera V (2007) Collagen stiffness regulates cellular contraction and matrix remodeling gene expression. J Biomed Mater Res, Part A 83A(3):887–894

Kim DH, Wirtz D (2013) Focal adhesion size uniquely predicts cell migration. FASEB J 27(4):1351–1361

Kim J, Mao X, Jones CAR, Feng J, Sun B, Sander LM, Levine H (2017) Stress-induced plasticity of dynamic collagen networks. Nat Commun 8(1):842

Kim J, Zheng Y, Alobaidi AA, Nan H, Tian J, Jiao Y, Sun B (2020) Geometric Dependence of 3D Collective Cancer Invasion. Biophys J 118(5):1177–1182

Kirkpatrick S, Gelatt CD, Vecchi MP (1983) Optimization by simulated annealing. Science 220(4598):671–680

Kong F, García AJ, Mould AP, Humphries MJ, Zhu C (2009) Demonstration of catch bonds between an integrin and its ligand. J Cell Biol 185(7):1275–1284

Lang NR, Münster S, Metzner C, Krauss P, Schürmann S, Lange J, Aifantis KE, Friedrich O, Fabry B, Lange J, Friedrich O, Münster S, Lang NR, Schürmann S, Krauss P, Fabry B (2013) Estimating the 3D pore size distribution of biopolymer networks from directionally biased data. Biophys J 105(9):1967–1975

Lee B, Zhou X, Riching K, Eliceiri KW, Keely PJ, Guelcher SA, Weaver AM, Jiang Y (2014) A three-dimensional computational model of collagen network mechanics. PLoS ONE 9(11):1–12

Lerche M, Elosegui-Artola A, Guzmán C, Georgiadou M, Kechagia JZ, Gulberg D, Roca-Cusachs P, Peuhu E, Ivaska J (2019) Integrin binding dynamics modulate ligand-specific mechanosensing in mammary gland fibroblasts. iScience 23(9):101507

Liang L, Jones C, Chen S, Sun B, Jiao Y (2016) Heterogeneous force network in 3D cellularized collagen networks. Phys Biol 13(6):1–11

Lindström SB, Vader DA, Kulachenko A, Weitz DA (2010) Biopolymer network geometries: Characterization, regeneration, and elastic properties. Phys Rev E Stat Nonlin Soft Matter Phys 82(5):051905

López-García M, Selhuber-Unkel C, Spatz JP, Erdmann T, Schwarz US, Kessler H (2010) Cell Adhesion Strength Is Controlled by Intermolecular Spacing of Adhesion Receptors. Biophys J 98(4):543–551

Lu P, Takai K, Weaver VM, Werb Z (2011) Extracellular Matrix degradation and remodeling in development and disease. Cold Spring Harb Perspect Biol 3(12):1–24

Ma X, Schickel ME, Stevenson MD, Sarang-Sieminski AL, Gooch KJ, Ghadiali SN, Hart RT (2013) Fibers in the extracellular matrix enable long-range stress transmission between cells. Biophys J 104(7):1410–1418

Malandrino A, Trepat X, Kamm RD, Mak M (2019) Dynamic filopodial forces induce accumulation, damage, and plastic remodeling of 3D extracellular matrices. PLoS Comput Biol 15(4):1–26

Mammoto A, Mammoto T, Ingber DE (2012) Mechanosensitive mechanisms in transcriptional regulation. J Cell Sci 125(13):3061–3073

Mann A, Sopher RS, Goren S, Shelah O, Tchaicheeyan O, Lesman A (2019) Force chains in cell-cell mechanical communication. J R Soc Interface 16(159):20190348

Marenzana M, Wilson-Jones N, Mudera V, Brown RA (2006) The origins and regulation of tissue tension: Identification of collagen tension-fixation process in vitro. Exp Cell Res 312(4):423–433

Mason DE, Collins JM, Dawahare JH, Nguyen TD, Lin Y, Voytik-Harbin SL, Zorlutuna P, Yoder MC, Boerckel JD (2019) YAP and TAZ limit cytoskeletal and focal adhesion maturation to enable persistent cell motility. J Cell Biol 218(4):1369–1389

Mauri A, Hopf R, Ehret AE, Picu CR, Mazza E (2016) A discrete network model to represent the deformation behavior of human amnion. J Mech Behav Biomed Mater 58:45–56

Mickel W, Münster S, Jawerth LM, Vader DA, Weitz DA, Sheppard AP, Mecke K, Fabry B, Schröder-Turk GE (2008) Robust pore size analysis of filamentous networks from three-dimensional confocal microscopy. Biophys J 95(12):6072–6080

Miroshnikova YA, Jorgens DM, Spirio L, Auer M, Sarang-Sieminski AL, Weaver VM (2011) Engineering strategies to recapitulate epithelial morphogenesis within synthetic three-dimensional extracellular matrix with tunable mechanical properties. Phys Biol 8(2):026013

Mogilner A, Oster G (2003) Force Generation by Actin Polymerization II : The Elastic Ratchet and Tethered Filaments. Biophys J 84(3):1591–1605

Moore SW, Roca-Cusachs P, Sheetz MP (2010) Stretchy proteins on stretchy substrates: The important elements of integrin-mediated rigidity sensing. Dev Cell 19(2):194–206

Motte S, Kaufman LJ (2013) Strain stiffening in collagen I networks. Biopolymers 99(1):35–46

Müller KW, Bruinsma RF, Lieleg O, Bausch AR, Wall WA, Levine AJ (2014) Rheology of semiflexible bundle networks with transient linkers. Phys Rev Lett 112(23):1–5

Müller KW, Cyron CJ, Wall WA (2015) Computational analysis of morphologies and phase transitions of cross-linked, semiflexible polymer networks. Proc R Soc A 471(2182):20150332

Murtada SC, Kroon M, Holzapfel GA (2010) A calcium-driven mechanochemical model for prediction of force generation in smooth muscle. Biomech Model Mechanobiol 9(6):749–762

Murtada SC, Arner A, Holzapfel GA (2012) Experiments and mechanochemical modeling of smooth muscle contraction: Significance of filament overlap. J Theor Biol 297:176–186

Nam S, Hu KH, Butte MJ, Chaudhuri O (2016) Strain-enhanced stress relaxation impacts nonlinear elasticity in collagen gels. Proc Natl Acad Sci 113(20):5492–5497

Nan H, Jiao Y, Liu R, Chen G, Liu L, Liang L (2018) Realizations of highly heterogeneous collagen networks via stochastic reconstruction for micromechanical analysis of tumor cell invasion. Phys Rev E 97(3):33311

Nguyen DT, Nagarajan N, Zorlutuna P (2018) Effect of Substrate Stiffness on Mechanical Coupling and Force Propagation at the Infarct Boundary. Biophys J 115(10):1966–1980

Notbohm J, Lesman A, Tirrell DA, Ravichandran G (2015) Quantifying cell-induced matrix deformation in three dimensions based on imaging matrix fibers. Integr Biol 7(10):1186–1195

Reissner E (1981) On finite deformations of space-curved beams. ZAMP Zeitschrift für Angew Math und Phys 32(6):734–744

Ringer P, Weißl A, Cost A-L, Freikamp A, Sabass B, Mehlich A, Tramier M, Rief M, Grashoff C (2017) Multiplexing molecular tension sensors reveals piconewton force gradient across talin-1. Nat Methods 14(11):1090–1096

Ronceray P, Broedersz CP, Lenz M (2016) Fiber networks amplify active stress. Proc Natl Acad Sci 113(11):2827–2832

Ross TD, Coon BG, Yun S, Baeyens N, Tanaka K, Ouyang M, Schwartz MA (2013) Integrins in mechanotransduction. Curr Opin Cell Biol 25(5):613–618

Rycroft CH (2009) VORO++: A three-dimensional Voronoi cell library in C++. Chaos 19(4):1–16

Schwartz MA (1995) Integrins: Emerging Paradigms of Signal Transduction. Annu Rev Cell Dev Biol 11(1):549–599

Seo BR, Chen X, Ling L, Song YH, Shimpi AA, Choi S, Gonzalez J, Sapudom J, Wang K, Eguiluz RCA, Gourdon D, Shenoy VB, Fischbach C (2020) Collagen microarchitecture mechanically controls myofibroblast differentiation. Proc Natl Acad Sci 117(21):11387–11398

Sethi KK, Yannas IV, Mudera V, Eastwood M, McFarland C, Brown RA (2002) Evidence for sequential utilization of fibronectin, vitronectin, and collagen during fibroblast-mediated collagen contraction. Wound Repair Regen 10(6):397–408

Shi Q, Ghosh RP, Engelke H, Rycroft CH, Cassereau L, Sethian JA, Weaver VM, Liphardt JT (2013) Rapid disorganization of mechanically interacting systems of mammary acini. Proc Natl Acad Sci 111(2):658–663

Simo J C (1985) A finite strain beam formulation. The three-dimensional dynamic problem. Part I. Comput Methods Appl Mech Eng 49(1):55–70

Simo J C, Vu-Quoc L (1986) A three-dimensional finite-strain rod model. part II: Computational aspects. Comput Methods Appl Mech Eng 58(1):79–116

Simon DD, Horgan CO, Humphrey JD (2012) Mechanical restrictions on biological responses by adherent cells within collagen gels. J Mech Behav Biomed Mater 14:216–226

Simon DD, Niklason LE, Humphrey JD (2014) Tissue Transglutaminase, Not Lysyl Oxidase, Dominates Early Calcium-Dependent Remodeling of Fibroblast-Populated Collagen Lattices. Cells Tissues Organs 200(2):104–117

Stehbens SJ, Wittmann T (2014) Analysis of focal adhesion turnover: a quantitative live-cell imaging example. Methods Cell Biol 123:335–346

Stein AM, Vader DA, Jawerth LM, Weitz DA, Sander LM (2008) An algorithm for extracting the network geometry of three-dimensional collagen gels. J Microsc 232(3):463–475

Stein AM, Vader DA, Weitz DA, Sander LM (2010) The Micromechanics of Three-Dimensional Collagen-I Gels. Complexity 16(4):22–28

Sukharev S, Sachs F (2012) Molecular force transduction by ion channels - diversity and unifying principles. J Cell Sci 125(13):3075–3083

Truong T, Shams H, Mofrad MRK (2015) Mechanisms of integrin and filamin binding and their interplay with talin during early focal adhesion formation. Integr Biol 7(10):1285–1296

Van Der Rijt JAJ, Van Der Werf KO, Bennink ML, Dijkstra PJ, Feijen J (2006) Micromechanical testing of individual collagen fibrils. Macromol Biosci 6(9):699–702

Wang H, Abhilash AS, Chen CS, Wells RG, Shenoy VB (2014) Long-Range Force Transmission in Fibrous Matrices Enabled by Tension-Driven Alignment of Fibers. Biophys J 107(11):2592–2603

Wang Y, Wang G, Luo X, Qiu J, Tang C (2012) Substrate stiffness regulates the proliferation, migration, and differentiation of epidermal cells. Burns 38(3):414–420

Weng S, Shao Y, Chen W, Fu J (2016) Mechanosensitive subcellular rheostasis drives emergent single-cell mechanical homeostasis. Nat Mater 15(9):961–967

Wiseman PW (2004) Spatial mapping of integrin interactions and dynamics during cell migration by Image Correlation Microscopy. J Cell Sci 117(23):5521–5534

Xie J, Bao M, Bruekers SMC, Huck WTS (2017) Collagen Gels with Different Fibrillar Microarchitectures Elicit Different Cellular Responses. ACS Appl Mater Interfaces 9(23):19630–19637

Yao M, Goult BT, Chen H, Cong P, Sheetz MP, Yan J (2014) Mechanical activation of vinculin binding to talin locks talin in an unfolded conformation. Sci Rep 4:4610

Yao M, Goult BT, Klapholz B, Hu X, Toseland CP, Guo Y, Cong P, Sheetz MP, Yan J (2016) The mechanical response of talin. Nat Commun 7:11966

Yeong CLY, Torquato S (1998) Reconstructing Random Media I and II. Phys Rev E 58(1):224–233

Zemel A (2015) Active mechanical coupling between the nucleus, cytoskeleton and the extracellular matrix, and the implications for perinuclear actomyosin organization. Soft Matter 11(12):2353–2363

Zheng Y, Nan H, Liu Y, Fan Q, Wang X, Liu R, Liu L, Ye F, Sun B, Jiao Y (2019) Modeling cell migration regulated by cell extracellular-matrix micromechanical coupling. Phys Rev E 100(4):43303

Zhou D, Zhang L, Mao X (2018) Topological Edge Floppy Modes in Disordered Fiber Networks. Phys Rev Lett 120(6):68003

Zhu C, Pérez-González C, Trepat X, Chen Y, Castro N, Oria R, Roca-Cusachs P, Elosegui-Artola A, Kosmalska A (2016) Mechanical regulation of a molecular clutch defines force transmission and transduction in response to matrix rigidity. Nat Cell Biol 18(5):540–548

Zhu YK, Umino T, Liu XD, Wang HJ, Romberger DJ, Spurzem JR, Rennard SI (2001) Contraction of Fibroblast-Containing Collagen Gels: Initial Collagen Concentration Regulates the Degree of Contraction and Cell Survival. Vitro Cell Dev Biol Anim 37(1):10–16

Ziegler W, Gingras A, Critchley D, Emsley J (2008) Integrin connections to the cytoskeleton through talin and vinculin. Biochem Soc Trans 36(2):235–239

Appendix D

Paper D

What do cells regulate in soft tissue on short time scales?

Jonas F. Eichinger, Daniel Paukner, Roland C. Aydin, Wolfgang A. Wall, Jay D. Humphrey, Christian J. Cyron

published in

Acta Biomaterialia, 10.1016/j.actbio.2021.07.054

Acta Biomaterialia xxx (xxxx) xxx

Contents lists available at ScienceDirect

Acta Biomaterialia

journal homepage: www.elsevier.com/locate/actbio

Full length article

What do cells regulate in soft tissues on short time scales?

Jonas F. Eichinger[a,b,*], Daniel Paukner[b,c], Roland C. Aydin[c], Wolfgang A. Wall[a], Jay D. Humphrey[d], Christian J. Cyron[b,c]

[a] Institute for Computational Mechanics, Technical University of Munich, Boltzmannstrasse 15, 85748, Garching, Germany
[b] Institute for Continuum and Material Mechanics, Hamburg University of Technology, Eissendorfer Str. 42, 21073, Hamburg, Germany
[c] Institute of Material Systems Modeling, Helmholtz-Zentrum Hereon, Max-Planck-Strasse 1, 21502, Geesthacht, Germany
[d] Department of Biomedical Engineering, Yale University, 55 Prospect Street, New Haven, CT 06520, USA

ARTICLE INFO

Article history:
Received 9 April 2021
Revised 15 July 2021
Accepted 22 July 2021
Available online xxx

Keywords:
Homeostasis
Mechanosensing
Mechanoregulation
Cell-matrix interactions
Discrete fiber model

ABSTRACT

Cells within living soft biological tissues seem to promote the maintenance of a mechanical state within a defined range near a so-called set-point. This mechanobiological process is often referred to as mechanical homeostasis. During this process, cells interact with the fibers of the surrounding extracellular matrix (ECM). It remains poorly understood, however, what individual cells actually regulate during these interactions, and how these micromechanical regulations are translated to the tissue-level to lead to what we observe as biomaterial properties. Herein, we examine this question by a combination of experiments, theoretical analysis, and computational modeling. We demonstrate that on short time scales (hours) - during which deposition and degradation of ECM fibers can largely be neglected - cells appear to not regulate the stress / strain in the ECM or their own shape, but rather only the contractile forces that they exert on the surrounding ECM.

Statement of significance

Cells in soft biological tissues sense and regulate the mechanical state of the extracellular matrix to ensure structural integrity and functionality. This so-called mechanical homeostasis plays an important role in the natural history of various diseases such as aneurysms in the cardiovascular system or cancer. Yet, it remains poorly understood to date which target quantity cells regulate on the mircroscale and how it translates to the macroscale. In this paper, we combine experiments, computer simulations, and theoretical analysis to compare different hypotheses about this target quantity. This allows us to identify a likely candidate for it at least on short time scales and in the simplified environment of tissue equivalents.

1. Introduction

While many engineering materials remain stress-free, or in their respective production-induced stress state, in the absence of external loading, living soft tissues generally seek to establish a preferred mechanical state that is not stress-free. This state is often referred to as *homeostatic*. Notwithstanding this near steady state, cells are yet highly active. They constantly probe and transduce environmental cues into intracellular signaling pathways (mechanosensing) and adjust their interactions with the surrounding tissue fibers (mechanoregulation) accordingly [1–7]. To this end, cells use transmembrane receptors such as integrins to connect the intracellular cytoskeleton to fibers of the extracellular matrix (ECM). This unique dynamic regulatory system allows cells to establish and maintain a preferred mechanical state via a process that is often referred to as *tensional* [8] or *mechanical* [9] *homeostasis*. Compromised or lost mechanical homeostasis, and its underlying mechanosensitive and mechanoregulatory processes, are linked to some of the most predominant causes of death, including aneurysms [10–13] or cancer [14–19] on the organ scale, and

* Corresponding author.
E-mail addresses: eichinger@lnm.mw.tum.de (J.F. Eichinger), daniel.paukner@hereon.de (D. Paukner), roland.aydin@hereon.de (R.C. Aydin), wall@lnm.mw.tum.de (W.A. Wall), jay.humphrey@yale.edu (J.D. Humphrey), christian.cyron@tuhh.de (C.J. Cyron).

https://doi.org/10.1016/j.actbio.2021.07.054

to altered cellular processes such as cell migration [20–23], differentiation [24–26], and even survival [27–30].

Despite the prominent role of mechanical homeostasis in various physiological and pathophysiological processes, it remains unclear which mechanical quantity is regulated on a tissue level. In simple constrained tissue equivalents, it has been hypothesized that this ubiquitous control may seek to develop and maintain a certain state of tension in the tissue. Although continuum metrics of stress, strain, and those derived from them are unlikely to be sensed directly by cells [31], such metrics can nevertheless be good surrogate markers sufficient for data analysis and computation [8,32–37]. To address this open question, experiments using tissue equivalents have attracted increasing attention over recent decades [38]. Tissue equivalents are simple model systems of living soft tissues that consist often of collagen fibers seeded with living cells. When fixed at their boundaries in an initially stress-free configuration, tissue equivalents exhibit a characteristic behavior observed in numerous independent studies [8,32–45]. First, they rapidly build up a certain level of internal tension (phase I). Second, this level of tension is maintained for a prolonged period (phase II). If this steady state is perturbed (e.g., by stretching or releasing the tissue equivalent slightly), cells seem to regulate their activity such that the tension in the gel is restored toward the value prior to the perturbation [8,32,33]. It remains unclear, however, whether this value is recovered within a range consistent with homeostasis, noting that “homeo” means similar to in contrast with “homo” which means the same as [46].

In general, different time scales are involved in mechanical homeostasis. On short time scales (minutes to hours), cells can adapt the forces they exert on the surrounding ECM. On longer time scales (several days to months), cells may additionally turnover the ECM, that is, inelastically reorganize its microstructure or deposit and degrade matrix fibers (growth and atrophy) [39,47–49]. This article focuses on short time scales, in which the regulation of cellular forces can be assumed to be the dominant mechanism of mechanical homeostasis. Not only different time scales, but also different spatial scales are involved. On the microscale, individual cells likely sense and regulate elementary quantities such as forces in or displacements of surrounding fibers [31]. By contrast, on the tissue scale, this cellular activity leads to changes of continuum mechanical quantities such as stress, strain, or stiffness.

In this paper, we consider the question of which mechanical quantity individual cells regulate on the microscale on short time scales (where growth and remodeling can largely be neglected), and how this behavior translates into changes of continuum mechanical quantities on the tissue level. We address this question by a combination of three tools. First, we performed biaxial tissue culture experiments with a custom-built bioreactor [33]. Second, we developed a simple theoretical mechanical analog model to understand the governing principles of our experimental observations. Third, we used a detailed computational model resolving cell-ECM interactions on the level of discrete cells and fibers [50] to validate the results of our theoretical analysis.

2. Material and methods

2.1. Experimental study

Device and experimental procedure

To study the evolution of cell-generated tension in cell-seeded collagen gels we used our custom-built biaxial bioreactor, previously described in [33]. Briefly, the device consists of a bath, two force transducers, and four motors (Fig. 1). The device is placed within a humidified incubator (NU-8520, NuAire) at 37°C and a CO_2 level of 5% to ensure appropriate culture conditions. Two highly sensitive force transducers (World Precision Instruments), one for each axis, measure generated forces in the gel in the range of $0–1mN$ over multiple hours with negligible drift. Four high resolution stepper motors (Advanced Micro Systems) precisely control complex biaxial loading conditions. The device is controlled by a custom-written LabView code. Due to their fragility, the gels were polymerized inside the device to avoid unnecessary movements. To this end, a 3D-printed cruciform mold, which yields a homogeneous stress field in the central region of the specimen, is placed in the middle of the bath of an already assembled device. The collagen solution including the cells is prepared as described below and then pipetted into the mold. The liquid solution evenly distributes within the mold and around porous inserts which are firmly attached to the force transducers. Due to the change in temperature (the collagen solution is prepared on ice) the initially liquid solution starts polymerizing, forming over $30–45min$ a gel connected to the transducers used to control the gel strain. Subsequently, the bath is immersed within $80ml$ of culture medium. At this point, the mold is removed allowing the gel to float freely in the culture medium. This marks the start of the experiment. After an initial stress-free phase of approximately $30–60min$, the cells start to generate tension within the gel which is measured by the force transducers through the deflection of cantilever beams. The initial gel has a width of $\sim 10mm$ in the arms, a thickness of $\sim 4mm$ and a length of $\sim 25mm$ (between the porous inserts). The initial stiffness of a gel in the small deformation regime is estimated using the above dimensions and a strain of 1% (strain rate $0.1\%/s$), resulting in a Young’s modulus of approximately $1kPa$. The same strain rate was applied in all the experiments described herein.

Preparation of tissue equivalents

Primary smooth muscle cells (SMCs) were isolated from 13–15 week old male C57BL/6 wild-type mouse aortas. Cells extracted from the medial layer of the descending, suprarenal, and infrarenal aorta (all having a mesoderm embryonic lineage [51]) were mixed and then expanded in culture. Cells were maintained in culture medium consisting of Dulbecco’s Modified Eagles’s Medium (DMEM) (Gibco, Life Technologies, D5796), 20% heat-inactivated fetal bovine serum (FBS) (Gibco, Life Technologies), and 1% penicillin-streptomycin (ThermoFisher) in an incubator at 37°C and 5% CO_2. After cell extraction, cells were grown in one well of a 6-well plate before being transferred to a T25 flask in passage 1 (P1). In P2 and P3, cells were grown in T75 flasks. Cells were passaged at $70-80\%$ confluence roughly every 6 days. Passages 4 and 5 were used in all experiments. Cells were starved in medium containing 2.0% FBS for $24h$ prior to the experiments to inhibit proliferation during the experiments.

SMC-seeded collagen gels were prepared on ice following a protocol slightly modified from [33]. Briefly, $1.428ml$ of $5x$ DMEM, $0.683ml$ of a $10x$ reconstitution buffer (0.1N NaOH and $20mM$ HEPES; Sigma), and $0.790ml$ of high concentration, type-I rat tail collagen ($8.22mg/ml$; Corning) were mixed with $4.1ml$ of experimental culture medium containing $3.5 \cdot 10^6$ SMCs for a total volume of $7.0ml$ of gel solution. This resulted in a collagen concentration of 1.0mg/ml and a cell density of 0.5×10^6 cells/ml. Variations in cell density and collagen concentration (the latter automatically associated with changes of stiffness and pore size [52,53]) change the level of the homeostatic plateau tension, but not the general observed behavior [33]. The experimental culture medium consisted of DMEM supplemented with 2.0% FBS and 1% penicillin-streptomycin. To avoid proliferation and to minimize parasitic effects of fluctuating concentrations of FBS components that naturally appear between batches, we used only 2% FSB in the experimental culture medium. The final gel solution was pipetted into a cruciform mold as described in the previous section. Subsequently, the experiment was started. During an experiment (which lasted

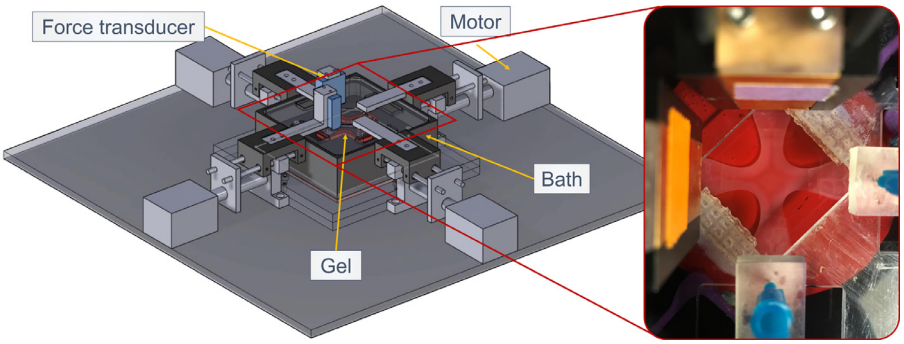

Fig. 1. Biaxial testing device for cell-seeded collagen gels as introduced in [33]: schematic drawing (left) and cruciform-shaped gel sample (right). The base plate upon which the system rests (left) is placed on a shelf within a custom incubator, with all wires exteriorized through a custom sealed port and connected to the power source or controlling computer.

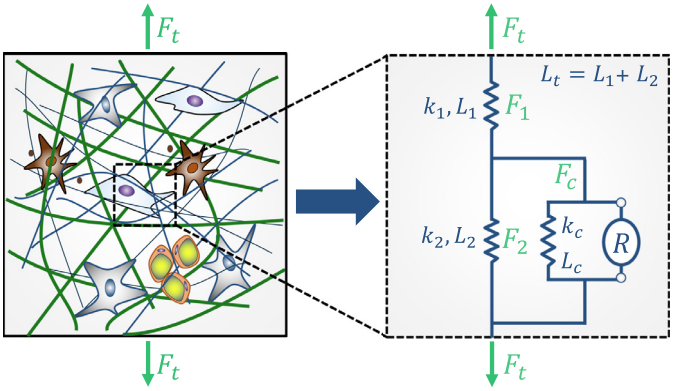

Fig. 2. Mechanical analog model of a three-dimensional fiber matrix with embedded cells: the sum of all cellular forces in the direction of interest is given by F_c composed of an active component mediated by the regulator element R and a passive component dictated by the spring constant k_c. In this way, cells pull on ECM fibers. These fibers are connected via the network to other fibers parallel to the cell (category 2), which are in general compressed when cells exert contractile forces. Both sets of fibers are represented by elastic springs. Displacements are fixed at the outer boundary of the system. The resulting force on the tissue level (as measured, for example, by force sensors at clamped boundaries) corresponds to the force F_t in the mechanical analog model. L_1, L_2, and L_t describe the lengths at deformed/homeostatic states reached by cellular contraction. Note, the analog model can also be understood as the smallest possible representative volume element (RVE) for soft tissues.

less than 48h), the medium was not changed to avoid disturbing the highly sensitive force measurements.

2.2. Mechanical analog model for soft tissue mechanical homeostasis on short time scales

To understand the underlying principles of mechanical homeostasis of soft tissues, we developed a simplified mechanical analog model (Fig. 2). The ECM, that is, the mechanical environment in which cells reside, was modeled as an elastic network of fibers. For simplicity, we focus only on a single direction, noting that an analogous discussion would be possible in any other direction. The scenario of a single direction leads to the mechanical analog model depicted in Fig. 2, consisting of two categories of fibers 1 and 2 and cells. Cells in vivo (and in vitro) attach to nearby matrix fibers via focal adhesions and then contract. This leads, in a connected fiber network, to fibers that are compressed (category 2, represented by elastic elements in parallel to cells in the analog model) and fibers that are stretched (category 1, represented by elastic elements in series to cells in the analog model). Note that this is true in any direction and can occur in several independent spatial directions at the same time in case of a multi-axial stress state. In general, the mechanical function of the fibers is represented by elastic spring elements. The forces in the spring elements (i.e., the forces transmitted through all fibers of category 1 and 2, respectively, with unit [N]) are denoted by F_1 and F_2. Cells are represented by an elastic spring (representing their passive stiffness) with a regulator element in parallel. The latter represents the active forces exerted by the stress fibers in the cytoskeleton on the surrounding ECM fibers. The force exerted by all cells in the direction of interest is denoted by F_c. It is composed of an active component exerted by the regulator element R and a passive component. Generally, the passive elastic forces of the different elements are characterized by the overall stiffness k_i and a length L_i in the direction of interest with $i \in \{1, 2, c\}$. That is, for the passive elastic parts of our model, changes of length and force are related by

$$\Delta F_i = k_i \Delta L_i, \quad i \in \{1, 2, c\}. \tag{1}$$

The overall force of the tissue (with length L_t) in the direction of interest is denoted by F_t. It is important to note that this model can also be interpreted as the smallest possible representative volume element (RVE) of a uniaxially loaded or constrained soft tissue. Viscoelastic effects were neglected because they manifest in the ECM on time scales much shorter than that for mechanical homeostasis.

2.3. Three-dimensional discrete fiber and cell model

Network model

To simulate soft tissue mechanics on the level of individual cells and fibers, we used the computational framework presented in [50] and shown Fig. 3. Briefly, we reconstructed periodic RVEs of fiber networks using stochastic optimization that neatly matched the crucial microstructural characteristics of actual collagen gels, that is, their valency, free fiber length, and orientation distributions. These descriptors are predominantly responsible for the mechanical properties of fibrous networks [54]. Individual fibers were discretized with nonlinear beam finite elements, which are well-known to capture the most important modes of the mechanical deformation of fibers, that is, axial tension, torsion, bending, and shear. Networks were formed by coupling both translational and rotational degrees of freedom at entanglement points of two fibers. Fibers were assumed to have circular cross-sections with a diameter of 180nm [55] and an elastic modulus of 1.1MPa [56] to mimic the collagen type-I fibers that were used in our experiments.

Cell adhesion model

Biologically, intracellular structures such as the actomyosin cytoskeleton are physically coupled to the surrounding ECM fibers via transmembrane integrins that cluster to form focal adhesions [4,7]. This coupling allows cells to receive mechanical cues from their environment and to react to them, for example, by adapting their contractility. We model cells as particles that can form elastic connections to predefined binding spots on nearby matrix fibers with a certain probability (Fig. 3). These connections represent the

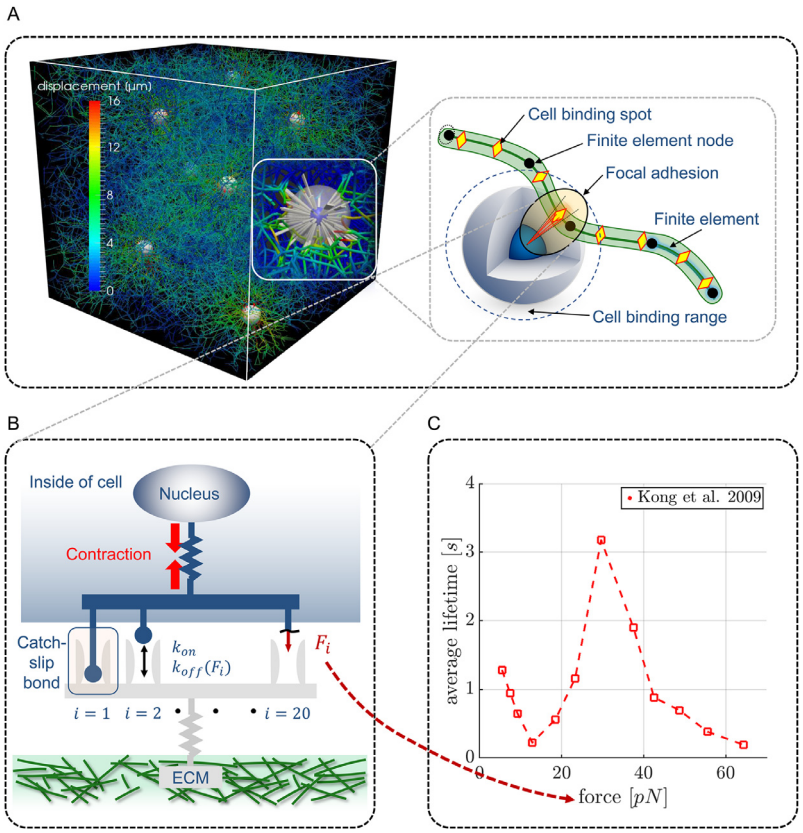

Fig. 3. (A) RVE of our three-dimensional discrete fiber and cell model. Fibers are modeled as nonlinear beam elements, on which cells can exert contractile forces via elastic links representing focal adhesions. (B) Each focal adhesion consists of up to 50 so-called integrin clusters, one of which is shown here, each formed by up to 20 integrins. We model each integrin cluster as being connected to one actin stress fiber. Integrins are modeled as molecular clutches, i.e., they bind and unbind according to specific binding kinetics. (C) [45] determined a catch-slip bond behavior for single integrins, which we model with a force-dependent lifetime for each bond matching this experimental data.

entire cell-matrix adhesion complex, consisting of the contractile cytoskeleton and the focal adhesions. The latter are modeled as multiple integrin clusters, each of which consists of 20 integrins (Fig. 3B). The on- and off-rates of the bonds between integrins and the ECM ligands were chosen to mimic their characteristic catch-slip bond behavior [57,58] (Fig. 3C), that is, a force-dependent lifetime of each integrin connection peaking at some preferred load state. Cell contractility was modeled by the contraction of established cell-ECM connections at a rate of $0.1 \mu m/s$ [59,60]. This increasing contraction automatically limits the lifetime of individual cell-ECM connections, which dissolve with increasing probability beyond a critical level of loading. Our model thereby captures typical lifetimes of focal adhesions on the order of minutes, while the turnover rate for most proteins involved in the adhesion complex is on the order of seconds. This implies that our model realistically describes the lifetime of focal adhesions as being determined by the interactions of many individual binding and unbinding events of integrins [61].

All simulations were performed using displacement-controlled boundary conditions for the considered RVEs, consistent with the experimental system. The entire computational framework was implemented in the in-house finite element code BACI [62].

3. Results

3.1. Experimental results

Experimental studies of cell-seeded collagen gels (tissue equivalents) subject to mechanical perturbations so far largely suffer from the unsatisfactory short periods over which the gels have been monitored after the perturbations (e.g., only 30 *min* in [8,32]). Therefore, it has remained unclear whether tissue equivalents recover the prior state of tension or only to some extent after perturbations. To close this gap, we performed our experiments with cruciform-shaped tissue equivalents (leading to uniaxially loaded arms and a biaxially loaded central region) over prolonged periods up to 40*h*. After 24*h* we strained some of the gels by 2% or −2%, respectively, allowing another 16*h* to observe possible recovery. Interestingly, the addition of Triton X after 40*h* to induce cell lysis led to a rapid decrease of the gel tension to zero (Fig. 4A inset). This implies that all forces measured were actively applied by the cells, with no inelastic change of the stress-free configuration of the matrix. Similar results were found before [44]. Because the turnover of collagen (i.e., deposition and degradation of collagen fibers by cells) typically happens on the time scale of 3+ days, it appears also justified to assume that mass turnover can most likely be neglected in our experiments [2,48,49,63,64].

In this setting, we initially observed the well-known increase of tension up to a homeostatic plateau [8,32,39–45]. Also as previously reported for porcine SMCs [65], this first stage was followed by a slight decline of tension (Fig. 4A). In cases where tissue equivalents were strained by a 2% step at 24*h*, gel tension first increased in a step-wise manner (elastic response of cells and matrix resulting in a step-like increase in F_t of $\sim 50\%$) followed by a period where tension decreased back toward the level prior to the perturbation (some isolated cellular response). However, even after 16*h*, the original level of tension was not fully recovered, but rather re-established within $\sim 10-15\%$ deviation from the prior value (Fig. 4B). Analogously, if the gels were released by 2% at 24*h*, one first observed a step-wise drop of tension (elastic response of cells

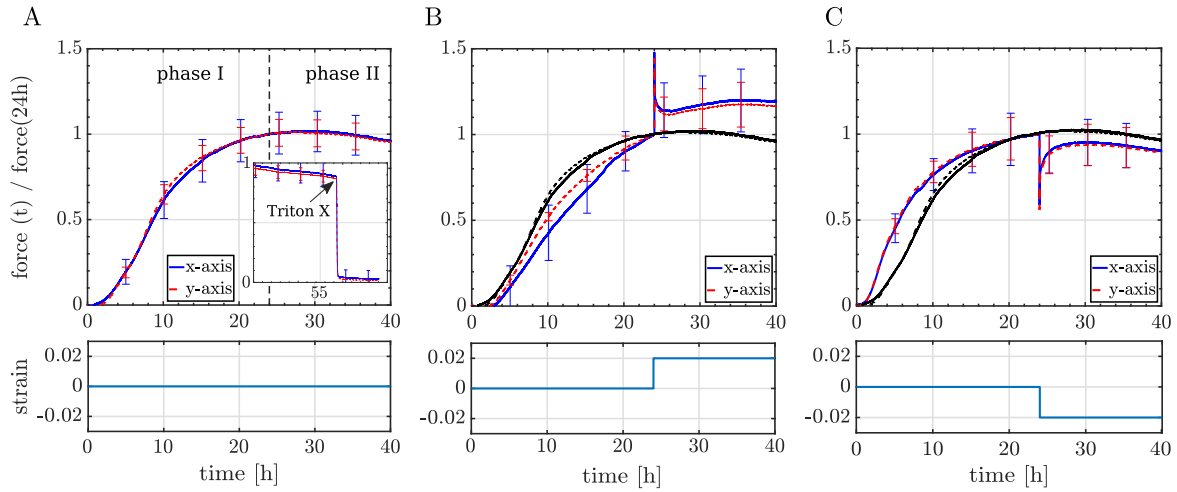

Fig. 4. Normalized force F_t at the outer boundary of cruciform-shaped collagen gels (arms of the gel aligned with x- and y-axis, respectively) seeded with primary aortic SMCs. Each curve shows the mean ± SEM of three identical experiments using a collagen concentration of $1.0 mg/ml$ and a cell density of $0.5 \cdot 10^6 cells/ml$. (A) Unperturbed tissue equivalents (normalized with $F_x(24h) = 720\mu N$ and $F_y(24h) = 729\mu N$) suggested a nearly isotropic biaxial response. (B) Tissue equivalents perturbed with an equibiaxial strain step of 2% at $24h$ (normalized with $F_x(24h) = 602\mu N$ and $F_y(24h) = 588\mu N$). (C) Tissue equivalents perturbed with an equibiaxial step-wise release by 2% at $24h$ (normalized with $F_x(24h) = 664\mu N$ and $F_y(24h) = 626\mu N$). Lines without error bars in (B) and (C) represent experiments without perturbation from (A), hence revealing some specimen-to-specimen variations.

and matrix resulting in a step-like decrease in F_t of $\sim 40\%$), followed by a period where tension increased back toward the level prior to the perturbation (some isolated cellular response). Again, however, even after $16h$ the original level of tension was not fully recovered (Fig. 4C), but rather re-established within $\sim 5-10\%$ deviation from the prior value.

It is worth mentioning that the presented data show a slight decrease of tension in phase II and therefore not an exact conservation of a specific tension. Such a behavior could arise for several reasons. First, a gradual slippage of the gel from the clamping mechanism could be responsible. We excluded this possible reason by pulling on the tested gels after the experiments with a higher force than during the experiments, which was not observed to result in any significant slippage. A second possible origin of the decline in tension is the low serum concentration of 2% that was used in the experimental medium. In preliminary studies, we confirmed that an increased serum concentration leads to higher tension. However, a decline of tension after approximately $24h$ was observed regardless of the serum concentration. Thus, the concentration of FBS in the experimental medium is presumably not responsible for the decline in tension in phase II. In [38], we compared the evolution of tension in constrained tissue equivalents across a large number of studies using a setup similar to ours. Different force generation patterns over time were observed (including decline of tension), depending on factors such as cell type, cell extraction method, and growth factors [38]. We therefore conclude that the slight decline of force is probably cell type specific. This assumption is supported by the study of [65], which reported a similar declining behavior for arterial SMCs. It is worth mentioning that free-floating collagen gels often exhibit a contractility persisting even beyond $48h$ [47,66]. Yet, the free-floating gel is a very different boundary value problem where the cells are not able to reach the same uniform (homeostatic) tension [66], and it is thus not suitable for a direct comparison with uni- or biaxially constrained gels.

3.2. Mechanical analog model

The primary observation of the previous section is: when cell-seeded tissue equivalents were perturbed from the apparent homeostatic state achieved over $24h$, they did not recover precisely F_t (over a period of $16h$). To understand the origin of this behavior, we employed the mechanical analog model introduced in Section 2. In this model, the external force on the tissue F_t needs to equal the elastic force F_1 in the tissue region under tension in series with the cells, which has to balance the sum of the cellular force F_c and the elastic forces F_2 in the tissue region under compression. This yields

$$F_t = F_1 = F_2 + F_c. \tag{2}$$

We now assume the system to be in a homeostatic state (Fig. 5A), in which the initially stress-free regions 1 and 2 were deformed by tensile cell forces $F_c > 0$. One can easily show that this results in an initial homeostatic force on the tissue level, in case of fixed displacements at the outer boundary, of

$$F_{t0} = \left(1 - \frac{k_2}{k_1 + k_2}\right) F_c. \tag{3}$$

We then subject the tissue to a step-wise stretch or release by a change of length ΔL_t (Fig. 5B). Keeping ΔL_t constant after the perturbation results in a permanent change of tissue length

$$\Delta L_t = \Delta L_1 + \Delta L_2. \tag{4}$$

The elastic response of the system will be a step-wise increase of F_t, the quantity that can be measured externally. The subsequent evolution of the forces in the tissue is directly governed by cellular mechanoregulation if we assume that the fiber network only deforms elastically (neither growth nor inelastic remodeling on the short time scales considered).

In the following, we discuss on the basis of our mechanical analog model competing hypotheses regarding the quantity that cells actually regulate. We discuss the observations on the macroscale that these hypotheses would yield and compare them with those in our experiments. It appears reasonable to assume that cells could possibly sense and thus regulate on the microscale three quantities (cf. also [31]): their shape (hypothesis I), the active force they exert through their focal adhesions (hypothesis II), or the strain of the fibers to which they are connected by focal adhesions (hypothesis III). This yields three hypotheses which will be discussed in the following. We assume for simplicity a linear-elastic behavior at the microscale, that is, deformation-independent stiffnesses k_i.

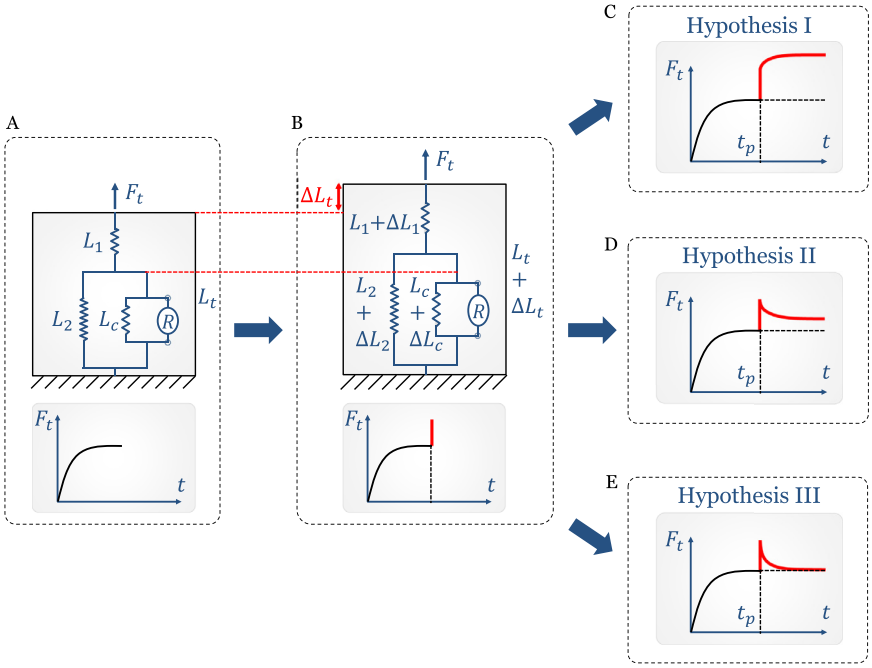

Fig. 5. Short-term response of the (A) mechanical analog model at steady state (after the force $F_c > 0$ built up over time) to a (B) strain step assuming different regulatory targets of an individual cell formulated in (C) hypothesis I (regulation of cell shape), (D) hypothesis II (regulation of contractile forces of cells on ECM), and (E) hypothesis III (regulation of tissue strain). Note that only hypothesis II agrees with experimental observations.

3.2.1. Hypothesis I: cells restore their shape

If cells restore their shape after perturbations, they restore L_c and thus also L_2 and F_2. To this end, cells have to contract after an initial step-wise stretch of the whole tissue and thus have to increase F_c. After regulation, $\Delta L_1 = \Delta L_t$ and with F_2 fully restored,

$$\Delta F_t = \Delta F_1 = \Delta F_c = k_1 \Delta L_1 = k_1 \Delta L_t. \tag{5}$$

Therefore, ΔF_t increases its magnitude compared to that after the perturbation, which is $|\Delta F_t| = |k_1(\Delta L_t - \Delta L_2)|$. This behavior is illustrated in (Fig. 5C), and is in contradiction to our experimental observations.

3.2.2. Hypothesis II: cells restore cellular forces

As discussed previously [38,58,67], cells have a tendency to build stable bonds to the ECM fibers only in a certain constant range of forces. Thus, we examine the response of our analog model if cells restore the cellular forces after perturbations, i.e., F_c. As Eq. (2) must hold also for changes of forces due to changes of lengths, we have, once F_c has been restored,

$$k_1 \Delta L_1 = \Delta F_1 = \Delta F_2 = k_2 \Delta L_2. \tag{6}$$

Combining Eqs. (1), (4), and (6) yields

$$\Delta F_t = \Delta F_1 = \Delta F_2 = \frac{k_1 k_2}{k_1 + k_2} \Delta L_t. \tag{7}$$

Thus, a restoration of F_c after the perturbation necessarily implies a permanent increased value of both F_2 and F_1 and thus also of F_t for $\Delta L_t > 0$, and a permanently decreased value for $\Delta L_t < 0$ (Fig. 5D). This is the behavior observed in our experiments.

Strikingly, this may suggest that most short-term tissue equivalent experiments do not study a regulation of the mechanical state of the ECM, but rather a superposition of the passive matrix response (according to Eq. (7) equal to the remaining offset) and the cellular regulation of a specific contractile force, which represents a relaxation (recovery) in case of extension (release) as an external mechanical perturbation. A direct quantitative comparison between experimental data and our analog model is presented in the supplementary material.

Therefore, our results agree with the findings of [67], which showed that isolated cells restore a specific cellular tensional state. Here we predict this in a three-dimensional fibrous, multi-cellular environment compared to a single cell on a two-dimensional substrate.

Moreover, the changes represented by Eq. (7) suggest a simple additional test of hypothesis II by future experiments. By performing the experiments shown herein in the future with two or more different fiber concentrations (implying different network stiffnesses [62,64,66]) and measuring the resulting residual offset ΔF_t, one could check whether the latter is in agreement with Eq. (7). If so, it should - ceteris paribus - increase by the same factor as the network stiffness.

3.2.3. Hypothesis III: cells restore strain in ECM fibers

If cells restore the strain in the ECM fibers on which they are pulling after the prescribed perturbations, they restore L_1 and thereby also F_1 and F_t. Thus, hypothesis III also contradicts our experiments, where F_t is not exactly restored after perturbations. To understand the problem of hypothesis III, note that it implies $\Delta L_2 = \Delta L_t$ in the long run (that is, after a step-wise elastic deformation and the subsequent mechanoregulation by the cells). It thus implies $\Delta F_2 = k_2 \Delta L_t$. With $0 = \Delta F_1 = \Delta F_2 + \Delta F_c$, one obtains

$$\Delta F_c = -\Delta F_2 = -k_2 \Delta L_t. \tag{8}$$

From this equation we see a possible reason why cells apparently do not restore the strain and thereby not exactly the tension in the fibers on which they are pulling. As apparent from Eq. (8), they would require information about the stiffness or forces in the region under compression. However, this would require that the cells not only sense the general stiffness of the surrounding tissue, but also specifically the extensional stiffness of the part of the ECM which they compress. Moreover, cells do not have information about ΔL_t. Thus, it appears that cells do not have the information necessary to regulate the strain of the fibers on which they pull, which explains why hypothesis III seems to be in disagreement with our experiments.

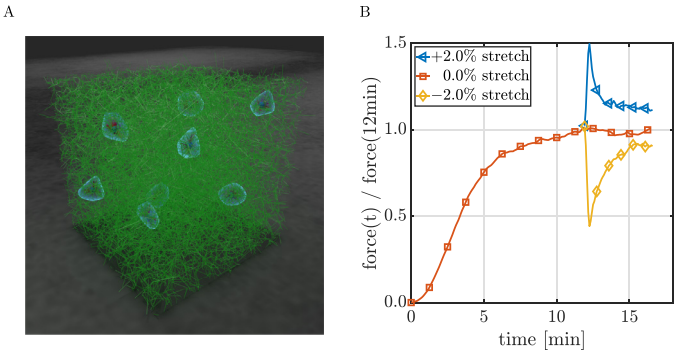

Fig. 6. (A) RVE simulated with a discrete fiber model; triaxial boundary conditions are applied to externally perturb the system. Cell shape is reconstructed around cell-matrix links using three-dimensional Delaunay triangulation. (B) Tissue tension in simulations initially increases to a plateau value. If this plateau value is perturbed, the prior level of tension is restored toward, but not precisely to, the prior steady state value, consistent with the concept of homeostasis now with a mechanistic understanding.

3.3. Discrete fiber network model

The main conclusion drawn from our experimental data and our simple mechanical analog model is: on short time scales, cells do not - and in fact cannot - control the tension in the tissue to a specific value. Cells only regulate the forces they exert on the surrounding fibers. This naturally leads to a residual offset in the tissue tension after perturbations on time scales too short for remodeling or de novo deposition and degradation of fibers. To corroborate this understanding of cellular mechanoregulation, we performed computer simulations with a discrete fiber-network model introduced in [50]. We studied an RVE with a covalently cross-linked fiber matrix (Fig. 6). The size, fiber concentration, and cell concentration of the simulated RVE were chosen to be equivalent to the cell and collagen density in our experiments.

Following [58], catch-slip bonds were assumed between cells and ECM fibers. These bonds are chemically the most enduring in a very specific regime of forces. Our objective was to test whether this behavior of the catch-slip bonds together with cellular contractility alone allows cells within the overall system to effectively control the forces they exert on the surrounding fibers [67] (i.e., F_c in our mechanical analog model), and whether this leads to a residual offset of the tissue tension after mechanical perturbations. As Fig. 6 reveals, this is indeed the case, confirming that the catch-slip bond is a key factor enabling cells to accurately control the contractile forces they exert on surrounding ECM fibers.

A notable difference between the simulation results in Fig. 6 and the experimental results in Fig. 4 is the time scale. In our simulations, mechanical homeostasis develops over a few minutes and thus matches well with experimental results of single cells on purely elastic substrates [67,68]. Yet, in our experiments the homeostatic state is established over many hours. A possible explanation for the difference in the time scale are viscoelastic effects that occur in the gel on the time scale of hours and are not included in the model. Another reason might be that gels increase their stiffness over time when placed in the incubator for multiple hours due to progressing polymerization. Possibly, also complex biochemical interactions between different cells could delay the homeostatic state, which is also not accounted for in the model.

4. Discussion and conclusions

A major shortcoming of previous studies about how tissue equivalents restore a preferred level of tension after an external perturbation (e.g., [8,32]) is the short period of less than an hour over which restoration of tension was monitored. Within such short periods, no new steady state of tension was re-established, leaving unanswered the question, within which tolerance the prior tension is restored after perturbations. This made it difficult to understand which mechanical target quantity is actually preserved by mechanical homeostasis. To overcome this problem, we used herein the device introduced in [33] to track the restoration of tension after perturbations over periods around 30 times longer than previous studies. These data formed the basis of a combined theoretical and computational analysis.

First, to unravel micromechanical principles underlying cellular mechanoregulation, we developed a mechanical analog model to test three competing hypotheses regarding what cells sense and regulate on the microscale. Hypothesis I assumed that cells regulate their own dimension. Hypothesis II, motivated by the experiments of [67], assumed that cells regulate the contractile forces they exert on the ECM. Hypothesis III assumed that cells regulate the strain in the surrounding tissue. Only hypothesis II was consistent with the observed behavior. We therefore conclude that it is likely that cells in gel-like tissue equivalents regulate only the forces they exert on the ECM (at least on short time scales), which by Newton's third law implies the forces that the ECM exerts on the cells, rather than any tissue-intrinsic quantity.

Using an advanced computational model resolving discrete fibers, cells, and their interactions, we confirmed that the catch-slip bond by which integrins connect cells and matrix fibers can endow cells with an ability to regulate the contractile forces they exert on the ECM. In general, catch-slip bonds differ from most chemical bonds in that their lifetime does not monotonically decrease with increasing mechanical load on the bond. There is rather a specific optimal loading at which the stability of these bonds attains a maximum [58]. In agreement with experiments [67], our studies reveal that this maximum determines the level at which cells can regulate the contractile forces they exert on ECM. It is worth noting that the computational studies with our discrete fiber model can support the assumption that the catch-slip bond is sufficient for cells to regulate the forces they exert on the ECM. Yet, these studies cannot prove that this is the only mechanism by which cells can or do act in this setting.

An important conclusion from both our mechanical analog model and simulations with our discrete fiber model is that the passive elasticity of the ECM acts in parallel with the cells to form an essential part of the mechanoregulatory system on the tissue level. Our findings suggest that the residual offset between the matrix tension before and after strain perturbations can be explained only from the passive elasticity of the ECM acting in parallel. To the authors' knowledge, this insight is new and can be used to design future experiments. To study mechanical homeostasis on the level of single cells, cells have been placed between an elastic cantilever and a rigid substrate (Fig. 7A, [69]), and on top of a stretchable micropost array (Fig. 7B, [67]). In both cases, the elastic effect of fibers acting in parallel with the contractile forces exerted by the cells is missing as illustrated in Fig. 7C. This means, neither of these systems mimic well that which defines mechanical homeostasis on the tissue scale. Hence, it will be essential to develop additional experimental set-ups that model the critically important cell-matrix interactions.

An important question for future work is, how can the conclusions drawn here be tested further by additional experiments. As discussed above, a simple test for our conclusion, that the contractile forces exerted by cells are the quantity controlled by the cells on short time scales at a tissue level, could be performed by running the experiments shown herein with several different collagen concentrations and observing whether the residual offset between the tissue tension before and after the perturbation scales with (approximately) the same factor as the tissue stiffness.

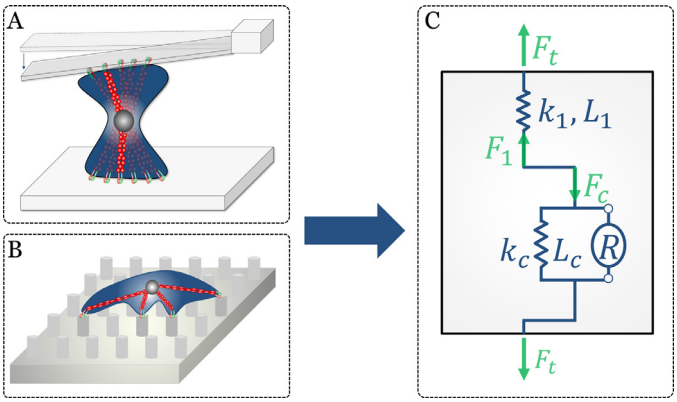

Fig. 7. Schematic drawing of experimental set-ups used by (A) [65] and (B) [46] to study mechanical homeostasis on the level of single cells. Both set-ups miss the elastic fibers acting in parallel to cells in real tissues and thus an important element defining how tissues respond to perturbations of their homeostatic state.

Another way to test these conclusions would be to perform a series of experiments with a varying cell density. While the residual offset between the matrix tension before and after a perturbation was shown in Eq. (7) to be independent of the contractile forces of the cells in the pre-perturbed state, Eq. (3) reveals that homeostatic tissue tension prior to the perturbation scales linearly with the magnitude of these forces. That is, findings herein predict a decreasing relative offset of tension before and after the perturbation as the cell density increases. Future experiments with varying cell density can easily test this.

In summary, the central result of this paper is that, on short time scales that preclude deposition and degradation of ECM, mechanical homeostasis on the tissue level likely results primarily from the contractile forces exerted by the cells on the surrounding tissue. Cells thereby re-establish a state only similar to the one prior to the perturbation. Using the mechanical analog model and computational framework presented in this paper to study the response of cell-seeded collagen gels and soft tissues to perturbations on longer time scales is a promising avenue of future research.

Declaration of Competing Interest

The authors declare that they have no known competing financial interests or personal relationships that could have appeared to influence the work reported in this paper.

Acknowledgments

This work was supported by the Deutsche Forschungsgemeinschaft (DFG, German Research Foundation) Projektnummer 257981274, Projektnummer 386349077. The authors gratefully acknowledge financial support by the International Graduate School of Science and Engineering (IGSSE) of Technical University of Munich, Germany. In addition, we thank Lydia Ehmer and Lea Haeusel for conducting some of the experiments and Isabella Jennings for advice and assistance with the experiments. We further gratefully thank Diane Tchibozo and Lisa Pretsch for contributing to Fig. 6A. Finally, we thank Abhay Ramachandra for his support in isolating the primary cells.

Supplementary material

Supplementary material associated with this article can be found, in the online version, at doi:10.1016/j.actbio.2021.07.054.

References

[1] J.J. Tomasek, G. Gabbiani, B. Hinz, C. Chaponnier, R.A. Brown, Myofibroblasts and mechano-regulation of connective tissue remodelling, Nat. Rev. Mol. Cell Biol. 3 (5) (2002) 349–363.
[2] J.D. Humphrey, E.R. Dufresne, M.A. Schwartz, Mechanotransduction and extracellular matrix homeostasis, Nat. Rev. Mol. Cell Biol. 15 (12) (2014) 802–812.
[3] G. Jiang, A.H. Huang, Y. Cai, M. Tanase, M.P. Sheetz, Rigidity sensing at the leading edge through $\alpha v\beta 3$ integrins and RPTPα, Biophys. J. 90 (5) (2006) 1804–1809.
[4] E.A. Cavalcanti-Adam, T. Volberg, A. Micoulet, H. Kessler, B. Geiger, J.P. Spatz, Cell spreading and focal adhesion dynamics are regulated by spacing of integrin ligands, Biophys. J. 92 (8) (2007) 2964–2974.
[5] D. Ben-Yaakov, R. Golkov, Y. Shokef, S.A. Safran, Response of adherent cells to mechanical perturbations of the surrounding matrix, Soft Matter 11 (7) (2015) 1412–1424.
[6] H. Wang, X. Xu, Continuum elastic models for force transmission in biopolymer gels, Soft Matter 16 (48) (2020) 10781–10808.
[7] M. Lerche, A. Elosegui-Artola, J.Z. Kechagia, C. Guzmán, M. Georgiadou, I. Andreu, D. Gullberg, P. Roca-Cusachs, E. Peuhu, J. Ivaska, Integrin binding dynamics modulate ligand-specific mechanosensing in mammary gland fibroblasts, iScience 23 (3) (2020) 100907.
[8] R.A. Brown, R. Prajapati, D.A. McGrouther, I.V. Yannas, M. Eastwood, Tensional homeostasis in dermal fibroblasts: mechanical responses to mechanical loading in three-dimensional substrates, J. Cell. Physiol. 175 (3) (1998) 323–332.
[9] J.D. Humphrey, Vascular adaptation and mechanical homeostasis at tissue, cellular, and sub-cellular levels, Cell Biochem. Biophys. 50 (2) (2008) 53–78.
[10] A.B. Kassam, M. Horowitz, Y.F. Chang, D. Peters, I.A. Awad, C.J. Hodge, G. Schackert, R.J. Dempsey, Altered arterial homeostasis and cerebral aneurysms: a molecular epidemiology study, Neurosurgery 54 (6) (2004) 1450–1460.
[11] J.D. Humphrey, D.M. Milewicz, G. Tellides, M.A. Schwartz, Dysfunctional mechanosensing in aneurysms, Science 344 (6183) (2014) 477–479.
[12] C.J. Cyron, J.D. Humphrey, Vascular homeostasis and the concept of mechanobiological stability, Int. J. Eng. Sci. 85 (2014) 203–223.
[13] Y. Yamashiro, H. Yanagisawa, The molecular mechanism of mechanotransduction in vascular homeostasis and disease, Clin. Sci. 134 (17) (2020) 2399–2418.
[14] V.M. Weaver, O.W. Petersen, F. Wang, C.A. Larabell, P. Briand, C. Damsky, M.J. Bissell, Reversion of the malignant phenotype of human breast cells in three-dimensional culture and in vivo by integrin blocking antibodies, J. Cell Biol. 137 (1) (1997) 231–245.
[15] D. Boettiger, D.A. Hammer, G.I. Rozenberg, K.R. Johnson, S.S. Margulies, V.M. Weaver, M. Dembo, C.A. Reinhart-King, A. Gefen, J.N. Lakins, N. Zahir, M.J. Paszek, Tensional homeostasis and the malignant phenotype, Cancer Cell 8 (3) (2005) 241–254.
[16] T. Yeung, P.C. Georges, L.A. Flanagan, B. Marg, M. Ortiz, M. Funaki, N. Zahir, W. Ming, V. Weaver, P.A. Janmey, Effects of substrate stiffness on cell morphology, cytoskeletal structure, and adhesion, Cell Motil. Cytoskeleton 60 (1) (2005) 24–34.
[17] K.R. Levental, H. Yu, L. Kass, J.N. Lakins, M. Egeblad, J.T. Erler, S.F. Fong, K. Csiszar, A. Giaccia, W. Weninger, M. Yamauchi, D.L. Gasser, V.M. Weaver, Matrix crosslinking forces tumor progression by enhancing integrin signaling, Cell 139 (5) (2009) 891–906.
[18] D.T. Butcher, T. Alliston, V.M. Weaver, A tense situation: forcing tumour progression, Nat. Rev. Cancer 9 (2) (2009) 108–122.
[19] P. Lu, V.M. Weaver, Z. Werb, The extracellular matrix: a dynamic niche in cancer progression, J. Cell Biol. 196 (4) (2012) 395–406.
[20] J. Kim, Y. Zheng, A.A. Alobaidi, H. Nan, J. Tian, Y. Jiao, B. Sun, Geometric dependence of 3d collective cancer invasion, Biophys. J. 118 (5) (2020) 1177–1182.
[21] J. Xie, M. Bao, S.M.C. Bruekers, W.T.S. Huck, Collagen gels with different fibrillar microarchitectures elicit different cellular responses, ACS Appl. Mater. Interfaces 9 (23) (2017). 1963, 0–19637.
[22] M.S. Hall, F. Alisafaei, E. Ban, X. Feng, C.-Y. Hui, V.B. Shenoy, M. Wu, Fibrous nonlinear elasticity enables positive mechanical feedback between cells and ECMs, Proc. Natl. Acad. Sci. 113 (49) (2016) 14043–14048.
[23] F. Grinnell, W.M. Petroll, Cell motility and mechanics in three-dimensional collagen matrices, Annu. Rev. Cell Dev. Biol. 26 (1) (2010) 335–361.
[24] M. Chiquet, L. Gelman, R. Lutz, S. Maier, From mechanotransduction to extracellular matrix gene expression in fibroblasts, Biochim. Biophys. Acta 1793 (5) (2009) 911–920.
[25] A. Mammoto, T. Mammoto, D.E. Ingber, Mechanosensitive mechanisms in transcriptional regulation, J. Cell Sci. 125 (13) (2012) 3061–3073.
[26] A. Zemel, Active mechanical coupling between the nucleus, cytoskeleton and the extracellular matrix, and the implications for perinuclear actomyosin organization, Soft Matter 11 (12) (2015) 2353–2363.
[27] R.C. Bates, L.F. Lincz, G.F. Burns, Involvement of integrins in cell survival, Cancer Metastasis Rev. 14 (3) (1995) 191–203.
[28] Y.K. Zhu, T. Umino, X.D. Liu, H.J. Wang, D.J. Romberger, J.R. Spurzem, S.I. Rennard, Contraction of fibroblast-containing collagen gels: initial collagen concentration regulates the degree of contraction and cell survival, Vitr. Cell. Dev. Biol. Anim. 37 (1) (2001) 10–16.
[29] S. Sukharev, F. Sachs, Molecular force transduction by ion channels — diversity and unifying principles, J. Cell Sci. 125 (13) (2012) 3075–3083.
[30] M.A. Schwartz, Integrins: emerging paradigms of signal transduction, Annu. Rev. Cell Dev. Biol. 11 (1) (1995) 549–599.

[31] J.D. Humphrey, Stress, strain, and mechanotransduction in cells, J. Biomech. Eng. 123 (6) (2001) 638–641.
[32] D.G. Ezra, J.S. Ellis, M. Beaconsfield, R. Collin, M. Bailly, Changes in fibroblast mechanostat set point and mechanosensitivity: an adaptive response to mechanical stress in floppy eyelid syndrome, Investig. Ophthalmol. Vis. Sci. 51 (8) (2010) 3853–3863.
[33] J.F. Eichinger, D. Paukner, J.M. Szafron, R.C. Aydin, J.D. Humphrey, C.J. Cyron, Computer-controlled biaxial bioreactor for investigating cell-mediated homeostasis in tissue equivalents, J. Biomech. Eng. 142 (7) (2020) 1–22.
[34] H. Wolinsky, S. Glagov, A lamellar unit of aortic medial structure and function in mammals, Circ. Res. 20 (1) (1967) 99–111.
[35] R.E. Shadwick, Mechanical design in arteries, J. Exp. Biol. 202 (Pt 23) (1999) 3305–3313.
[36] C. Zhu, C. Pérez-González, X. Trepat, Y. Chen, N. Castro, R. Oria, P. Roca-Cusachs, A. Elosegui-Artola, A. Kosmalska, Mechanical regulation of a molecular clutch defines force transmission and transduction in response to matrix rigidity, Nat. Cell Biol. 18 (5) (2016) 540–548.
[37] A. Elosegui-Artola, X. Trepat, P. Roca-Cusachs, Control of mechanotransduction by molecular clutch dynamics, Trends Cell Biol. 28 (5) (2018) 356–367.
[38] J.F. Eichinger, L.J. Haeusel, D. Paukner, R.C. Aydin, J.D. Humphrey, C.J. Cyron, Mechanical homeostasis in tissue equivalents - a review, Biomech. Model. Mechanobiol. 20 (3) (2021) 833–850.
[39] M. Marenzana, N. Wilson-Jones, V. Mudera, R.A. Brown, The origins and regulation of tissue tension: identification of collagen tension-fixation process in vitro, Exp. Cell Res. 312 (4) (2006) 423–433.
[40] R.A. Brown, K.K. Sethi, I. Gwanmesia, D. Raemdonck, M. Eastwood, V. Mudera, Enhanced fibroblast contraction of 3d collagen lattices and integrin expression by TGF-β1 and -β3: mechanoregulatory growth factors? Exp. Cell Res. 274 (2) (2002) 310–322.
[41] C. Courderot-Masuyer, Mechanical properties of fibroblasts, in: Agache's Measuring the Skin, Springer, 2017, pp. 903–909.
[42] B.H. Campbell, W.W. Clark, J.H.C. Wang, A multi-station culture force monitor system to study cellular contractility, J. Biomech. 36 (1) (2003) 137–140.
[43] A.H. Dahlmann-Noor, B. Martin-Martin, M. Eastwood, P.T. Khaw, M. Bailly, Dynamic protrusive cell behaviour generates force and drives early matrix contraction by fibroblasts, Exp. Cell Res. 313 (20) (2007) 4158–4169.
[44] D. Karamichos, R.A. Brown, V. Mudera, Collagen stiffness regulates cellular contraction and matrix remodeling gene expression, J. Biomed. Mater. Res. Part A 83 (3) (2007) 887–894.
[45] K.K. Sethi, I.V. Yannas, V. Mudera, M. Eastwood, C. McFarland, R.A. Brown, Evidence for sequential utilization of fibronectin, vitronectin, and collagen during fibroblast-mediated collagen contraction, Wound Repair Regen. 10 (6) (2002) 397–408.
[46] W.B. Cannon, Organization for physiological homeostasis, Physiol. Rev. IX (3) (1929) 399–431.
[47] D.D. Simon, L.E. Niklason, J.D. Humphrey, Tissue transglutaminase, not lysyl oxidase, dominates early calcium-dependent remodeling of fibroblast-populated collagen lattices, Cells Tissues Organs 200 (2) (2014) 104–117.
[48] T. Matsumoto, K. Hayashi, Mechanical and dimensional adaptation of rat aorta to hypertension, J. Biomech. Eng. 116 (3) (1994) 278–283.
[49] Y. Nakagawa, M. Totsuka, T. Sato, Y. Fukuda, K. Hirota, Effect of disuse on the ultrastructure of the achilles tendon in rats, Eur. J. Appl. Physiol. Occup. Physiol. 59 (3) (1989) 239–242.
[50] J.F. Eichinger, M.J. Grill, R.C. Aydin, W.A. Wall, J.D. Humphrey, C.J. Cyron, A computational framework for modeling cell-matrix interactions in soft biological tissues, Biomech. Model Mechanobiol. (2021).
[51] M.W. Majesky, Developmental basis of vascular smooth muscle diversity, Arterioscler. Thromb. Vasc. Biol. 27 (6) (2007) 1248–1258.
[52] Y.A. Miroshnikova, D.M. Jorgens, L. Spirio, M. Auer, A.L. Sarang-Sieminski, V.M. Weaver, Engineering strategies to recapitulate epithelial morphogenesis within synthetic three-dimensional extracellular matrix with tunable mechanical properties, Phys. Biol. 8 (2) (2011) 026013.
[53] J. Joshi, G. Mahajan, C.R. Kothapalli, Three-dimensional collagenous niche and azacytidine selectively promote time-dependent cardiomyogenesis from human bone marrow-derived MSC spheroids, Biotechnol. Bioeng. 115 (8) (2018) 2013–2026.
[54] I. Davoodi-Kermani, M. Schmitter, J.F. Eichinger, R.C. Aydin, C.J. Cyron, Computational study of the geometric properties governing the linear mechanical behavior of fiber networks, Comput. Mater. Sci. 199 (2021) 110711.
[55] J.A.J. Van Der Rijt, K.O. Van Der Werf, M.L. Bennink, P.J. Dijkstra, J. Feijen, Micromechanical testing of individual collagen fibrils, Macromol. Biosci. 6 (9) (2006) 699–702.
[56] K.A. Jansen, A.J. Licup, A. Sharma, R. Rens, F.C. MacKintosh, G.H. Koenderink, The role of network architecture in collagen mechanics, Biophys. J. 114 (11) (2018) 2665–2678.
[57] W. Chen, J. Lou, E.A. Evans, C. Zhu, Observing force-regulated conformational changes and ligand dissociation from a single integrin on cells, J. Cell Biol. 199 (3) (2012) 497–512.
[58] F. Kong, A.J. García, A.P. Mould, M.J. Humphries, C. Zhu, Demonstration of catch bonds between an integrin and its ligand, J. Cell Biol. 185 (7) (2009) 1275–1284.
[59] D. Choquet, D.P. Felsenfeld, M.P. Sheetz, N. Carolina, Extracellular matrix rigidity causes strengthening of integrin cytoskeleton linkages, Cell 88 (1) (1997) 39–48.
[60] S.W. Moore, P. Roca-Cusachs, M.P. Sheetz, Stretchy proteins on stretchy substrates: the important elements of integrin-mediated rigidity sensing, Dev. Cell 19 (2) (2010) 194–206.
[61] S.J. Stehbens, T. Wittmann, Analysis of focal adhesion turnover: a quantitative live-cell imaging example, Methods Cell Biol. 123 (2014) 335–346.
[62] BACI: A Comprehensive Multi-Physics Simulation Framework 2021. https://baci.pages.gitlab.lrz.de/website (Accessed June 23, 2021).
[63] R. Nissen, G.J. Cardinale, S. Udenfriend, Increased turnover of arterial collagen in hypertensive rats, Proc. Natl. Acad. Sci. 75 (1) (1978) 451–453.
[64] E. Gineyts, P.A. Cloos, O. Borel, L. Grimaud, P.D. Delmas, P. Garnero, Racemization and isomerization of type i collagen c-telopeptides in human bone and soft tissues: assessment of tissue turnover, Biochem. J. 345 (Pt 3) (2000) 481–485.
[65] S.M. Hall, A. Soueid, T. Smith, R.A. Brown, S.G. Haworth, V. Mudera, Spatial differences of cellular origins and in vivo hypoxia modify contractile properties of pulmonary artery smooth muscle cells: lessons for arterial tissue engineering, J. Tissue Eng. Regen. Med. 1 (4) (2007) 287–295.
[66] D.D. Simon, L.O. Horgan, J.D. Humphrey, Mechanical restrictions on biological responses by adherent cells within collagen gels, J. Mech. Behav. Biomed. Mater. 14 (2012) 216–226.
[67] S. Weng, Y. Shao, W. Chen, J. Fu, Mechanosensitive subcellular rheostasis drives emergent single-cell mechanical homeostasis, Nat. Mater. 15 (9) (2016) 961–967.
[68] M. Hippler, K. Weißenbruch, K. Richler, E.D. Lemma, M. Nakahata, B. Richter, C. Barner-kowollik, Y. Takashima, A. Harada, E. Blasco, M. Wegener, M. Tanaka, M. Bastmeyer, Mechanical stimulation of single cells by reversible host-guest interactions in 3d microscaffolds, Sci. Adv. 6 (39) (2020) eabc2648.
[69] K.D. Webster, W.P. Ng, D.A. Fletcher, Tensional homeostasis in single fibroblasts, Biophys. J. 107 (1) (2014) 146–155.

Appendix E

Literature review on gel constituents

Cell Type	Cell Density $\left[\frac{10^6\ cells}{mL}\right]$	Isolation Process	Passage Number	Reference
human dermal FB	0.20 0.40	explant growth	unknown	Delvoye et al. (1991)
human dermal FB	1.10	collagenase digestion, explant growth	unknown	Eastwood et al. (1994)
human dermal FB	unknown	collagenase digestion, explant growth (primarily)	unknown	Eastwood et al. (1996)
human dermal FB	1.00	explant growth	P6 - P9	Jenkins et al. (1999)
human dermal FB	1.00	explant growth	P6 - P7	Brown et al. (2002)
human dermal FB	0.29	unknown	unknown	Campbell et al. (2003)
human dermal FB	1.00	explant	P3 - P7	Karamichos et al. (2007)
human osteosarcoma FB	1.00	unknown	unknown	Jenkins et al. (1999)
human ocular FB	7.00 scleral 1.00 Tenon's, corneal	dispase digestion	P2 - P10	Dahlmann-Noor et al. (2007)
human tarsal plate FB	1.00	collagenase digestion	P3 - P4	Ezra et al. (2010)
human fascial tissue FB	1.00	unknown	up to P5	Bisson et al. (2004) Bisson et al. (2009)
calf dermal FB	0.20	explant growth	unknown	Delvoye et al. (1991)
chick embryo FB	0.77	unknown	P2	Kolodney and Wysolmerski (1992)
rabbit tendon FB	unknown	explant growth	unknown	Eastwood et al. (1996)
rabbit tendon FB	1.00	collagenase digestion	P0 - P6	Sawadkar et al. (2020)
rat tendon FB	1.00	collagenase digestion, explant growth	up to P8	Marenzana et al. (2006)
NIH 3T3 FB	0.20 0.50 1.00	unknown	P4 - P5	Eichinger et al. (2020)
porcine pulmonary arterial SMC	1.00	enzyme digestion	P3 - P6	Hall et al. (2007)

Table E.1: Supplementary information on cells used in previous studies.

Gel Volume $[mL]$	Cell Type	Number of Cells $[10^6\ cells]$	Collagen Concentr. $[\frac{mg}{mL}]$	FBS (Gel) $[vol\%]$	5xDMEM (Gel) $[vol\%]$	Other Gel Constituents	Reference
14.8	human dermal FB calf dermal FB	3.0 6.0 3.0	0.46	10.0	18.0	19.32 mM HEPES, 3.05 mM NaOH	Delvoye et al. (1991)
5.0	human dermal FB	5.5	1.00	1.0	21.8	0.1% glutamine, 0.1% Pen-Strep, 2.5 mM HEPES, NaOH	Eastwood et al. (1994)
5.0	human dermal FB rabbit tendon FB	unknown	0.80	0.0	22.0	NaOH	Eastwood et al. (1996)
6.0	human dermal FB human osteosarcoma FB	6.0	1.50	10.0	unknown	NaOH	Jenkins et al. (1999)
6.7	human dermal FB	6.7	1.70	0.0	21.6	15 M HCl, NaOH	Brown et al. (2002)
7.0	human dermal FB	2.0	1.83	2.9	5.1	7.14% 10×PBS, 7.14 mM NaOH	Campbell et al. (2003)
5.0	human dermal FB	5.0	unknown	0.0	2.0	10% 10×MEM, NaOH	Karamichos et al. (2007)
2.0	human ocular FB	14.0 2.0	1.50	unknown	unknown	L-glutamine, $NaHCO_3$, NaOH	Dahlmann-Noor et al. (2007)
2.85	human tarsal plate FB	2.85	1.58	10.2	21.4	1.1% L-glutamine, 0.21% $NaHCO_3$	Ezra et al. (2010)
5.0	human fascial tissue FB	5.0	1.88	1.0	1.8	8.2% 10×MEM, 0.2 mM L-glutamine, 10 U/ml, 10 g/ml Pen-Strep, 100 mM HEPES	Bisson et al. (2004) Bisson et al. (2009)
13.0	chick embryo FB	10.0	0.87	10.0	17.9	Pen-Strep, 2.90 mM NaOH	Kolodney and Wysolmerski (1992)
5.0	rabbit tendon FB	5.0	unknown	0.0	2.0	10% 10×MEM, NaOH	Sawadkar et al. (2020)
6.7	rat tendon FB	6.7	1.70	0.0	21.6	HCl, NaOH	Marenzana et al. (2006)
3.5 uniaxial 6.5 biaxial	NIH 3T3 FB	0.7 1.75 3.5 6.5	0.80 1.50 2.50 1.50	5.4	27.1	9.0 mM NaOH, 1.8 mM HEPES, 5.40% porcine serum, 0.54% Pen-Strep, 0.54% antibiotic/ antimycotic	Eichinger et al. (2020)
5.0	porcine pulmonary arterial SMC	5.0	1.00	1.0	21.8	0.1% glutamine, 0.1% Pen-Strep, 2.5 mM HEPES, NaOH	Hall et al. (2007)

Table E.2: Composition of gels used in previous studies. 5x DMEM concentration is a theoretical value representing the amount of 5x DMEM necessary to obtain the same final concentration of DMEM in the collagen gel as specified in the respective publication (although a differently concentrated DMEM might have been used).

Appendix F

Technical drawings for novel biaxial bioreactor

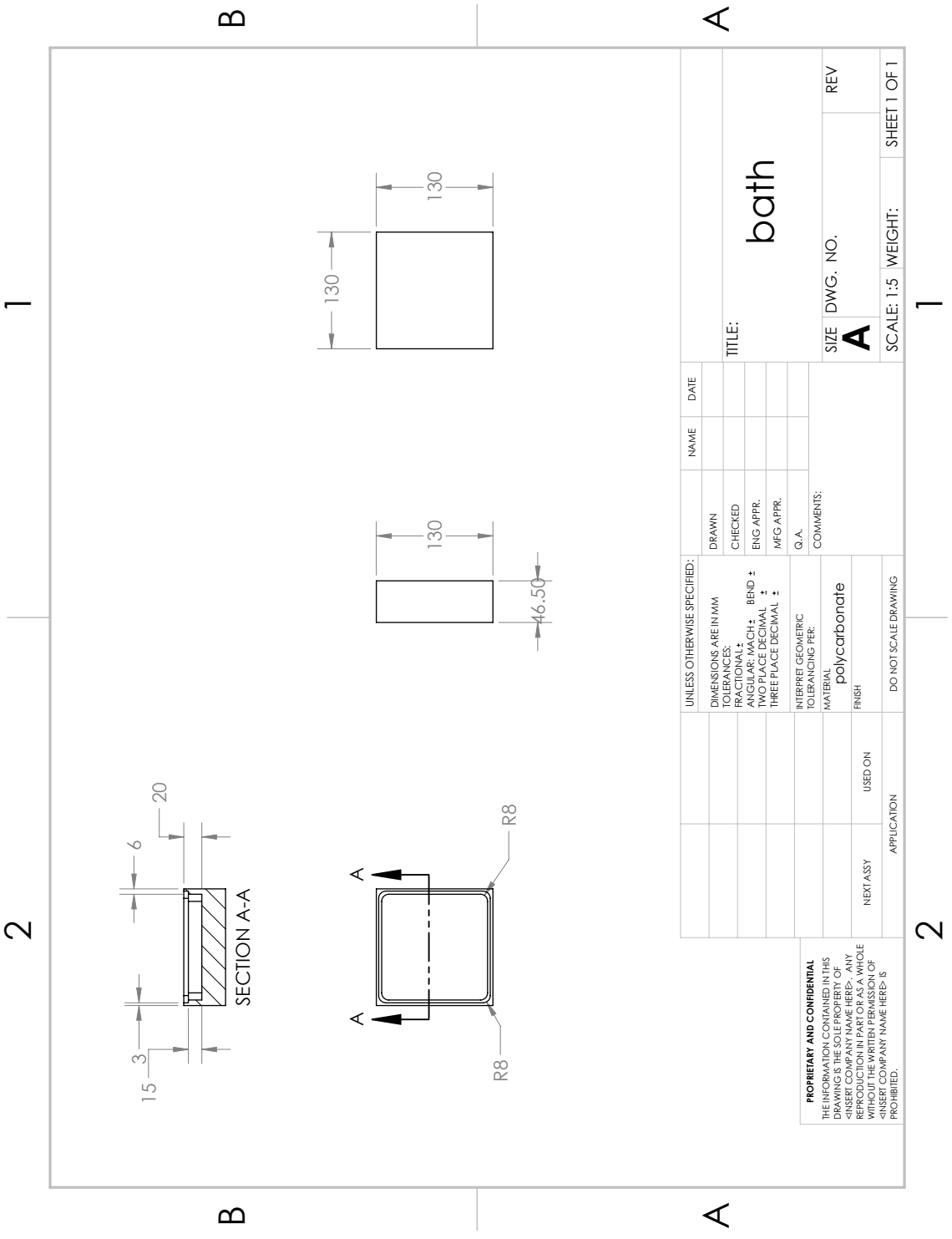

Figure F.1: Technical drawing of the bath of the device which contains the gel immersed in experimental medium.

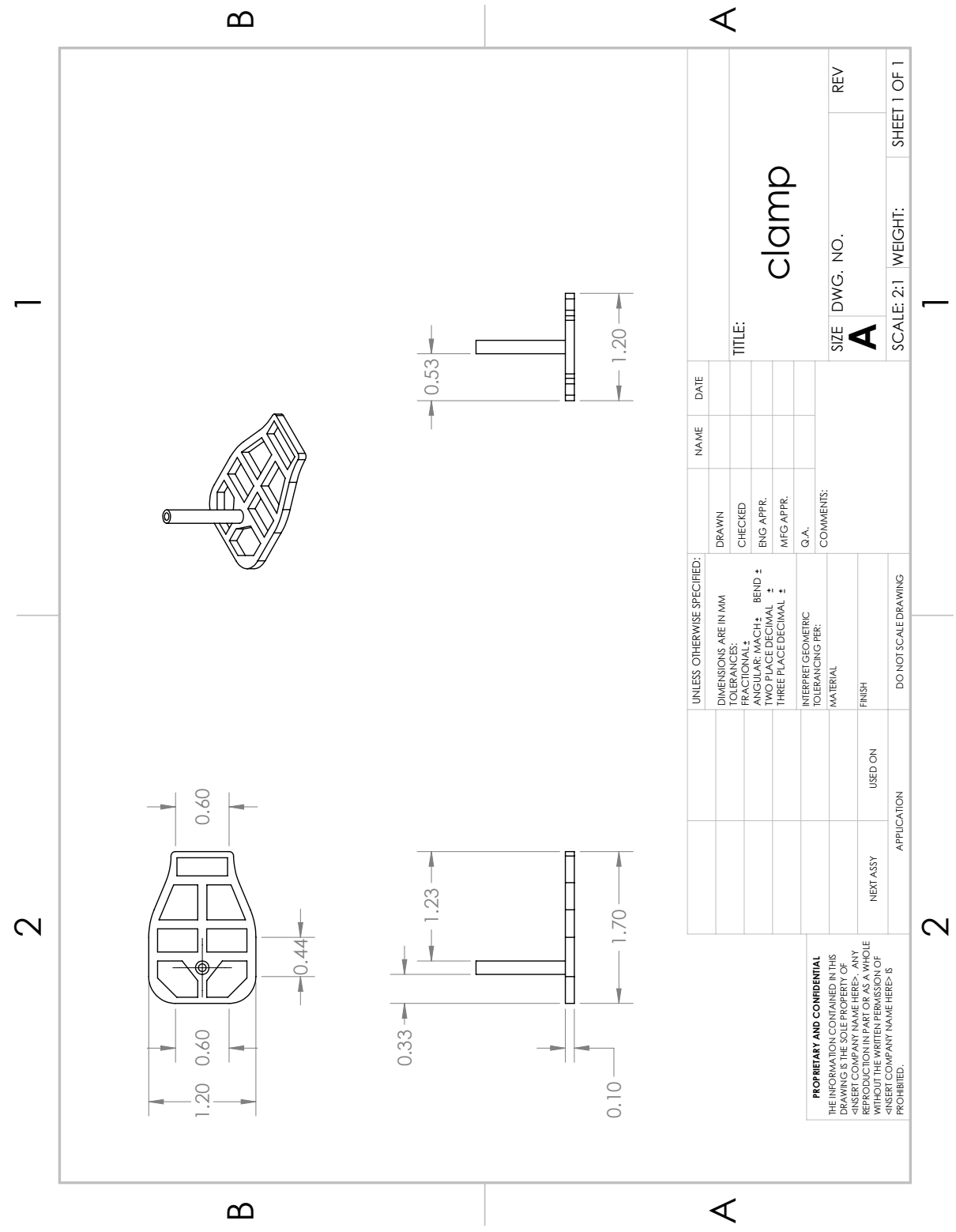

Figure F.2: Technical drawing of the inset used to attach the gel to the device.

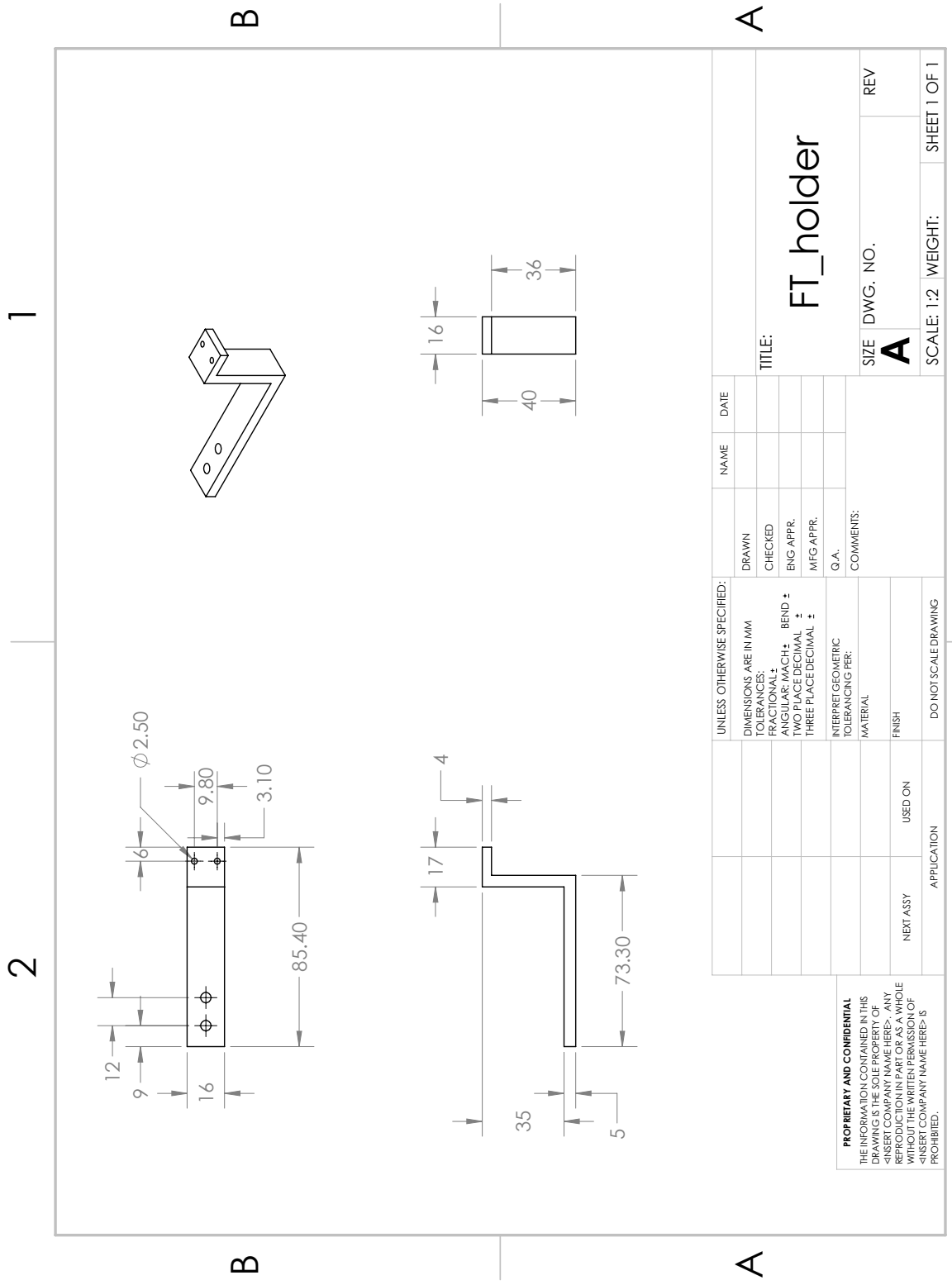

Figure F.3: Technical drawing of the part that holds a force transducers.

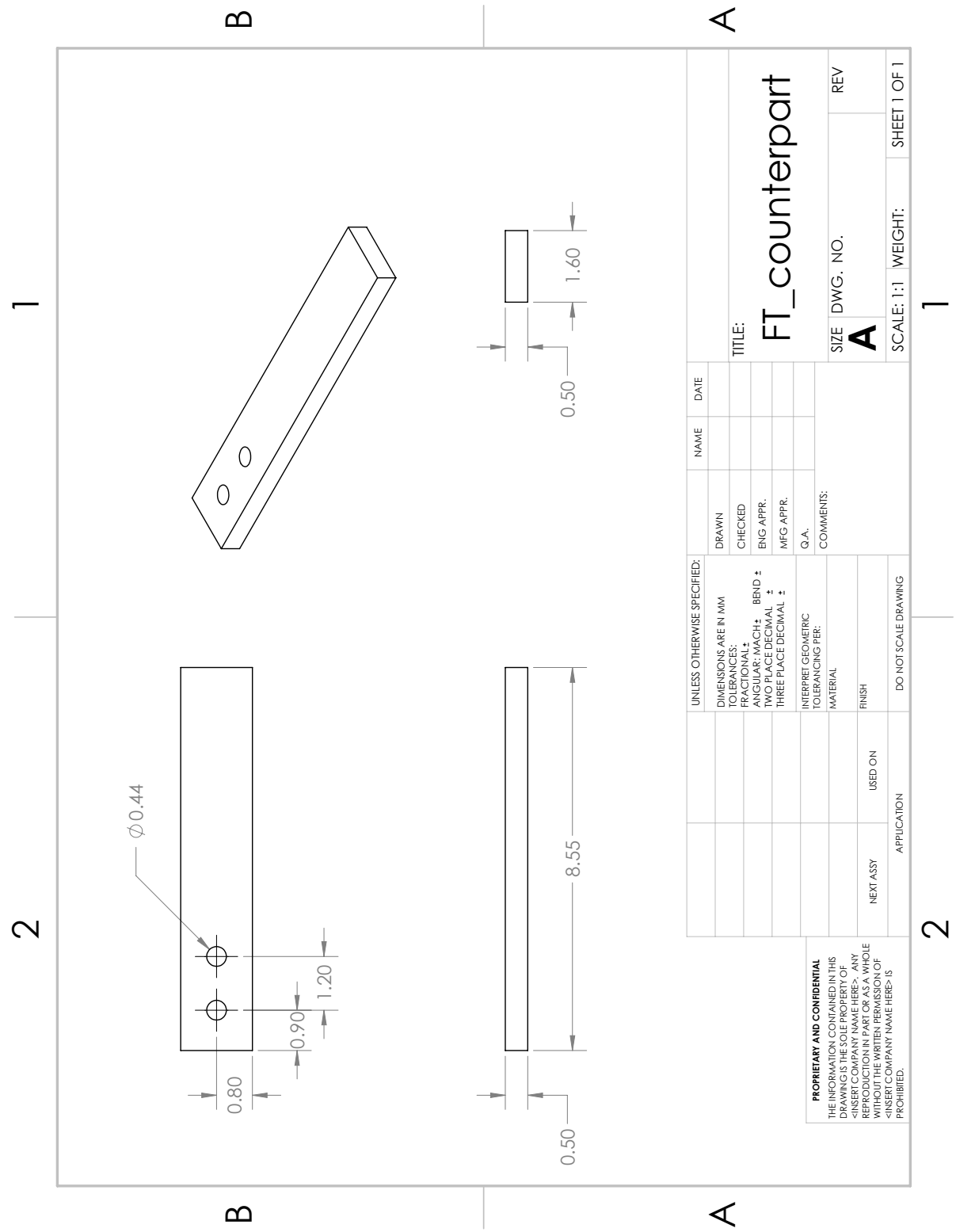

Figure F.4: Technical drawing of the part that is installed in two the directions that do not have a force transducer.

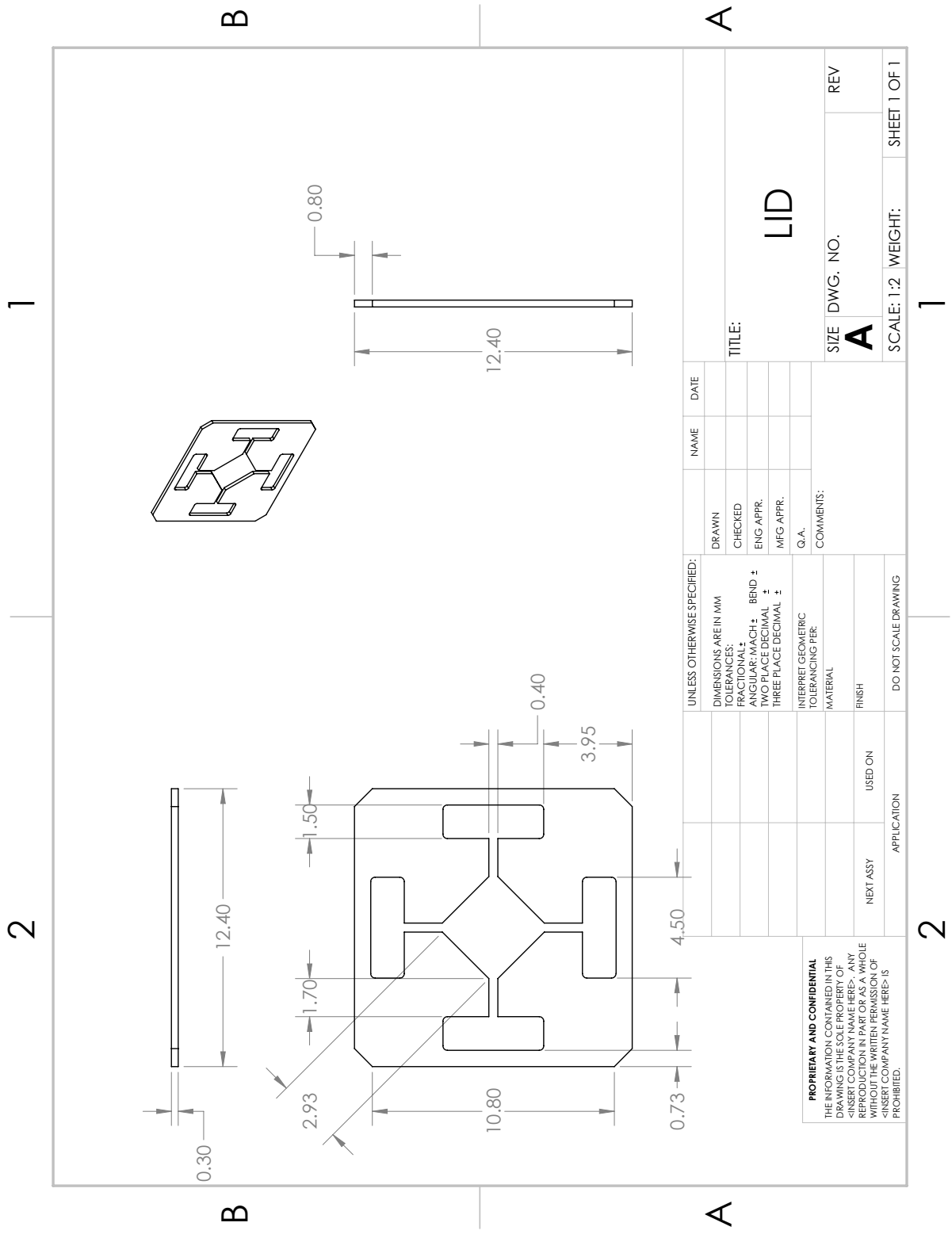

Figure F.5: Technical drawing of the lid to cover the bath.

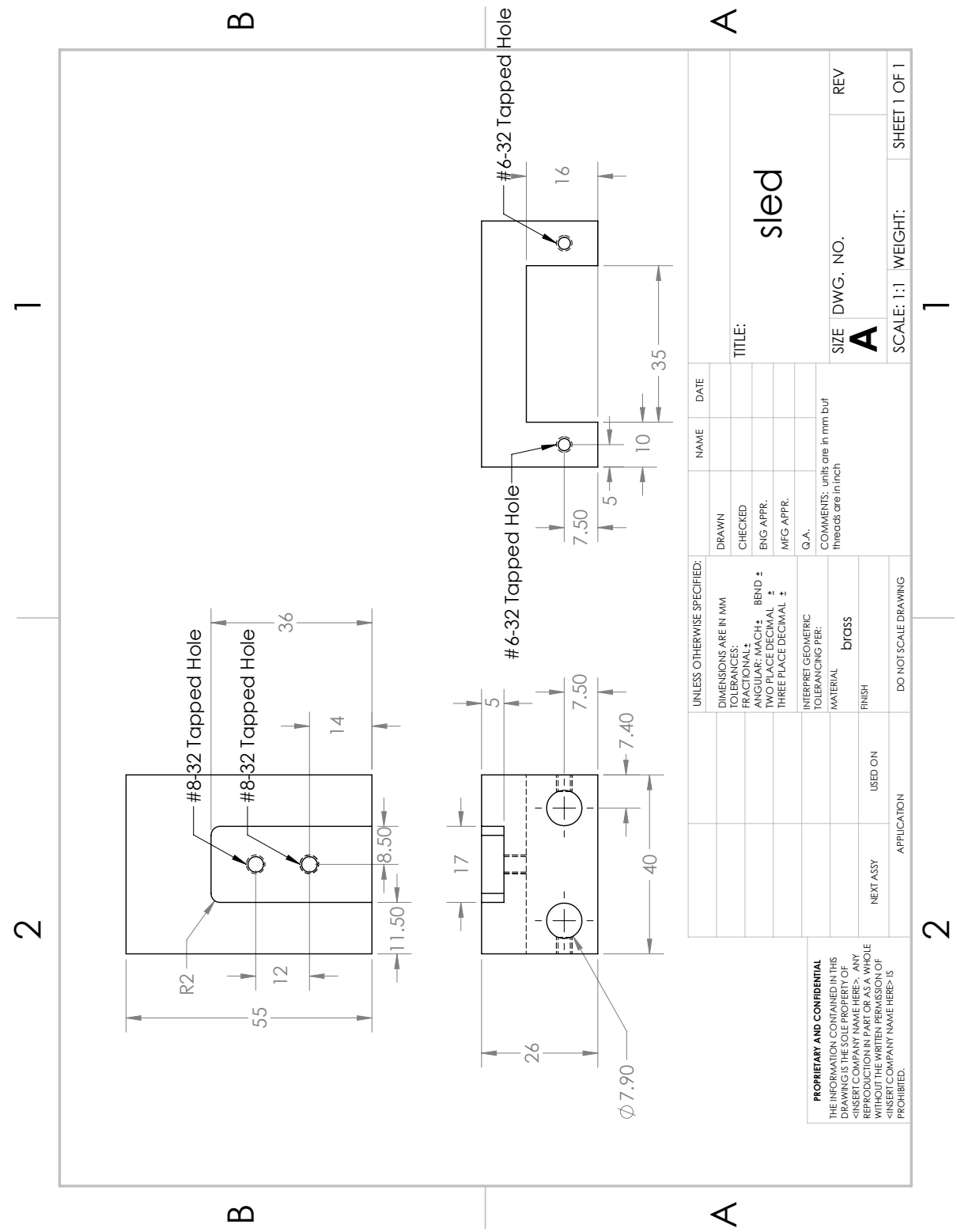

Figure F.6: Technical drawing of the sled that ensures the ability of the device to move its four arms.

Appendix G

Experimental protocols

G.1 Thawing cells from liquid nitrogen

This protocol describes the process of thawing cells from liquid nitrogen. Numbers refer to thawing 4x 1 million cells with a seeding density of 2 million cells per T75 flask. For NIH/3T3 fibroblasts, a seeding density of 1 million cells per flask is enough and is therefore used. With this seeding density, cells need roughly 6 days to get confluent. Therefore, cells need to be thawed every other day so that experiments can be performed every other day.

1. 1h before thawing: add 3ml of fibronectin to a sterile T75 flasks (only for primary cells)
2. After 1h, heat 10% of the cell type specific culture medium in water bath
3. Put in hood: 1000μN pipetter, 2x 15ml falcon tubes, 4x aspiration pipette, 2x 10ml pipette
4. Aspirate fibronectin from T75 flask, wait 15min (only for primary cells)
5. When medium is warm, transfer it to hood and put 8 ml of warm medium in each 15 ml falcon tube
6. Get 4x 1 million cells from liquid nitrogen, thaw (not heat) in water bath, put in hood
7. Add 2x 1ml of thawed cell solution to each falcon tube (so each has in total 10ml)
8. Transfer 15ml falcon tubes (with 10ml fluid) to centrifuge (spin with 500G for primary cells and 1000RPM for NIH/3T3s for 5min)
9. Add 10ml of warm medium to T75 flask, label flasks
10. Get cells from centrifuge, aspirate supernatant and re-suspend in 1ml warm medium
11. Add 1ml of cells (2 Mio), coming from each falcon tube, to each T75 flask
12. Transfer flask to incubator
13. Clean and turn off flow hood

G.2 Preparation of cell-seeded collagen gels

A) Clean and re-assemble device:

1. Move motors to initial position, turn off LabVIEW
2. Turn on heater under incubator to avoid a temperature drop inside the incubator, set CO_2 level to 0.0%

3. Prepare small petri dish with 70% Ethanol and put on top of incubator
4. Remove arms of device, then gently clean feet by immersing them in ethanol and wipe gently with small Kimwipe
5. Take out bath
6. Close door and start cleaning baths (with ethanol and sometimes bleach), molds and all other parts
7. After cleaning, put everything back in incubator and re-assemble device

B) Prepare two collagen gels for two devices:

1. Heat culture medium with 10% FBS, PBS, and (2x) Trypsin in water bath
2. Prepare lab notebook
3. Add labels 1 and 2 on 50ml falcon tube, 15ml falcon tube, and Eppendorf tubes to distinguish the gels
4. Prepare pipettes, pipettors, falcon tubes and Eppendorf tubes. Then, after sterilization with 70% ethanol, put them in hood (number indicates how many are needed):
   - **4x** aspiration pipettes
   - **6x** 5ml pipettes
   - **4x** 10ml pipettes
   - **2x** 15ml falcon tubes
   - **2x** 50ml falcon tubes
   - **1x** 50 μl pipettor
   - **1x** 1000 μl pipettor
   - **2x** Eppendorf tubes
5. Prepare cell counting (Neubauer chamber, Trypan blue, 10μl pipettor, counter)
6. Get cell flasks from incubator, check under microscope if confluent, then put in flow hood (no sterilization) together with Trypsin (sterilize with ethanol)
7. Aspirate flasks, add Trypsin, do cruciform motion and put back in incubator for 5min (use timer)
8. Get ice, 5x DMEM, reconstitution buffer, collagen and cold experimental medium (put all of them on ice), sterilize with 70% ethanol, then transfer to flow hood
9. Put warm 10% medium and warm PBS under flow hood

10. Get cell flasks from incubator, tab on all three sides, check under microscope if cell detached from bottom of flask, (if needed, put back in incubator for further 30s), then put (no sterilization for cells) under hood

11. Add 10ml (warm) medium to each flask, aspirate with same pipette approximately 12ml and put in 50ml falcon tube

12. Add 10 ml (warm) PBS to each flask, aspirate the rest of fluid into 50ml falcon tube with same pipette

13. Transfer 50ml falcon tubes to centrifuge and spin for 5min with 500G (primary cells) or 1000RPM (NIH/3T3), take PBS and 10% medium to refrigerator

14. Start preparing gels: Put correct amount of 5x DMEM and reconstitution buffer in 5ml falcon tubes (adapt numbers depending on exact concentration of the used collagen batch)

15. Get cells from centrifuge

16. Add correct amount of collagen to 15ml Falcon tubes and mix gently (no bubbles) with pre-added 5x DMEM and reconstitution buffer

17. Aspirate 50ml Falcon tube number 1, re-suspend with 4.2ml or, if only few cells, e.g. 2.2ml cold experimental medium $\rightarrow$ put 50μl in Eppendorf tube 1

18. Aspirate 50ml Falcon tube number 1, re-suspend with 4.2ml or, if only few cells, e.g. 2.2ml cold experimental medium $\rightarrow$ put 50μl in Eppendorf tube 2

19. Take both Eppendorf tubes plus 50μl pipettor out of hood, add 50μl of Trypan blue, mix roughly 30 times

20. Take 10μl out of each Eppendorf tube and count cells, calculate number of cells per ml for gel 1 and for gel 2 and write in lab notebook

$$\text{cells per ml} = \text{cells per square} * \text{dilution factor} * 10^4 \tag{G.1}$$

21. Calculate how many ml

$$(x\ ml = 3.5\text{million cell}/\text{million cells per ml}) \tag{G.2}$$

of each cell suspension you need to have 3.5 million cells in each gel (for a cell density of 1 million cells per ml), calculate how many ml of pure cold experimental medium needs to be added to each gel

$$(4.1ml - x\ ml = y\ ml) \tag{G.3}$$

22. Turn on heater, put CO_2 level of incubator back to 5%

23. Mix prepared collagen gel solution

24. Add x_1 ml (cells) and y_1 ml (pure medium) to gel 1, mix gel gently

25. Add x_2 ml (cells) and y_2 ml (pure medium) to gel 2, mix gel gently
26. Take all of gel 1 in 5ml pipette and transfer to device
27. Mix gel 2, take all of gel 2 in 5ml pipette and transfer to device
28. Turn off heater, set timer to 30min (time for gel polymerization before experiment is started)
29. Take 4x 50ml Falcon tubes and experimental floating medium to hood, fill up falcon tubes
30. Then, heat floating medium in water bath
31. Clean lab and hood, turn of microscope
32. After 30min, turn on heater, remove molds, fix them to corners and start experiment, turn off heater and bottom light

Bibliography

A. S. Abhilash, B. M. Baker, B. Trappmann, C. S. Chen, and V. B. Shenoy. Remodeling of fibrous extracellular matrices by contractile cells: Predictions from discrete fiber network simulations. *Biophys. J.*, 107(8):1829–1840, 2014. DOI: 10.1016/j.bpj.2014.08.029.

J. Alcaraz, H. Mori, C. M. Ghajar, D. Brownfield, R. Galgoczy, and M. J. Bissell. Collective epithelial cell invasion overcomes mechanical barriers of collagenous extracellular matrix by a narrow tube-like geometry and MMP14-dependent local softening. *Integr. Biol.*, 3(12): 1153–1166, 2011. DOI: 10.1039/c1ib00073j.

D. Ambrosi, G. Ateshian, E. Arruda, S. Cowin, J. Dumais, A. Goriely, G. Holzapfel, J. Humphrey, R. Kemkemer, E. Kuhl, J. Olberding, L. Taber, and K. Garikipati. Perspectives on biological growth and remodeling. *J. Mech. Phys. Solids*, 59(4):863–883, 2010. DOI: 10.1016/j.jmps.2010.12.011.

S. M. Arribas, A. Hinek, and M. C. González. Elastic fibres and vascular structure in hypertension. *Pharmacol. Ther.*, 111(3):771–791, 2006. DOI: 10.1016/j.pharmthera.2005.12.003.

K. Austen, P. Ringer, A. Mehlich, A. Chrostek-Grashoff, C. Kluger, C. Klingner, B. Sabass, R. Zent, M. Rief, and C. Grashoff. Extracellular rigidity sensing by talin isoform-specific mechanical linkages. *Nat. Cell Biol.*, 17(12):1597–1606, 2015. DOI: 10.1038/ncb3268.

BACI. A Comprehensive Multi-Physics Simulation Framework. `https://baci.pages.gitlab.lrz.de/website`. Accessed: 2021-11-10.

B. M. Baker and C. S. Chen. Deconstructing the third dimension – how 3D culture microenvironments alter cellular cues. *J. Cell Sci.*, 125(13):3015–3024, 2012. DOI: 10.1242/jcs.079509.

B. M. Baker, B. Trappmann, W. Y. Wang, M. S. Sakar, I. L. Kim, V. B. Shenoy, J. A. Burdick, and C. S. Chen. Cell-mediated fibre recruitment drives extracellular matrix mechanosensing in engineered fibrillar microenvironments. *Nat. Mater.*, 14(12):1262–1268, 2015. DOI: 10.1038/nmat4444.

E. Ban, J. M. Franklin, S. Nam, L. R. Smith, H. Wang, R. G. Wells, O. Chaudhuri, J. T. Liphardt, and V. B. Shenoy. Mechanisms of Plastic Deformation in Collagen Networks Induced by Cellular Forces. *Biophys. J.*, 114(2):450–461, 2018. DOI: 10.1016/j.bpj.2017.11.3739.

E. Ban, H. Wang, J. M. Franklin, J. T. Liphardt, P. A. Janmey, and V. B. Shenoy. Strong triaxial coupling and anomalous Poisson effect in collagen networks. *Proc. Natl. Acad. Sci.*, 116(14): 6790–6799, 2019. DOI: 10.1073/pnas.1815659116.

B. L. Bangasser, S. S. Rosenfeld, and D. J. Odde. Determinants of maximal force transmission in a motor-clutch model of cell traction in a compliant microenvironment. *Biophys. J.*, 105 (3):581–592, 2013. DOI: 10.1016/j.bpj.2013.06.027.

R. C. Bates, L. F. Lincz, and G. F. Burns. Involvement of integrins in cell survival. *Cancer Metastasis Rev.*, 14(3):191–203, 1995. DOI: 10.1007/BF00690291.

E. Bell, B. Ivarsson, and C. Merrill. Production of a tissue-like structure by contraction of collagen lattices by human fibroblasts of different proliferative potential in vitro. *Proc. Natl. Acad. Sci.*, 76(3):1274–8, 1979. DOI: 10.1073/pnas.76.3.1274.

A. D. Bershadsky, N. Q. Balaban, and B. Geiger. Adhesion-Dependent Cell Mechanosensitivity. *Annu. Rev. Cell Dev. Biol.*, 19:677–695, 2003. DOI: 10.1146/annurev.cellbio.19.111301.153011.

A. P. Bhole, B. P. Flynn, M. Liles, N. Saeidi, C. A. Dimarzio, and J. W. Ruberti. Mechanical strain enhances survivability of collagen micronetworks in the presence of collagenase: implications for load-bearing matrix growth and stability. *Philos. Trans. R. Soc. A Math. Phys. Eng. Sci.*, 367(1902):3339–3362, 2009. DOI: 10.1098/rsta.2009.0093.

K. Bircher, M. Zündel, M. Pensalfini, A. E. Ehret, and E. Mazza. Tear resistance of soft collagenous tissues. *Nat. Commun.*, 10(1):1–13, 2019. DOI: 10.1038/s41467-019-08723-y.

M. A. Bisson, V. Mudera, D. A. McGrouther, and A. O. Grobbelaar. The contractile properties and responses to tensional loading of Dupuytren's disease-derived fibroblasts are altered: A cause of the contracture? *Plast. Reconstr. Surg.*, 113(2):611–621, 2004. DOI: 10.1097/01.PRS.0000101527.76293.F1.

M. A. Bisson, K. S. Beckett, D. A. McGrouther, A. O. Grobbelaar, and V. Mudera. Transforming Growth Factor-β1 Stimulation Enhances Dupuytren's Fibroblast Contraction in Response to Uniaxial Mechanical Load Within a 3-Dimensional Collagen Gel. *J. Hand Surg. Am.*, 34(6): 1102–1110, 2009. DOI: 10.1016/j.jhsa.2009.02.008.

E. J. Blain, S. J. Gilbert, R. J. Wardale, S. J. Capper, D. J. Mason, and V. C. Duance. Upregulation of matrix metalloproteinase expression and activation following cyclical compressive loading of articular cartilage in vitro. *Arch. Biochem. Biophys.*, 396(1):49–55, 2001. DOI: 10.1006/abbi.2001.2575.

D. Boettiger, D. A. Hammer, G. I. Rozenberg, K. R. Johnson, S. S. Margulies, V. M. Weaver, M. Dembo, C. A. Reinhart-King, A. Gefen, J. N. Lakins, N. Zahir, and M. J. Paszek. Tensional homeostasis and the malignant phenotype. *Cancer Cell*, 8(3):241–254, 2005. DOI: 10.1016/j.ccr.2005.08.010.

C. Bonnans, J. Chou, and Z. Werb. Remodelling the extracellular matrix in development and disease. *Nat. Rev. Mol. Cell Biol.*, 15(12):786–801, 2014. DOI: 10.1038/nrm3904.

F. A. Braeu, A. Seitz, R. C. Aydin, and C. J. Cyron. Homogenized constrained mixture models for anisotropic volumetric growth and remodeling. *Biomech. Model. Mechanobiol.*, 16(3): 889–906, 2017. DOI: 10.1007/s10237-016-0859-1.

C. P. Broedersz, X. Mao, T. C. Lubensky, and F. C. Mackintosh. Criticality and isostaticity in fibre networks. *Nat. Phys.*, 7(12):983–988, 2011. DOI: 10.1038/NPHYS2127.

R. A. Brown, R. Prajapati, D. A. McGrouther, I. V. Yannas, and M. Eastwood. Tensional homeostasis in dermal fibroblasts: Mechanical responses to mechanical loading in three-dimensional substrates. *J. Cell. Physiol.*, 175(3):323–332, 1998. DOI: 10.1002/(SICI)1097-4652(199806)175:3¡323::AID-JCP10¿3.0.CO;2-6.

R. A. Brown, K. K. Sethi, I. Gwanmesia, D. Raemdonck, M. Eastwood, and V. Mudera. Enhanced fibroblast contraction of 3D collagen lattices and integrin expression by TGF-β1 and -β3: Mechanoregulatory growth factors? *Exp. Cell Res.*, 274(2):310–322, 2002. DOI: 10.1006/excr.2002.5471.

B. Burkel, M. Proestaki, S. Tyznik, and J. Notbohm. Heterogeneity and nonaffinity of cell-induced matrix displacements. *Phys. Rev. E*, 98(5):1–13, 2018. DOI: 10.1103/PhysRevE.98.052410.

D. T. Butcher, T. Alliston, and V. M. Weaver. A tense situation: Forcing tumour progression. *Nat. Rev. Cancer*, 9(2):108–122, 2009. DOI: 10.1038/nrc2544.

J. P. Califano and C. A. Reinhart-King. Substrate stiffness and cell area predict cellular traction stresses in single cells and cells in contact. *Cell. Mol. Bioeng.*, 3(1):68–75, 2010. DOI: 10.1007/s12195-010-0102-6.

B. H. Campbell, W. W. Clark, and J. H. C. Wang. A multi-station culture force monitor system to study cellular contractility. *J. Biomech.*, 36(1):137–140, 2003. DOI: 10.1016/S0021-9290(02)00325-1.

W. B. Cannon. Organization for Physiological Homeostasis. *Physiol. Rev.*, IX(3):399–431, 1929. DOI: 10.1152/physrev.1929.9.3.399.

W. B. Cannon. *The Wisdom of the Body*. W. W. Norton and Company, Inc., New York, 1932.

L. Cardamone, A. Valentin, J. Eberth, and J. D. Humphrey. Origin of Axial Prestretch and Residual Stress in Arteries. *Biomech. Model. Mechanobiol.*, 8(6):431–446, 2009. DOI: 10.1007/s10237-008-0146-x.

A. Carisey, R. Tsang, A. M. Greiner, N. Nijenhuis, N. Heath, A. Nazgiewicz, R. Kemkemer, B. Derby, J. Spatz, and C. Ballestrem. Vinculin regulates the recruitment and release of core focal adhesion proteins in a force-dependent manner. *Curr. Biol.*, 23(4):271–281, 2013. DOI: 10.1016/j.cub.2013.01.009.

E. A. Cavalcanti-Adam, T. Volberg, A. Micoulet, H. Kessler, B. Geiger, and J. P. Spatz. Cell Spreading and Focal Adhesion Dynamics Are Regulated by Spacing of Integrin Ligands. *Biophys. J.*, 92(8):2964–2974, 2007. DOI: 10.1529/biophysj.106.089730.

C. E. Chan and D. J. Odde. Traction dynamics of filopodia on compliant substrates. *Science*, 322(5908):1687–1691, 2008. DOI: 10.1126/science.1163595.

A. P. Chatterjee. Nonuniform fiber networks and fiber-based composites: Pore size distributions and elastic moduli. *J. Appl. Phys.*, 108(6):063513, 2010. DOI: 10.1063/1.3485823.

W. Chen, J. Lou, E. A. Evans, and C. Zhu. Observing force-regulated conformational changes and ligand dissociation from a single integrin on cells. *J. Cell Biol.*, 199(3):497–512, 2012. DOI: 10.1083/jcb.201201091.

Q. Cheng, Z. Sun, G. Meininger, and M. Almasri. PDMS elastic micropost arrays for studying vascular smooth muscle cells. *Sens. Actuators B Chem.*, 188:1055–1063, 2013. DOI: 10.1016/j.snb.2013.08.018.

M. Chiquet, L. Gelman, R. Lutz, and S. Maier. From mechanotransduction to extracellular matrix gene expression in fibroblasts. *Biochim. Biophys. Acta*, 1793(5):911–920, 2009. DOI: 10.1016/j.bbamcr.2009.01.012.

R. Chovatiya and R. Medzhitov. Stress, inflammation, and defense of homeostasis. *Mol. Cell*, 54(2):281–288, 2014. DOI: 10.1016/j.molcel.2014.03.030.

C. Courderot-Masuyer. Mechanical Properties of Fibroblasts. In *Agache's Meas. Ski.*, chapter 91, pages 903–909. Springer, 2017. DOI: 10.1007/978-3-319-32383-1.

T. R. Cox and J. T. Erler. Remodeling and homeostasis of the extracellular matrix: implications for fibrotic diseases and cancer. *Dis. Model. Mech.*, 4(2):165–178, 2011. DOI: 10.1242/dmm.004077.

Y. Cui, F. M. Hameed, B. Yang, K. Lee, C. Q. Pan, S. Park, and M. Sheetz. Cyclic stretching of soft substrates induces spreading and growth. *Nat. Commun.*, 6:1–8, 2015. DOI: 10.1038/ncomms7333.

C. J. Cyron and R. C. Aydin. Mechanobiological free energy: a variational approach to tensional homeostasis in tissue equivalents. *Zeitschrift für Angew. Math. und Mech.*, 97(9):1011–1019, 2017. DOI: 10.1002/zamm.201600126.

C. J. Cyron and J. D. Humphrey. Vascular homeostasis and the concept of mechanobiological stability. *Int. J. Eng. Sci.*, 85:203–223, 2014. DOI: 10.1016/j.ijengsci.2014.08.003.

C. J. Cyron and J. D. Humphrey. Growth and remodeling of load-bearing biological soft tissues. *Meccanica*, 52(3):645–664, 2017. DOI: 10.1007/s11012-016-0472-5.

C. J. Cyron, K. W. Müller, K. M. Schmoller, A. R. Bausch, W. A. Wall, and R. F. Bruinsma. Equilibrium phase diagram of semi-flexible polymer networks with linkers. *Epl*, 102(3):38003, 2013a. DOI: 10.1209/0295-5075/102/38003.

C. J. Cyron, J. S. Wilson, and J. D. Humphrey. Mechanobiological stability: A new paradigm to understand the enlargement of aneurysms? *J. R. Soc. Interface*, 11(100):20140680, 2014. DOI: 10.1098/rsif.2014.0680.

C. J. Cyron, R. C. Aydin, and J. D. Humphrey. A homogenized constrained mixture (and mechanical analog) model for growth and remodeling of soft tissue. *Biomech. Model. Mechanobiol.*, 15(6):1389–1403, 2016. DOI: 10.1007/s10237-016-0770-9.

C. J. Cyron. *Micromechanical Continuum Approach for the Analysis of Biopolymer Networks*. Dissertation, Technical University of Munich, 2011.

C. J. Cyron, K. W. Müller, A. R. Bausch, and W. A. Wall. Micromechanical simulations of biopolymer networks with finite elements. *J. Comput. Phys.*, 244:236–251, 2013b. DOI: 10.1016/j.jcp.2012.10.025.

C. Cyron and W. A. Wall. Numerical method for the simulation of the Brownian dynamics of rod-like microstructures with three-dimensional nonlinear beam elements. *Int. j. numer. method. biomed. eng.*, 90(8):955–987, 2012. DOI: doi.org/10.1002/nme.3351.

A. H. Dahlmann-Noor, B. Martin-Martin, M. Eastwood, P. T. Khaw, and M. Bailly. Dynamic protrusive cell behaviour generates force and drives early matrix contraction by fibroblasts. *Exp. Cell Res.*, 313(20):4158–4169, 2007. DOI: 10.1016/j.yexcr.2007.07.040.

M. Das, S. Subbayya Ithychanda, J. Qin, and E. F. Plow. Mechanisms of talin-dependent integrin signaling and crosstalk. *Biochim. Biophys. Acta*, 1838(2):579–588, 2014. DOI: 10.1016/j.bbamem.2013.07.017.

M. W. Davidson, S. Ruehland, M. A. Baird, S. Teo, N. Bate, P. Kanchanawong, W. I. Goh, Y. Wang, H. Goh, D. R. Critchley, and J. Liu. Talin determines the nanoscale architecture of focal adhesions. *Proc. Natl. Acad. Sci.*, 112(35):E4864–E4873, 2015. DOI: 10.1073/pnas.1512025112.

K. J. A. Davies. Adaptive homeostasis. *Mol. Aspects Med.*, 49:1–7, 2016. DOI: 10.1016/j.mam.2016.04.007.

H. G. Davis. *Conservative Surgery*. Appleton & Co., New York, 1867.

I. Davoodi-Kermani, M. Schmitter, J. F. Eichinger, R. C. Aydin, and C. J. Cyron. Computational study of the geometric properties governing the linear mechanical behavior of fiber networks. *Comput. Mater. Sci.*, 199:110711, 2021. DOI: 10.1016/j.commatsci.2021.110711.

A. del Rio, R. Perez-Jimenez, R. Liu, P. Roca-Cusachs, J. M. Fernandez, and M. P. Sheetz. Stretching Single Talin Rod. *Science*, 323(5914):638–641, 2009. DOI: 10.1126/science.1162912.

P. Delvoye, P. Wiliquet, J.-L. Levêque, B. V. Nusgens, and C. M. Lapière. Measurement of Mechanical Forces Generated by Skin Fibroblasts Embedded in a Three-Dimensional Collagen Gel. *J. Invest. Dermatol.*, 97(5):898–902, 1991. DOI: 10.1098/rsfs.2015.0080.

S. Domaschke, A. Morel, G. Fortunato, and A. E. Ehret. Random auxetics from buckling fibre networks. *Nat. Commun.*, 10(1):1–8, 2019. DOI: 10.1038/s41467-019-12757-7.

S. Dong, Z. Huang, L. Tang, X. Zhang, Y. Zhang, and Y. Jiang. A three-dimensional collagen-fiber network model of the extracellular matrix for the simulation of the mechanical behaviors and micro structures. *Comput. Methods Biomech. Biomed. Engin.*, 20(9):991–1003, 2017. DOI: 10.1080/10255842.2017.1321113.

B. J. DuChez, A. D. Doyle, E. K. Dimitriadis, and K. M. Yamada. Durotaxis by Human Cancer Cells. *Biophys. J.*, 116(4):670–683, 2019. DOI: 10.1016/j.bpj.2019.01.009.

D. W. Dumbauld, H. Shin, N. D. Gallant, K. E. Michael, H. Radhakrishna, and A. J. García. Contractility modulates cell adhesion strengthening through focal adhesion kinase and assembly of vinculin-containing focal adhesions. *J. Cell. Physiol.*, 223(3):746–756, 2010. DOI: 10.1002/jcp.22084.

D. W. Dumbauld, T. T. Lee, A. Singh, J. Scrimgeour, C. A. Gersbach, E. A. Zamir, J. Fu, C. S. Chen, J. E. Curtis, and S. W. Craig. How vinculin regulates force transmission. *Proc. Natl. Acad. Sci.*, 110(24):9788–9793, 2013. DOI: 10.1073/pnas.1216209110.

K. Duval, H. Grover, L. H. Han, Y. Mou, A. F. Pegoraro, J. Fredberg, and Z. Chen. Modeling physiological events in 2D vs. 3D cell culture. *Physiology*, 32(4):266–277, 2017. DOI: 10.1152/physiol.00036.2016.

K. Dzobo, N. E. Thomford, D. A. Senthebane, H. Shipanga, A. Rowe, C. Dandara, M. Pillay, and K. S. C. M. Motaung. Advances in regenerative medicine and tissue engineering: Innovation and transformation of medicine. *Stem Cells Int.*, 2018:2495848, 2018. DOI: 10.1155/2018/2495848.

M. Eastwood, R. Porter, U. Khan, G. McGrouther, and R. Brown. Quantitative analysis of collagen gel contractile forces generated by dermal fibroblasts and the relationship to cell morphology. *J. Cell. Physiol.*, 166(1):33–42, 1996. DOI: 10.1002/(SICI)1097-4652(199601)166:1¡33::AID-JCP4¿3.0.CO;2-H.

M. Eastwood, D. A. McGrouther, and R. A. Brown. A culture force monitor for measurement of contraction forces generated in human dermal fibroblast cultures: evidence for cell-matrix mechanical signalling. *Biochim. Biophys. Acta*, 1201(2):186–192, 1994. DOI: 10.1016/0304-4165(94)90040-X.

J. F. Eichinger, D. Paukner, J. M. Szafron, R. C. Aydin, J. D. Humphrey, and C. J. Cyron. Computer-Controlled Biaxial Bioreactor for Investigating Cell-Mediated Homeostasis in Tissue Equivalents. *J. Biomech. Eng.*, 142(7):1–22, 2020. DOI: 10.1115/1.4046201.

J. F. Eichinger, M. J. Grill, R. C. Aydin, W. A. Wall, J. D. Humphrey, and C. J. Cyron. A computational framework for modeling cell-matrix interactions in soft biological tissues. *Biomech. Model. Mechanobiol.*, 20(5):1851–1870, 2021a. DOI: 10.1007/s10237-021-01480-2.

J. F. Eichinger, L. J. Haeusel, D. Paukner, R. C. Aydin, J. D. Humphrey, and C. J. Cyron. Mechanical homeostasis in tissue equivalents - a review. *Biomech. Model. Mechanobiol.*, 20(3):833–850, 2021b. DOI: 10.1007/s10237-021-01433-9.

J. F. Eichinger, D. Paukner, R. C. Aydin, W. A. Wall, J. D. Humphrey, and C. J. Cyron. What do cells regulate in soft tissues on short time scales? *Acta Biomater.*, 134:348–356, 2021c. DOI: 10.1016/j.actbio.2021.07.054.

A. Elosegui-Artola and R. Oria. Cell Migration: Deconstructing the Matrix. *Curr. Biol.*, 30(20): R1266–R1268, 2020. DOI: 10.1016/j.cub.2020.08.013.

A. Elosegui-Artola, E. Bazellières, M. D. Allen, I. Andreu, R. Oria, R. Sunyer, J. J. Gomm, J. F. Marshall, J. L. Jones, X. Trepat, and P. Roca-Cusachs. Rigidity sensing and adaptation through regulation of integrin types. *Nat. Mater.*, 13(6):631–637, 2014. DOI: 10.1038/nmat3960.

A. Elosegui-Artola, X. Trepat, and P. Roca-Cusachs. Control of Mechanotransduction by Molecular Clutch Dynamics. *Trends Cell Biol.*, 28(5):356–367, 2018. DOI: 10.1016/j.tcb.2018.01.008.

M. C. Evans and V. H. Barocas. The Modulus of Fibroblast-Populated Collagen Gels is not Determined by Final Collagen and Cell Concentration: Experiments and an Inclusion-Based Model. *J. Biomech. Eng.*, 131(10):101014, 2009. DOI: 10.1115/1.4000064.

D. G. Ezra, J. S. Ellis, M. Beaconsfield, R. Collin, and M. Bailly. Changes in fibroblast mechanostat set point and mechanosensitivity: An adaptive response to mechanical stress in floppy eyelid syndrome. *Investig. Ophthalmol. Vis. Sci.*, 51(8):3853–3863, 2010. DOI: 10.1167/iovs.09-4724.

B. P. Flynn, A. P. Bhole, N. Saeidi, M. Liles, C. A. Dimarzio, and J. W. Ruberti. Mechanical strain stabilizes reconstituted collagen fibrils against enzymatic degradation by mammalian collagenase matrix metalloproteinase 8 (MMP-8). *PLoS One*, 5(8):21–23, 2010. DOI: 10.1371/journal.pone.0012337.

B. P. Flynn, G. E. Tilburey, and J. W. Ruberti. Highly sensitive single-fibril erosion assay demonstrates mechanochemical switch in native collagen fibrils. *Biomech. Model. Mechanobiol.*, 12 (2):291–300, 2013. DOI: 10.1007/s10237-012-0399-2.

M. F. Fournier, R. Sauser, D. Ambrosi, J. J. Meister, and A. B. Verkhovsky. Force transmission in migrating cells. *J. Cell Biol.*, 188(2):287–297, 2010. DOI: 10.1083/jcb.200906139.

F. Gao, M. Watanabe, and T. Matsuzawa. Stress analysis in a layered aortic arch model under pulsatile blood flow. *Biomed. Eng. Online*, 5:1–11, 2006. DOI: 10.1186/1475-925X-5-25.

A. Gautieri, S. Vesentini, A. Redaelli, and M. J. Buehler. Hierarchical structure and nanomechanics of collagen microfibrils from the atomistic scale up. *Nano Lett.*, 11(2):757–766, 2011. DOI: 10.1021/nl103943u.

M. Ghibaudo, A. Saez, L. Trichet, A. Xayaphoummine, J. Browaeys, P. Silberzan, A. Buguin, and B. Ladoux. Traction forces and rigidity sensing regulate cell functions. *Soft Matter*, 4(9): 1836–1843, 2008. DOI: 10.1039/b804103b.

E. Gineyts, P. A. Cloos, O. Borel, L. Grimaud, P. D. Delmas, and P. Garnero. Racemization and isomerization of type I collagen C-telopeptides in human bone and soft tissues: Assessment of tissue turnover. *Biochem. J.*, 345(3):481–485, 2000. DOI: 10.1042/0264-6021:3450481.

C. Grashoff, B. D. Hoffman, M. D. Brenner, R. Zhou, M. Parsons, M. T. Yang, M. A. McLean, S. G. Sligar, C. S. Chen, T. Ha, and M. A. Schwartz. Measuring mechanical tension across vinculin reveals regulation of focal adhesion dynamics. *Nature*, 466:263–266, 2010. DOI: 10.1038/nature09198.

M. J. Grill, J. F. Eichinger, J. Koban, C. Meier, O. Lieleg, and W. A. Wall. A Novel Modeling and Simulation Approach for the Hindered Mobility of Charged Particles in Biological Hydrogels. *Proc. R. Soc. A*, 477(2249):20210039, 2021. DOI: 10.1098/rspa.2021.0039.

M. J. Grill. *Computational Models and Methods for Molecular Interactions of Deformable Fibers in Complex Biophysical Systems*. Dissertation, Technical University of Munich, 2020.

P. Grimmer and J. Notbohm. Displacement Propagation in Fibrous Networks Due to Local Contraction. *J. Biomech. Eng.*, 140(4):1–11, 2017. DOI: 10.1115/1.4038744.

F. Grinnell and W. M. Petroll. Cell Motility and Mechanics in Three-Dimensional Collagen Matrices. *Annu. Rev. Cell Dev. Biol.*, 26(1):335–361, 2010. DOI: 10.1146/annurev.cellbio.042308.113318.

M. Grossman, N. Ben-Chetrit, A. Zhuravlev, R. Afik, E. Bassat, I. Solomonov, Y. Yarden, and I. Sagi. Tumor cell invasion can be blocked by modulators of collagen fibril alignment that control assembly of the extracellular matrix. *Cancer Res.*, 76(14):4249–4258, 2016. DOI: 10.1158/0008-5472.CAN-15-2813.

M. S. Hall, F. Alisafaei, E. Ban, X. Feng, C.-Y. Hui, V. B. Shenoy, and M. Wu. Fibrous nonlinear elasticity enables positive mechanical feedback between cells and ECMs. *Proc. Natl. Acad. Sci.*, 113(49):14043–14048, 2016. DOI: 10.1073/pnas.1613058113.

S. M. Hall, A. Soueid, T. Smith, R. A. Brown, S. G. Haworth, and V. Mudera. Spatial differences of cellular origins and in vivo hypoxia modify contractile properties of pulmonary artery smooth muscle cells: lessons for arterial tissue engineering. *J. Tissue Eng. Regen. Med.*, 1: 287–295, 2007. DOI: 10.1002/term.

M. A. Heroux and J. Willenbring. A New Overview of the Trilinos Project. *Sci. Program.*, 20: 83–88, 2012.

C. Heussinger and E. Frey. Force distributions and force chains in random stiff fiber networks. *Eur. Phys. J. E*, 24(1):47–53, 2007. DOI: 10.1140/epje/i2007-10209-1.

G. A. Holzapfel and R. W. Ogden. Modelling the layer-specific three-dimensional residual stresses in arteries, with an application to the human aorta. *J. R. Soc. Interface*, 7(46):787–799, 2019. DOI: 10.1098/rsif.2009.0357.

G. A. Holzapfel, T. C. Gasser, and R. W. Ogden. A new constitutive framework for arterial wall mechanics and a comparative study of material models. *J. Elast.*, 61:1–48, 2000. DOI: 10.1023/A:1010835316564.

J. D. Humphrey. Constrained Mixture Models of Soft Tissue Growth and Remodeling Twenty Years After. *J. Elast.*, 145:49–75, 2021. DOI: 10.1007/s10659-020-09809-1.

J. D. Humphrey and K. R. Rajagopal. A constrained mixture model for growth and remodeling of soft tissues. *Math. Model. Methods Appl. Sci.*, 12(3):407–430, 2002. DOI: 10.1142/S0218202502001714.

J. D. Humphrey and C. A. Taylor. Intracranial and abdominal aortic aneurysms: Similarities, differences, and need for a new class of computational models. *Annu. Rev. Biomed. Eng.*, 10: 221–246, 2008. DOI: 10.1146/annurev.bioeng.10.061807.160439.

J. D. Humphrey and G. Tellides. Central artery stiffness and thoracic aortopathy. *Am. J. Physiol. Hear. Circ. Physiol.*, 316(1):H169–H182, 2019. DOI: 10.1152/ajpheart.00205.2018.

J. D. Humphrey, P. B. Wells, S. Baek, J.-J. Hu, K. McLeroy, and A. T. Yeh. A theoretically-motivated biaxial tissue culture system with intravital microscopy. *Biomech. Model. Mechanobiol.*, 7(4):323–334, 2008. DOI: 10.1007/s10237-007-0099-5.

J. D. Humphrey, E. R. Dufresne, and M. A. Schwartz. Mechanotransduction and extracellular matrix homeostasis. *Nat. Rev. Mol. Cell Biol.*, 15(12):802–812, 2014a. DOI: 10.1038/nrm3896.

J. D. Humphrey, D. M. Milewicz, G. Tellides, and M. A. Schwartz. Dysfunctional Mechanosensing in Aneurysms. *Science*, 344(6183):477–479, 2014b. DOI: 10.1126/science.1253026.

D. L. Humphries, J. A. Grogan, and E. A. Gaffney. Mechanical Cell-Cell Communication in Fibrous Networks: The Importance of Network Geometry. *Bull. Math. Biol.*, 79(3):498–524, 2017. DOI: 10.1007/s11538-016-0242-5.

D. Humphries, J. Grogan, and E. Gaffney. The mechanics of phantom Mikado networks. *J. Phys. Commun.*, 2(5):055015, 2018. DOI: 10.1088/2399-6528/aac07a.

D. E. Ingber. Mechanobiology and diseases of mechanotransduction. *Ann. Med.*, 35(8):564–577, 2003. DOI: 10.1080/07853890310016333.

K. A. Jansen, P. Atherton, and C. Ballestrem. Mechanotransduction at the cell-matrix interface. *Semin. Cell Dev. Biol.*, 71:75–83, 2017. DOI: 10.1016/j.semcdb.2017.07.027.

K. A. Jansen, D. M. Donato, H. E. Balcioglu, T. Schmidt, E. H. J. Danen, and G. H. Koenderink. A guide to mechanobiology: Where biology and physics meet. *Biochim. Biophys. Acta*, 1853 (11):3043–3052, 2015. DOI: 10.1016/j.bbamcr.2015.05.007.

G. Jelenić and M. A. Crisfield. Geometrically exact 3D beam theory: Implementation of a strain-invariant finite element for statics and dynamics. *Comput. Methods Appl. Mech. Eng.*, 171(1-2):141–171, 1999. DOI: 10.1016/S0045-7825(98)00249-7.

G. Jenkins, K. L. Redwood, L. Meadows, and M. R. Green. Effect of gel re-organization and tensional forces on $\alpha 2\beta 1$ integrin levels in dermal fibroblasts. *Eur. J. Biochem.*, 263(1):93–103, 1999. DOI: 10.1046/j.1432-1327.1999.00468.x.

L. Jiang, Z. Sun, X. Chen, J. Li, Y. Xu, Y. Zu, J. Hu, D. Han, and C. Yang. Cells sensing mechanical cues: Stiffness influences the lifetime of cell-extracellular matrix interactions by affecting the loading rate. *ACS Nano*, 10(1):207–217, 2016. DOI: 10.1021/acsnano.5b03157.

T. Jin, L. Li, R. C. M. M. Siow, and K.-K. K. Liu. A novel collagen gel-based measurement technique for quantitation of cell contraction force. *J. R. Soc. Interface*, 12(106):20141365, 2015. DOI: 10.1098/rsif.2014.1365.

C. A. R. Jones, L. Liang, D. Lin, Y. Jiao, and B. Sun. The spatial-temporal characteristics of type I collagen-based extracellular matrix. *Soft Matter*, 10(44):8855–8863, 2014. DOI: 10.1039/C4SM01772B.

J. Joshi, G. Mahajan, and C. R. Kothapalli. Three-dimensional collagenous niche and azacytidine selectively promote time-dependent cardiomyogenesis from human bone marrow-derived MSC spheroids. *Biotechnol. Bioeng.*, 115(8):2013–2026, 2018. DOI: 10.1002/bit.26714.

K. E. Kadler, C. Baldock, J. Bella, and R. P. Boot-Handford. Collagens at a glance. *J. Cell Sci.*, 120(12):1955–1958, 2007. DOI: 10.1242/jcs.03453.

D. Karamichos, R. A. Brown, and V. Mudera. Collagen stiffness regulates cellular contraction and matrix remodeling gene expression. *J. Biomed. Mater. Res. Part A*, 83(3):887–894, 2007. DOI: 10.1002/jbm.a.31423.

J. Kim, X. Mao, C. A. R. Jones, J. Feng, B. Sun, L. M. Sander, and H. Levine. Stress-induced plasticity of dynamic collagen networks. *Nat. Commun.*, 8(1):842, 2017. DOI: 10.1038/s41467-017-01011-7.

J. Kim, Y. Zheng, A. A. Alobaidi, H. Nan, J. Tian, Y. Jiao, and B. Sun. Geometric Dependence of 3D Collective Cancer Invasion. *Biophys. J.*, 118(5):1177–1182, 2020. DOI: 10.1016/j.bpj.2020.01.008.

M. S. Kolodney and R. B. Wysolmerski. Isometric Contraction by Fibroblasts and Endothelial Cells in Tissue Culture: A Quantitative Study. *J. Cell Biol.*, 117(1):73–82, 1992. DOI: 10.1083/jcb.117.1.73.

F. Kong, A. J. García, A. P. Mould, M. J. Humphries, and C. Zhu. Demonstration of catch bonds between an integrin and its ligand. *J. Cell Biol.*, 185(7):1275–1284, 2009. DOI: 10.1083/jcb.200810002.

S. O. Koskinen, K. M. Heinemeier, J. L. Olesen, H. Langberg, and M. Kjaer. Physical exercise can influence local levels of matrix metalloproteinases and their inhibitors in tendon-related connective tissue. *J. Appl. Physiol.*, 96(3):861–864, 2004. DOI: 10.1152/japplphysiol.00489.2003.

M. E. Kotas and R. Medzhitov. Homeostasis, Inflammation, and Disease Susceptibility. *Cell*, 160(5):816–827, 2015. DOI: 10.1016/j.cell.2015.02.010.

N. R. R. Lang, S. Münster, C. Metzner, P. Krauss, S. Schürmann, J. Lange, K. E. E. Aifantis, O. Friedrich, and B. Fabry. Estimating the 3D pore size distribution of biopolymer networks from directionally biased data. *Biophys. J.*, 105(9):1967–1975, 2013. DOI: 10.1016/j.bpj.2013.09.038.

M. Latorre and J. D. Humphrey. Mechanobiological stability of biological soft tissues. *J. Mech. Phys. Solids*, 125:298–325, 2019. DOI: 10.1016/j.jmps.2018.12.013.

B. Lee, X. Zhou, K. Riching, K. W. Eliceiri, P. J. Keely, S. A. Guelcher, A. M. Weaver, and Y. Jiang. A three-dimensional computational model of collagen network mechanics. *PLoS One*, 9(11):1–12, 2014. DOI: 10.1371/journal.pone.0111896.

W. R. Legant, A. Pathak, M. T. Yang, V. S. Deshpande, R. M. McMeeking, and C. S. Chen. Microfabricated tissue gauges to measure and manipulate forces from 3D microtissues. *Proc. Natl. Acad. Sci.*, 106(25):10097–10102, 2009. DOI: 10.1073/pnas.0900174106.

M. Lerche, A. Elosegui-Artola, J. Z. Kechagia, C. Guzmán, M. Georgiadou, I. Andreu, D. Gullberg, P. Roca-Cusachs, E. Peuhu, and J. Ivaska. Integrin Binding Dynamics Modulate Ligand-Specific Mechanosensing in Mammary Gland Fibroblasts. *iScience*, 23(3):100907, 2020. DOI: 10.1016/j.isci.2020.100907.

K. R. Levental, H. Yu, L. Kass, J. N. Lakins, M. Egeblad, J. T. Erler, S. F. Fong, K. Csiszar, A. Giaccia, W. Weninger, M. Yamauchi, D. L. Gasser, and V. M. Weaver. Matrix Crosslinking Forces Tumor Progression by Enhancing Integrin Signaling. *Cell*, 139(5):891–906, 2009. DOI: 10.1016/j.cell.2009.10.027.

L. Liang, C. Jones, S. Chen, B. Sun, and Y. Jiao. Heterogeneous force network in 3D cellularized collagen networks. *Phys. Biol.*, 13(6):1–11, 2016. DOI: 10.1088/1478-3975/13/6/066001.

O. Lieleg, M. M. Claessens, C. Heussinger, E. Frey, and A. R. Bausch. Mechanics of bundled semiflexible polymer networks. *Phys. Rev. Lett.*, 99(8):3–6, 2007. DOI: 10.1103/PhysRevLett.99.088102.

O. Lieleg, M. M. Claessens, and A. R. Bausch. Structure and dynamics of cross-linked actin networks. *Soft Matter*, 6(2):218–225, 2010. DOI: 10.1039/b912163n.

S. B. Lindström, D. A. Vader, A. Kulachenko, and D. A. Weitz. Biopolymer network geometries: Characterization, regeneration, and elastic properties. *Phys. Rev. E*, 82(5):2–6, 2010. DOI: 10.1103/PhysRevE.82.051905.

C. M. Lo, H. B. Wang, M. Dembo, and Y. L. Wang. Cell movement is guided by the rigidity of the substrate. *Biophys. J.*, 79(1):144–152, 2000. DOI: 10.1016/S0006-3495(00)76279-5.

S. Loerakker, T. Ristori, and F. P. Baaijens. A computational analysis of cell-mediated compaction and collagen remodeling in tissue-engineered heart valves. *J. Mech. Behav. Biomed. Mater.*, 58:173–187, 2016. DOI: 10.1016/j.jmbbm.2015.10.001.

P. Lu, K. Takai, V. M. Weaver, and Z. Werb. Extracellular Matrix degradation and remodeling in development and disease. *Cold Spring Harb. Perspect. Biol.*, 3(12):1–24, 2011. DOI: 10.1101/cshperspect.a005058.

P. Lu, V. M. Weaver, and Z. Werb. The extracellular matrix: A dynamic niche in cancer progression. *J. Cell Biol.*, 196(4):395–406, 2012. DOI: 10.1083/jcb.201102147.

M. W. Majesky. Developmental basis of vascular smooth muscle diversity. *Arterioscler. Thromb. Vasc. Biol.*, 27(6):1248–1258, 2007. DOI: 10.1161/ATVBAHA.107.141069.

M. W. Majesky, X. R. Dong, V. Hoglund, W. M. Mahoney, and G. Daum. The adventitia: A dynamic interface containing resident progenitor cells. *Arterioscler. Thromb. Vasc. Biol.*, 31 (7):1530–1539, 2011. DOI: 10.1161/ATVBAHA.110.221549.

A. Mammoto, T. Mammoto, and D. E. Ingber. Mechanosensitive mechanisms in transcriptional regulation. *J. Cell Sci.*, 125(13):3061–3073, 2012. DOI: 10.1242/jcs.093005.

A. Mann, R. S. Sopher, S. Goren, O. Shelah, O. Tchaicheeyan, and A. Lesman. Force chains in cell-cell mechanical communication. *J. R. Soc. Interface*, 16(159):20190348, 2019. DOI: 10.1098/rsif.2019.0348.

M. Marenzana, N. Wilson-Jones, V. Mudera, and R. A. Brown. The origins and regulation of tissue tension: Identification of collagen tension-fixation process in vitro. *Exp. Cell Res.*, 312 (4):423–433, 2006. DOI: 10.1016/j.yexcr.2005.11.005.

M. Marino. Molecular and intermolecular effects in collagen fibril mechanics: a multiscale analytical model compared with atomistic and experimental studies. *Biomech. Model. Mechanobiol.*, 15(1):133–154, 2016. DOI: 10.1007/s10237-015-0707-8.

J. P. Marquez, G. M. Genin, G. I. Zahalak, and E. L. Elson. Thin bio-artificial tissues in plane stress: The relationship between cell and tissue strain, and an improved constitutive model. *Biophys. J.*, 88(2):765–777, 2005. DOI: 10.1529/biophysj.104.040808.

T. Matsumoto and K. Hayashi. Mechanical and dimensional adaptation of rat aorta to hypertension. *J. Biomech. Eng.*, 116(3):278–283, 1994. DOI: 10.1115/1.2895731.

T. Matsumoto and K. Hayashi. Response of Arterial Wall to Hypertension and Residual Stress. In *Biomech. Funct. Adapt. Remodel.*, pages 93–119. Springer Japan, Tokyo, 1996. DOI: 10.1007/978-4-431-68317-9_5.

A. Mauri, R. Hopf, A. E. Ehret, C. R. Picu, and E. Mazza. A discrete network model to represent the deformation behavior of human amnion. *J. Mech. Behav. Biomed. Mater.*, 58:45–56, 2016. DOI: 10.1016/j.jmbbm.2015.11.009.

B. S. McEwen and J. C. Wingfield. What is in a name? Integrating homeostasis, allostasis and stress. *Horm. Behav.*, 57(2):105–111, 2010. DOI: 10.1016/j.yhbeh.2009.09.011.

W. Mickel, S. Münster, L. M. Jawerth, D. A. Vader, D. A. Weitz, A. P. Sheppard, K. Mecke, B. Fabry, and G. E. Schröder-Turk. Robust pore size analysis of filamentous networks from three-dimensional confocal microscopy. *Biophys. J.*, 95(12):6072–6080, 2008. DOI: 10.1529/biophysj.108.135939.

Y. A. Miroshnikova, D. M. Jorgens, L. Spirio, M. Auer, A. L. Sarang-Sieminski, and V. M. Weaver. Engineering strategies to recapitulate epithelial morphogenesis within synthetic three-dimensional extracellular matrix with tunable mechanical properties. *Phys. Biol.*, 8(2): 026013, 2011. DOI: 10.1088/1478-3975/8/2/026013.

T. Mitchison and M. Kirschner. Cytoskeletal dynamics and nerve growth. *Neuron*, 1(9):761–772, 1988. DOI: 10.1016/0896-6273(88)90124-9.

A. Mogilner and G. Oster. Force Generation by Actin Polymerization II : The Elastic Ratchet and Tethered Filaments. *Biophys. J.*, 84(3):1591–1605, 2003. DOI: 10.1016/S0006-3495(03)74969-8.

S. W. Moore, P. Roca-Cusachs, and M. P. Sheetz. Stretchy proteins on stretchy substrates: The important elements of integrin-mediated rigidity sensing. *Dev. Cell*, 19(2):194–206, 2010. DOI: 10.1016/j.devcel.2010.07.018.

S. Motte and L. J. Kaufman. Strain stiffening in collagen I networks. *Biopolymers*, 99(1):35–46, 2013. DOI: 10.1002/bip.22133.

K. W. Müller, R. F. Bruinsma, O. Lieleg, A. R. Bausch, W. A. Wall, and A. J. Levine. Rheology of semiflexible bundle networks with transient linkers. *Phys. Rev. Lett.*, 112(23):1–5, 2014. DOI: 10.1103/PhysRevLett.112.238102.

K. W. Müller, C. J. Cyron, and W. A. Wall. Computational analysis of morphologies and phase transitions of cross-linked, semi-flexible polymer networks. *Proc. R. Soc. A Math. Phys. Eng. Sci.*, 471(2182):20150332, 2015. DOI: 10.1098/rspa.2015.0332.

K. W. Müller. *Simulation of self-assembly and mechanics of transiently crosslinked, semiflexible biopolymer networks*. Dissertation, Technical University of Munich, 2014.

S. C. Murtada, A. Arner, and G. A. Holzapfel. Experiments and mechanochemical modeling of smooth muscle contraction: Significance of filament overlap. *J. Theor. Biol.*, 297:176–186, 2012. DOI: 10.1016/j.jtbi.2011.11.012.

S.-I. Murtada, M. Kroon, and G. A. Holzapfel. A calcium-driven mechanochemical model for prediction of force generation in smooth muscle. *Biomech. Model. Mechanobiol.*, 9(6):749–762, 2010. DOI: 10.1007/s10237-010-0211-0.

Y. Nakagawa, M. Totsuka, T. Sato, Y. Fukuda, and K. Hirota. Effect of disuse on the ultrastructure of the achilles tendon in rats. *Eur. J. Appl. Physiol. Occup. Physiol.*, 59(3):239–242, 1989. DOI: 10.1007/BF02386194.

S. Nam, K. H. Hu, M. J. Butte, and O. Chaudhuri. Strain-enhanced stress relaxation impacts nonlinear elasticity in collagen gels. *Proc. Natl. Acad. Sci.*, 113(20):5492–5497, 2016. DOI: 10.1073/pnas.1523906113.

N. M. Nguyen, C. Angely, S. Andre Dias, E. Planus, M. Filoche, G. Pelle, B. Louis, and D. Isabey. Characterisation of cellular adhesion reinforcement by multiple bond force spectroscopy in alveolar epithelial cells. *Biol. Cell*, 109(7):255–272, 2017. DOI: 10.1111/boc.201600080.

R. Nissen, G. J. Cardinale, and S. Udenfriend. Increased turnover of arterial collagen in hypertensive rats. *Proc. Natl. Acad. Sci.*, 75(1):451–453, 1978. DOI: 10.1073/pnas.75.1.451.

J. Notbohm, A. Lesman, D. A. Tirrell, and G. Ravichandran. Quantifying cell-induced matrix deformation in three dimensions based on imaging matrix fibers. *Integr. Biol.*, 7(10):1186–1195, 2015. DOI: 10.1039/c5ib00013k.

Y. Okabe and R. Medzhitov. Tissue biology perspective on macrophages. *Nat. Immunol.*, 17(1):9–17, 2016. DOI: 10.1038/ni.3320.

M. Parsons, E. Kessler, G. J. Laurent, R. A. Brown, and J. E. Bishop. Mechanical load enhances procollagen processing in dermal fibroblasts by regulating levels of procollagen C-proteinase. *Exp. Cell Res.*, 252(2):319–331, 1999. DOI: 10.1006/excr.1999.4618.

B. Patel, A. R. Gingras, A. A. Bobkov, L. M. Fujimoto, M. Zhang, R. C. Liddington, D. Mazzeo, J. Emsley, G. C. Roberts, I. L. Barsukov, and D. R. Critchley. The activity of the vinculin binding sites in talin is influenced by the stability of the helical bundles that make up the talin rod. *J. Biol. Chem.*, 281(11):7458–7467, 2006. DOI: 10.1074/jbc.M508058200.

S. R. Peyton and A. J. Putnam. Extracellular matrix rigidity governs smooth muscle cell motility in a biphasic fashion. *J. Cell. Physiol.*, 204(1):198–209, 2005. DOI: 10.1002/jcp.20274.

S. V. Plotnikov, A. M. Pasapera, B. Sabass, and C. M. Waterman. Force fluctuations within focal adhesions mediate ECM-rigidity sensing to guide directed cell migration. *Cell*, 151(7):1513–1527, 2012. DOI: 10.1016/j.cell.2012.11.034.

B. Pontes, P. Monzo, L. Gole, A. L. Le Roux, A. J. Kosmalska, Z. Y. Tam, W. Luo, S. Kan, V. Viasnoff, P. Roca-Cusachs, L. Tucker-Kellogg, and N. C. Gauthier. Membrane tension controls adhesion positioning at the leading edge of cells. *J. Cell Biol.*, 216(9):2959–2977, 2017. DOI: 10.1083/jcb.201611117.

R. T. Prajapati, B. Chavally-Mis, D. Herbage, M. Eastwood, and R. A. Brown. Mechanical loading regulates protease production by fibroblasts in three-dimensional collagen substrates. *Wound Repair Regen.*, 8(3):226–237, 2000. DOI: 10.1046/j.1524-475X.2000.00226.x.

E. Reissner. On finite deformations of space-curved beams. *Zeitschrift für Angew. Math. und Phys.*, 32(6):734–744, 1981. DOI: 10.1007/BF00946983.

P. Ringer, A. Weißl, A. L. Cost, A. Freikamp, B. Sabass, A. Mehlich, M. Tramier, M. Rief, and C. Grashoff. Multiplexing molecular tension sensors reveals piconewton force gradient across talin-1. *Nat. Methods*, 14(11):1090–1096, 2017. DOI: 10.1038/nmeth.4431.

P. Roca-Cusachs, T. Iskratsch, and M. P. Sheetz. Finding the weakest link exploring integrin-mediated mechanical molecular pathways. *J. Cell Sci.*, 125(13):3025–3038, 2012. DOI: 10.1242/jcs.095794.

L. M. Romero, M. J. Dickens, and N. E. Cyr. The reactive scope model - A new model integrating homeostasis, allostasis, and stress. *Horm. Behav.*, 55(3):375–389, 2009. DOI: 10.1016/j.yhbeh.2008.12.009.

P. Ronceray, C. P. Broedersz, and M. Lenz. Fiber networks amplify active stress. *Proc. Natl. Acad. Sci.*, 113(11):2827–2832, 2016. DOI: 10.1073/pnas.1514208113.

T. D. Ross, B. G. Coon, S. Yun, N. Baeyens, K. Tanaka, M. Ouyang, and M. A. Schwartz. Integrins in mechanotransduction. *Curr. Opin. Cell Biol.*, 25(5):613–618, 2013. DOI: 10.1016/j.ceb.2013.05.006.

P. Sawadkar, D. Player, L. Bozec, and V. Mudera. The mechanobiology of tendon fibroblasts under static and uniaxial cyclic load in a 3D tissue engineered model mimicking native extracellular matrix. *J. Tissue Eng. Regen. Med.*, 14(1):135–146, 2020. DOI: 10.1002/term.2975.

H. B. Schiller and R. Fässler. Mechanosensitivity and compositional dynamics of cell-matrix adhesions. *EMBO Rep.*, 14(6):509–519, 2013. DOI: 10.1038/embor.2013.49.

M. A. Schwartz. Integrins: Emerging Paradigms of Signal Transduction. *Annu. Rev. Cell Dev. Biol.*, 11(1):549–599, 1995. DOI: 10.1146/annurev.cellbio.11.1.549.

K. K. Sethi, I. V. Yannas, V. Mudera, M. Eastwood, C. McFarland, and R. A. Brown. Evidence for sequential utilization of fibronectin, vitronectin, and collagen during fibroblast-mediated collagen contraction. *Wound Repair Regen.*, 10(6):397–408, 2002. DOI: 10.1046/j.1524-475X.2002.10609.x.

R. E. Shadwick. Mechanical design in arteries. *J. Exp. Biol.*, 202(23):3305–3313, 1999. DOI: 10.1242/jeb.202.23.3305.

V. P. Sharma, B. T. Beaty, A. Patsialou, H. Liu, M. Clarke, D. Cox, J. S. Condeelis, and R. J. Eddy. Reconstitution of in vivo macrophage-tumor cell pairing and streaming motility on one-dimensional micro-patterned substrates. *IntraVital*, 1(1):77–85, 2012. DOI: 10.4161/intv.22054.

Q. Shi, R. P. Ghosh, H. Engelke, C. H. Rycroft, L. Cassereau, J. A. Sethian, V. M. Weaver, and J. T. Liphardt. Rapid disorganization of mechanically interacting systems of mammary acini. *Proc. Natl. Acad. Sci.*, 111(2):658–663, 2013. DOI: 10.1073/pnas.1311312110.

J. C. Simo. A finite strain beam formulation. The three-dimensional dynamic problem. Part I. *Comput. Methods Appl. Mech. Eng.*, 49(1):55–70, 1985. DOI: 10.1016/0045-7825(85)90050-7.

J. C. Simo and L. Vu-Quoc. A three-dimensional finite-strain rod model. part II: Computational aspects. *Comput. Methods Appl. Mech. Eng.*, 58(1):79–116, 1986. DOI: 10.1016/0045-7825(86)90079-4.

D. D. Simon, C. O. Horgan, and J. D. Humphrey. Mechanical restrictions on biological responses by adherent cells within collagen gels. *J. Mech. Behav. Biomed. Mater.*, 14:216–226, 2012. DOI: 10.1016/j.jmbbm.2012.05.009.

D. D. Simon, L. E. Niklason, and J. D. Humphrey. Tissue Transglutaminase, Not Lysyl Oxidase, Dominates Early Calcium-Dependent Remodeling of Fibroblast-Populated Collagen Lattices. *Cells Tissues Organs*, 200(2):104–117, 2014. DOI: 10.1159/000381015.

D. D. Simon. *Biomechanics and remodeling of free-floating tissue equivalents*. Dissertation, Yale University, 2014.

S. J. Stehbens and T. Wittmann. Analysis of focal adhesion turnover: a quantitative live-cell imaging example. *Methods Cell Biol.*, 123:335–346, 2014. DOI: 10.1016/B978-0-12-420138-5.00018-5.Analysis.

A. M. Stein, D. A. Vader, D. A. Weitz, and L. M. Sander. The Micromechanics of Three-Dimensional Collagen-I Gels. *Complexity*, 16(4):22–28, 2010. DOI: 10.1002/cplx.

S. Sukharev and F. Sachs. Molecular force transduction by ion channels diversity and unifying principles. *J. Cell Sci.*, 125(13):3075–3083, 2012. DOI: 10.1242/jcs.092353.

M. Sun, A. B. Bloom, and M. H. Zaman. Rapid quantification of 3D collagen fiber alignment and fiber intersection correlations with high sensitivity. *PLoS One*, 10(7):e0131814, 2015. DOI: 10.1371/journal.pone.0157379.

G. Taraboletti, D. D. Roberts, and L. A. Liotta. Thrombodspondin-induced tumor cell migration: Haptotaxis and chemotaxis are mediated by different molecular domains. *J. Cell Biol.*, 105 (5):2409–2415, 1987. DOI: 10.1083/jcb.105.5.2409.

A. D. Theocharis, S. S. Skandalis, C. Gialeli, and N. K. Karamanos. Extracellular matrix structure. *Adv. Drug Deliv. Rev.*, 97:4–27, 2016. DOI: 10.1016/j.addr.2015.11.001.

T. Truong, H. Shams, and M. R. K. Mofrad. Mechanisms of integrin and filamin binding and their interplay with talin during early focal adhesion formation. *Integr. Biol.*, 7(10):1285–1296, 2015. DOI: 10.1039/c5ib00133a.

T. Wakatsuki, M. S. Kolodney, G. I. Zahalak, and E. L. Elson. Cell Mechanics Studied by a Reconstituted Model Tissue. *Biophys. J.*, 79(5):2353–2368, 2000. DOI: 10.1016/S0006-3495(00)76481-2.

H. Wang, A. S. Abhilash, R. G. Wells, C. S. Chen, V. B. Shenoy, R. G. Wells, and V. B. Shenoy. Long-Range Force Transmission in Fibrous Matrices Enabled by Tension-Driven Alignment of Fibers. *Biophys. J.*, 107(11):2592–2603, 2014. DOI: 10.1016/j.bpj.2014.09.044.

P. N. Watton, N. A. Hill, and M. Heil. A mathematical model for the growth of the abdominal aortic aneurysm. *Biomech. Model. Mechanobiol.*, 3(2):98–113, 2004. DOI: 10.1007/s10237-004-0052-9.

V. M. Weaver, O. W. Petersen, F. Wang, C. A. Larabell, P. Briand, C. Damsky, and M. J. Bissell. Reversion of the malignant phenotype of human breast cells in three- dimensional culture and in vivo by integrin blocking antibodies. *J. Cell Biol.*, 137(1):231–245, 1997. DOI: 10.1083/jcb.137.1.231.

B. Weigelin, G.-J. Bakker, and P. Friedl. Intravital third harmonic generation microscopy of collective melanoma cell invasion. *IntraVital*, 1(1):32–43, 2012. DOI: 10.4161/intv.21223.

S. Weng, Y. Shao, W. Chen, and J. Fu. Mechanosensitive subcellular rheostasis drives emergent single-cell mechanical homeostasis. *Nat. Mater.*, 15(9):961–967, 2016. DOI: 10.1038/nmat4654.

K. Wolf, M. te Lindert, M. Krause, S. Alexander, J. te Riet, A. L. Willis, R. M. Hoffman, C. G. Figdor, S. J. Weiss, and P. Friedl. Physical limits of cell migration: Control by ECM space and nuclear deformation and tuning by proteolysis and traction force. *J. Cell Biol.*, 201(7): 1069–1084, 2013. DOI: 10.1083/jcb.201210152.

J. Wolff. *Das Gesetz der Transformation der Knochen*. Hirschwald, Berlin, 1892.

H. Wolinsky and S. Glagov. A lamellar unit of aortic medial structure and function in mammals. *Circ. Res.*, 20(1):99–111, 1967. DOI: 10.1161/01.RES.20.1.99.

H. Wolinsky. Effects of Hypertension and Its Reversal on the Thoracic Aorta of Male and Female Rats. *Circ. Res.*, 28(6):622–637, 1971. DOI: 10.1161/01.RES.28.6.622.

P.-H. Wu, A. Giri, S. X. Sun, and D. Wirtz. Three-dimensional cell migration does not follow a random walk. *Proc. Natl. Acad. Sci.*, 111(11):3949–3954, 2014. DOI: 10.1073/pnas.1318967111.

T. A. Wynn, A. Chawla, and J. W. Pollard. Macrophage biology in development, homeostasis and disease. *Nature*, 496(7446):445–455, 2013. DOI: 10.1038/nature12034.

J. Xie, M. Bao, S. M. C. Bruekers, and W. T. S. Huck. Collagen Gels with Different Fibrillar Microarchitectures Elicit Different Cellular Responses. *ACS Appl. Mater. Interfaces*, 9(23): 19630–19637, 2017. DOI: 10.1021/acsami.7b03883.

K. M. Yamada and M. Sixt. Mechanisms of 3D cell migration. *Nat. Rev. Mol. Cell Biol.*, 20(12): 738–752, 2019. DOI: 10.1038/s41580-019-0172-9.

M. Yao, B. T. Goult, H. Chen, P. Cong, M. P. Sheetz, and J. Yan. Mechanical activation of vinculin binding to talin locks talin in an unfolded conformation. *Sci. Rep.*, page 4610, 2014. DOI: 10.1038/srep04610.

M. Yao, B. T. Goult, B. Klapholz, X. Hu, C. P. Toseland, Y. Guo, P. Cong, M. P. Sheetz, and J. Yan. The mechanical response of talin. *Nat. Commun.*, 7:11966, 2016. DOI: 10.1038/ncomms11966.

T. Yeung, P. C. Georges, L. A. Flanagan, B. Marg, M. Ortiz, M. Funaki, N. Zahir, W. Ming, V. Weaver, and P. A. Janmey. Effects of substrate stiffness on cell morphology, cytoskeletal structure, and adhesion. *Cell Motil. Cytoskeleton*, 60(1):24–34, 2005. DOI: 10.1002/cm.20041.

A. Zemel. Active mechanical coupling between the nucleus, cytoskeleton and the extracellular matrix, and the implications for perinuclear actomyosin organization. *Soft Matter*, 11(12): 2353–2363, 2015. DOI: 10.1039/c4sm02425g.

D. Zhou, L. Zhang, and X. Mao. Topological Edge Floppy Modes in Disordered Fiber Networks. *Phys. Rev. Lett.*, 120(6):068003, 2018. DOI: 10.1103/PhysRevLett.120.068003.

C. Zhu, C. Pérez-González, X. Trepat, Y. Chen, N. Castro, R. Oria, P. Roca-Cusachs, A. Elosegui-Artola, and A. Kosmalska. Mechanical regulation of a molecular clutch defines force transmission and transduction in response to matrix rigidity. *Nat. Cell Biol.*, 18(5): 540–548, 2016. DOI: 10.1038/ncb3336.

Y. K. Zhu, T. Umino, X. D. Liu, H. J. Wang, D. J. Romberger, J. R. Spurzem, and S. I. Rennard. Contraction of Fibroblast-Containing Collagen Gels: Initial Collagen Concentration Regulates the Degree of Contraction and Cell Survival. *In Vitro Cell Dev. Biol. Anim.*, 37(1):10–16, 2001. DOI: 10.1290/1071-2690(2001)037<0010:COFCCG>2.0.CO;2.

W. H. Ziegler, A. R. Gingras, D. R. Critchley, and J. Emsley. Integrin connections to the cytoskeleton through talin and vinculin. *Biochem. Soc. Trans.*, 36(2):235–239, 2008. DOI: 10.1042/bst0360235.

Verzeichnis der betreuten Studienarbeiten

Im Rahmen dieser Dissertation entstanden am Lehrstuhl für Numerische Mechanik (LNM) in den Jahren von 2017 bis 2020 unter wesentlicher wissenschaftlicher, fachlicher und inhaltlicher Anleitung des Autors die im Folgenden aufgeführten studentischen Arbeiten. Der Autor dankt allen Studierenden für ihr Engagement bei der Unterstützung dieser wissenschaftlichen Arbeit.

Studierende(r)	**Studienarbeit**
Lea Häusel	*Study of Cell-Mediated Homeostasis in Tissue Equivalents in Computer-controlled Biaxial Tests*, Bachelorarbeit, 2020, eingeflossen in Kapitel 3.2 und 3.5.
Lydia Ehmer	*Study of Tensional Homeostasis in Higher Dimensions Using Cell Seeded Collagen Gels*, Semesterarbeit, 2019, eingeflossen in Kapitel 3.5.
Lydia Ehmer	*Simulation of the Viscoelastic Behavior of Acellular Collagen Gels and Quantitative Comparison with Experimental Results*, Bachelorarbeit, 2019.
Daniel Paukner	*Design and Validation of a Biaxial Bioreactor for Cell-Seeded Collagen Gels*, Masterarbeit, 2018, eingeflossen in Kapitel 2.3 und 3.3.
Niklas Klinkertz	*Equilibrium Morphologies of Semiflexible, Transiently Crosslinked, Heterogeneous Biopolymer Networks*, Bachelorarbeit, 2017.
Daniel Paukner	*Simulation of the Brownian Dynamics of Slender Biopolymers using Beam Finite Elements*, Semesterarbeit, 2017.